CHAPTER 7

Membrane-Bound Proteins

7.1 INTRODUCTION

The plasma membrane is a lipid body containing proteins and carbohydrate units. It defines the shape of the cell and acts as a physical barrier between the cytoplasm and the external environment (*exoplasm*). Since these two environments are very different in terms of their chemical composition, the formation of the first membranes signified the evolutionary emergence of the first biological organisms; this event took place between 3.2 and 3.8 billion years ago [1–4]. The cells of all organisms are enveloped by plasma membranes, and some cells contain other membranes as well. Gram-negative bacteria, for example, also have an outer membrane, which has its own set of characteristic proteins, and is rich in polysaccharides. Eukaryotic cells, which evolved about 1.5 billion years ago, contain inner membranes, which define the various organelles.

The primary role of the plasma membrane is to maintain the unique chemical environment of the cell, which includes the following:

1. **Ions.** Intracellular ions are chemically diverse. Some are elements such as Na^+, K^+, Cl^-, Mg^{2+}, Mn^{2+}, Cu^{2+}, Zn^+, Co^{2+} and $Fe^{2+/3+}$, whereas others are molecules of various sizes (e.g., PO_2^{3-}). Maintaining a constant concentration of these ions inside the cell is crucial for the routine execution of numerous cellular and physiological processes. First, by stabilizing charged groups in the active sites of enzymes, or participating in the binding of atoms and molecules, ions enable routine biochemical pathways to take place [5,6]. Second, the concentration gradient of Na^+, K^+ and Cl^- across the plasma membrane is responsible for its electric potential, which is used to drive processes such as cellular transport, neural transmission, and muscle contraction. Finally, the physiological ionic balance is important for the regulation of body hydration.

2. **Small metabolites.** Small organic molecules, such as ATP, amino acids, monosaccharides and disaccharides, nucleotides, pyruvate, and others, participate in, and are formed by, metabolic processes.

3. **Macromolecules.** Proteins, carbohydrates, lipids, and nucleic acids are the functional units of cells and tissues, as explained in Chapter 1.

Many of these chemicals are polar (neutral or charged), which explains why the type of barrier chosen by evolution to keep them inside the cell is based on a lipid structure, whose permeability to such molecules is extremely low. In order for a polar compound to cross the

membrane, it must first transfer from the aqueous environment (cytoplasm or exoplasm) into the membrane itself. This process is highly unlikely, due to the desolvation of the polar compound. The transfer energy can be estimated using the Born equation of solvation (Equation (2.2)), as follows.

Assuming that ion transfer into the membrane is determined by electrostatic contributions, the transfer free energy is:

$$\Delta G_{\text{transfer}} = G_m - G_w = 166\left(\frac{q}{r}\right)\left(\frac{1}{\varepsilon_m} - \frac{1}{\varepsilon_w}\right) \tag{7.1}$$

(where m and w are the membrane and aqueous environments, respectively; q is the net charge of the molecule; r is its effective radius; and ε is the dielectric. See Chapter 2 for more details.).

For simplicity, let us consider a simple spherical ion of radius 1 Å and charge +1. Taking the dielectrics of the membrane and aqueous environment to be 2 and 80, respectively, we obtain $\Delta G_{\text{transfer}} = +80$ kcal/mol. Thus, the fraction of ions that transfer into the membrane (Equation (4.3b)) is: $P \propto e^{(-\Delta G/RT)} = e^{(-80/0.6)} \approx 1 \times 10^{-58}$. **Thus, in essence, at a physiological ion concentration of about 150 mM, no cation will partition into the membrane.** Computational [7] and experimental [8] studies show that this is also true for large ions, such as the side chains of charged amino acids.

Since most of the compounds inside cells are produced and utilized constantly by metabolic processes, it is not enough to prevent them from leaving the cell; keeping their concentrations fixed requires the constant import of some compounds and the export of others. In addition, the entire process must be carefully controlled, so as to avoid the loss of important metabolites or the internalization of wastes and/or toxic chemicals. As in the other cases we have encountered, here too evolution has assigned the job to proteins. There are two types of *transport proteins*: *channels* and *transporters*. A channel crosses the entire length of the membrane, and contains a water annulus, which enables polar chemicals (often ions) to move across the membrane, down their electrochemical gradient. A transporter binds polar chemicals on one side of the membrane and releases them on the other side. Some transporters span the entire width of the membrane, whereas others (*carriers*) do not, and have to diffuse from one side to the other in order to release the 'substrate' into the right compartment. While some transporters transfer molecules down their electrochemical gradient, others (*pumps*) do so in the opposite direction, by using an external source of energy, which can be direct (ATP), or indirect (the electrochemical gradient of another molecule). The transport process is controlled in both channels and transporters; channels only let in molecules that are small enough to enter the water annulus, and can also open or close in response to different signals, such as ligand binding, change in cross-membrane voltage, or application of mechanical pressure. Transporters can bind or release their 'substrates' when the latter are present, but in many cases they do so pending the binding of the right regulatory ligand. The function of transport proteins is so basic that in microorganisms they constitute 40% to 50% of all membrane proteins [9].

In addition to transport, membrane proteins play other important roles, most of which are mentioned in Chapter 1:

1. **Communication and signal transduction.** Numerous cellular proteins are membrane-bound receptors. These act as antennae, and pass communication signals arriving

from the external environment into the cell. Most of these receptors respond to chemical messengers, such as hormones, neurotransmitters, pheromones, odorants, and local mediators, whereas others respond to other types of signals, such as electromagnetic radiation (light) or mechanical pressure. Thus, the proper functioning of these proteins is crucial not only to individual cells, but also to entire physiological systems, specifically, the nervous, endocrine, and immune systems. Receptors span the entire width of the membrane, with their extracellular side designed to bind or respond to the external messenger, and their intracellular side interacting with different cytoplasmic proteins. The latter transmit messages into the cell, often by catalyzing enzymatic reactions. For example, *growth factor receptors* relay the message 'grow' or 'divide' into the cell by promoting phosphorylation of various cellular components. While most of the cytoplasmic proteins receiving this message are water-soluble, some, such as *G-proteins* or the enzymes *protein kinase A and C* are membrane-bound, at least part of the time.

2. **Cell-cell and cell-ECM recognition.** Certain membrane-bound proteins, such as *integrins* or *cadherins*, bind proteins or other elements that reside either on other cells or in the extracellular matrix (ECM). Such interactions are important, e.g., for the cell's ability to recognize its neighbors or become anchored to its biological tissue.

3. **Energy production and photosynthesis.** A number of proteins that reside inside the inner mitochondrial membrane (or the plasma membrane of bacteria) participate in the extraction of chemical energy from foodstuff, and its storage in a freely available form, ATP. Most of these proteins act as electron carriers and proton pumps, whereas others construct the ATP-producing component of this system. A similar system functions in the thylakoid membrane of plants and algae (or the plasma membrane of photosynthetic bacteria), in the assimilation of solar energy, i.e., photosynthesis.

4. **Defense.** Certain membrane-bound proteins participate in the defense of the cell or the entire body against invading pathogens, i.e., bacteria, viruses, and parasites. These proteins may fulfill different functions, most of which involve recognition of pathogen-related molecules. A well-known example is the *T-cell receptor*, which spans the membrane of a T lymphocyte, and recognizes peptides that have been taken from degraded pathogens.

5. **Cellular trafficking.** Membrane proteins often serve as attachment points for other proteins. This function enables cells to concentrate metabolic enzymes or signal transduction proteins in certain locations. The trafficking of vesicles carrying lipids and proteins between cellular compartments is also affected by certain membrane-bound proteins.

The significance of membrane proteins is reflected not only in their functions but also in their prevalence; it is estimated that 20% to 30% of any genome codes for membrane proteins [10,11], and a recent, extensive survey of the human proteome indicates a similar value, 23% [12]. Defects in membrane proteins manifest as various pathologies, including neural or cardiovascular disorders, depression, obesity, and cancer. Accordingly, it is estimated that ~60% of approved pharmaceutical drugs act on membrane proteins [13,14], most of which are G protein-coupled receptors (GPCRs; see below) [15,16].

We discussed earlier how proteins are structurally, thermodynamically, and functionally affected by their environments. It therefore stands to reason that in order to understand the behavior of membrane proteins, one must first understand the nature of biological membranes. This conclusion is reinforced by the fact that membranes are by nature much more complex, both chemically and physically, than the aqueous solution constituting the cytoplasm. In the following section we review the key characteristics of the biological membrane, and in Section 7.4 we focus on the effects of these properties on the behavior of membrane proteins, and *vice versa*.

7.2 STRUCTURE AND ORGANIZATION OF BIOLOGICAL MEMBRANES

7.2.1 General structure and properties

In 1972, Singer and Nicolson proposed their well-known *fluid mosaic (FM) model* to describe the structures and characteristics of biological membranes [17]. The model depicts the membrane as a structure made of two layers of lipid molecules (*lipid bilayer*), in which various proteins reside (Figure 7.1a). These proteins are separated into two general types:

1. **Integral proteins** reside inside the lipid bilayer, with one or more segments of their polypeptide chain crossing the full width of the bilayer (*transmembrane (TM) domain*). Isolating these proteins requires the disruption of the bilayer structure by detergents.

2. **Peripheral proteins** are loosely attached to one of the lipid monolayers, or to an integral protein. Isolating such proteins does not require membrane disruption; a mild treatment, e.g., elevating the salt concentration, is sufficient.

In addition to lipids and proteins, membranes also contain different types of carbohydrates, in the form of long and branched chains. These are attached to both lipid and protein molecules on the extracellular side of the membrane. The entire carbohydrate coat of the membrane is referred to as the *'glycocalyx'*. Contrary to its depiction in old biochemistry and cell biology books, the glycocalyx is of formidable size, and is visible to the electron microscope. The carbohydrate chains provide physical protection to the membrane, but also participate in molecular recognition processes. These can be between cells, or between the cell and a water-soluble molecule within the body.

The bilayer structure, on which the entire membrane is based, is made of numerous lipid molecules packed tightly against one another (Figure 7.1b). Nevertheless, the FM model posits that since each lipid molecule is inherently dynamic, the bilayer is only mildly viscous (hence the term 'fluid' in the name of the model). To test this posit, early studies focused on the protein-to-lipid ratio in different biological membranes. They concluded that although most biological membranes have a weight ratio of ~0.5, some membranes differ considerably in this parameter. For example, in the myelin membrane, which surrounds the axons of nerve cells, the ratio is ~0.2, whereas in the inner mitochondrial membrane it is ~0.8. A study carried out on red blood cells took a slightly different approach by considering a different parameter, the proportion of the membrane surface occupied by the protein component [18]. The results demonstrated that proteins occupy at least 23% of the membrane surface, i.e., a much higher value than expected based on the protein-to-lipid

ratio. This high value was attributed to the fact that many integral membrane proteins have large extramembrane domains, and also to the fact that such proteins tend to form large oligomers. These results suggested that, contrary to the fluid depiction put forward by the FM model and studies carried out in pure lipid bilayers — an approach that had dominated the scientific view up until that point — biological membranes have a certain rigidity. Today, the membrane is considered to have intermediary properties between fluid and gel, which enable it to block the free movement of polar solutes, but at the same time retain its flexibility, which is highly important for its function. For example, flexibility is important for the formation of transport vesicles, which carry protein and lipid cargo between intracellular membranes and the plasma membrane. The cargo molecules may reside in the membrane or be secreted in a process of exocytosis [19,20]. Transport vesicles also enable polar solutes to be internalized by the cell through endocytosis.

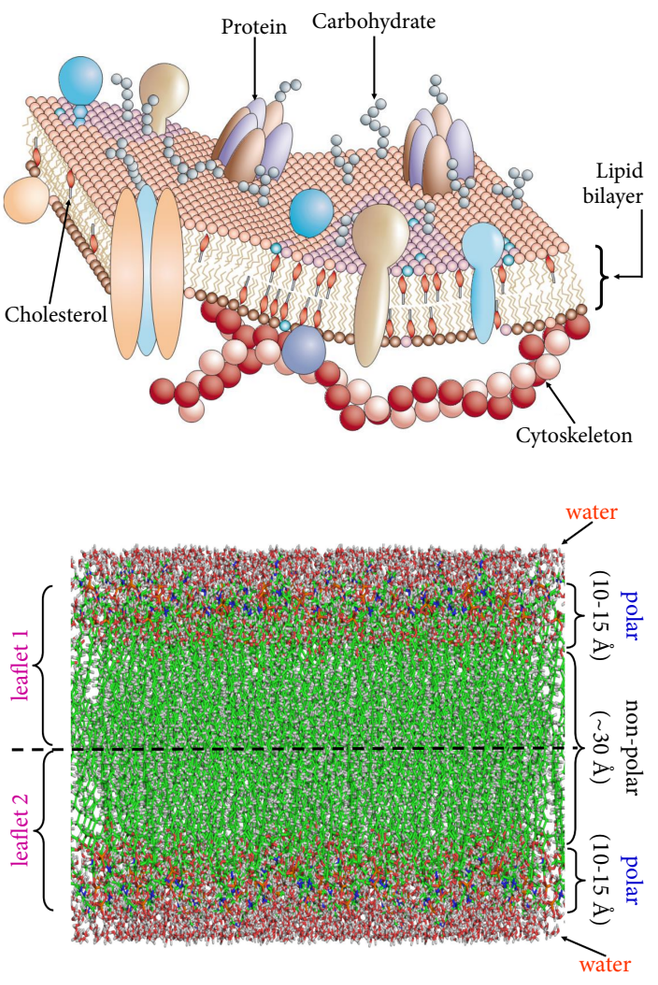

FIGURE 7.1 **The biological membrane.** (a) The fluid mosaic model of the cell membrane. The image was adapted from [21]. (b) An atomistic representation of the hydrated lipid bilayer. The polar and nonpolar regions are noted, as well as their lengths (from [22]). The dashed line marks the border between two leaflets. For clarity, the lipid bilayer is shown in its ordered phase. In reality, the lipid chains are disordered and dynamic.

7.2.2 Composition of lipid bilayer

The biological membrane contains numerous lipid molecules of different types [23,24]. Even red blood cells, which are considered to be highly simple, contain in their plasma membranes over 200 different types of lipids [25]. The following subsections summarize the structures and properties of the main types.

7.2.2.1 Glycerophospholipids

Glycerophospholipids are the most abundant type of lipids in biological membranes [26]. Their name alludes to their chemical structure; each contains two fatty acids esterified to a glycerol backbone, with the third glycerol carbon attached to a negatively charged phosphate group (Figure 7.2a). In most phospholipids, the phosphate group is attached on its other side to an alcohol group, which can be *serine*, *choline*, *ethanolamine*, *inositol 4,5-bisphosphate* (IP_2), or even *glycerol* [27] (Figure 7.2b). The name of each phospholipid includes the prefix *'phosphatidyl'*, followed by the name of the alcohol group it contains. Since the various phospholipids differ only in the identity of their respective alcohol groups, it is the alcohol group that determines the overall physicochemical uniqueness of each phospholipid, including its size and electric charge (Table 7.1). *Cardiolipin* differs substantially from other phospholipids in its shape. Its alcohol group is an entire phosphatidylglycerol group, which means it contains two phosphate groups, two glycerol groups, and four acyl chains[*1] [28]. The acyl chain in the first glycerol position (*sn-1*) tends to be either saturated[*2] or monounsaturated[*3], whereas that in the second position *(sn-2)* tends to be polyunsaturated[*4] [29]. Most acyl chains in biological membranes contain 18 carbons [30], which creates an average hydrophobic width of ~30 Å [31].

TABLE 7.1 **Glycerophospholipids composing biological membranes.**

Full Name	Abbreviation	Acyl Chains	Alcoholic Head Group	Net Charge
Phosphatidyl**choline**	PC	2	trimethylammonium	0
Phosphatidyl**ethanolamine**	PE	2	amino	0
Phosphatidyl**serine**	PS	2	amino/carboxyl	−1
Phosphatidyl**inositol bisphosphate**	PIP_2	2	hydroxyl/phosphate	−5
Phosphatidyl**glycerol**	PG	2	hydroxyl	−1
Diphosphatidyl**glycerol** (cardiolipin)	CL	4	hydroxyl/diacyl	−2

7.2.2.2 Sphingolipids

Sphingolipids have similar properties to glycerophospholipids, except for the following:

1. The backbone of the molecule contains *dihydrosphingosine* instead of glycerol (Figure 7.3a).

[*1] When attached to another molecule or group, the fatty acids are called 'acyl chains'.
[*2] That is, devoid of any double bonds.
[*3] That is, containing one double bond.
[*4] That is, containing several double bonds.

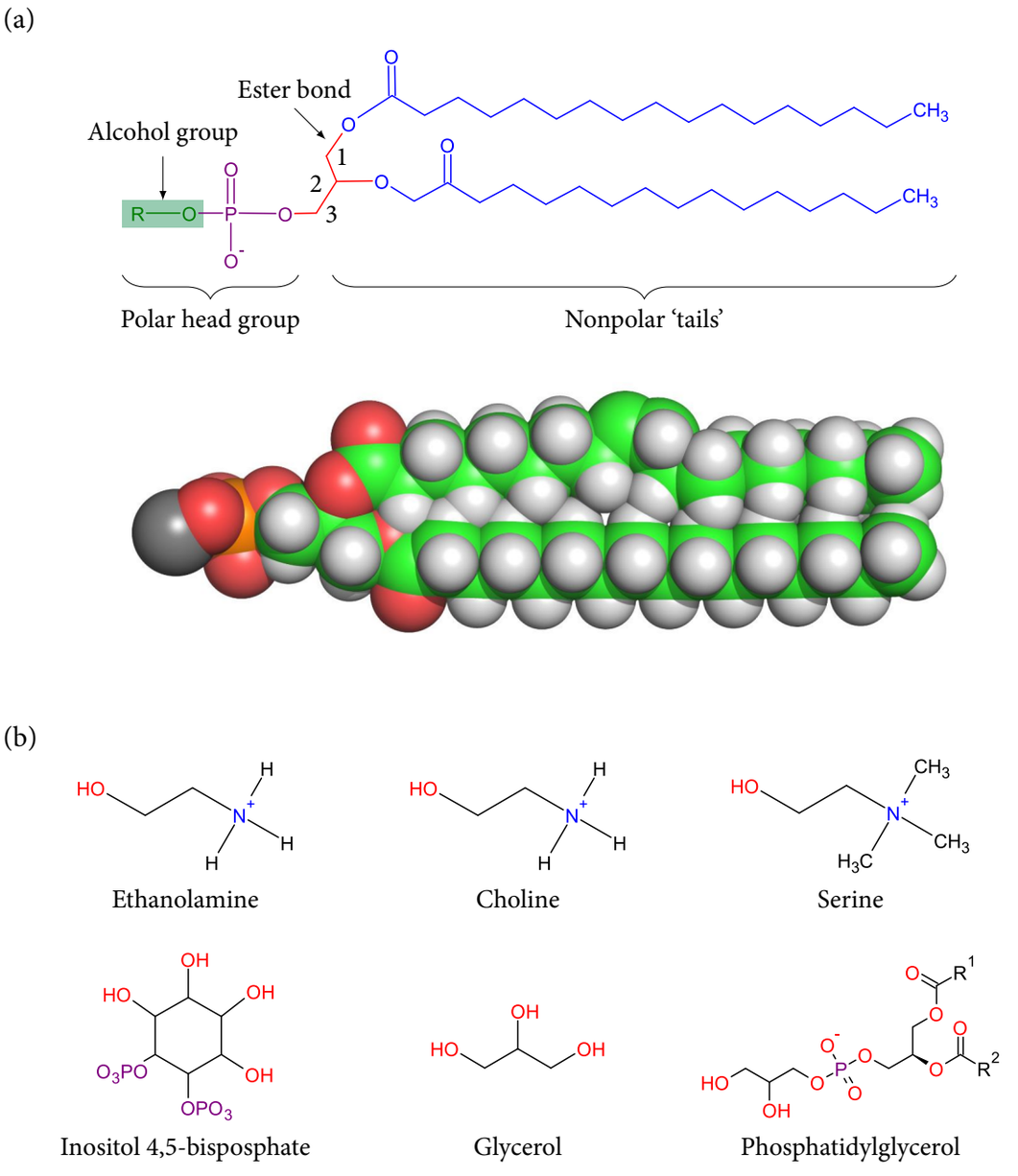

FIGURE 7.2 **Glycerophospholipids.** (a) General structure. *Top*: Chemical structure. The glycerol backbone is colored in red and numbered; the acyl chains are colored in blue; and the alcohol group (R–OH) is surrounded by a green box. The nonpolar and polar parts of the phospholipid define the corresponding regions of the lipid bilayer (see Figure 7.1). *Bottom*: Three-dimensional structure. The atoms are colored by atom type, with the R moiety colored in grey. (b) Common types of alcohol groups that appear in phospholipids.

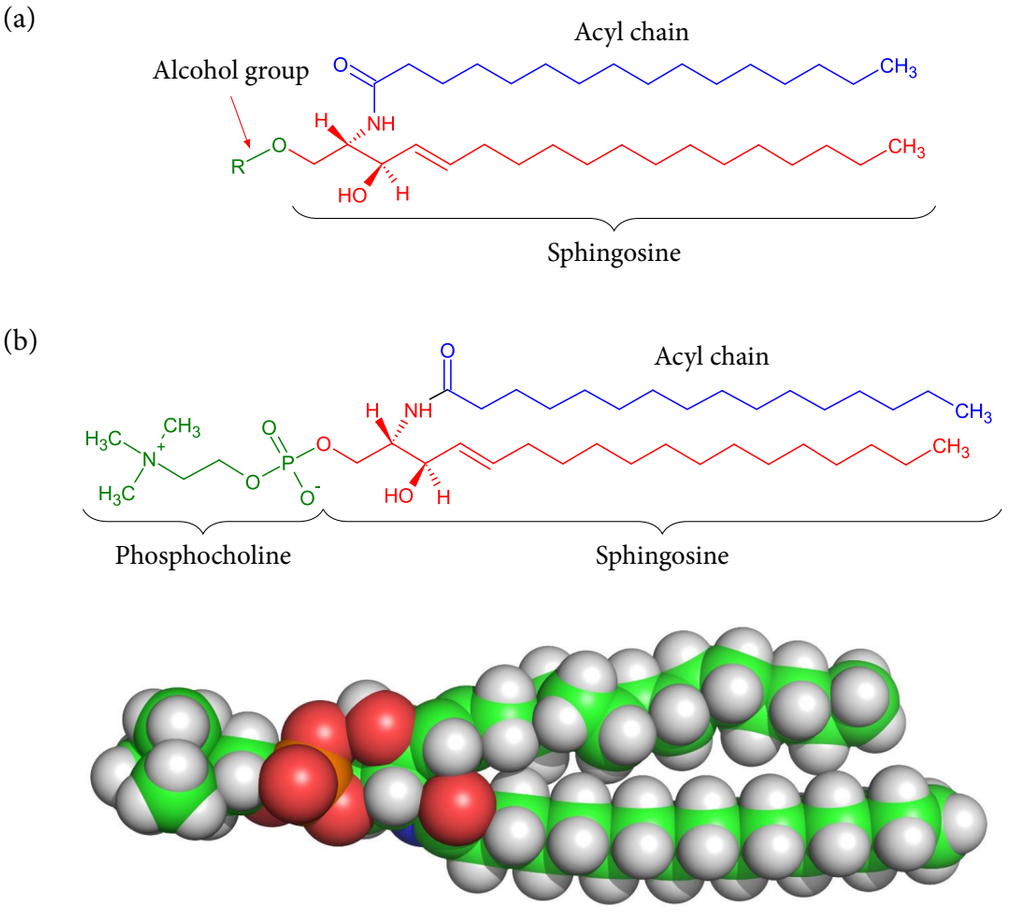

FIGURE 7.3 **Sphingolipids.** (a) General structure, demonstrated on a ceramide molecule. The sphingosine backbone of the molecule is colored in red, the acyl chain in blue, and the alcohol moiety in green. (b) *Top*: The chemical structure of sphingomyelin, colored as in (a). *Bottom*: The three-dimensional structure of sphingomyelin.

2. Only one acyl chain is present, attached to the sphingosine backbone (this conjugate is called *'ceramide'*). However, since the structure of sphingosine itself includes a long hydrocarbon chain that resembles an acyl chain, the general shape of the lipid molecule is still similar to that of glycerol phospholipids.

3. Although in many cases the carbon at the third position of sphingosine is attached to a phosphocholine group (this molecule is called *sphingomyelin* [32]; Figure 7.3b), in other cases the phosphate group may be replaced by a large carbohydrate group. Such complex molecules are referred to as *'glycosphingolipids'* (*GSLs*). Some GSLs contain a *sialic acid* group (*N-acetylneuraminic acid*) covalently attached to the sugar moiety. These GSLs are called *'gangliosides'*, and are particularly prevalent in neuronal membranes, where they constitute 2% to 10% of the total lipid component [33].

GSLs are ubiquitous components of animal cell membranes [33] and constitute a particularly interesting category of sphingolipids. The complex carbohydrate patterns in GSLs, and the

fact that most GSLs reside on the outer leaflet of the lipid bilayer, make these molecules highly suitable for molecular recognition processes. Indeed, GSLs are known to interact with an extensive set of extracellular ligands, such as lectins, toxins, hormones, and viruses. The membrane composition of GSLs is carefully regulated, and is known to depend on the developmental condition of the cell. In addition, this composition has been found to change dramatically in some abnormal events, such as neurological diseases and cancerous transformation of cells.

7.2.2.3 Sterols

In eukaryotes, a third type of lipid, the *sterol*, can be found. Sterols have a characteristic structure of four fused rings with a hydroxyl group at one end of the molecule and a lipid 'tail' at the other end (Figure 7.4a). The specific type of sterol in the membrane depends on the type of organism: Plants, fungi and animals contain *stigmasterol*, *ergosterol*, and *cholesterol*, respectively [34] (Figure 7.4b–d). Compared to the slender-flexible phospholipids, sterols are bulky and rigid. These two properties of sterols have an important effect on the properties of the entire membrane, as explained below. The general importance of cholesterol in the mammalian membrane is reflected in its narrow concentration range in the membrane [34,35]. This range is actively monitored by the cell.

7.2.2.4 Ethers

Archaeans are among the most ancient organisms on Earth. Not surprisingly, they tend to live in niches such as the hydrothermal vents at the bottom of the ocean, which have extreme conditions resembling those that dominated our planet ~3.5 billion years ago. Though they are considered prokaryotes, Archaeans have several characteristics that distinguish them from eubacteria ('modern' bacteria), as well as from eukaryotes. One of these differences lies in the chemistry of their membrane lipids. While in eukaryotes and eubacteria most membrane lipids include fatty acids esterified to glycerol backbones, in Archaeans the lipid chain in the first position is attached to the glycerol via an *ether bond* (e.g., in *plasmalogen*) (Figure 7.5). It is possible that the ether bond, which is more stable than an ester, confers an important advantage at the extreme conditions these organisms live in.

7.2.2.5 Variability

Cells possess different mechanisms that enable them to control the lipid composition in their membranes [36–38]. Although the compositions of most membranes share several general characteristics (e.g., the dominance of phospholipids), substantial variability is observed across membranes from different origins, as follows:

1. **Different groups of organisms.** In eukaryotes the major phospholipid is phosphatidylcholine (PC; ~20% of the lipids in the rat liver plasma membrane [39]), whereas in most bacteria it is phosphatidylethanolamine (PE) or phosphatidylglycerol (PG) [40]. Conversely, in the mycobacteria *M. tuberculosis* the dominant phospholipid is cardiolipin (CL) [41].

2. **Different tissues within the same organism.** For example, the intestinal brush border membrane has no CL, whereas membranes in the nervous system that are rich in

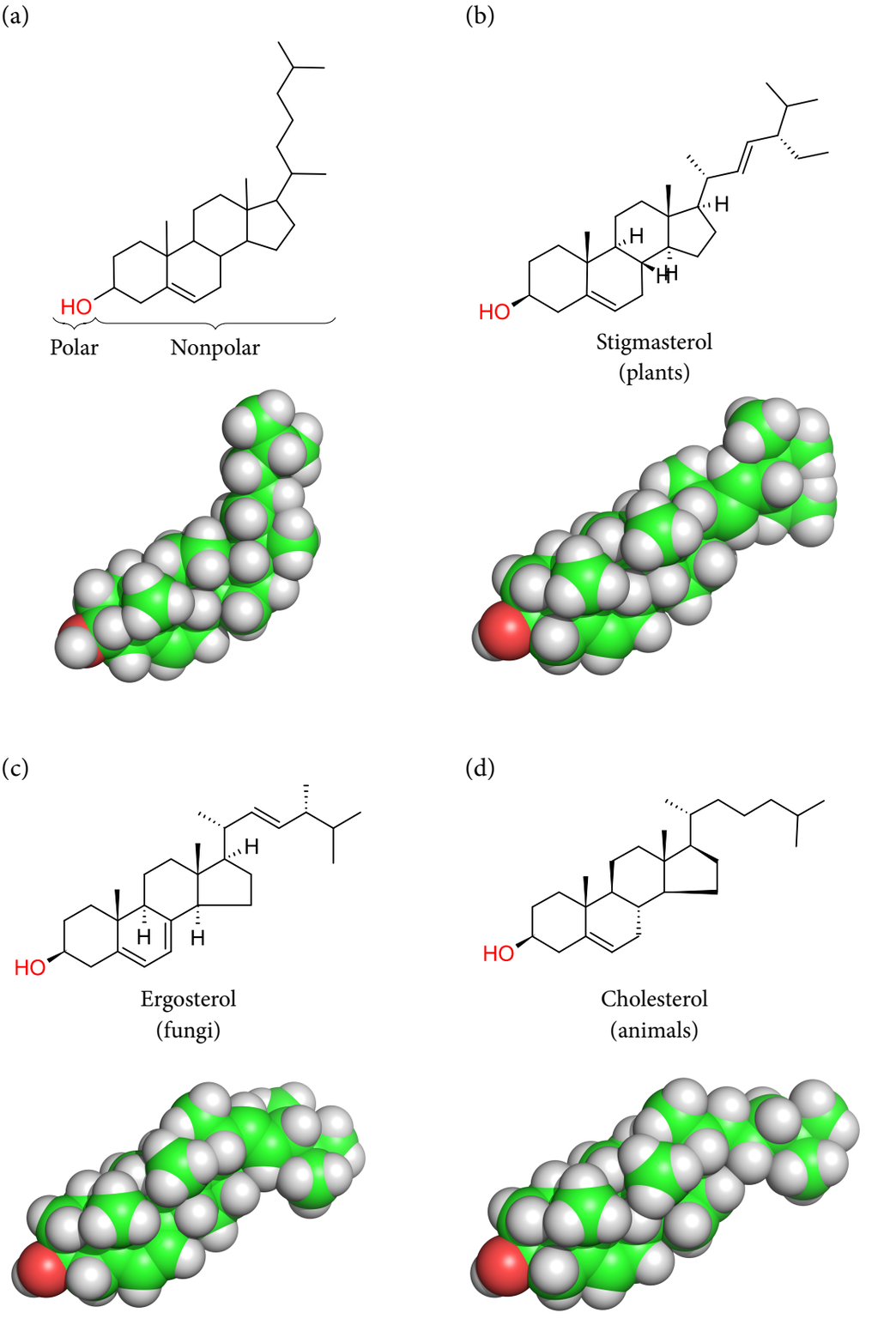

FIGURE 7.4 **Sterols.** (a) The general sterol structure, containing four fused rings, a hydrophobic tail, and a hydroxyl group on the other side. (b) Stigmasterol. (c) Ergosterol. (d) Cholesterol. *Top*: The chemical structures of the lipids. *Bottom*: The three-dimensional structures of the lipids.

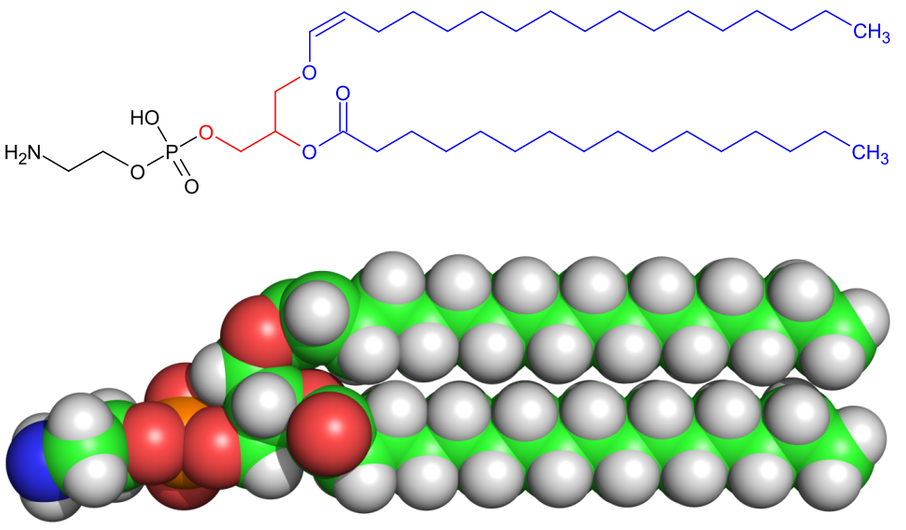

FIGURE 7.5 **Ether-linked lipids.** *Top*: The chemical structure of these lipids is exemplified by plasmalogen. The glycerol and acyl chains are shown as in Figure 7.2. *Bottom*: The three-dimensional structure of plasmalogen.

cholinergic receptors have very little sphingomyelin (SM) and no phosphatidylinositol (PI) [42].

3. **Plasma versus inner membranes in eukaryotes.** For example, CL constitutes ~20% of lipids in the mitochondrial inner membrane, whereas it is virtually absent in the ER and plasma membranes [43]. In addition, animal cholesterol resides mainly in the plasma membrane, and is present only in negligible amounts in the ER membrane [44–46]. Finally, most of the SM in the cell is concentrated in the plasma membrane and the lysosomal membrane [42].

4. **Cytoplasmic versus exoplasmic leaflets of the plasma membrane.** In eukaryotic membranes, the exoplasmic leaflet contains mainly choline phospholipids (PC and SM), whereas the cytoplasmic leaflet contains mainly amino phospholipids (PS and PE), as well as PI, in much smaller quantities [47–50]. Since both PC and SM are electrically neutral, whereas phosphatidylserine (PS) and PI are negatively charged, the lipid asymmetry leads to a charge difference between the two leaflets. That is, **the cytoplasmic leaflet is negative compared to the exoplasmic leaflet**. In the bacterial inner membrane the exoplasmic leaflet is enriched with PG, whereas the cytoplasmic leaflet is enriched with PE and PI [50].

5. **Different regions of the same membrane.** Certain lipid molecules of similar characteristics tend to gather at defined regions of the membrane, called *microdomains*, or *rafts* [51,52]. The formation of microdomains is one of the results of lipid-protein interactions, and usually has functional implications. For example, PIP_2 microdomains are important for certain signal transduction processes (see Subsection 7.4.1.2.2 below for details).

7.2.3 Lipid property effects on membranes

7.2.3.1 Amphipathicity

Despite their marked differences, lipid molecules in biological membranes share one common characteristic, namely, *amphipathicity*. That is, each membrane lipid includes a polar region and a nonpolar region. For example, in glycerophospholipids the polar region includes the ester-glycerol-phosphate-alcohol (or carbohydrate) groups, whereas the nonpolar region includes the acyl chains. These two regions are often referred to as the *'polar head'* and *'nonpolar tails'*, respectively. In cholesterol, the fused ring structure and attached hydrophobic tail constitute the nonpolar region, and the hydroxyl group constitutes the polar region. In the aqueous environment typical to biological systems, the hydrophobic effect and amphipathic nature of these lipids drive them to form larger structures, in which the polar regions face the aqueous medium and the nonpolar regions face each other. One such stable structure is the lipid bilayer. As described earlier, this structure is organized so the nonpolar tails of all lipids create a ~30-Å hydrophobic core[*1], and their head groups form two ~10 to 15-Å polar layers facing the external aqueous environment [53] (Figure 7.1b). This structural organization is fundamental to the lipid bilayer's most important trait, i.e., *impermeability* to most polar solutes. Again, because of the membrane's impermeability, the cell can tightly regulate the concentration of its metabolites by using specific transport proteins as the sole means of entry into and exit from the cytoplasm.

7.2.3.2 Asymmetry

As explained in Subsection 7.2.2.5 above, the membrane is asymmetric in terms of its lipid distribution. For example, in eukaryotic membranes the exoplasmic leaflet contains mainly the choline-containing lipids PC and SM, as well as glycolipids, whereas the cytoplasmic leaflet contains mainly the amino lipids PS and PE [33,47–50,54]. Since phospholipids can change sides in a matter of hours, the asymmetry must be maintained by an active mechanism: namely, membrane-bound enzymes that transfer lipids from one side of the bilayer to the other, using ATP as an energy source [54,55]. In particular, there are two enzymes working in opposite directions:

1. **Flippase** (aminophospholipid translocase) transfers the amino peptides PS and PE from the exoplasmic side of the bilayer to the cytoplasmic side.

2. **Floppase** transfers PC and cholesterol (in some tissues) from the cytoplasmic side to the exoplasmic side.

Membrane lipid asymmetry is diminished by certain processes, such as programmed or accidental cell death (apoptosis and necrosis, respectively), as well as cancerous transformation of cells [49]. This reduction of asymmetry happens as a result of either a decrease in the activity of flippase or activation of another enzyme, *scramblase*, which transfers phospholipids equally to both sides of the bilayer. The loss of asymmetry may in turn affect the cell and tissue, at least in the case of PS [49]. Specifically, the presence of PS in the exoplasmic leaflet has been found to mediate several physiological processes that involve cellular recognition:

[*1] The width of the hydrophobic core is measured between the glycerol groups of the two opposite layers.

1. **Recognition of apoptotic cells by macrophages.** As explained earlier, macrophages are phagocytes that are able to engulf and internalize a variety of entities, from single proteins to entire cells. In doing this, they play a double role. First, they kill invading bacteria that may harm the body. Second, they assist in disposing of dead cells from tissues. The latter role is important not only for cleaning purposes, but also for preventing the development of a harmful inflammatory response in the tissue following the apoptosis of cells. Conversely, when cells die by necrosis, which is not 'planned' by the body but rather inflicted by some kind of trauma, inflammation ensues rapidly. PS on the surface of apoptotic cells has been implicated in macrophages' capacity to recognize these cells, and therefore has a role in the prevention of inflammation.

2. **Recognition of activated endothelial cells by T-lymphocytes.** One of the roles of the immune system is to detect tissues invaded by pathogens and to act quickly to eradicate the invaders. The problem is that lymphocytes are normally on the move inside circulating blood and lymph, and do not linger in one place. Thus, when pathogens are detected in a certain tissue, it is necessary to prevent lymphocytes in the vicinity of this tissue from moving elsewhere. This is done by nearby endothelial cells, i.e., cells that line the blood vessels at the vicinity of the invaded tissue. These undergo a process that exposes their PS to the extracellular environment, and the latter is recognized and bound by nearby T-lymphocytes.

3. **Recognition of bacteria by the complement system.** The complement system includes several proteins that normally exist in an inert state. However, when activated during pathogenic invasion, they form a complex that attacks the invading cells. The attack involves damaging both the membrane and the cytoplasmic components of those cells. In most cases, the complement system is activated against invading bacteria, already recognized by antibodies. However, alternative activation pathways also exist, and they seem to involve PS on the exoplasmic leaflet of the invading bacteria. If this is indeed the case, it is likely that cancer cells are also recognized this way, as such cells are known to have lower membrane lipid asymmetry compared with healthy cells.

7.2.3.3 Degree of order and thickness

Though the lipid bilayer is commonly depicted as being overall fluid (in accordance with the fluid mosaic model), its fluidity may vary within a certain range. This variation is determined by the degree of order of the individual lipids, and specifically their hydrophobic tails. Linear tails are tightly packed within the bilayer structure, making it more viscous [56]. Such a structure is referred to as *'liquid ordered'* (l_o). Conversely, bent tails form a less tightly packed and more fluid structure, referred to as *'liquid disordered'* (l_d). Under physiological conditions the two types (or *phases*) coexist within the lipid bilayer, each contributing to its biological properties: The l_o phase enhances the bilayer's capacity to serve as a physical barrier for polar solutes, whereas the l_d phase provides it with a certain degree of dynamics. Indeed, bilayer regions that assume the l_d phase allow individual lipids not only to diffuse along the surface of the bilayer (*lateral diffusion*), but also to 'flip' from one leaflet to another (*transverse diffusion*). Moreover, the l_d phase allows the membrane to undergo structural organization that is needed for certain biological processes, such as the formation, budding, and fusion of transport vesicles.

The packing tightness of individual lipids is determined by two main factors:

1. **Degree of lipid saturation.** Fully saturated lipids have linear hydrophobic tails, which tend to form an l_o-type of bilayer. Conversely, lipids containing one or more double bonds have bent tails that pack in an l_d-type of structure.

2. **Presence of sterols in the bilayer.** Sterols have a dual effect on the properties of the lipid bilayer [34,57]. On the one hand, the sterol acts as a plug that prevents the free passage of solutes through the cavities between phospholipids. On the other hand, the rigid and bent structure of the sterol molecule creates a spatial disturbance in the tight phospholipid packing of the lipid bilayer, which prevents the bilayer from solidifying. This is important for the biological function of the membrane, which requires the bilayer to remain dynamic. **Thus, sterols allow biological membranes to remain dynamic without losing their basic function as a physical barrier.**

The cell can modulate the two factors to achieve the right balance between different properties. For example, the ER membrane contains small quantities of sterols [44–46], but retains flexibility due to large quantities of unsaturated phospholipids. Studies evaluating lipid composition, sensitivity to detergents, and biophysical measurements of lipid motions suggest that **extensive regions in biological membranes exist in the l_o phase** [51], and that **the l_d phase is usually restricted to those regions involved in dynamic activity**, such as the formation of transport vesicles.

An important trait of the lipid bilayer that is derived from its degree of order is its thickness. Measurements in pure lipid bilayers indicate that the bilayer has an average thickness of ~50 to 60 Å, with a ~30-Å nonpolar core and two polar lipid-water interfaces measuring ~10 to 15 Å each [53] (Figure 7.1b). These values vary (within a certain range) across different organisms, and even among different compartments of the same cell. In liver cells, for example, the *apical membrane*, which faces the lumen, is ~5 Å thicker than the ER membrane, and ~7 Å thicker than the *basolateral membrane*, which faces other cells [57]. When a region of the lipid bilayer changes from the l_o to the l_d phase, it becomes thinner due to a decrease in the length of the acyl chains. This difference affects the interactions between the phospholipids and the integral membrane proteins in their vicinity. Since such effects also influence the stability of the latter, proteins tend to concentrate in regions of the membrane in which only one of the phases exists, and, as a result, groups of membrane proteins tend to be physically separated from one another. The concentration of proteins in certain membrane regions is often used to enhance signal transduction pathways, which require proximity of their components. Finally, changes in protein-lipid interactions following phase changes may directly affect the activity of the former. These issues are further discussed in Section 7.4 below.

7.2.3.4 Curvature

Although the lipid bilayer is traditionally depicted as planar, it may curve temporarily in certain regions [58]. This phenomenon facilitates various processes, such as the vesicular transport of proteins and lipids among the ER, Golgi apparatus, and plasma membrane. Vesicular transport begins with the gradual curving of the source membrane until the vesicle is formed, continues with the separation of the vesicle from the membrane (*budding*) and its diffusion towards the target membrane, and finally ends with fusion of the two [19]

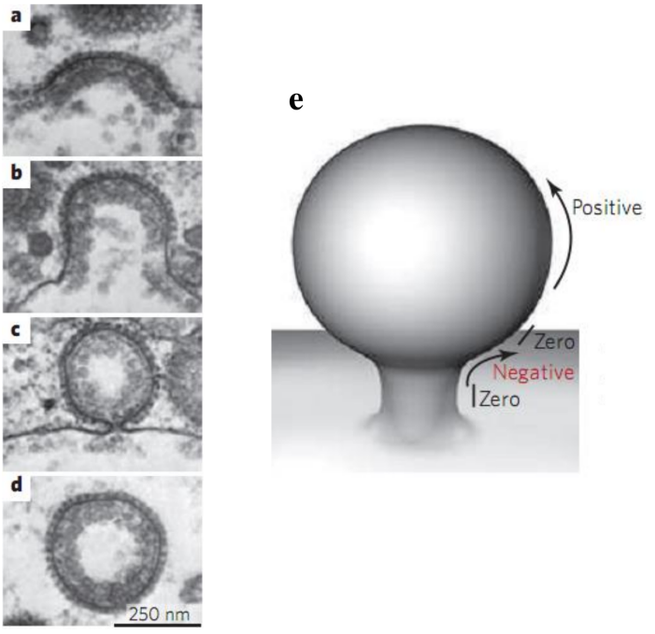

FIGURE 7.6 **Curvature changes in the budding of transport vesicles [58].** (a) through (d) Stages in vesicle budding. (e) Positive and negative curvatures in the transport vesicle.

(Figure 7.6). Exocytosis, endocytosis [20], and inter-organelle exchange all involve this process.

Membrane curvature is affected by lipid and protein composition. The effect of lipids involves the ratio between the effective cross-section area of the lipids' head groups and that of their tails. When the ratio is ~1, the lipids arrange side-by-side in parallel, forming a roughly planar bilayer structure. Conversely, when there is a mismatch between the area of the head group region and that of the tail group region, the lipids form a curved membrane [59]. There are two such cases:

1. **Positive membrane curvature** forms when the head group section is wider than the tail section, as is the case with choline-containing lipids (PC and SM), as well as with PG. The leaflet formed by these lipids has an inherent tendency to curve convexly (Figure 7.7a).

2. **Negative membrane curvature** forms when the head group section is narrower than the tail section, as is the case with PE (Figure 7.7b). The leaflet formed by these lipids has an inherent preference to form a concave curvature. Lipids that induce negative curvature reduce the stability of the bilayer membrane, which might ultimately lead to bilayer disintegration.

Biological membranes feature a mixture of lipids of different curvature preferences, as well as proteins, and it is not always easy to predict the exact shape that will arise from a certain lipid composition. For example, the bacterial plasma membrane remains, in essence, planar, despite the fact that PE constitutes 70% of its lipids [40]. This is because the remaining 30% are PGs, which induce a compensational positive curvature. In fact, studies show that as long as the concentration of negative curvature-inducing lipids is less than ~20%, the membrane will remain planar and whole even in the absence of compensatory lipids [60]. Nevertheless, the presence of a mix of lipids with different curvature-inducing properties

does create mechanical frustration within the membrane. It has been suggested that cells use this so-called *'curvature frustration'* to render the membrane metastable, which is advantageous in cases where the membrane's biological function requires frequent curvature changes (e.g., in intracellular transport) [61]. Thus, the effect of lipid shape on bilayer curvature is present, yet weak. Lipid shape makes the ER and Golgi membranes, for example, slightly curved. Integral membrane proteins exert a much stronger effect on membrane curvature; these are responsible for dramatic changes such as formation of transport vesicles. This issue is further discussed in Section 7.4.2 below.

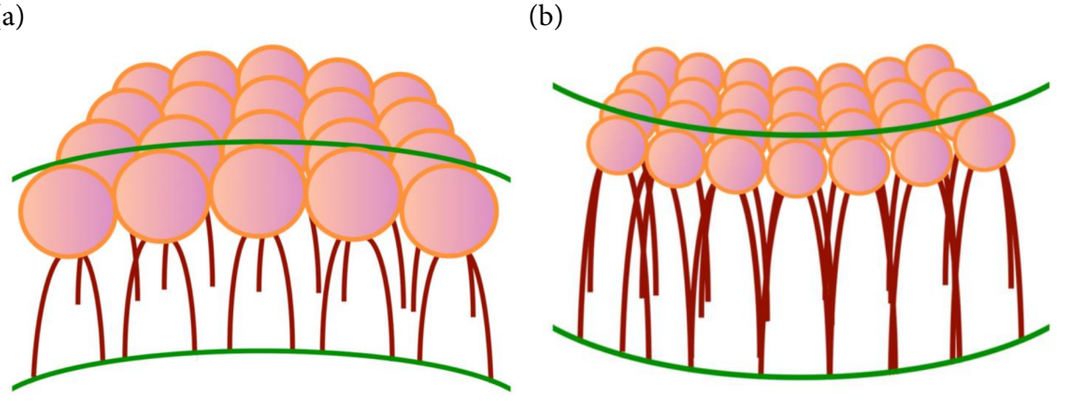

FIGURE 7.7 **Effects of different lipids on membrane curvature.** The figure shows a highly schematic illustration of the following: (a) Formation of positive curvature and convex membrane by lipids with large head group sections and small tails. (b) Formation of negative curvature and concaved membrane by lipids with a small head group sections and large tail sections. In both images, only one leaflet of the lipid bilayer is shown. The shape of the other leaflet depends on its lipid composition.

7.3 PRINCIPLES OF MEMBRANE PROTEIN STRUCTURE

7.3.1 Overview

Membrane-bound proteins can be separated into two major groups: integral proteins and peripheral proteins. **The membrane-spanning region of an integral protein may appear in two forms. The first includes α-helical segments (Figure 7.8a), whereas the second is structured as a β-barrel (Figure 7.8b)** (see details in Subsection 7.3.2 below). Certain antibiotic peptides such as gramicidin have alternating D and L amino acids, which allow them to create a third type of structure, the β-helix (Figure 7.8c). The β-helix is wider than the α-helix, and can therefore function as a channel, transferring monovalent ions through the membrane. In this section we focus primarily on helical membrane proteins, which constitute the vast majority of integral membrane proteins [62]. A discussion of the properties of β-barrel membrane proteins is provided in Section 7.3.2.2.2 below. Helical membrane proteins may be separated into subgroups according to the number of membrane-crossing segments they contain. *Bitopic* membrane proteins contain a single transmembrane segment (Figure 7.8d), whereas *polytopic* membrane proteins contain several such segments (Figure 7.8e). Comparison among different organisms suggests that in unicellular organisms, integral membrane proteins containing 6 or 12 transmembrane segments are more

common than others, whereas in higher organisms (*Caenorhabditis elegans* and *Homo sapiens*) there is a weak preference for membrane proteins containing seven transmembrane segments each [10]. GPCRs are a well-known example of the latter type of protein; these proteins play a central role in animal physiology and constitute a major target for pharmaceutical drugs [63,64]. GPCRs are the focus of the last section of this chapter.

Integral membrane proteins constitute most of the membrane protein population, and have diverse roles. Monotopic[*1] and bitopic proteins tend to function as recognition and/or adhesion molecules, as well as receptors to growth-factor-like messengers. Their extracellular region is responsible for binding the chemical messenger, whereas their cytoplasmic region passes the signal into the cell by binding soluble elements or cytoskeletal proteins. Polytopic proteins usually function as receptors or transporters. For example, GPCRs, mentioned above, respond to a variety of messengers, including hormones, neurotransmitters, odorants, pheromones, and even electromagnetic radiation (i.e., light) [65,66]. Peripheral membrane proteins are anchored to membrane lipids or integral proteins on either side of the membrane. Lipid attachment may be direct or mediated by carbohydrate moieties.

As integral membrane proteins are surrounded by the lipid bilayer, their structure (more specifically, the structure of their transmembrane domains) is determined by rules quite different from those corresponding to water-soluble proteins. Therefore, our discussion will focus primarily on the structure of integral membrane proteins, whereas peripheral proteins, which are mostly surrounded by a water-based environment, will be discussed mainly with respect to their membrane anchoring.

7.3.2 Structures of integral membrane proteins

Integral membrane proteins are considered to be globular, like their cytoplasmic counterparts. However, their presence in an environment so different from the aqueous cytoplasm suggests that the energy determinants of their structural stability might differ from those affecting the structure of water-soluble proteins. Understanding these determinants requires analysis of numerous structures, as has been done in the last decades for water-soluble proteins. As explained in Chapter 3, determining the structure of a membrane protein is challenging, due to the difficulty to overexpress, extract and purify such proteins, as well as to crystallize them [67]. The crystallization problem is usually addressed by replacing the surrounding lipids with detergent molecules, though the new environment might change the structure of the protein, making findings irrelevant. In the last few years, researchers have made impressive progress in the experimental determination of membrane protein structure [67]. This progress includes the development and perfection of methods such as electron cryomicroscopy (cryo-EM), circular dichroism (CD), and small-angle X-ray scattering (SAXS) (see Chapter 3), which have provided valuable information on hard-to-crystallize membrane proteins, as well as on the supra-molecular assemblies they form. In addition, X-ray crystallography has advanced substantially in various aspects, including (*i*) the capacity to overexpress proteins in different hosts; (*ii*) the development of new detergents and lipids for more efficient solubilization and crystallization; (*iii*) protein stabilization via mutations, fusion with other proteins, or binding to monoclonal antibodies; (*iv*) hardware-related methods for optimizing the crystallization process; and (*v*) developments in beamline and synchrotron radiation (see recent review in [67]). And yet, despite all this progress, the membrane proteins whose structures have been experimentally determined constitute only ~3.5% of all known protein structures (as of Dec 2017). Fortunately, while the lipid bi-

[*1] Proteins that are anchored to the membrane from one side.

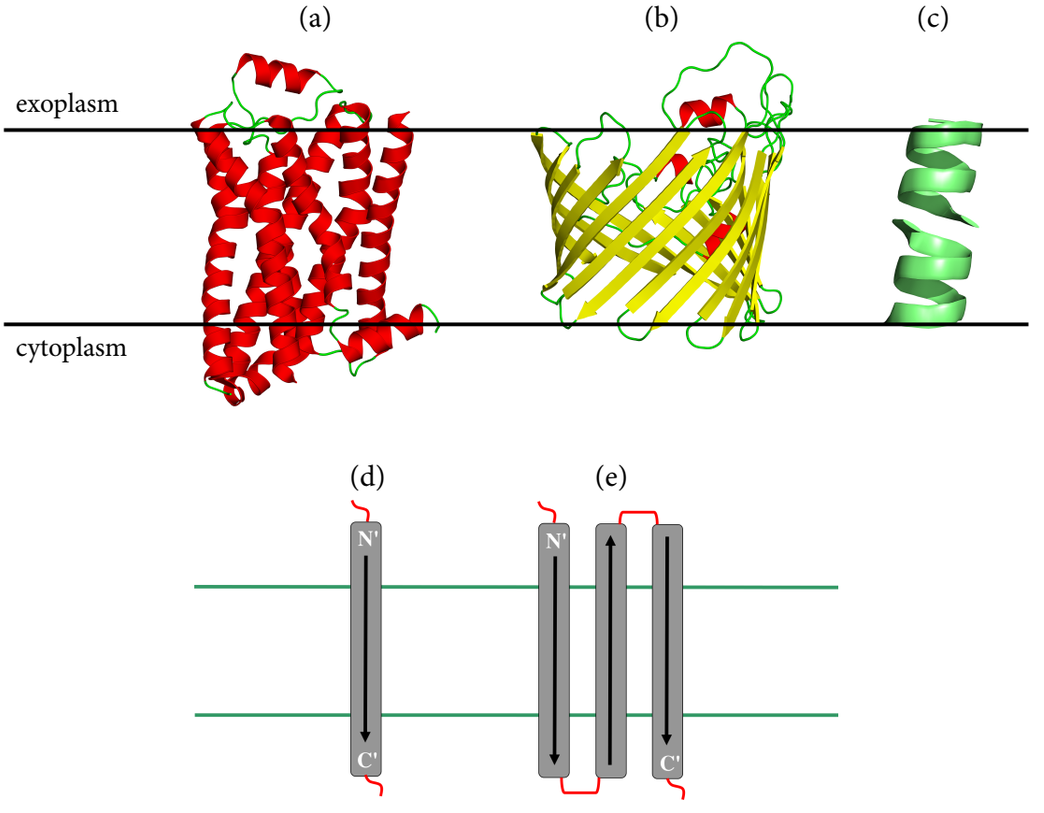

FIGURE 7.8 **General classification of integral membrane proteins.** (a) α-helical (β_1-adrenergic receptor; PDB entry 2vt4). (b) β-barrel (bacterial porin; PDB entry 2por). (c) β-helical (head-to-head gramicidin dimer; PDB entry 1grm). (d) Bitopic (single-pass). The transmembrane segment of each protein is represented by a grey cylinder, with the termini and the direction of the polypeptide chain marked. (e) Polytopic (multi-pass). The extramembrane connections between the transmembrane segments are shown in red.

layer surrounding membrane proteins impedes crystallization, it makes the understanding and even the prediction of their structure easier than in water-soluble proteins. This is because of the anisotropic and chemically complex nature of the lipid bilayer, which imposes constraints on the structure of resident proteins [68]. As a result, the general architecture of membrane proteins is relatively simple, and fewer structures are needed for understanding the basic principles determining that architecture [69].

The main determinant of integral membrane protein structure is the energetic cost of burying the protein's polar peptide bonds inside the hydrophobic hydrocarbon core of the lipid bilayer [70,71]. To compensate for this cost, the sequences of the transmembrane segments are highly hydrophobic [72], and have a strong tendency to form organized secondary structures [9,53]. Additional determinants exist, with secondary, yet important influence on membrane protein structure. In the following subsections we review the principles determining membrane protein structure, as we understand them today, according to the structural hierarchy used for water-soluble proteins. For further details, we recommend the reviews written by von Heijne [73,74], White [75], Engelman [76], and Bowie [77,78].

7.3.2.1 Primary structure

7.3.2.1.1 Polarity and length

The polypeptide chain of an integral membrane protein crosses the lipid bilayer at least once. The hydrocarbon core of the bilayer is highly hydrophobic, which requires the transmembrane domains of the proteins to be hydrophobic as well [8,53,72] (Figure 7.9a). Indeed, **the most pronounced trait of integral membrane proteins is their low polarity compared to water-soluble proteins, particularly in their transmembrane segments.** Though all types of nonpolar residues are common in transmembrane segments, Leu, Ile, Val, and Phe are particularly highly enriched in integral membrane proteins in comparison to water-soluble proteins [72]. **Polar residues also appear in transmembrane domains, but they are less common, especially in single-pass proteins, where they constitute in total only** ~20% **of the sequence [79]. In multi-pass membrane proteins polar residues are usually buried in the core (especially if they are charged) rather than facing the membrane, which is more hydrophobic.** As in the cores of water-soluble proteins, here too the presence of polar residues in a highly hydrophobic environment serves a specific function, justifying the unavoidable structural destabilization [80]*1. The destabilization is mitigated to some extent by the fact that the buried polar residue is surrounded by water molecules, other polar residues [81,82], or both (e.g., in the voltage-sensing K^+ channel [83–85]). Integral membrane proteins are inserted into the ER membrane co-translationally, via the translocon machinery [75]*2. How, then, is the translocon able to scan the nested polypeptide chain and detect transmembrane segments? Structural studies show that, in addition to the main channel pore that accommodates the nested polypeptide chain, the translocon structure contains a 'side gate', which opens to the lipid bilayer at a certain frequency, thus exposing the sequences inside it [86].

Another characteristic trait of transmembrane segments is their length. **Statistical analyses demonstrate that though helical transmembrane segments may include 15 to 39 residues, the 'average' transmembrane helix includes 21 to 26 residues, and there is strong preference for helices with over 20 residues [72,87,88].** Again, this is a result of the restrictions imposed by the membrane environment combined with the structural properties of α-helices. That is, **because of the characteristic 1.5 Å rise per residue along the helix axis, a 20-residue-long α-helical transmembrane segment would correspond to a length of** ~30 Å**, matching the average thickness of the hydrocarbon core of the lipid bilayer.** Obviously, to cross the membrane, the helix should be hydrophobic enough. As we will see later, longer helices usually tilt to maximize their nonpolar interactions with the membrane's core (see Section 7.4 below). For comparison, in water-soluble proteins, whose environment does not impose the restrictions observed in the bilayer, α-helices tend to be shorter on average, with a broader length distribution (15 ± 9 residues [72]).

The significance of the low polarity and characteristic length of transmembrane segments is demonstrated by the fact that these characteristics can be successfully used to detect membrane proteins automatically in whole genomes and to predict the number of their transmembrane segments, according to sequence alone. Algorithms that are used for this purpose are discussed in Box 7.1.

---

*1 This also explains the evolutionary conservation of polar residues in transmembrane proteins.

*2 This enables cells to prevent non-specific aggregation of the highly nonpolar membrane proteins in the aqueous environment of the cytoplasm.

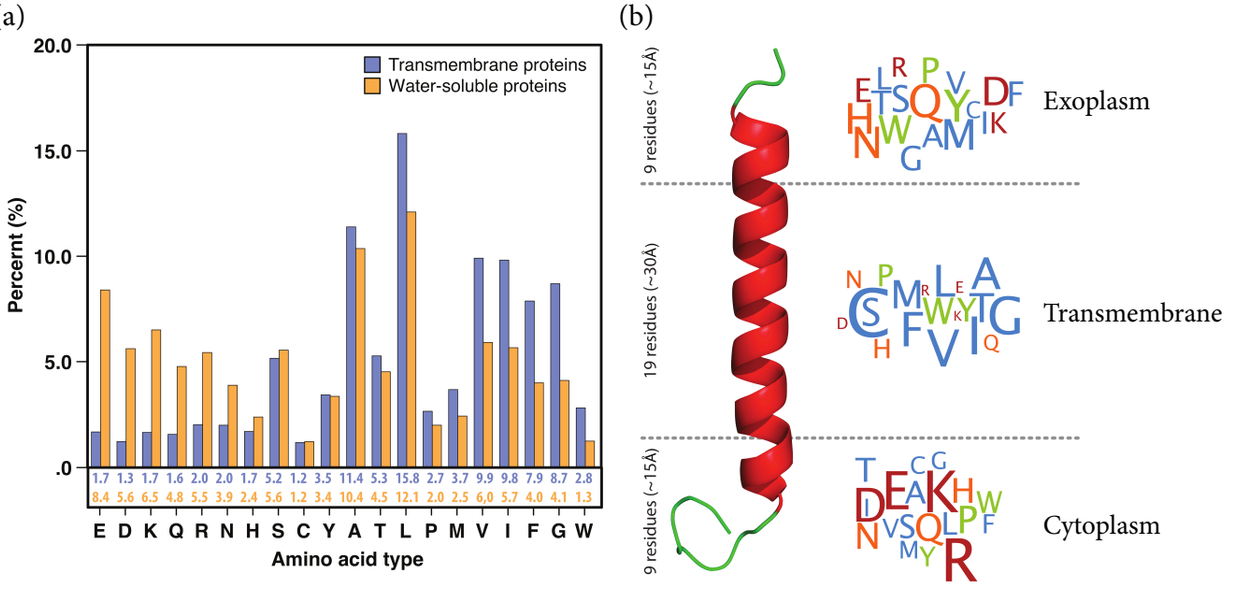

FIGURE 7.9 **Amino acid preferences in water-soluble and transmembrane proteins.** (a) Amino acid type distributions from 792 transmembrane and 7,348 water-soluble helices from a set of non-redundant proteins of known structure. The distribution for transmembrane helices is in blue, and the distribution for water-soluble helices is in orange. (b) Amino acid location prevalence in a membrane. Letter size is proportional to the relative prevalence of a given amino acid in the corresponding region in the membrane. Colors: red – charged amino acids (KRED), orange – polar-uncharged amino acids (QHN), green – aromatic amino acids plus Pro (PYW), blue – other amino acids (CMTSGVFAIL). The images are taken from [72].

7.3.2.1.2 Pro and Gly

Transmembrane segments arranged as α-helices often include Pro and Gly, as well as β-branched residues (Figure 7.9b). This is highly unexpected, as such residues rarely appear in α-helices of globular proteins (see Chapter 2, Section 2.3.6.1). Proline is particularly common in helical transmembrane segments, and is usually adjacent to Ser or Thr [89]. Structural analysis shows why these residues are so important in membrane proteins; this is discussed in Section 7.3.2.2.1 below.

7.3.2.1.3 Aromatic residues

Transmembrane segments tend to have 'aromatic belts' near the boundaries of the hydrocarbon region of the lipid bilayer [90–92] (Figure 7.10a). Such a belt includes the aromatic residues Trp and Tyr, which are normally rare in proteins. This is intriguing, especially in the case of Trp, whose frequency in membrane proteins is three times higher than in water-soluble proteins [91,93]. The location of the aromatic residues is near the termini of transmembrane helices, placing them at the interface between the nonpolar tails and the polar head group region of the lipid bilayer. There, they can participate in complex interactions with both parts of the lipid (see Subsection 7.4 below). According to the accepted theory, these interactions are used to anchor the transmembrane segments to the bilayer, thus preventing them from 'sliding' into the cell or out of it [94,95]. The affinity of Trp and Tyr

to the interface area may be explained by their amphipathic nature, which allows them to interact with the amphipathic membrane interface. That is, their polar NH and OH groups hydrogen-bond with the polar lipid head groups of the interface, whereas their large surface area allows them to interact with the nonpolar lipid tails. In addition, the rigid, bulky side chains of Trp and Tyr are expected to disfavor insertion into the highly disordered acyl chains of the membrane core.

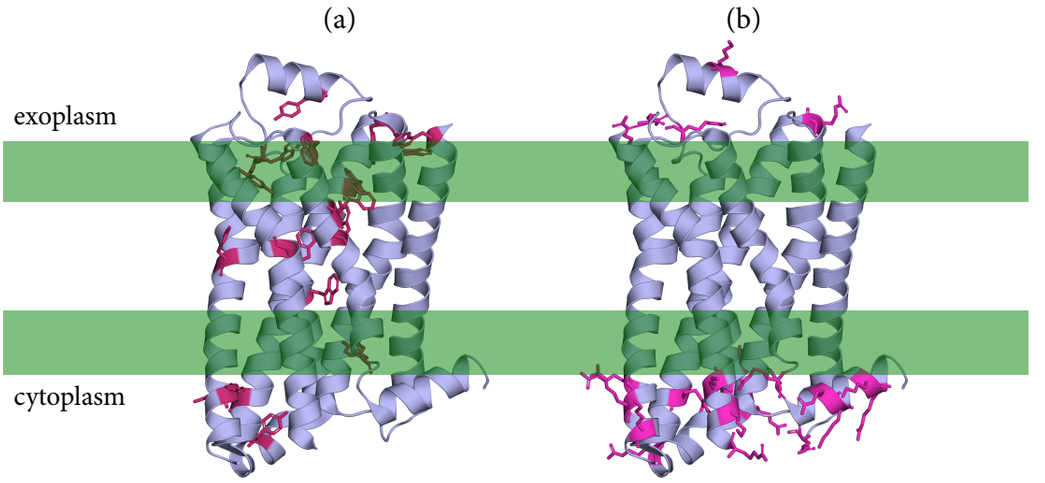

FIGURE 7.10 **Locations of aromatic (Trp and Tyr; (a)) and basic (Arg and Lys; (b)) residues in the β_1-adrenergic receptor (PDB entry 2vt4).** The residues are colored purple, and the polar head group regions of the bilayer are in light blue. As the figure demonstrates, most aromatic residues are concentrated near the acyl-head group interface, and some are buried in the protein. Most of the basic residues are positioned on the cytoplasmic side of the membrane, in accordance with the 'positive inside' rule (see also Figure 7.9b).

7.3.2.1.4 Basic residues

Transmembrane segments tend to include the basic residues Lys and Arg in their cytoplasmic regions [72,96,97] (Figure 7.9b and 7.10b). This tendency was discovered by von Heijne, who referred to it as 'the positive inside rule' [96]. Histidine also displays such a preference, though the prevalence of His in these regions is half that of Lys or Arg [97]. This makes sense, considering that the His side chain has almost equal probabilities of being positively charged or electrically neutral at physiological pH. There are several possible explanations for the positive inside tendency. For example, it may have to do with the inherent phospholipid asymmetry of lipid bilayers. We have seen earlier that eukaryotic membranes place electrically neutral phospholipids (PC and SM) at the exoplasmic leaflet of the bilayer, and negatively charged phospholipids (PS, and PI) at the cytoplasmic leaflet (see Subsection 7.2.3.2 above). In inner bacterial membranes both the exoplasmic and cytoplasmic leaflets contain negatively charged lipids (PG and PI, respectively). Thus, in both prokaryotic and eukaryotic membranes, transmembrane segments that have basic residues at their cytoplasmic regions could form salt bridges with these negatively charged lipids, and stabilize the protein-membrane system. The opposite, i.e., presence of acidic residues on the exoplasmic side of the bilayer, does not occur, as the lipid bilayer does not include any positively charged lipids.

Other reasons for the positive inside rule may be the 'membrane potential', i.e., the electric potential across biological membranes, where the cytoplasm is more negative than the periplasm. Alternatively, the positive inside rule could reflect bias in the translocon machinery. Finally, the compatibility of Lys and Arg with the membrane interface probably has to do with their side chains, which each include a polar group at the end of a long nonpolar chain. Thus, the polar group can interact favorably with phospholipid head groups even when the residue is positioned deeper inside the hydrocarbon core of the bilayer. This phenomenon is referred to as *'snorkeling'* [98]. Interestingly, a recent study suggests that only Arg significantly stabilizes the cytoplasmic side of the membrane, although its preference for this region is similar to that of Lys [97]. This may have to do with the electronic delocalization on the side chain of Arg (which is not present in Lys), which spreads the stabilizing positive charge over a larger area. Also, compared with that of Lys, the side chain of Arg can participate in more hydrogen bonds with phospholipid head groups.

In the β-barrel proteins of the Gram-negative bacterial membrane (see below), the distribution of positive residues is the opposite of that in other membrane proteins [68]. That is, basic residues appear mainly in the outside-facing loops of the protein ('positive outside') [99]. This distribution serves a purpose; in contrast to other cellular membranes, the bacterial outer membrane is highly negatively charged on its exoplasmic side due to the abundance of lipopolysaccharides (LPS). The basic residues of membrane proteins in this region stabilize the negatively charged LPS through ionic interactions. On its opposite side, a bacterial outer-membrane protein is enriched in negatively charged residues; these interact with periplasmic cationic chaperones, such as Skp, which assist in the insertion and folding of the β-barrel proteins into the outer membrane [100].

7.3.2.1.5 Small residues

Small residues such as Gly, Ala, and Ser are common in transmembrane segments. These residues tend to appear in α-helices, and allow adjacent helices to optimize their van der Waals interactions, as well as their hydrogen bonds. This topic is further discussed below.

BOX 7.1 PREDICTING LOCATIONS AND MEMBRANE TOPOLOGIES OF TRANSMEMBRANE SEGMENTS IN AMINO ACID SEQUENCES

Predicting the three-dimensional structures of membrane proteins has been an important goal of computational-structural biologists for decades, particularly considering the lack of experimentally determined structures. Paradoxically, because of the lack of structures, progress towards this goal has been slow, due to the difficulty in understanding the basic rules governing membrane proteins at the atomic level. And yet, different prediction methods have emerged (see Section 7.3.2.3.4 below for details). This process happened gradually; early trials began with relatively humble goals, such as locating transmembrane segments of membrane proteins, or trying to predict their overall topology, i.e., the sidedness of their termini in the membrane. These tasks relied on simple rules at the sequence level, and were therefore a good starting point for the prediction process. In the following paragraphs we give a short description of these methods.

I. Locating transmembrane segments

I.I. Hydrophobicity scales and hydropathy plots

The transmembrane segments of an integral membrane protein contain mainly nonpolar residues, whose number in each segment tends to fit roughly the thickness of the hydrophobic core of the membrane (see main text for details). In α-helical proteins, which constitute the bulk of integral membrane proteins, this number is ~20 residues. This understanding has prompted scientists to devise computer algorithms that can locate transmembrane segments within genomes, based on these tendencies [71,101]. The first attempt was carried out by Kyte and Doolittle [102]. Their general idea was to use a (virtual) sliding window covering ~20 amino acid positions, to locate transmembrane segments along the protein sequence. For each position of the window along the sequence, either the overall or average hydrophobicity of the 20-amino acid-long sequence was calculated. In those places where the calculated value exceeded a certain threshold, the segment covered by the window was considered to be a potential transmembrane segment. The results of this procedure were presented as a *hydropathy plot* (Figure 7.1.1), which represents the probability of each consecutive 20-residue segment in the sequence to be a transmembrane segment.

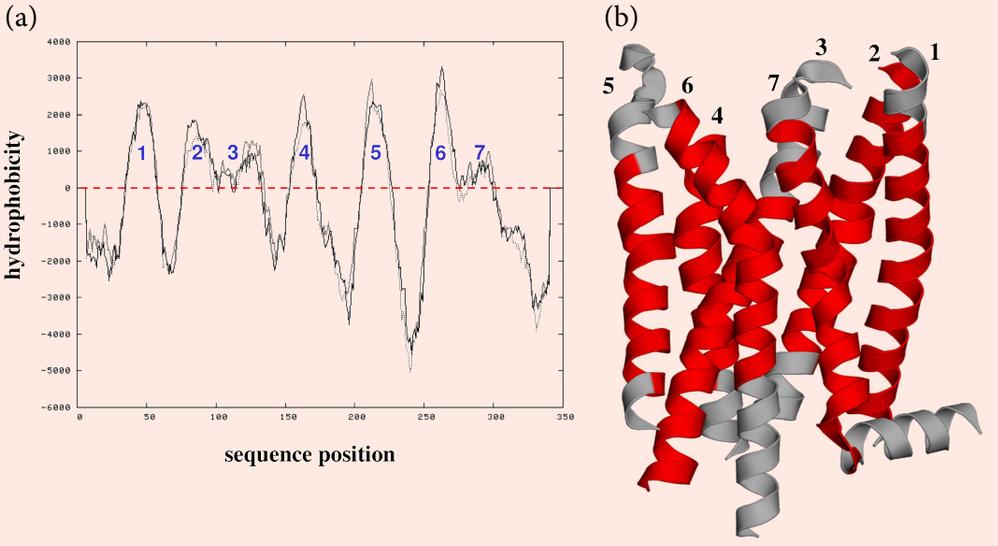

FIGURE 7.1.1 **Hydropathy plot.** (a) A hydropathy plot calculated for the GPCR bovine rhodopsin using TMpred [103,104]*a. The calculation was based on Kyte and Doolittle's scale. The red dashed line marks the threshold, above which the sequence is considered to be hydrophobic enough to span the membrane. The seven peaks in the figure correspond to the seven transmembrane segments of rhodopsin. (b) The three-dimensional structure of bovine rhodopsin with the predicted transmembrane segments colored in red. The image demonstrates the main problem of such prediction algorithms: Although they often provide a rough indication of the locations of the transmembrane segments, they fail in identifying their exact boundaries.

*a http://www.ch.embnet.org/software/TMPRED_form.html

The critical component of this method was (and still is) the calculation of the hydrophobicity of each candidate sequence. This was carried out by using a *hydrophobicity scale*, in which each of the 20 natural amino acid types was assigned a hydrophobicity value. The construction of this scale may seem trivial at first, but it is (still) a matter of controversy. First, there is the matter of selecting the physical quantity that can be used to represent hydrophobicity. The first quantity that comes to mind is the polarity of the molecule. However, despite the fact that polarity (inversely) affects hydrophobicity, it does not necessarily account for it fully. This is because polarity results merely from the geometric distribution of electronegative atoms, whereas hydrophobicity reflects all the qualities contributing to the molecule's tendency to prefer a nonpolar medium over a polar one. Thus, as explained in Chapter 1, a large residue such as tyrosine, which is considered to be polar due to its side chain OH group, might still turn out to be hydrophobic if its large phenyl group can produce strong enough nonpolar interactions. Accordingly, the Kyte-Doolittle (KD) scale [102] was produced empirically, based on the partition of the amino acids between polar (water) and nonpolar (vacuum) media (Figure 7.1.2). The result were converted into an energy-like value using Equation (4.1) (see Chapter 4):

$$\Delta G^0 = -RT \ln K_p$$

(where K_p is the equilibrium constant of partitioning). However, the empirical values were not used 'as is', but rather were normalized, in some cases using arbitrary considerations.

This leads us to the second problem associated with producing a hydrophobicity scale, namely, the types of media used in the measurement of hydrophobicity. In order for such measurement to be efficient, the polar and nonpolar media chosen for measuring the hydrophobicity values must be as close as possible to what they represent, i.e., the cytoplasm and the lipid bilayer, respectively. Whereas water has always been accepted as representative of the cytoplasm, disagreement has arisen concerning the medium that should be chosen to represent the lipid bilayer [96,102,105–107]. Vacuum, which was used by Kyte and Doolittle, is indeed nonpolar ($\varepsilon = 1$; a value even lower than that of the hydrocarbon region of the membrane); however it is not amphipathic, and therefore cannot faithfully represent the biological membrane. To take this important property of the membrane into account, other scales have been produced by using octanol (e.g., [108]), and even real lipid bilayers (e.g., the Goldman, Engelman, and Steitz (GES) scale [106]) as the nonpolar medium. White, von Heijne and coworkers took another step in making the hydrophobicity values more accurate [109–111]; instead of measuring the spontaneous, yet artificial partitioning of residues between simple polar and nonpolar media, they used a reconstructed system containing all the biological components involved in the insertion of transmembrane segments into the membrane in real cells, including the ribosome-translocon complex. The hydrophobicity scale they produced is perhaps more realistic than the scales produced by transferring amino acids and/or peptides between simple media. However, the amino acid transfer energies obtained by White, von Heijne, and coworkers were significantly lower in magnitude than those obtained by the above studies [112], which raised doubts as to their accuracy. It was suggested that these low energies might have resulted from several approximations that were made in the study [113] and/or interactions of the inserted peptides with other

membrane components [114]. Notably, a recent study of amino acids transfer energetics, which, like the study of White, von Heijne and coworkers, used a real biological membrane, yielded similar transfer energies to those obtained in the studies that used simple media [97]. These results support the reliability of the latter studies and suggest that simple organic solvents faithfully represent the hydrophobicity at the core of biological membranes.

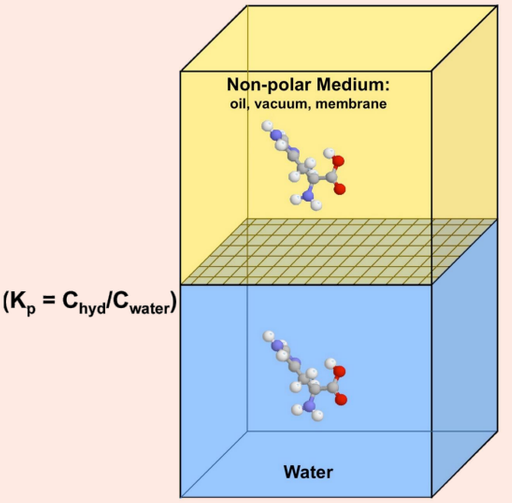

FIGURE 7.1.2 **Partitioning between polar and nonpolar media.** The amino acid residue is put in one of the compartments, and its equilibrium concentrations in each (C, representing molar concentrations) are measured to produce the partitioning constant K_p, from which the free energy of transfer is derived.

The use of knowledge-based scales circumvents the two problems discussed above, i.e., selecting the physical quantity that should be used to construct the hydropathy scales and the type of media that should be used for the amino acid transfer experiments [92,115,116]. These relatively new scales replace the physically meaningful hydrophobicity with the non-physical probability of a residue to appear inside a transmembrane segment. The probability is calculated on the basis of statistical data collected from membrane proteins of known 3D structure. Such data were not available until recently, due to the lack of membrane protein structures, but with the growth in the number of such structures over the past decades it is now possible to extract this information. It should be noted that knowledge-based scales are biased by functional constraints. This bias is especially prominent in the case of charged residues, whose real transfer energies into nonpolar media are highly unfavorable; yet their statistical tendency to appear in transmembrane domains is higher than suggested by these energies because they are needed for functional reasons (binding, catalysis, etc.).

The third controversial issue associated with producing hydrophobicity scales is determining how to represent the residues in the transmembrane segment. The KD and GES scales use individual amino acids, despite the fact that in reality the amino acids are interconnected by peptide bonds. The bonds reduce the full electric charges on the α-amino and α-carboxyl groups of the amino acids into mere partial dipoles. Since the

partitioning between polar and nonpolar media depends considerably on the magnitude of the charge on the molecule, it has been suggested that the use of individual amino acids is methodologically flawed. To solve this problem, Wimley and White [105] used whole peptides in producing their own hydrophobicity scale, following the *'host-guest'* approach. The peptides they used in the various measurements were identical except for one position, which contained a different residue in each case. Like Goldman, Engelman, and Steitz, Wimley and White also used a lipid bilayer instead of a simple nonpolar mimic. However, due to their short sequences (5 or 6 residues), the host-guest peptides could not span the entire length of the lipid bilayer, and partitioned only into the polar head group region. As a result, the scale produced by this procedure could not be applied to transmembrane segments. In a computational study, Kessel and Ben-Tal [8] used host-guest peptides of 20 residues, which were able to span the entire length of the bilayer. Moreover, the peptides possessed an α-helical conformation, in which the polar backbone groups were paired in hydrogen bonds, as in real transmembrane segments. As discussed in Chapter 2, Section 2.3.4, the formation of such bonds is crucial for the insertion of transmembrane segments into the membrane.

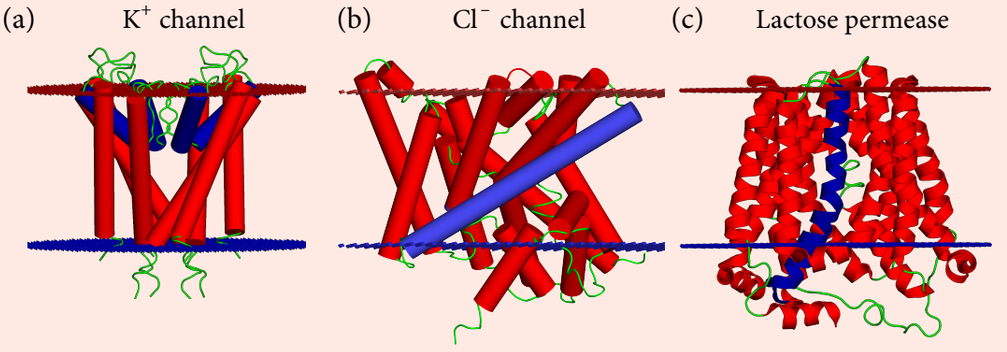

FIGURE 7.1.3 **Examples of non-canonical transmembrane α-helices.** (a) Four short helices within the 're-entrant loops' of the potassium ion channel (PDB entry 1bl8), which are too short to span the entire thickness of the lipid bilayer. As a result, one polar terminus of each of these four 'half-helices' resides roughly in the bilayer midplane. The termini are shielded from the lipid tails because of their location in the protein core. The red and blue planes mark the predicted boundaries of the membrane respectively (the OPM database [117]). The polar head group regions of the bilayer are in light green. Note that in reality, the membrane probably deforms to match its thickness to the hydrophobic lengths of the transmembrane segments of the proteins. (b) A transmembrane α-helix in the chloride channel (PDB entry 1otu) whose hydrophobic length far exceeds the thickness of the lipid bilayer core. Water exposure of nonpolar groups is reduced by the tilting of the helix. (c) Core exposure of polar groups in the middle of lactose permease (PDB entry 1pv6), due to a helix-distorting kink (circled). The figure was prepared following [118].

I.II. Shortcomings and future leads

The first algorithms for identifying transmembrane segments were designed and used at a time when only a few 3D structures of membrane proteins existed. As structures

started to emerge, such as those of the K^+ channel [119], it became clear that the length and hydrophobicity values of some of the transmembrane segments deviated from the basic tendencies assumed by the prediction algorithms [101,120]. First, certain transmembrane segments were buried inside the core of the membrane, despite the fact that they were too short to span its entire thickness (Figure 7.1.3a). Nevertheless, the unpaired polar groups in the termini of these segments were not exposed to the hydrophobic core, as they were electrostatically masked by polar groups on adjacent segments, or by water molecules filling the intramembrane pore. Other transmembrane segments were found to have hydrophobic lengths that exceeded the hydrophobic thickness of the membrane (Figure 7.1.3b). These segments usually acquired a tilted orientation with respect to the membrane normal, in order to allow as many nonpolar residues as possible to interact with the hydrocarbon region of the membrane. Finally, some segments appeared to be kinked in a way that distorted the helical structure (Figure 7.1.3c). These observations have made it clear that, in order to be efficient, predictions of transmembrane segments must incorporate data beyond sequence tendencies.

II. Predicting topologies of transmembrane segments

The search for rules of thumb describing transmembrane segments has led scientists to the issue of topology, i.e., predicting which regions of each segment face the cytoplasmic or exoplasmic sides of the membrane. This type of prediction constitutes a critical preliminary step in the prediction of the overall structure of an integral membrane protein, as it limits the number of ways in which the transmembrane segments can be spatially organized with respect to each other. The first algorithm designed for this purpose, *TopPred* [96], combined the general tendency of transmembrane segments for hydrophobicity with the aforementioned 'positive inside' rule. Algorithms that were designed later, such as *MEMSAT* [121] and *TMHMM* [122], mainly relied on statistical data concerning the locations of transmembrane segments in proteins of known structure. Today, numerous prediction methods and algorithms are fully accessible to the general public, and anyone can use them to produce a good starting model. For example, the current TMHMM algorithm [123], which is accessible via server[*a], has been demonstrated to achieve 80% success in predicting the topology of transmembrane segments in bacterial membrane proteins [124].

Similarly, the MEMSAT-SVM, which integrates both signal peptide predictions and re-entrant helix predictions, can achieve an accuracy level of 89% [125]. This method is also freely available, via the PsiPred server[*b]. Again, the accuracy of these tools usually decreases considerably in the case of short-buried helices (half-helices, re-entrant helices) and those that possess kinks.

[*a] URL: http://www.cbs.dtu.dk/services/TMHMM/
[*b] URL: http://bioinf.cs.ucl.ac.uk/psipred/

A recent graph-based method called *'TopGraph'*[*a] represents an approach that differs from the aforementioned methods, in that it relies on extensive empirical data. TopGraph uses apparent insertion free energies of host peptides into membranes by the bacterial TOXCAT-β-lactamase system [126]. It is especially useful for predicting the topologies of membrane proteins with low similarities to known structures, as it does not rely on data that were derived for specific structures. It also allows constraints to be added on the basis of prior knowledge regarding the query protein (e.g., an amino acid known to be on the cytoplasmic side of the membrane). Finally, there are prediction methods that focus on β-barrels, e.g., BOCTOPUS [127][*b] (see additional methods in [128]). However, most of these tools have been trained on proteins of the bacterial outer membrane, and can therefore deal only with single-chain β-barrels [128].

7.3.2.2 Secondary structure

One of the most prominent characteristics of integral membrane proteins is the substantial extent to which α-helical (and to a lesser extent the β-strand) conformations occupy their transmembrane segments [70,86] (Figure 7.10a and b). In Chapter 2 we saw that one of the main purposes of the α and β conformations in water-soluble proteins is to pair backbone polar groups in hydrogen bonds, thus lowering the energetic penalty associated with their exposure to the nonpolar protein core during folding (see Chapter 2, Section 2.3.4). The reason for the high prevalence of these conformations in membrane proteins is essentially the same, and even more salient; the transmembrane segments of such proteins are exposed to the cores of both the protein and the lipid bilayer, with the latter being extremely nonpolar. Electrostatic masking of backbone polar groups is therefore even more critical in membrane proteins than in their water-soluble counterparts [53]. The tendency of transmembrane segments to have extensive α-helical and β-strand/sheet content has been exploited in algorithms for structural prediction of membrane proteins. In particular, specific algorithms have been developed for GPCRs (see details in [71,101]).

7.3.2.2.1 α-Helical proteins

Most transmembrane segments in integral membrane proteins are organized as α-helices. As mentioned above, these helices have a high content of Pro residues [129], despite the 'helix-breaking' properties of this residue (Figure 7.11a, Box 7.1) and its low prevalence in the cores of helical segments of water-soluble proteins [130]. On the basis of their MD simulations, Sansom and coworkers proposed that **Pro residues act as hinges of motion in transmembrane segments, thus allowing better adjustment of helices' orientations, as well as mediating functionally-important conformational changes [131].** As we will see later, conformational changes are highly important to the function of integral membrane proteins, e.g., for facilitating gating in channels, and transitions between inside- and outside-open states in transporters, or between active and inactive states in receptors and enzymes. These changes include a range of motions in the protein, from hinge bending or displacement of

[*a] URL: http://topgraph.weizmann.ac.il/
[*b] URL: http://boctopus.cbr.su.se/

individual helices in screw or pivot motions, to positional changes of whole domains and subunits. As mentioned above, Pro is known to create kinks in helices and confer rigidity to the polypeptide chain. Therefore, the importance of Pro to conformational changes in transmembrane proteins may seem surprising at first. However, Pro residues in transmembrane segments tend to appear within certain sequence motifs, which also contain Ser and Thr, such as *(S/T)P*, *(S/T)AP*, *PAA(S/T)* [89]. Simulations demonstrate that these residues compensate for the structural distortion created by the Pro, and suggest that these structural effects allow the helices to undergo the required conformational changes [89]. Experiments support this proposition, showing that replacement of Ser and Thr within these motifs changes the activity of the protein [132–134]. Still, one may wonder why these phenomena are observed almost exclusively in integral membrane proteins rather than in all proteins. This may have to do with the restrictions imposed on membrane protein motions by the lipid bilayer structure. That is, since integral membrane proteins are more restricted by their environment than water-soluble proteins, special characteristics such as inclusion of Pro residues inside secondary structures may have developed as a means of providing these proteins with the same degree of flexibility that normally exists in their water-soluble counterparts. Thus, in the absence of the surrounding membrane, many of the advantages conferred by Pro are likely to become liabilities. This proposition raises the interesting possibility that Pro may also be important to membrane proteins through so-called *'negative design'*. Specifically, it prevents membrane proteins from folding outside the membrane, in which case they would be unstable and subject to degradation. A different study has shown that the mere presence of Pro residues in certain positions on transmembrane segments can protect membrane proteins from misfolding, by disfavoring non-native structures that contain an array of β-strands [135].

Transmembrane segments may contain other structural distortions as well, such as tight turns of 3_{10} helices and wide turns of π-helices [76]. The latter two irregularities have been studied less extensively than Pro-induced kinks, so it is still unclear whether they play a functional role. One of the advantages conferred by such distortions is that they allow proximity between polar groups in adjacent helices, thereby facilitating better electrostatic masking than that achieved by intrahelical interactions alone. Indeed, nearly 40% of the transmembrane helices in membrane proteins are distorted, compared to only 19% of the helices in water-soluble proteins [87]. In addition, transmembrane helices may be discontinuous or penetrate halfway into the membrane core, forming re-entrant loops [68] (Figure 7.11b, Box 7.1). The latter are particularly common in channels such as aquaporins and K^+-channels, where the exposed residues in the re-entrant loops usually serve as binding sites for ions or other substrates (see Figure 7.15b below).

7.3.2.2.2 β-Sheet proteins

Integral membrane proteins with extended (β) conformations [136,137] are less common than those having α-helical conformations, and are estimated to constitute only a small percentage of the total proteome [62]. These structures, called β-barrels, usually consist of a single chain but can also comprise multiple chains. Most β-barrels belong to the porin superfamily of small molecule channels, which reside in the membranes of Gram-negative bacteria [138,139], as well as in the outer membranes of mitochondria and chloroplasts [140–143]. In bacteria, the exposure of porins to the external environment turns many of them into attachment sites for phages and bacterial toxins [9]. In fact, some of the toxins (e.g., *α-hemolysin*

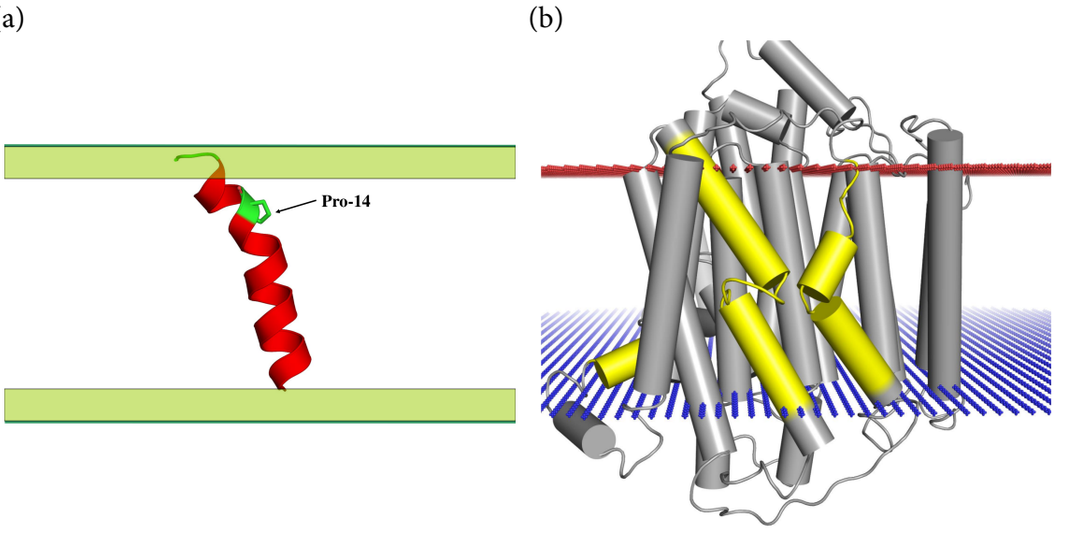

FIGURE 7.11 **Irregularities in transmembrane helices.** (a) A kink-inducing Pro in the transmembrane peptide alamethicin. The peptide is represented as a ribbon, with Pro-14 shown also as sticks (PDB entry 1amt). The polar head group regions of the bilayer are in light green. (b) Distorted helices, half-helices and membrane-exposed loops in one of the subunits of the membrane domain of respiratory complex I from *E. coli* (PDB entry 3rko). For clarity, the helices are presented as cylinders. The protein is colored in grey with irregular helices colored in yellow. The red and blue planes mark the predicted boundaries of the membrane, respectively (the OPM database [117]).

from *Staphylococcus aureus* [144]) create a β-barrel structure in the host membrane. In the barrel structure, the strands are anti-parallel, connected by short loops at the periplasmic side, and long loops at the external side of the cell or organelle [145] (Figure 7.8b). Based on this structure, it has been suggested that the β-hairpin motif is the principal evolutionary unit of all β-barrel proteins [146]. In accordance with the role of porins, the barrel structure is amphipathic[*1], with a water-filled center and nonpolar exterior. Moreover, the large width of the barrel is associated with low selectivity. As a result, porins are able to transport a larger variety of polar molecules, compared with the channels that reside in the plasma membrane or inner mitochondrial membrane, all of which are made up of α-helical bundles. Finally, porins tend to oligomerize within the membrane [147]. Porins should not be confused with aquaporins, which are α-helical channels that belong to the *major intrinsic protein* (*MIP*) superfamily (see Subsection 7.3.2.3.3 below).

7.3.2.3 Tertiary structure

7.3.2.3.1 Key characteristics

Integral membrane proteins exist within a lipid environment, which explains why they have nonpolar exteriors, as well as the fact that many of their polar residues tend to face the protein interior. On the basis of these observations, it was initially proposed that these proteins are *'inside-out'* versions of water-soluble proteins. However, with the structural characterization of different membrane-bound proteins, this assumption has turned out to be an oversimplification [75,148]. Rather, the structure of integral membrane proteins is similar in

[*1] Contains polar residues on one face and nonpolar residues on the opposite face.

certain aspects to structures of water-soluble proteins [86,149]. First, in both protein types, the core is tightly packed, contains mainly nonpolar residues with few functionally important polar residues, and is evolutionarily more conserved than the surface of the protein [150]. The high conservation of the core probably results from the fact that inter-residue packing is tighter than residue-lipid packing, such that the residues in the core are more structurally constrained [71]. Second, the loops in the structures of both protein types serve similar roles in ligand binding and signal transduction.

As mentioned above, the transmembrane segments of integral membrane proteins tend to include small residues such as Ala, Ser, and Gly, which facilitate tight packing of helices. The packing is important not only for helices within polytopic proteins, but also for bitopic proteins, which tend to dimerize or oligomerize within the membrane [151]. Moreover, the distribution of the small residues among larger residues produces *grooves and ridges* (respectively) along the helix, which creates geometric complementarity between adjacent helices (*'knobs-into-holes' packing*) (Figure 7.12a,b). Since these ridges and grooves are not geometrically parallel, but rather curl around each helix, the best fit between adjacent helices requires them to tilt across the membrane. Indeed, **though transmembrane helices in membrane proteins may have a 5° to 35° tilt [77], their average tilt is** ~20°**, which seems to be optimal for interhelical packing [88,152].**

One of the most common models used for studying helix-helix interactions in membrane proteins is *glycophorin A*, which forms an α-helical dimer when solubilized in detergent or lipid bilayers. The protein contains the sequence motif *LIxxGVxxGVxxT* (x is any residue), located within the helix-helix interface. When these residues are replaced with mutations, the protein dimer separates into two monomers. The motif includes a smaller motif, *GxxxG*, which is over-represented in transmembrane segments [129,153], and also appears in many interacting helices of water-soluble proteins. As explained in Chapter 2, the two Gly residues are located on the same face of the helix, a turn away from each other, and allow the two interacting helices to become separated by only 6 Å. This short distance optimizes van der Waals interactions and allows the C_α–H group of one helix to hydrogen-bond to a backbone carbonyl group (C=O) in the other [154]. Many cases have been observed, however, in which the small residues Ser and Ala appear instead of Gly residues, thus extending the *GxxxG* motif into a *'GxxxG-like (or GAS) motif'* [129,155,156]. Other motifs suggested to mediate tertiary interactions in membrane proteins include the *leucine-isoleucine zipper* [157][*1] (Figure 7.12c), the heptad *serine zipper* (e.g., *SxxLxxx*) [158], and the *GxxxGxxxG glycine zipper* [159] motifs. These and other linear motifs that mediate helix-helix and protein-protein interactions can be found in the MeMotif database [160], which can also identify such motifs in specific sequences[*2].

Finally, the charged residues Glu, Asp, Lys, and Arg within transmembrane helices have been implicated as mediators of helix-helix interactions [82,151] (Figure 7.12d). The energetic implications of such interactions are discussed in the following subsection. As in water-soluble proteins (see Chapter 4), polar interactions inside the protein have an added benefit; they are more specific than nonpolar interactions that rely on steric complementarity alone.

Certain structural arrangements found in integral membrane proteins tend to recur [161]. The most common is by far the α-helical bundle, which reappears in different

[*1] As we saw in Chapter 2, the leucine zipper motif mediates interhelical interactions in coiled coil-forming water-soluble and fibrous proteins as well. In membrane proteins, however, this motif often appears coincidental due to the high prevalence of Leu, Ile, and Val in transmembrane segments.

[*2] URL: http://projects.biotec.tu-dresden.de/memotif/en/Special:Search

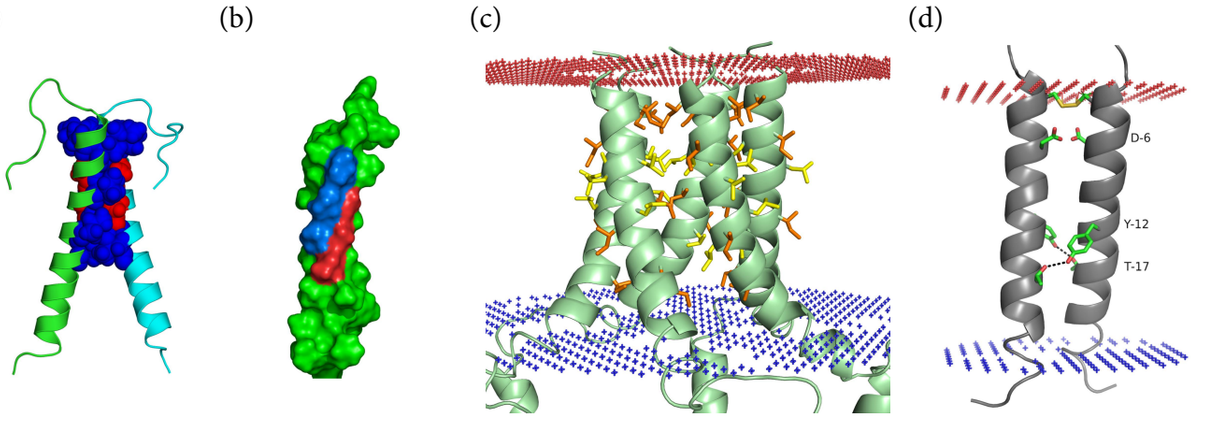

FIGURE 7.12 **Packing motifs and interhelical interactions in transmembrane segments.** (a) and (b) Ridges and grooves. (a) The dimeric structure of glycophorin A in detergent micelles (PDB entry 1afo), prepared after Figure 12 in [53]. The backbone is shown as a ribbon, and the side chains of the helix-helix interface are shown as spheres. Valine and isoleucine residues, forming the ridges, are colored in blue. Glycine and threonine residues, forming the grooves, are colored in red. (b) The ridges and grooves in the interface of one of the chains. (c) Leucine and isoleucine zipper in the pentameric structure of phospholamban (PDB entry 1zll). The backbone is shown as a ribbon, and the side chains of the helix-helix interface are shown as sticks. Leucine and isoleucine residues are colored in yellow and orange, respectively. The red and blue dashed lines mark the predicted boundaries of the membrane, respectively (the OPM database [117]). (d) Polar interactions. The image shows hydrogen bonds involving two Asp residues and two Tyr-Thr pairs in the TCR-ζ chain dimer (PDB entry 2hac). The close proximity of the two Asp residues suggests that one of them is protonated. Furthermore, NMR studies indicate that these residues are stabilized by an extensive hydrogen bond network with a buried water molecule (absent in the presented structure) and other residues. The two chains are also connected by a disulfide bond.

forms. For example, GPCRs include a characteristic seven-helical bundle, some transporter groups include 12 or 14 helical bundles, and so on. A less common structural motif is the β-barrel, which characterizes channels with low selectivity in the outer membranes of bacteria and eukaryotic organelles of bacterial origin [136,137] (see Subsection 7.3.2.2.2 above).

7.3.2.3.2 Energetics

Integral membrane proteins reach their final active state in the membrane through a complex process, during which each transmembrane segment undergoes the following major steps [74–76,162,163]:

1. Translation by the ribosome
2. Insertion by the translocon complex into the membrane
3. Acquiring secondary structure
4. Assembly with the other transmembrane segments into the mature protein, usually in the form of an α-helical bundle

Since membrane insertion often depends on secondary structure formation in transmembrane segments [105,164–166] steps 2 and 3 are usually referred to as a single coupled step. In

any case, the entire four-step process is complex, and although recent structural studies have clarified some of the complexities [75], it is still not entirely understood. One alternative for studying this process, with all the biological components included therein, is to use model systems that are based either on whole proteins [167] or on isolated peptides, and to focus on the energetics of the four key steps instead of getting into the numerous kinetic barriers and minima that the complex translocon system involves. Studies with such systems, as well as with more realistic setups [109], have produced estimates of the energies associated with the key steps, especially the first three (see [8,53] and references therein). Generally speaking, the energetics of transfer of transmembrane segments from the aqueous phase into the membrane is dominated by the following [75]:

1. The free energy penalty associated with partitioning of the (polar) peptide backbone into the lipid environment. This penalty has been calculated as +2.1 kcal/mol for C=O and N–H backbone groups that are hydrogen-bonded to each other, and +6.4 kcal/mol when the hydrogen bond is not satisfied [168,169].

2. The favorable free energy contribution due to the hydrophobic effect. On the basis of simple partition experiments, this free energy value has been estimated at $\sim -25 \pm 30\%$ cal/mol per Å^2 of the protein involved in nonpolar interactions [108,170–173]. Experiments using a more realistic system, in which peptides were inserted into the ER membrane by the Sec61 translocon [174], produced a smaller value of −10 cal/mol per Å^2.

The favorable free energy must therefore compensate for the free energy penalty, as well as for the cost of inserting polar side chains, in order for the net membrane-partitioning free energy to be favorable (i.e., negative).

Inside the membrane, the nonpolar environment induces secondary structure formation in the inserted segments [105,164–166]. The energetics of this step is essentially the same as the energetics of the induction of secondary structure in water-soluble proteins upon folding (see Chapter 2). **Atomic force microscopy measurements carried out on bacteriorhodopsin indicate that the free energy of the coupled insertion-folding process of a single α-helical transmembrane segment is** −1.3 kcal/mol **per residue [175].** Estimates concerning the insertion of each of the transmembrane segments into the membrane can be presented in the form of a scale. In the scale, each of the naturally occurring amino acids is assigned a value describing the free energy of its insertion into the polar head group region [105,108] or the hydrocarbon core [8] (see also Box 7.1).

In the final step of membrane protein formation, each of the folded transmembrane segments interacts inside the membrane with its neighbors to form the fully folded protein [75]*1. The net energy of this process has recently been measured for bacteriorhodopsin as ~ -11 kcal/mol [178], which is on the scale of the energy of water-soluble protein folding. However, compared with the earlier stages of membrane insertion and acquisition of secondary structure of each transmembrane segments, this stage is associated with much more controversy with regard to its energy components and their magnitude [86]. We have seen

*1Note that this also pertains to dimerization and oligomerization of (helical) membrane proteins; here, too, the process involves interhelical packing, with the only exception being that the interacting transmembrane segments are not connected by loops. Dimerization and oligomerization are common in membrane proteins [176], with 50% to 70% of the complexes containing the same chains (homodimers and oligomers) [177].

that in water-soluble proteins the driving force for folding is the hydrophobic effect (nonpolar interactions). Integral membrane proteins are surrounded by a lipid medium, which means the driving force for their folding must be different. Studies show that the stability of membrane-bound proteins correlates with the amount of surface area of the protein that becomes buried during folding [179]. In the absence of the hydrophobic effect, this correlation should reflect mainly van der Waals interactions. Indeed, **van der Waals interactions are expected to play a more significant role in driving the folding of membrane proteins compared to their water-soluble counterparts**. This expectation stems mainly from the fact that water molecules, being smaller than lipid molecules, are better at rearranging around the unfolded protein and forming a tight interaction shell. As a result, the van der Waals interactions between the unfolded protein and the molecules of its environment should be stronger in the case of water-soluble proteins than in the case of membrane proteins. This means that the increase in strength of these interactions during folding is more pronounced in membrane proteins. In addition, the aforementioned motifs in membrane proteins facilitate especially tight packing of transmembrane segments, which, in turn, optimizes the van der Waals interactions between them.

Aside from van der Waals interactions, the stability-surface area correlation may also reflect another effect, which is entropic in nature, and is reminiscent of the hydrophobic effect in water-soluble proteins [180]. The lipids that make up the membrane have a certain freedom of movement, which decreases when a protein is inserted into the membrane. This restriction of movement pertains mostly to lipids that are in direct physical contact with protein residues. During protein folding, some of those lipids are released into the bulk, and as a result their freedom of movement increases. In other words, **folding decreases the entropy of the polypeptide chain but increases the entropy of the lipid bilayer. Since this process is favorable, it can be considered as a driving force of folding.** This process is analogous to the hydrophobic effect in water-soluble proteins, because in both cases folding of the protein releases 'solvent' molecules (lipids or water), thereby increasing the overall entropy. Quantitatively speaking, this effect is probably weaker than the hydrophobic effect, as the change in the freedom of movement of lipids is expected to be smaller than in the case of the much smaller water molecules.

As in the case of water-soluble proteins, the exact effect of electrostatic interactions on membrane protein folding is also not entirely clear [86]. We saw earlier that various motifs known to promote helix-helix packing in membrane proteins include polar residues, suggesting that polar interactions are overall favorable in this setting. Indeed, studies that focused on hydrogen bonds between transmembrane segments suggested that these bonds are favorable and drive the assembly of the protein [181–183]. For example, DeGrado and coworkers studied this issue using helical model peptides that dimerize [183]. When hydrogen bonds involving the amino acid residues Asn, Gln, Asp and Glu were disrupted by mutagenesis, dimerization did not occur. Thermodynamically, it makes sense that hydrogen bonds contribute favorably to the assembly of the helices into a folded protein, since in their isolated state (inside the lipid bilayer) the potential hydrogen bond donors and acceptors are surrounded by a less polar environment than in the folded state (Figure 7.13). Again, the fact that polar residues such as Ser and Thr are more prevalent inside membrane-bound proteins than inside water-soluble proteins supports this suggestion [152].

Assuming that transmembrane hydrogen bonds do stabilize the folded state of membrane proteins, how significant is the stabilization? A study by Bowie and coworkers [184] investigated this issue using bacteriorhodopsin, a bacterial light-activated proton pump of

known structure, which is often used as a model for membrane proteins. They mutated hydrogen-bonding pairs to non-hydrogen-bonding residues that were highly similar to the original residues (in this case, alanine) in all other aspects, and measured the resulting change in protein stability. Their results suggested that the average contribution of hydrogen bonds to stability is quite modest, on the scale of $1k_BT$ (i.e., 0.6 kcal/mol). What could be the evolutionary reason for maintaining such marginally stabilizing forces? First, the additive stabilization achieved with multiple hydrogen bonds between transmembrane segments that contain several polar residues can be substantial. Second, Bowie and coworkers speculated that, as in the case of Pro-related hinges, these weak interactions might just be what membrane proteins need to remain highly flexible and form the helical distortions characterizing their structure. Finally (as controversies go), some studies suggest that hydrogen bonds destabilize membrane proteins [185,186].

The effects of ionic interactions like salt bridges on membrane protein stability are more complicated, as the exposure of charged residues to the core of the protein involves a large desolvation penalty. As discussed at length in Chapter 4, studies carried out on salt bridges in the cores of water-soluble proteins indicate that such interactions may be overall stabilizing if they are optimized spatially and constitute part of a larger network of electrostatic interactions that include also hydrogen bonds [187–189]. In membrane proteins the salt bridges may also be partially exposed to the lipid environment, which should make the desolvation penalty even larger than in water-soluble proteins. However, the fact that salt bridges are found in transmembrane segments, where they are organized as motifs that promote helix-helix interactions, suggests that these interactions are overall stabilizing in membrane proteins.

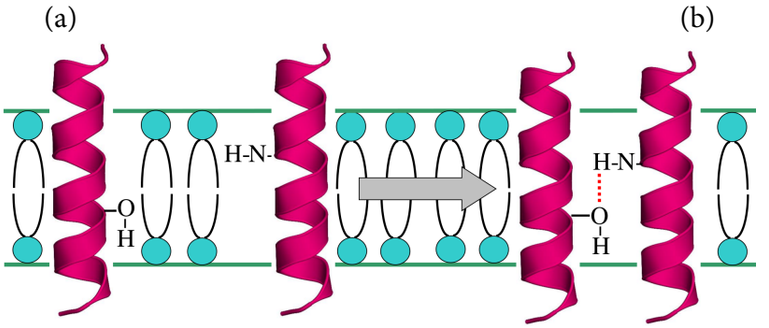

FIGURE 7.13 **Polar interactions in integral membrane proteins.** (a) Polar groups in unfolded membrane proteins are exposed to the hydrophobic region of the membrane, which is energetically unfavorable. (b) Assembly of transmembrane segments allows these polar groups to hydrogen-bond and mask each other in the slightly less hydrophobic environment of the protein core.

7.3.2.3.3 Architecture

As mentioned above, the constraints imposed on membrane proteins by the chemically complex and highly anisotropic lipid bilayer have led to a collection of structures that share similar characteristics. For example, transmembrane segments are almost always arranged as α-helical bundles, and to a lesser extent as β-barrels. Nevertheless, the shared general architecture of membrane proteins may manifest in different forms, which are suited to the proteins' specific biological functions. Several important examples of such architectural

themes and their functional significance are reviewed by von Heijne [9] and by Gouaux and McKinnon [190]. Here we focus on proteins that are involved in the transport of polar molecules across biological membranes, i.e., channels and transporters. In Section 7.5 below we describe the structure-function relationship in the other major category of membrane proteins, ligand-activated receptors.

1. **Aquaporins**
   Aquaporins are ancient channels that can be found in a wide range of organisms, where they facilitate the passive movement of water in cells and tissues [191]. In animals, for example, they participate in the re-absorption of water from urine in the kidneys. Certain aquaporins, termed *'aqua-glyceroporins'*, can also transport small solutes like glycerol, ammonia, CO_2, and O_2. Aquaporins are part of the major intrinsic protein superfamily and exist as tetramers in which each monomer is an independent pore. The pores created by aquaporins have an hourglass-shaped structure that includes six transmembrane segments and two half-helices (Figure 7.14a). The selectivity of the channel against molecules larger than water results from the narrow region at the center of the channel (2.8 Å). In fact, even the water molecules themselves can pass through the narrow channel only in single file, though the transport rate is extremely high (~10^9 molecules/sec). The narrow part of this region is formed from side chains that face the inner side of the pore, and which belong to two types of motifs:

   - Two conserved *Asn-Pro-Ala motifs* (*NPA*, yellow region in Figure 7.14a), which reside in the two half-helices (see more below).
   - An *ar/R motif* ('ar' for aromatic and 'R' for arginine), which resides ~8 Å away from the NPA motif, towards the extracellular side. This motif is considered to be the major barrier for large uncharged solutes. Indeed, in aqua-glyceroporins the ar/R residues create a wider opening, allowing larger solutes to be transported [192] (Figure 7.14b).

   As mentioned above, the *NPA* motif plays a secondary role in the selectivity of the channel against uncharged solutes. On the other hand, it is crucial for the selectivity of aquaporins against protons, which are smaller than water molecules. Protons are positively charged, and the selectivity mechanism is, predictably, electrostatic. Each water molecule that passes through the center of the channel reorients such that its partially negative oxygen atom can hydrogen-bond with the *NPA* asparagine residues surrounding it (Figure 7.14c). Protons are positively charged and therefore cannot form these interactions. The exclusion of protons is further assisted by the dipoles of the half-helices flanking the *NPA* motif. Thus, protons cannot pass through the channel, nor can they 'hop' between the single-file water molecules that reside in the pore [193]. Finally, the partial charges of the *NPA* asparagine have also been suggested to contribute to the fast passage of the water through the channel [194].

2. **Ion channels**
   Ion channels are involved in numerous physiological functions, such as neural transmission, molecular transport, muscle contraction, energy production, and more. Accordingly, malfunction of these proteins leads to various pathologies (*channelopathies*), which include cystic fibrosis, Bartter syndrome, and paralysis [195]. The

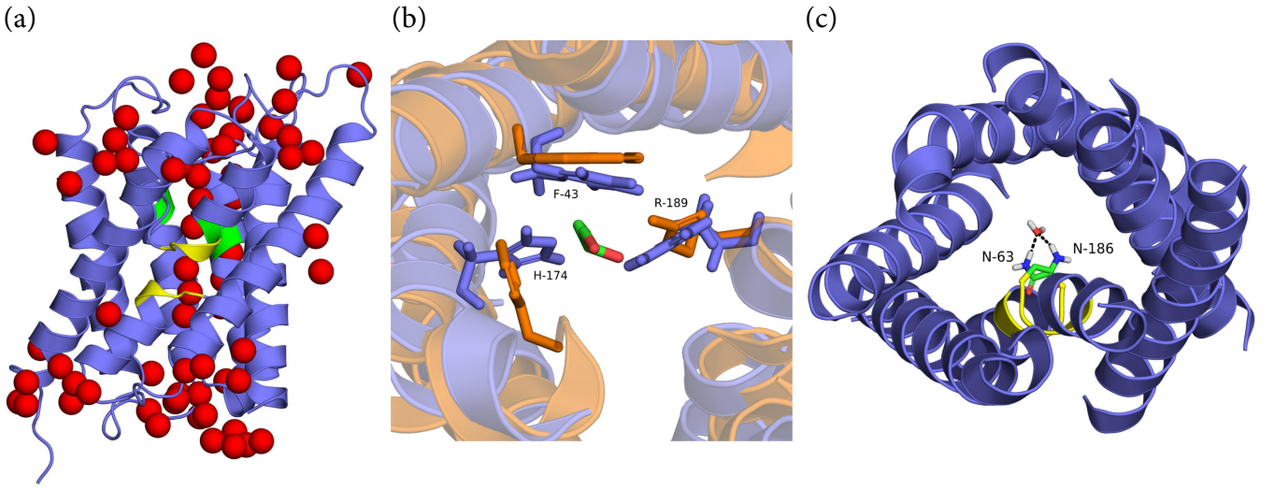

FIGURE 7.14 **Structural characteristics of aquaporins.** (a) A general view of the channel (PDB entry 1rc2). The image shows the single-file distribution of water molecules along the channel (oxygen atoms as red spheres), and the location of the two motifs that create the central constriction: the NPA (yellow), and the ar/R (green) motifs. (b) Superimposition of aquaporin (blue) and aquaglyceroporin (orange, PDB entry 1fx8). The residues forming the motif in aquaporin are noted. A glycerol molecule in the aqua-glyceroporin is shown as sticks. (c) Hydrogen bonds between asparagine residues of the NPA motif and a water molecule (as sticks) inside the channel.

structure of an ion channel is arranged around a central water-filled pore that traverses the lipid bilayer, and in which ions can dissolve without having to pay the energy cost of exposure to the hydrophobic environment of the bilayer core. One of the popular models for such channels is the pH-dependent bacterial K^+ channel (KcsA)[*1]. K^+ channels have a characteristic structure that includes a transmembrane domain and a long (35-residue) cytoplasmic domain, both of which are α-helical (Figure 7.15a). The channel is a tetramer, where each monomer contributes two transmembrane helices (TM1 and TM2) and one cytoplasmic helix at the C-terminus. The transmembrane domain has an inverted teepee structure, and includes a wide, water-filled pore that extends over 2/3 of the lipid bilayer. Thus, the potassium ion can diffuse freely most of its way across the membrane (Figure 7.15b). This property, as well as the electric repulsion between adjacent K^+ ions, leads to a very high K^+ passage rate (~10^8 ions per second). The cytoplasmic domain is an extension of the four TM2 helices that form the inner part of the channel. This domain influences different functional aspects of the transport (permeation, gating), stabilizes the channel, and allows it to interact with regulatory elements.

Despite the high variability of channels, in terms of shape, size, and diameter, virtually all possess some degree of specificity towards the ions they transport. The specificity can be broad, e.g., allowing all elemental ions of a certain charge to pass, or narrow, e.g., enabling only Ca^{2+} ions to pass. In most cases, the selection seems to require the 'candidate' ion to lose its solvation shell and to bind directly to channel residues. This mechanism enables the channel to assess the suitability of the ion. In the KcsA chan-

[*1]For solving the structure of the KcsA channel's transmembrane domain and elucidating the selectivity mechanism [119], Roderick MacKinnon received the 2003 Nobel Prize in Chemistry.

nel the selectivity-related residues appear at the end of the ion's path, in a loop-based substructure called the *'selectivity filter'* (Figure 7.15bI). The loop composing the selectivity filter in each chain includes four residues (the *TVGYG* signature sequence), forming four evenly-spaced K^+ binding sites termed S1 through S4 (Figure 7.15bII). The sites coordinate the four K^+ atoms via four backbone carbonyl groups and one side chain hydroxyl group. The filter determines whether or not the desolvated ion can keep moving all the way to the other side. The biological importance of the filter structure is reflected, for example, in the fact that it is targeted by toxins, such as *kaliotoxin*, produced by scorpions [196]. Whereas some ion channels use a simple size cutoff for selecting the right ion(s), others may be more sophisticated. This seems to be the case with the KcsA channel, which selects K^+ over Na^+, despite the smaller size of the latter. The selection mechanism can be referred to as *'molecular mimicry'*. That is, **the polar uncharged oxygen atoms that coordinate each K^+ ion in the selectivity filter are positioned in a way that precisely mimics the arrangement of water-derived oxygen atoms around the K^+ ion in bulk solution (Figure 7.15c).** Thus, the K^+ ion encounters virtually no energy barriers during its transfer from solution to the selectivity filter (i.e., desolvation). Being smaller, Na^+ ions can enter the selectivity filter, but they are too far from the filter's oxygen atoms to achieve efficient electrostatic masking by the latter. Therefore, they tend to remain in bulk solution, i.e., outside the channel. The molecular mimicry mechanism, which was proposed by MacKinnon in his Nobel Prize-winning work, is elegant and explains the 1,000-fold preference of the KcsA channel for K^+ over Na^+. However, data from later studies suggest that the selectivity mechanism is probably more complicated. For example, NMR measurements have demonstrated increased protein flexibility in the selectivity filter region, suggesting that this region should be able to adapt to ions smaller than K^+ [197]. Similarly, molecular dynamics (MD) simulations of the KcsA channel in a lipid membrane demonstrate fluctuations of the selectivity filter over a range of ion–carbonyl distances, sufficient to coordinate either ion [198]. The authors of the latter study suggested that selectivity is controlled by the intrinsic electrostatic properties of the coordinating carbonyl groups and not by the average size of the pore. Finally, a study combining electrophysiology, X-ray crystallography, and MD suggested that smaller ions like Na^+ and Li^+ can bind easily to the selectivity filter, but find it difficult to reach the filter from the intracellular side due to a K^+-dependent energy barrier [199]. Again, these studies suggest that the selectivity of ion channels is more complex than previously assumed. Interestingly, despite the fact that small elemental ions such as K^+ occupy very little space, their binding often involves considerable changes in channel conformation, as demonstrated for the K^+, Na^+ and Ca^{2+} channels [190].

As in the case of many cellular proteins, the transport carried out by ion channels must be regulated, i.e., it must occur only in response to the right signal. For this purpose, most channels have a gate that prevents the passage of ions in the resting state. The signal activating the channel may be electric, chemical or mechanical in nature. Accordingly, the gate always includes a region of amino acids that acts as a sensor and responds to an activating or inactivating signal. For example, in voltage-gated K^+ (K_v) channels, the sensor includes positively charged amino acids (Lys and Arg) that reside on S4 helices [200,201]. In the channel's resting state the abundance of Na^+ ions

on the extracellular side of the membrane repels the positively charged S4 helices, keeping the channel closed. However, when the membrane depolarizes during neuronal signaling, the significant decrease in the number of Na^+ ions at the extracellular side reduces the electric repulsion, enabling the S4 helices to be displaced, such that the channel opens. This process can be viewed as a conversion of electric energy into mechanical energy, which induces motion. As we will see later, energy conversions happen also in transporters that function as ion pumps, where the chemical energy stored in ATP, or the electrochemical energy stored in an ion gradient, is converted into motion, and vice versa.

The gating mechanism of the KcsA channel is rather complex and relies on two separate gates [202,203]:

(a) H^+-activated gate, which resides at the region covering the intracellular side of the transmembrane domain and the beginning of the cytoplasmic domain. This gate is closed at high pH levels and opens when the pH decreases.

(b) H^+-independent gate, which resides at the selectivity filter.

Understandably, most studies of KcsA gating have focused on the first gate, since it is the one that responds to a change in pH. Activation of this gate leads to conformational changes in the TM2 helices, in both the transmembrane and cytoplasmic domains. In the transmembrane domain, the helices undergo a ~15° hinge-bending motion around Gly-104 [204] (Figure 7.15dI). In the cytoplasmic domain, the conformational change is focused around a region in which the TM2 helices create a bulge, near Val-115 (Figure 7.15dII). There, at the narrowest point for K^+ permeation, each TM2 helix shifts ~4 Å outwardly upon activation, resulting in an overall ~20-Å opening of the channel[*1] [204,206]. The bulging region also seems to be the place where the pH sensing takes place; it contains three residues, Arg-117, Glu-118, and Glu-120, which have been implicated as the pH sensors of the KcsA channel (Figure 7.15dII) [207,208]. Although the exact mechanism of this sensing is not entirely clear, it has been suggested that a p*Ka* (~4.2) leads to protonation of the two glutamate residues (118 and 120), thus rendering them electrically neutral. As a result, these residues are no longer able to mask and stabilize the positive charges on Arg-117. The electrostatic repulsion that ensues between Arg-117 from adjacent monomers induces displacement of helices, and opening of the channel. As mentioned above, the channel also contains a second gate, at the selectivity filter. It is thought that the conformational change described for the H^+-activated gate affects the second gate allosterically, which leads the channel to assume a fully open state [205,209].

It addition to the active and resting states, ion channels can also exist in an inactivated state. Channels normally become inactivated after a period of activity, to attenuate the cell's response. There are two major types of inactivation in K^+ channels [210]. The first, called *N*-type inactivation, is observed in voltage-gated K channels. This is a fast process that involves physical blockage of the pore by an electrically charged *N*-terminal

[*1] Interestingly, when the large cytoplasmic domain is truncated, activation results in a ~32-Å opening of the transmembrane domain [205]. The ~20-Å opening obtained in the full-length structure [204] is probably a lower bound, as the large C-terminal domain was further stabilized by bound antibody fragments. Thus, the real opening of the channel is most likely somewhere between 20 Å and 32 Å.

(a)

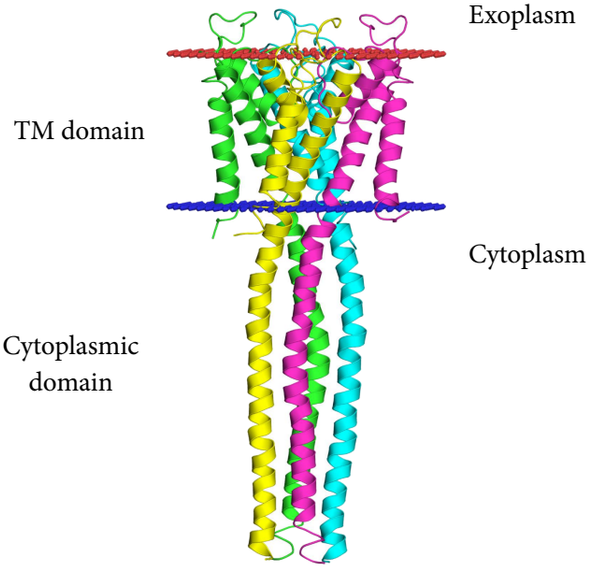
Exoplasm
TM domain
Cytoplasm
Cytoplasmic domain

(c)

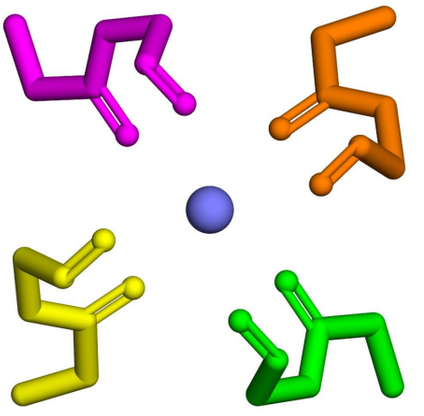

(b) (I)

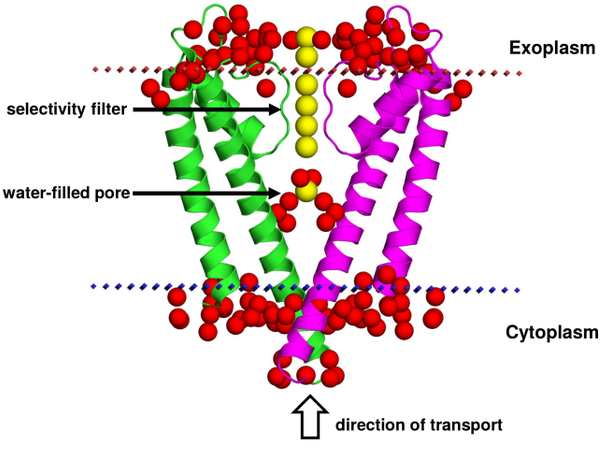
Exoplasm
selectivity filter
water-filled pore
Cytoplasm
direction of transport

(d) (I)

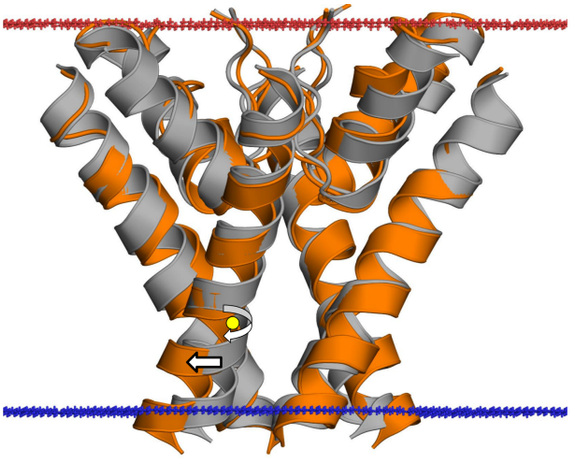

(II)

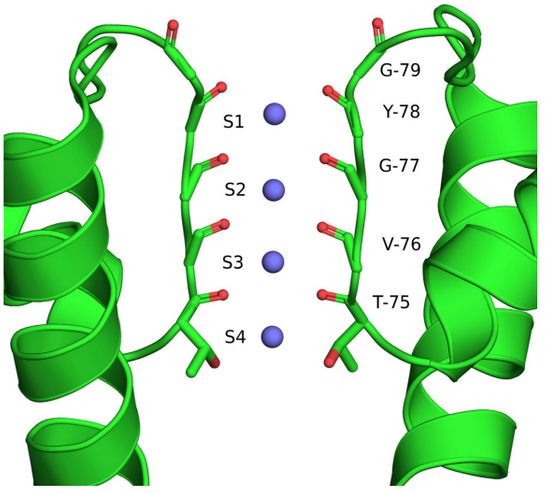
S1
S2
S3
S4
G-79
Y-78
G-77
V-76
T-75

(II)

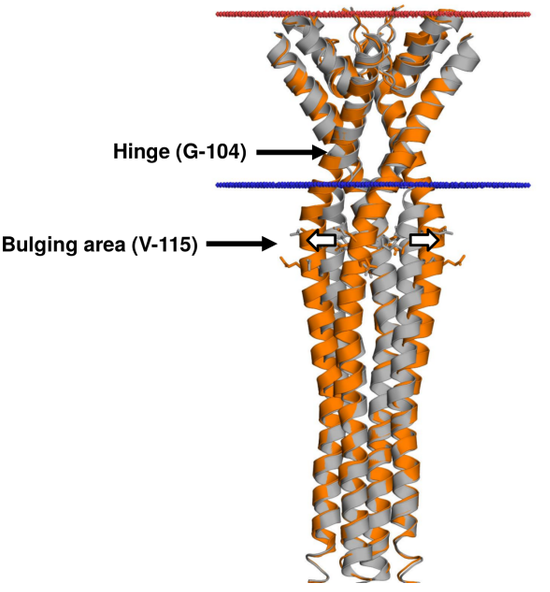
Hinge (G-104)
Bulging area (V-115)

segment of the channel. The second type of inactivation, called *C*-type inactivation, is observed in the KcsA channel, and is much slower than *N*-type inactivation. *C*-type inactivation is thought to involve the H^+-independent gate at the selectivity filter, through reorientation of the backbone carbonyls and subsequent destabilization of K^+ ions inside the filter [203]. Interestingly, though the large cytoplasmic domain limits the degree of opening of the transmembrane domain upon activation (see above), it also seems to slow the rate of channel inactivation [204].

3. **Transporters**
   Like ion channels, some transporters facilitate the passive transfer of ions down their electrochemical gradients. However, many other transporters transfer larger solutes (amino acids, sugars, etc.), and some transporters are even capable of transferring solutes against their electrochemical gradients, or in other words, 'pump' them. In any case, it is obvious that transporters must use a more sophisticated transport mechanism than the one used by channels. Indeed, **transporters do not form simple water-filled structures, but rather exist in (at least) two different states; one allows the ligand to enter the transporter on one side of the membrane, whereas the other releases it on the other side.** This model, abstractly introduced by Oleg Jardetzky, is commonly called 'the alternating access mechanism' [211]. Structurally, it requires each transporter to possess at least two distinct conformations, corresponding to the states mentioned above (Figure 7.16). Such a mechanism is observed in the *SemiSweet transporter* [212], which facilitates passive diffusion of sugars into bac-

FIGURE 7.15 **Structural characteristics of the KcsA K^+ channel.** (Opposite) (a) A general structure of the tetrameric channel in the closed state (PDB entry 3eff), colored by chain. The transmembrane and cytoplasmic domains are noted. The red and blue planes mark the predicted boundaries of the membrane, respectively (the OPM database [117]). (b) (I) The different parts of the transmembrane domain in the conductive channel at high K^+ concentration (PDB entry 1k4c). For clarity, only two of the four chains are shown, and are colored differently. K^+ ions are presented as yellow spheres, and the oxygen atoms of water molecules are shown as red spheres. Most of the transmembrane domain, from the cytoplasmic side, forms a water-filled pore (a hydrated K^+ ion is shown). The top third of the domain forms a selectivity filter that can accommodate four dehydrated K^+ ions. The last part of the domain is just outside the membrane, where the ions are hydrated again. The filter is made of the re-entrant loops interfacing with the K^+ ions. (II) The selectivity filter. The filter is composed of the signature *TVGYG* sequence, which binds the K^+ ions via four backbone carbonyls and one side chain hydroxyl per chain. Each K^+ ion is coordinated by oxygen atoms from two layers, and thus, the filter contains four K^+ binding sites, termed S1 through S4. (c) A view from above showing interactions between one of the K^+ ions (blue sphere, reduced size for clarity) and two layers of backbone carbonyl oxygen atoms in the selectivity filter (eight carbonyls altogether, shown as sticks, colored by chain). (d) Conformational changes in the pH-activated gate of the KcsA channel. (I) The hinge motion of the TM2 helices. The image shows a superposition of the closed-state (grey, PDB entry 3eff) and open-state (orange, PDB entry 3pjs) structures, with a close-up on the transmembrane domain. For clarity, the TM1 helices are not shown. The Gly-104 hinge is marked by the yellow circle, and the hinge motion is delineated by the curved arrow. The resulting shift of the cytoplasmic part of one of the TM2 helices is noted by the thick arrow. (II) The conformational change in the cytoplasmic domain, focused around the bulging area (V-115). The 4-Å shifts in two helices are noted by the thick arrows. The residues constituting the pH sensor are shown as sticks.

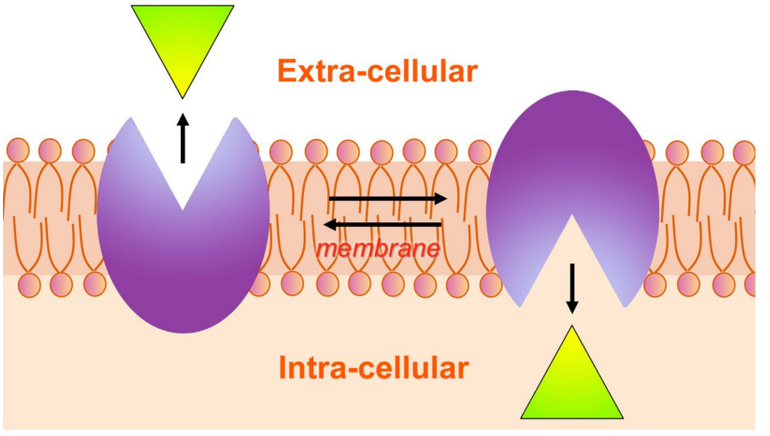

FIGURE 7.16 **The alternating access mechanism for substrate transfer in transporters.** A highly schematic illustration of the mechanism. The purple shapes symbolize two different equilibrium conformations of the transporter inside the membrane (cyan). In each conformation the substrate-binding site faces a different cellular compartment, where it binds or releases the substrate (yellow triangle). The figure demonstrates an import process, where the left 'conformation' binds the substrate in the exoplasm, and then changes into the right conformation to release the substrate into the cytoplasm. The shapes symbolizing the transporter, substrate, and membrane are grossly disproportionate to emphasize the main aspects of the transport process.

teria. The function of this transporter is analogous to that of the GLUT and SGLT transporters in humans, which are key elements in sugar metabolism. As Figure 7.17a shows, in the outward-open state of the transporter (left), the inner side is blocked by a cluster of aromatic and nonpolar residues (intracellular (IC) gate). The switch from the outward-open state to the inward-open state involves several conformational changes. First, a hinge motion of the cytoplasmic half of TM1 (TM1b), around the highly conserved Pro-21, tilts TM1b 30° with respect to the exoplasmic half of TM1 (TM1a). Second, a rotational movement of TM1a, TM2, TM3, and TM1b of the other monomer, leads to an overall 'binder clip' movement. That is, the exoplasmic parts of the transmembrane helices become closer to each other while their cytoplasmic parts are pushed away from each other. This motion leads to the simultaneous closure of the extracellular gate (EC gate) and opening of the cytoplasmic gate. The EC gate is composed of Tyr-53, Arg-57 and Asp-59. When the gate is closed, these residues form polar interactions with the equivalent residues in the adjacent monomer, thus stabilizing the closure.

An active transporter, or 'pump', transfers solutes against its electrochemical gradient. This process requires a source of energy, either ATP or the electrochemical gradient of a common cellular ion. Like passive transporters, active transporters switch between outward- and inward-facing conformations. However, in an active transporter the dominant conformation at any given time is determined by the binding of ATP/ADP/P_i or ions to a specific site in the protein[*1]. This is because the binding of each of these species to the protein stabilizes a different conformation. Thus, in an

[*1] The binding of the transported solute and possibly of other chemical species (common ions, lipids, etc.) is likely to stabilize certain transporter conformations as well, but the effects of these species are not necessarily unique to active transporters.

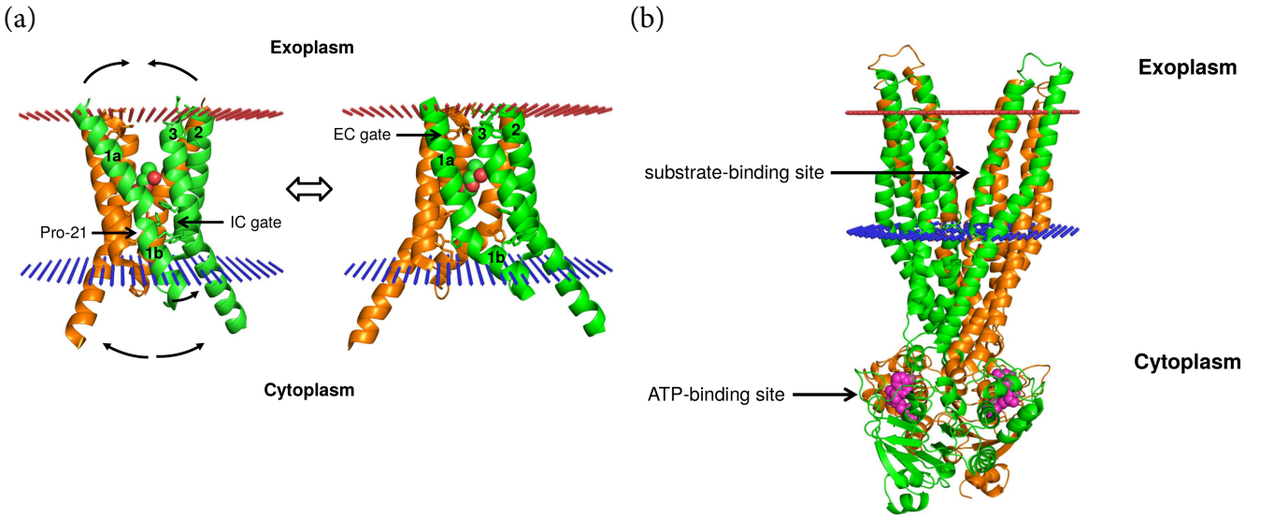

FIGURE 7.17 **Conformational changes in transporters.** (a) Outward (left) and inward (right) conformations of the bacterial SemiSweet transporter (PDB entry 4x5n). The dimeric structure is colored by chain. The glycerol moiety of 1-oleoyl-R-glycerol (PDB entry 4x5m), which mimics the transported sugar, is shown as spheres in the putative substrate-binding site between the two monomers. Residues belonging to the transporter's extracellular gate (EC gate) and intracellular gate (IC gate) are shown as sticks. The curved arrows show the 'binder clip' motion in which the protein shifts from its outward-open state into the inward-open state. (b) The ATP-bound state of the Sav1866 ABC transporter (PDB entry 2hyd), with its substrate-binding site open to the extracellular side of the membrane. The dimeric transporter is colored by chain, and the bound ADP molecules are shown as magenta spheres. The red and blue planes mark the predicted boundaries of the membrane, respectively (the OPM database [117]).

ATP-dependent transporter, a cycle that includes (1) ATP binding, (2) ATP hydrolysis to ADP and P_i, and (3) release of one or two of the latter, involves switching of the protein between different conformations that face different sides of the membrane. Such a mechanism is exemplified by the bacterial multidrug transporter Sav1866, which belongs to the group of *ATP-binding cassette (ABC) transporters*. These proteins appear in both prokaryotes and eukaryotes, where they pump small molecules from (or to) the cell. The action of these transporters is also medically important; some ABC transporters in bacteria pump out antibiotics, leading to resistance. Similarly, tumor cells use such transporters to pump out chemotherapeutic agents, which reduces the efficiency of the treatment. The solute export cycle of Sav1866 begins when the protein is in a monomeric state and its transmembrane domain is exposed to the cell's interior. This conformation enables the targeted solute to bind the transmembrane domain. ATP binding to the nucleotide-binding domains of two Sav1866 monomers induces dimerization and an outward-facing conformation (Figure 7.17b) [213,214]. ATP hydrolysis is thought to induce additional conformational changes that bring the transporter back to an inward-facing state, ready to bind a new solute molecule. It should be noted that the exact nature of the coupling between ATP binding or hydrolysis and the transport of solutes in ABC transporters is not always as simple as depicted above, and may sometimes (and in some variants) be very weak. For exam-

ple, the bacterial vitamin B12 importer $BtuC_2D_2$ hydrolyzes many ATP molecules for each substrate, and hydrolysis takes place even in the absence of the substrate [215].

The effects of nucleotide or ion binding on the shifts between inward- and outward-facing conformations in active transporters do not really explain how these transporters can draw a solute from a low-concentration compartment and release it into a high-concentration compartment. This capability has to do with the inherent *affinity* of each conformation to the solute. In passive transporters the affinity of the inward-facing conformation may be similar to that of the outward-facing conformation, since the binding and release of the solute are governed by its concentration in the two opposite compartments. In active transporters, the conformation facing the compartment that has low solute concentration must have a sufficiently high affinity to the solute to bind it, whereas the conformation facing the compartment with high solute concentration must have a sufficiently low affinity in order to release the solute [216,217]. By selectively stabilizing the two different conformation types, binding of nucleotides or ions indirectly determines changes in affinity during the transport cycle. For example, in the ABC transporters described above, ATP binding stabilizes the outward-facing conformation, which has a low affinity to the solute, thus enabling the solute to be released into the cell's exterior (see [217] and references therein). Some transporters are assisted by binding proteins that scavenge the solute and then bind to a certain domain in the transporter [213].

In conclusion, ATP hydrolysis and electrochemical gradient dissipation are able to fuel active transport, not by a direct release of energy, but rather through sequential binding of nucleotides or ions that stabilize distinct conformations of the transporter. These conformations differ from one another in (1) the exposure of the transporter's transmembrane domains to the inner or outer sides of the membrane, and (2) the affinity of the transmembrane domains to the transported solute.

The principles of active transport that are described above exist in *ATP-dependent ion transporters*. These proteins, which constitute key elements in any organism, are divided into the following groups [218]:

P-ATPases (E_1E_2-ATPases). These transporters are found in bacteria, in fungi, and in eukaryotic plasma membranes and organelles. They transport a variety of different ions across membranes, including H^+, Na^+, K^+, and Ca^{2+}. This category includes some of the cell's key primary active transport proteins, such as the Na^+/K^+-ATPase (Figure 7.18), H^+/K^+-ATPase, and the Ca^{2+}-ATPase (Figure 7.19). The electrochemical gradients formed by these proteins are used for different purposes. For example, bacteria use the proton gradient to drive processes such as chemotaxis and secondary active transport. P-ATPases contain cytoplasmic and transmembrane domains. The cytoplasmic domain includes phosphorylation (P)[*1], nucleotide-binding (N), and actuator (A) subdomains [219]. The transmembrane domain includes six helices, through which the membrane transport takes place. Most P-ATPases, however, also include additional transmembrane helices. For example, in the Na^+/K^+-ATPase and Ca^{2+}-ATPase the transmembrane domain includes 10 helices. These helices also contain cation-binding sites, and are thought to contribute to the ion selectivity of the transporter. Finally, some P-ATPases, such as the Na^+/K^+-ATPase and the H^+/K^+-ATPase,

[*1] The mechanism of P-ATPases includes a phosphorylated intermediate (aspartate in a *DKTG* motif, see more below), hence the name.

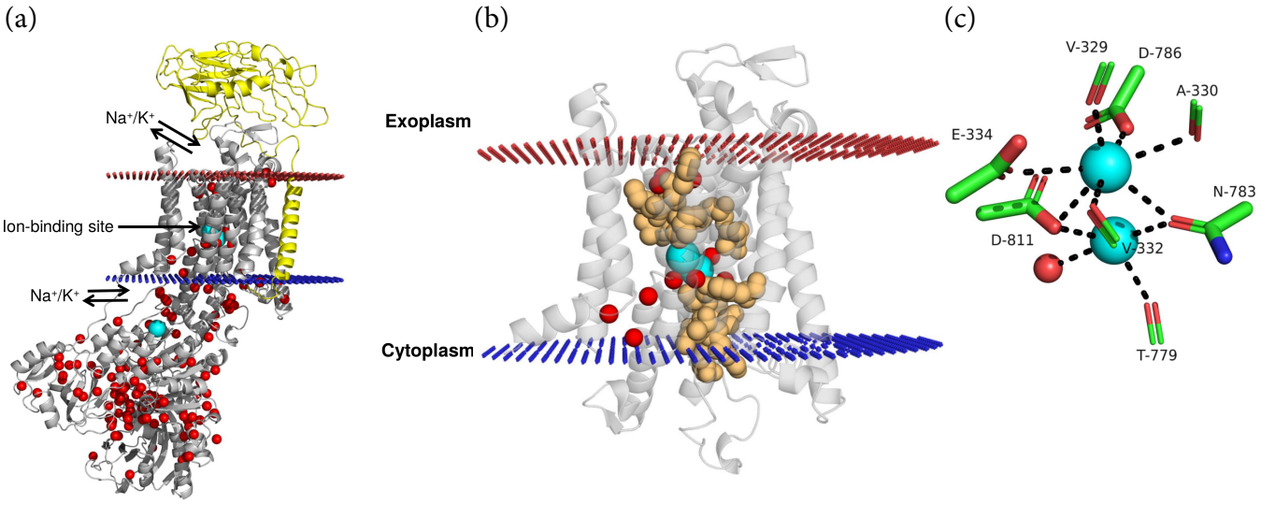

FIGURE 7.18 **Shark Na^+/K^+-ATPase bound to K^+ [221] (PDB entry 2zxe).** (a) A global view of the protein and its position inside the membrane. The α subunit (grey) is responsible for the ion transport and ATPase activity. The β subunit (yellow) is involved in the assembly and trafficking of the protein, and also in the binding of K^+ [221]. Potassium ions are colored in cyan, and water molecules (oxygen atoms only) in red. The entry and exit points of the ions with respect to the transmembrane domain are noted, as well as a transmembrane K^+ binding site. (b) Experimentally-determined K^+-binding sites in the transmembrane domain of the Na^+/K^+-ATPase [221,222]. The residues constituting the binding sites are shown as light-orange spheres. For clarity, the transmembrane helices are semi-transparent, and other parts of the protein have been removed. (c) Polar interactions (black dashed lines) between the two K^+ ions located in the transmembrane domain and protein groups. The ionization states of the acidic residues were predicted by MolProbity [223].

also include an extracellular β subunit that is important for the proper trafficking of the transporter to the plasma membrane [220], and that also affects other functional aspects of the transport.

F-ATPases (F_1F_O-ATPases). These H^+-ATPases reside in mitochondria, chloroplasts, and bacterial plasma membranes. F-ATPases operate in the opposite direction to P-ATPases; in F-ATPases, proton transport is used to fuel ATP synthesis, instead of the other way around. Specifically, F-ATPases use the H^+ electrochemical gradient that is created during cellular respiration (in mitochondria) or photosynthesis (in chloroplasts) to drive the synthesis of ATP. Thus, these proteins are usually referred to as *'ATP synthases'* rather than ATPases. The structure and mechanism of the mitochondrial F-ATPase are described in Chapter 9, Section 9.1.5.3.

V-ATPases (V_1V_O-ATPases). These H^+-ATPases are primarily found in the membranes engulfing eukaryotic organelles (e.g., vacuoles and lysosomes). In the latter, V-ATPases function in acidifying the organelle by pumping protons into it. In addition, in segments of the kidneys they contribute to the net excretion of acid into urine. They have a complex structure, containing more than 10 subunits (Figure 7.20).

A-ATPases (A_1A_O-ATPases) are found in Archaea and function similarly to F-ATPases.

E-ATPases are cell-surface enzymes that hydrolyze a range of nucleoside triphosphates (NTPs), including extracellular ATP.

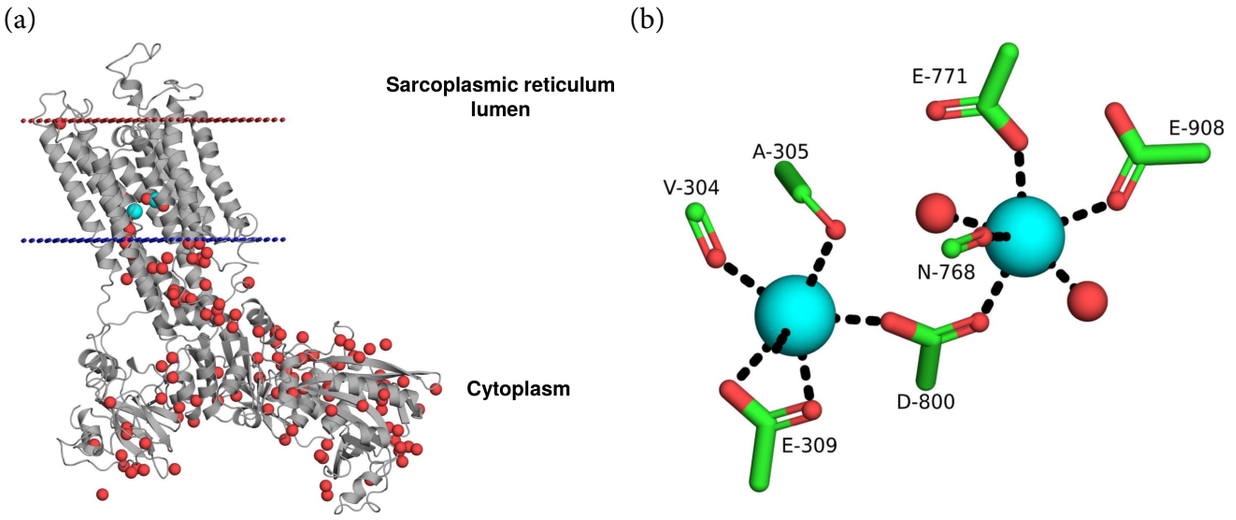

FIGURE 7.19 **Sarcoplasmic reticulum calcium ATPase (SERCA) bound to Ca^{2+} [224] (PDB entry 1su4).** (a) A global view of the protein and its position inside the membrane. The Ca^{2+} ion and water molecules are colored as in panel (b) Polar interactions between the two Ca^{2+} ions located in the transmembrane domain of the transporter and protein groups. The ionization states of the acidic residues were predicted by MolProbity [223].

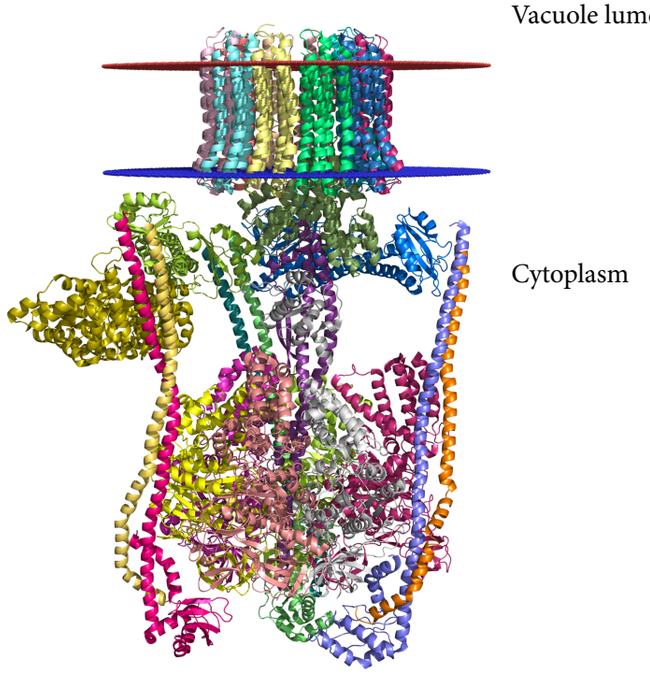

FIGURE 7.20 **A low-resolution electron microscopy structure of the complete V-ATPase pump from yeast [225] (PDB entry 3j9t).** The protein is colored by chain.

Like other transporters, ion pumps work by cycling among different conformations, which 'pick up' the solute on one side of the membrane and release it on the other side. Evidence of such a cycle can be seen in the three-dimensional structures of the Na^+/K^+-ATPase (Figure 7.18a) and the Ca^{2+}-ATPase (Figure 7.19a). Both structures demonstrate that in order to cross the membrane, the ions must 'hop' between amino acids inside the transporter, which serve as transient binding sites (see Figure 7.18b for the Na^+/K^+-ATPase). As Figures 7.18c and 7.19b show, the cation-binding sites in the Na^+/K^+-ATPase and the Ca^{2+}-ATPase include the negatively charged side chains of glutamate and aspartate residues, but also the partial charges of main chain or side chain carbonyl and hydroxyl groups, as well as individual molecules. **The involvement of partial charges that transiently bind desolvated ions is similar to what we have seen in the KcsA (potassium) channel. There too, the use of partial charges ensures that ions can move through the protein instead of getting stuck in one place.** The absence of a water-filled path in transporters may seem disadvantageous, but it is in fact one of the factors preventing the unwanted (simultaneous) exposure of the transported ion to both sides of the membrane, an event that would allow the ion to go back to the compartment from which it was taken.

We have seen earlier that in active ATP-dependent transporters (e.g., the ABC transporter Sav1866), the conformational changes that underlie the transport process are driven by ATP binding and hydrolysis. This is true for all ATPases, including the ion pumps described in the previous paragraphs. The mechanism through which ATPases translate these events into conformational changes involves the effects of ATP and of its hydrolysis products (ADP and P_i) on the transporter's energy landscape [219]. That is, the binding of ATP, ADP, or P_i to the transporter changes its energy, induces a conformational change, and brings it back to its energy minimum. Since ATP, ADP, and P_i have different effects on the energy of the transporter, the binding of each leads to a different conformation. The evolution of ATPases enabled them to cycle between conformations in accordance with the binding of ATP, ADP, and P_i, and this cycling results in ion transport. In P-ATPases such as the Na^+/K^+-, Ca^{2+}-, and H^+-ATPases, the conformational changes begin at the cytoplasmic domain with the movements of the A, N and P subdomains relative to each other, and propagate to the transmembrane domain through linkers and tertiary contacts. To illustrate the overall transport cycle we will look at the Na^+/K^+-ATPase, which transports three Na^+ ions from the cytoplasm to the cell's exterior and two K^+ ions in the reverse direction. The transport cycle includes the following steps (Figure 7.21):

- The ATP-bound form of the transporter, termed E1, has a high affinity to Na^+ ions, and its Na^+-binding site faces the cytoplasm. These properties result in the binding of three cytosolic Na^+ ions to the protein and occlusion of the binding site (Figure 7.21, step 1).

- The transporter has an inherent ATPase activity, and the hydrolysis of ATP is coupled to the transfer of the γ-phosphate to a conserved aspartate in the protein's P domain (Figure 7.21, step 2). This event, which is accompanied by ADP release, has two effects. First, it considerably reduces the affinity of the transporter to Na^+, and second, it promotes a conformational change that exposes the Na^+-binding site to the cytoplasm (the E2 state). These changes result in the release of the three Na^+ ions to the extracellular side of the membrane and binding of two K^+ ions, as well as protonation of the protein (Figure 7.21, steps 3 and 4).

- Binding of the K^+ ions promotes dephosphorylation of the protein's conserved aspartate and occlusion of the binding site (Figure 7.21, step 5), release of P_i (Figure 7.21, step 6), and binding of new ATP (Figure 7.21, step 7).
- The ATP-bound protein reverts to the E1 form, resulting in the release of the bound K^+ ions to the cytoplasm (Figure 7.21, step 8).

In P-ATPases that transport only one type of ion (e.g., Ca^{2+}-ATPase), the transport cycle does not include the steps involving binding and release of the second ion type (steps 4 and 8 in Figure 7.21, respectively).

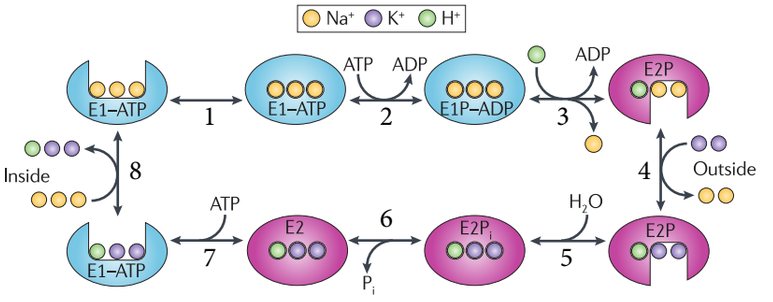

FIGURE 7.21 **A schematic representation of the transport process employed by the Na^+/K^+-ATPase.** Step 1 – occlusion of the Na^+-binding site. Step 2 – ATP hydrolysis and phosphorylation of the conserved aspartate in the protein. Step 3 – protonation of the transporter is accompanied by a conformational change of the protein from the E1 state to the low-affinity E2 state (binding site faces cell's exterior). The change also involves the release of ADP and one Na^+ atom. Step 4 – exchange of the two remaining Na^+ ions with two K^+ ions from the cell's exterior. Step 5 – dephosphorylation of the protein and occlusion of the binding site. Step 6 – release of P_i. Step 7 – ATP binding to the protein changes it back to the E1 form, in which the binding site is exposed to the cytoplasm and the affinity to Na^+ is high. Step 8 – deprotonation and release of the two K^+ ions from the protein to the cytoplasm, and binding of 3 new Na^+ ions. The image is taken from [219].

7.3.2.3.4 Structure prediction

We have seen how the strong sequence-related tendencies of transmembrane segments enable scientists to identify such segments in the amino acid sequence and to predict their topology with respect to the other parts of the protein. The two remaining steps for successful prediction of the entire structure relate to the orientations of helices and the conformation of the protein backbone (in cases in which the helices are distorted) and side chains. Thus, one way to classify structural prediction methods of membrane proteins is according to the properties they predict: secondary structure, topology, tertiary structure, etc. (see [128] for details). Another way of classifying structure prediction methods is by the information they use to carry out their predictions. According to the latter criterion, methods can be separated into three main groups [71,101]. The first group includes *ab initio* methods, which rely solely on physicochemical principles characteristic to membrane proteins, such as length, hydrophobicity, etc. PREDICT [226] is an example of such a method, one that was developed specifically for GPCRs. The greatest advantage of such methods is that they do not require any additional information regarding the protein, aside from the amino acid sequence. Their

main disadvantage is their requirement of massive conformational sampling, which is computationally demanding [227]. The second group includes methods that rely on statistical tendencies of residues to appear in certain regions of the protein. One example is kPROT [228], a scale of the propensities of amino acids to face either the lipid bilayer or the protein core; this scale was developed on the basis of statistical data extracted from bitopic and polytopic proteins, respectively. Three other statistical propensities successfully used in structure prediction algorithms are evolutionary conservation [229,230], correlated mutations [231] (see Box 3.3), and tight packing against other residues [232]. The third group of structural prediction methods of membrane proteins includes methods that rely on sequence-based similarity between the query protein and membrane proteins whose structure is already known (*template-based methods*). When the query and template proteins are homologous (sequence identity > ~30%), the preferred method is *homology modeling* (see Chapter 3, Subsection 3.4.3). However, this method, which is highly successful in water-soluble proteins, is less efficient in membrane proteins because of the limited number of homologues with known structure that can be used as templates. In such cases, *fold recognition* (*threading*) methods may be used (see Chapter 3, Subsection 3.4.3.3). In such methods, the template is chosen not by the similarity of its sequence to that of the query protein, but rather by similarity of sequence properties. Some of these properties are extracted statistically from multiple sequence alignments, whereas others are physically meaningful, e.g., propensity to form a certain secondary structure, to be exposed to the surrounding medium, to have certain dihedral angles, to interact with certain amino acids, etc.

Current prediction algorithms are often hybrid, i.e., they are based on a scoring function that includes expressions adopted from different approaches [233] (see Chapter 3, Subsection 3.4.4). For example, some of the expressions may rely on physicochemical considerations, whereas others rely heavily on statistically derived tendencies of certain amino acids to form certain structures or to be involved in certain physical interactions. Two well-known methods, *Rosetta* [234,235]*1 and *I-TASSER* [237]*2, offer a unified modeling framework in which different approaches are used for different modeling challenges [233]. Indeed, both methods have been tested on different proteins and yielded good predictions [236,239,240] (see more details in [233]).

Finally, a relatively new approach has been adopted that uses experimental data in order to make predictions more efficient [118] (see Chapter 3, Section 3.5). These data are derived from experimental methods that provide low-resolution structures of membrane proteins; such methods include mainly cryo-EM, SAXS, and NMR, but also CD and FRET. The general idea is to use the extracted data as spatial constraints that narrow down the conformational space searched by the prediction methods, and thus significantly increase their chances of providing the native protein structure [241–244]. Cryo-EM looks especially promising in this sense; EM methods have traditionally been used to provide data concerning the number, tilt, and overall locations of transmembrane helices in query structures [233]. However, recent technological developments in single-particle cryo-EM have facilitated the production of near-atomic-resolution structures (4 or 5 Å), at least for some proteins. Indeed, in recent years, several software programs have been designed or adapted to integrate experimentally derived constraints into the structure prediction and modeling process [245]. These programs include *Rosetta* [246–250] (mentioned above), *CHESHIRE* [251], *CS23D* [252],

*1 Rosetta has a version designed specifically for membrane proteins, called RosettaMembrane [234,236].

*2 I-TASSER has a version designed specifically for GPCRs, called GPCR-I-TASSER [238] (server: http://zhanglab.ccmb.med.umich.edu/GPCR-I-TASSER/).

and *SAXTER* [253]. Biochemical methods also provide experimental data that can be used to guide prediction tools; such methods include (1) proteolytic cleavage of extramembrane regions of the proteins or their identification using antibodies, (2) point mutations of different residues of the protein (conserved residues often face the core [150]), and (3) chemical crosslinking. One major problem in the use of such methods for structure prediction is that they are carried out on samples containing large numbers of molecules. As a result, they might provide data corresponding to different substates of the protein, thereby complicating the prediction process [233].

7.3.3 Peripheral membrane proteins

Peripheral membrane proteins are attached to either the exoplasmic side or the cytoplasmic side of the membrane, with the bulk of their surface in the aqueous solution (extracellular matrix or cytoplasm, respectively). Thus, the principles determining their structures are similar to those of water-soluble proteins. Accordingly, our discussion of peripheral membrane proteins focuses on their attachment to the lipid bilayer. This attachment can take place through the following three mechanisms:

1. **Electrostatic binding (Figure 7.22a).** Certain membrane proteins contain a binding site that is geometrically suited for binding a certain membrane phospholipid. In many cases the latter is negatively charged (PS, PG, PIP_2), and the binding site contains basic residues that are capable of interacting with it favorably (e.g., in the pleckstrin homology domain, Figure 7.22b). Other proteins, such as MARCKS, contain a *patch* of basic amino acids, which renders the entire region positively charged. This charge allows the protein to adhere non-specifically to areas of the lipid bilayer containing microdomains of negatively charged phospholipids [254–256]; in eukaryotes, such areas are present on the cytoplasmic side of the membrane. In these cases, the protein is positioned about 3 Å away from the phospholipid head group, a distance that is electrostatically optimal. That is, the Coulomb attraction between the two charged entities at this distance is maximal, and over-compensates for the unfavorable Born repulsion, which is minimal since a water layer separates the protein and lipid membrane. A well-known example of the two forms of electrostatic binding described here is given in Subsection 7.4.1.2 below, which discusses the interaction between proteins and membrane PIP_2.

2. **Covalent binding (Figure 7.22a).** Some proteins undergo post-translational modifications that enable them to bind covalently to membranes. The modifications include *N′*-myristoylation, *S*-palmitoylation, and *S*-prenylation (see also Chapter 2, Section 2.6). Such binding can be observed in certain key signal transduction proteins such as ras and src, which bind to lipid chains from the cytoplasmic side of the membrane.

3. **Integrated binding of amphipathic helices (Figure 7.22c).** Some membrane proteins contain amphipathic helices that enable them to partially penetrate one of the bilayer leaflets. In this mode of protein-membrane binding, the nonpolar residues of the hydrophobic face of the helix interact with the hydrocarbon core of the bilayer, and the polar residues on the opposite face interact with the lipid head groups (e.g. [257,258]). This form of binding is also observed in peptides [259,260], e.g., antimicrobial peptides attaching to bacterial membranes.

The last form of association is particularly interesting. First, it is observed both in membrane proteins and in peptides. Second, it affects the structure of the lipid bilayer, as further discussed in Section 7.4 below. Interestingly, none of the three forms of binding seems to be sufficient on its own, as demonstrated in the case of the signal transduction protein MARCKS. This protein uses the first two forms of binding, and possibly the third as well, to remain attached to the membrane. Upon phosphorylation or binding to calmodulin [261], the electrostatic component of the binding is nullified [262], which leads to the release of the protein into the cytoplasm.

7.4 PROTEIN-MEMBRANE INTERACTION

7.4.1 Lipid bilayer effects on membrane proteins

The lipid bilayer is a chemically complex medium, and as such it has diverse effects on its resident proteins [30]. Still, these effects, which result from the physicochemical interactions between the lipids and proteins, can be separated into two types. The first type results from the physical properties of the bilayer as a bulk, which can be considered as a complex solvent. Indeed, studies show that membrane proteins are affected by general properties of the lipid bilayer, such as topology [70,263], degree of order [264], viscosity [265], hydrophobic thickness [266], curvature [61], degree of acyl chain packing [267], free volume [268], rigidity [269], and more. The second type of bilayer effect is mediated via specific interactions between the proteins and certain lipid molecules. The two types of effects have been studied in the last decades using different techniques. The main findings are reviewed in the following subsections.

7.4.1.1 Effects of general bilayer properties

7.4.1.1.1 Topology

Transmembrane segments of membrane proteins tend to acquire an ordered secondary structure (mainly α-helical) to avoid the unfavorable exposure of their backbone polar groups to the hydrophobic core of the lipid bilayer. A similar phenomenon also occurs when amphipathic peptides or protein segments bind to the bilayer interface. That is, the amphipathic peptides or segments fold and acquire an ordered helical structure [70,263]. The folding in this case, however, is driven in part by the need to preserve the amphipathic nature of the peptide or segment, which allows it to interact favorably with the lipid bilayer (see Subsection 7.3.3 above). Thus, the basic polar/nonpolar topology of the lipid bilayer can affect the structure of proteins inside it.

7.4.1.1.2 Degree of order and thickness

Membrane proteins differ in their preference for regions in the membrane of particular degrees of lipid order. Studies show that many integral proteins prefer l_d-phase regions, yet some integral proteins have been shown to prefer l_o-phase regions [270,271]. The different preferences lead to *lateral segregation* of proteins within the membrane, and to the formation of microdomains that have their own unique lipid and protein compositions. In some cases the preference results from direct protein-lipid interactions, as in the case of proteins that are covalently attached to the bilayer via a fatty acid or other types of hydrocarbon chains. In such cases, the preference has to do with the degree of saturation of the acyl chain.

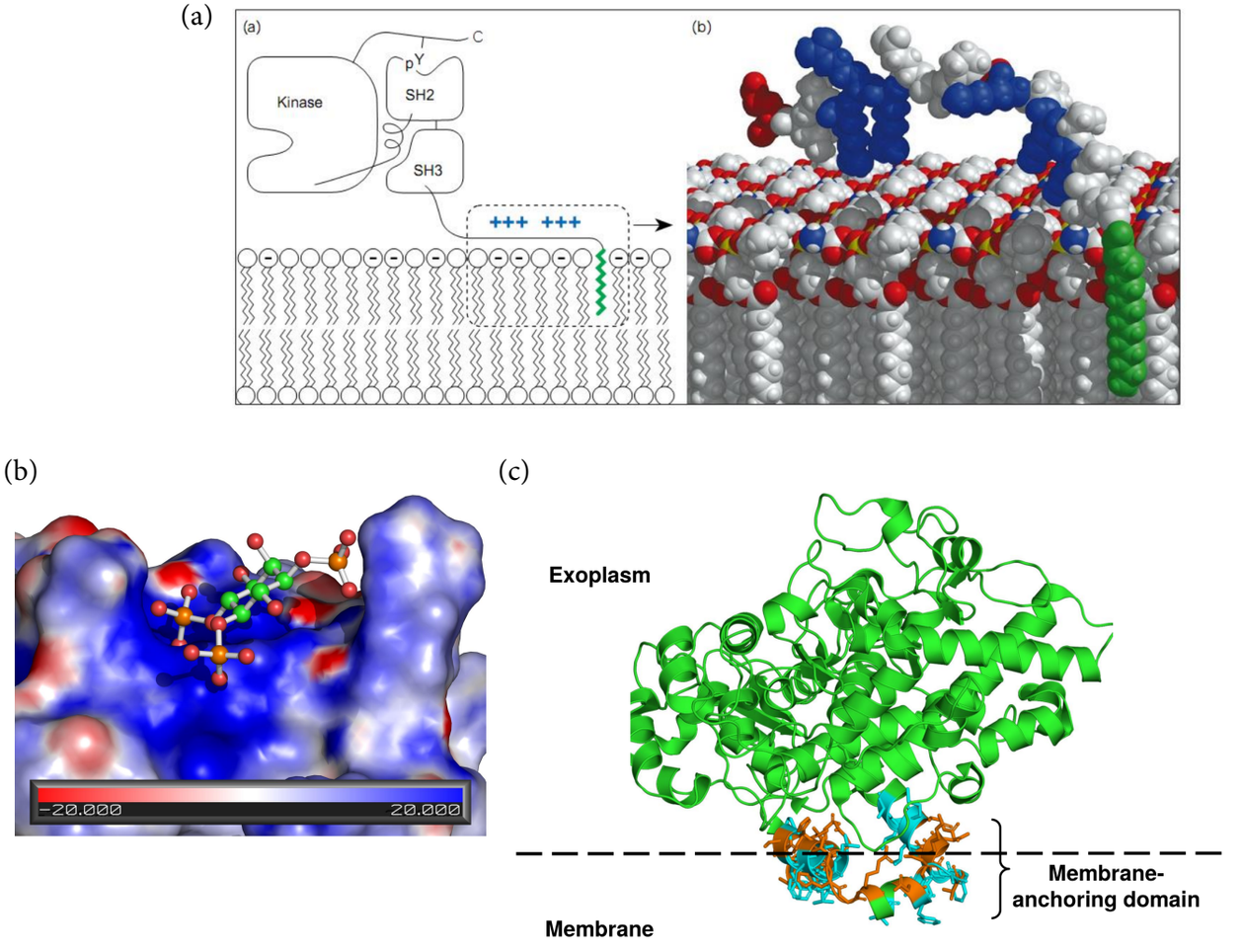

FIGURE 7.22 **Common interactions of peripheral proteins with biomembranes.** (a) Electrostatic adhesion and covalent binding to an acyl chain. The structure of c-Src is shown. The cartoon on the left shows the domain composition of the protein and suggests its orientation with respect to the membrane. The right image shows a blowup view of how the N' of the protein could interact electrostatically with the polar head groups of the lipid bilayer, and covalently with an acyl chain. Basic residues in c-Src are blue; acidic residues are red; and the acyl chain (myristate) bound to the protein is green. The membrane is represented here by a 2:1 PC:PS bilayer, with the acidic lipid, PS, identified by its exposed nitrogen, colored blue. The figures are taken from [254]. (b) Electrostatic and geometric compatibility of the pleckstrin homology (PH) domain binding site to inositol 1,4,5-trisphosphate. The image shows the structure of the PH domain of Arhgap9 (PDB entry 2p0d). The protein surface is colored according to electrostatic potential, in the range specified by the scale at the bottom of the figure (in k_BT/e units). Inositol 1,4,5-trisphosphate is shown as sticks and balls. The latter binds into a cleft on the surface of the protein, which is characterized by a strong positive potential, created by Arg and Lys residues. The positive potential of the protein cleft matches the negative potential of the ligand, which results from the three phosphate groups in the latter. (c) A schematic representation of the electrostatic and nonpolar interactions between the amphipathic helices of the enzyme cyclooxygenase-1 (PDB entry 1eqg) and the lipid bilayer. The membrane-anchoring region of the protein extends between positions 73 and 116 (shown as sticks). Polar residues are colored in orange, whereas nonpolar residues are colored in cyan. The dashed line marks the approximate location of the (exoplasmic) membrane core boundary.

For example, proteins that are covalently attached to GPI (glycophosphatidylinositol) prefer ordered regions of the bilayer (l_o), because the GPI's acyl chain is saturated [272]. This is also true for src and other kinases of that family, which are myristoylated or palmitoylated [273]. Conversely, GTPases of the ras family, which are attached to the unsaturated prenyl chain, prefer disordered (l_d) regions of the bilayer [274].

The bilayer's degree of order also affects proteins indirectly, by influencing the membrane's thickness. Saturated acyl chains are more extended than unsaturated ones, and therefore tend to form more ordered bilayers. The proteins are affected not by the overall thickness of the bilayer but rather by the thickness of the hydrocarbon region. As described earlier, nonpolar residues in transmembrane segments usually extend over a length that roughly matches the hydrophobic thickness of the lipid bilayer. Still, there are cases where transmembrane segments *hydrophobically mismatch* [266,267] the bilayer core. As we will see in Section 7.4.2 below, such a mismatch is likely to affect the shape of the lipid bilayer. Still, the protein may also undergo some changes in order to minimize the mismatch. *Positive hydrophobic mismatch* occurs when the thickness of the bilayer's core is smaller than the length of the nonpolar stretch in the transmembrane segment (Figure 7.23a). This prevents the nonpolar residues of the transmembrane segment from interacting fully with the core of the bilayer. In order to overcome this problem, the transmembrane segment may tilt with respect to the bilayer's vertical axis (Figure 7.23c). The opposite situation, i.e., when the thickness of the bilayer's core is greater than the length of the nonpolar stretch in the transmembrane segment (*negative hydrophobic mismatch*, Figure 7.23b), is much less favorable energetically. The problem is the partitioning of polar amino acid residues of the protein to the nonpolar environment of the bilayer core, which, as we have seen earlier, may seriously destabilize the system. There are several ways to minimize negative mismatch or its effects [264]:

1. **Lateral diffusion (Figure 7.23d).** The protein may move along the plane of the lipid bilayer towards regions with lower degrees of order and smaller hydrophobic thickness. This creates microdomains in the lipid bilayer. Signal transduction is an example of a cellular process that is highly dependent on the presence of such microdomains [52,270]. Specifically, signal transduction requires a concentration of certain protein and lipid elements in one confined region of the membrane. An example for such a requirement is given by PIP_2-dependent signal transduction processes (see Subsection 7.4.1.2.3 below). Another cellular process affected by microdomains is the trafficking of proteins inside the cell [275]. That is, a protein sent to a certain cellular compartment must hydrophobically match the membrane of that compartment[*1].

2. **Conformational changes in the protein (Figure 7.23e).** Membrane proteins that are large enough may undergo conformational changes in order to reduce hydrophobic mismatch. Such changes usually include screw or slide motions of structural protein units, such as helices or domains. Though they solve the mismatch problem, such conformational changes might create new problems by reducing the activity of the protein [276–279]. Such a reduction in activity occurs, e.g., in the enzyme Ca^{2+}-ATPase within the *sarcoplasmic reticulum* (*SR*)[*2] membranes of muscle cells, when the thickness of the latter becomes different from that of the plasma membrane [30,280]. The

[*1] The membranes of the different organelles have different lipid compositions, and therefore different thicknesses.

[*2] The equivalent of the ER in muscle cells.

implications of this reduction are not necessarily negative, as **it provides a means of regulating the activity of the enzyme under different conditions that change the thickness of the SR membrane.**

3. **Oligomerization (Figure 7.23f).** When two separate transmembrane segments interact unfavorably with the lipid bilayer (e.g., due to hydrophobic mismatch), the system can reduce the number of unfavorable interactions by replacing some of them with favorable protein-protein interactions. That is, the two transmembrane segments associate. In some cases association may facilitate activation. This is observed in the antibiotic protein gramicidin [281]. The association in this case allows two short segments to dimerize into a transmembrane segment long enough to span the membrane and function as an ion channel [282,283]. **This may reflect an evolutionary mechanism using protein-membrane (hydrophobic) mismatches to activate certain proteins and peptides.**

All the above-mentioned membrane-induced effects may lead to changes in the activity of the protein. Indeed, studies have already proved this to be the case in many proteins, such as Na/K-ATPase [278,284], cytochrome c oxidase [280], Ca^{2+}-ATPase [30,280], melibiose permease [285], and diacylglycerol kinase [279].

7.4.1.1.3 Viscosity

The activity of virtually all proteins requires them to dynamically shift between different conformations (see Chapter 5 for details). Most globular proteins are surrounded by water molecules, which can adjust rapidly to any new conformation the protein acquires. Such adjustment makes it easy for the protein to undergo structural changes, although it does involve friction due to water-water interactions (van der Waals, hydrogen bonds). Membrane proteins, in contrast, are surrounded by lipids, which are less mobile than water, and limited in their capacity to reorganize in response to conformational changes. As a result, conformational changes of integral membrane proteins involve significant friction with neighboring lipids, particularly with the acyl chains [30]. On the one hand, such friction opposes the change, but on the other hand it may make the change 'smoother' by inhibiting post-change vibrations. The importance of having constant viscosity in biological membranes is revealed in prokaryotes, which are exposed to changing environmental conditions. In these organisms membrane viscosity is a *homeostatic* property, i.e., it is kept constant; this homeostasis is achieved through the lipid composition of the bilayer, which can change in response to changes in environmental conditions [286]. For example, a bacterium will respond to elevation of the external temperature by increasing the percentage of long saturated phospholipids, which oppose the heat-induced rise in membrane dynamics.

7.4.1.1.4 Curvature

The capacity of the lipid bilayer to acquire positive or negative curvature in specific regions has been found to affect the activity of integral proteins in these regions. Many of the studies investigating this issue have focused on processes that create negative curvature in the bilayer. This is because in extreme cases such processes may lead to loss of planarity of the bilayer, and create, e.g., an inverted hexagonal phase [59]. The results demonstrate a complex situation, in which enrichment of PE, a lipid known to induce negative curvature, increases the activity of some proteins (e.g., see [287]) while decreasing the activity of others (e.g., see [288]).

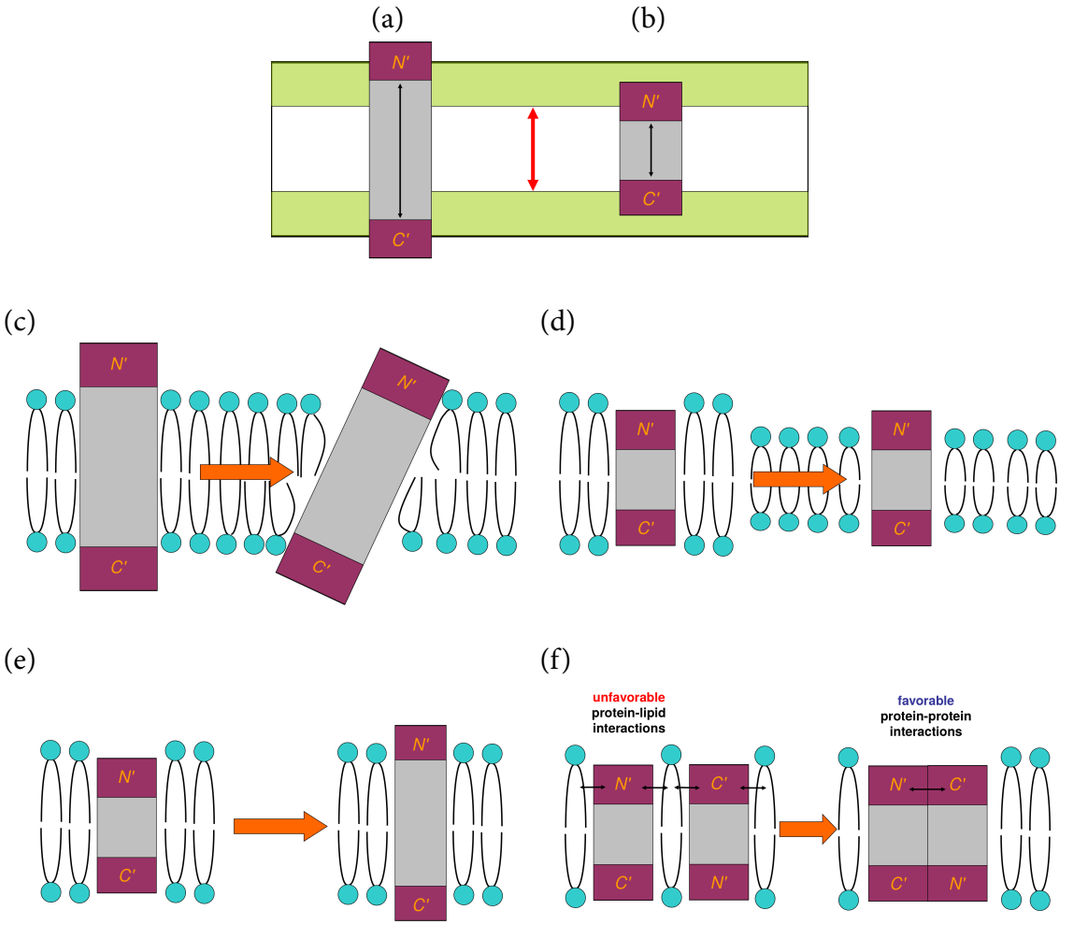

FIGURE 7.23 **Hydrophobic mismatch.** The figure illustrates (a) positive and (b) negative mismatches between the hydrophobic length of the transmembrane helix (or protein) and the thickness of the hydrocarbon region of the lipid bilayer. The transmembrane segments are depicted as rectangles, with their hydrophobic regions colored in grey, and their polar termini in purple. The hydrophobic lengths of the transmembrane segments are marked by the black arrows. The lipid bilayer is depicted as in Figure 7.11, with its hydrophobic thickness marked by the red arrow. (c) Tilting of the transmembrane segment reduces the positive mismatch. The transmembrane segments are depicted as in (a) and (b), and representative lipids of the bilayer are depicted schematically. (d) through (f) Adaptations of proteins to negative mismatch: (d) Lateral diffusion to a thinner area of the lipid bilayer; (e) Conformational changes that exclude the polar termini from the nonpolar bilayer core; (f) Oligomerization, which replaces unfavorable interactions between the polar termini of the transmembrane segments and the nonpolar core of the bilayer with favorable interactions between the polar termini of the two transmembrane segments. (The interactions are favorable because the two segments are positioned in an anti-parallel topology, allowing their partially positive N' to interact with their partially negative C').

7.4.1.1.5 Mechanical pressure

In prokaryotes exposed to environmental changes, a sudden drop in the solute concentration of the external environment leads to massive entry of water into the cell. This is a dangerous situation, because aside from the resulting drop in intracellular solute concentration, the stretching of the plasma membrane may lead to its rupture due to the immense pressure applied to it from within. In bacteria, the latter problem is solved by certain membrane proteins that function as mechanosensitive sensors [289]. Upon stretching the membrane, these proteins allow a rare event to happen: the massive efflux of cellular solutes. This leads to water efflux, which solves the problem. Interestingly, these proteins have been found to respond to membrane stretching only when the increase in membrane surface area reaches 4%, which happens to be the threshold for membrane rupture*1 [289].

7.4.1.2 Effects of specific bilayer lipids

7.4.1.2.1 General lipid types

Biological membranes include different kinds of lipids, as explained above in detail. However, in terms of their interactions with proteins, these lipids, regardless of type, can be divided into three basic categories [290]:

1. **Bulk lipids**, include all lipids that are not engaged in specific contacts with proteins, and whose diffusion is therefore determined by their interaction with neighboring lipids.

2. **Annular lipids**, include all lipids that form a contact layer around a protein but still move constantly between this layer and the bulk [291]. EPR measurements show this movement to be about one order of magnitude slower than the diffusion rate of bulk lipids [292]. This contact layer assists in positioning integral proteins vertically in the lipid bilayer, and seals the protein-lipid interface. Annular lipids are not confined to the periphery of the protein and can also be found in large spaces within multimeric proteins, as can be seen clearly in the structure of the V-Type Na^+-ATPase [293].

3. **Bound lipids**, include lipid molecules that interact strongly with the protein. The interaction inhibits the motions of these lipids considerably, allowing them to co-crystallize with the protein (Figure 7.24). They can therefore be seen in structures obtained by X-ray diffraction. Bound lipids may be found in clefts on the protein surface (usually located in inter-subunit interfaces), or buried within the protein [290]. Lipids that are deeply buried within a protein or complex are also called '*integral*'. The lipid-binding site often contains evolutionarily conserved residues [294] (for example, the cholesterol-binding motif in G-proteins; see Section 7.5 below). The bound lipid molecule tends to acquire a conformation that provides the best possible interaction with the protein, and this often leads to distortion of the lipid molecule. Such distortion is known to happen even when the lipid is saturated, and may result in its translation inward, towards the bilayer core. The lipid distortion may even lead to situations in which the lipid polar head group is positioned below the normal location of the phosphoester groups of the bilayer, or its acyl chains curve and wrap around α-helices of the protein [295].

*1 The low tolerance of the membrane to stretching probably results from the exposure of its nonpolar core to the aqueous solvent [30].

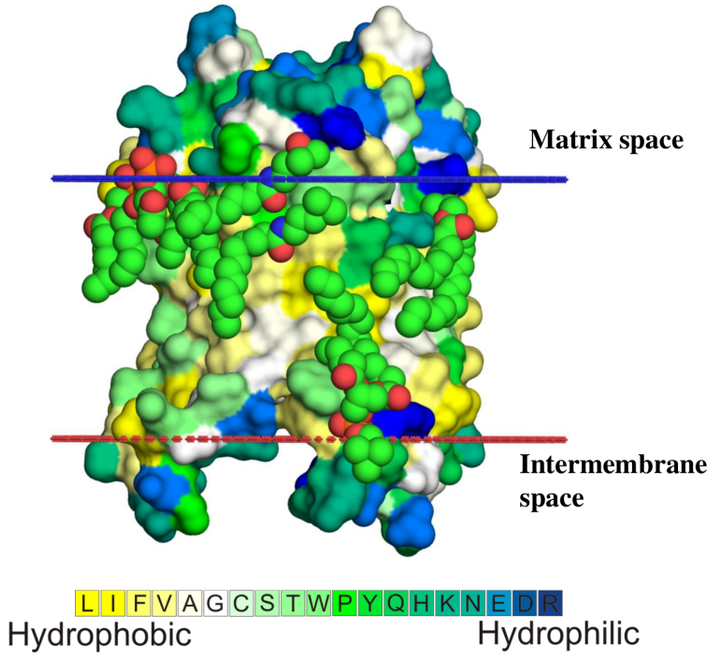

FIGURE 7.24 **Protein-bound lipids.** The structure of the mitochondrial ADP/ATP carrier complex with bound lipids is shown (PDB entry 1okc). The surface of the protein is colored by hydrophobicity using the Kessel-Ben-Tal Scale [8] (see Figure 2.7 for details), and the annular lipids are depicted as atom type-colored spheres. As the image clearly shows, some of the lipids are distorted significantly, which prevents the highly unfavorable interaction between the nonpolar tails and the polar regions of the protein. The red and blue lines mark the predicted boundaries of the membrane (the OPM database [117]).

7.4.1.2.2 Phospholipid-protein interaction

Specific protein-lipid interactions are mostly noncovalent, and include electrostatic interactions involving the lipid's polar head group [30], in addition to nonpolar and van der Waals interactions involving the acyl chains [290]. As mentioned earlier, some of the most favorable interactions involving lipid head groups are between basic protein residues and acidic head groups on the electronegative side of the membrane (the mitochondrial matrix, the stroma of chloroplasts, or the cytoplasmic side of the plasma membrane) [295,296]. While interactions involving the alcoholic groups of lipids are diverse [295], those that involve the phosphodiester group, common to all phospholipids, are mediated by several two-residue combinations of basic and polar-neutral residues [290]:

KT, KW, KY, RS, RW, RY, RN, HS, HW, HY

The primary interaction with the phosphodiester group involves the following residues, ranked by the number of occurrences:

Arg > Lys > Tyr > His > Trp, Ser, Asn

Other favorable interactions involve Thr and Gln. The interactions at the other, less electronegative side of the bilayer also involve recurring residues, most of which are polar-neutral, and very few of which are basic. In the case of PC, the main phospholipid on that

side of the membrane, the interactions do not involve Lys and Arg at all, probably because of the presence of the positively charged trimethylamino group. They do, however, involve a combination of His and Ser, or His, Ser, and Thr, separately. Another special case is that of cardiolipin (CL), which contains two phosphodiester groups. These interact with a three-residue motif, in which the first two are basic and the third is polar-neutral.

As mentioned above, the aromatic residues Tyr and Trp in transmembrane segments tend to appear near the polar-nonpolar interface, where they function as anchors preventing the segment from sliding out or in (see Subsection 7.3.2.1.3 above). Much of the anchoring effect results from complex interactions between these residues and adjacent phospholipids (Figure 7.25). These interactions rely on two properties of Tyr/Trp [297]:

1. **A ring structure.** This allows the residue to have significant van der Waals and non-polar interactions with the acyl chains of the phospholipid. The planarity of the ring makes these interactions geometry-dependent.

2. **Polarity.** This property results both from the chemical composition of the residue (OH group in Tyr and NH in Trp) and from its aromaticity (i.e., the delocalized π electrons). It allows the residue to interact electrostatically with polar head groups of adjacent lipids. Due to the location of the aromatic residue, the interaction primarily includes hydrogen bonds with phospholipid carbonyl groups, although a recent NMR study suggests that these are not important for membrane anchoring [298].

7.4.1.2.3 Effects on membrane proteins

Specific lipid molecules within the bilayer may affect the stability, folding, assembly, and activity of integral membrane proteins [290]. Evolutionary 'forces' made these effects beneficial in most cases, and **some proteins are already known to be active only when surrounded with certain lipids [299]**. For example, the activity of the metabolic proteins NADH dehydrogenase, ADP/ATP carriers, cytochrome c oxidase, ATP synthase, and cytochrome bc1 depends on cardiolipin [300–302], which is abundant in the inner mitochondrial membrane. In such cases, the lipid molecule is considered to be a cofactor. In some cases the three-dimensional structure of the protein and bound lipid sheds light on the molecular basis for the functional dependency. This is the case with the light-harvesting complex of photosystem II (LHC-II) in plants. The LHC is a trimer, whose formation (and therefore activity) depends on PG [303]. Close inspection of the structure of LHC shows that the phospholipid molecule is located at the subunit interface, where one of its acyl chains is positioned inside the trimer [304,305] (Figure 7.26). Thus, PG assists in stabilizing the oligomeric structure of LHC. Furthermore, PG also interacts with other lipids in the vicinity of LHC, such as chlorophyll and carotenoids, which help stabilize the loosely packed and marginally hydrophobic α-helices in the LHC structure [306]. Similarly, in cytochrome c oxidase, two cardiolipin molecules that face the mitochondrial intermembrane side of the protein seem to stabilize the dimeric structure of the protein, whereas two other cardiolipin molecules that face the matrix side seem to function as proton traps, thus facilitating proton translocation along the protein's surface [307]. Other examples of lipid molecules that can be attributed specific functional roles are given in [68,294]. Nevertheless, it is not always easy to deduce the molecular basis for the lipid dependency of the protein from its three-dimensional structure. This is the case with the tetrameric KcsA channel, the activity of which depends on PG. The

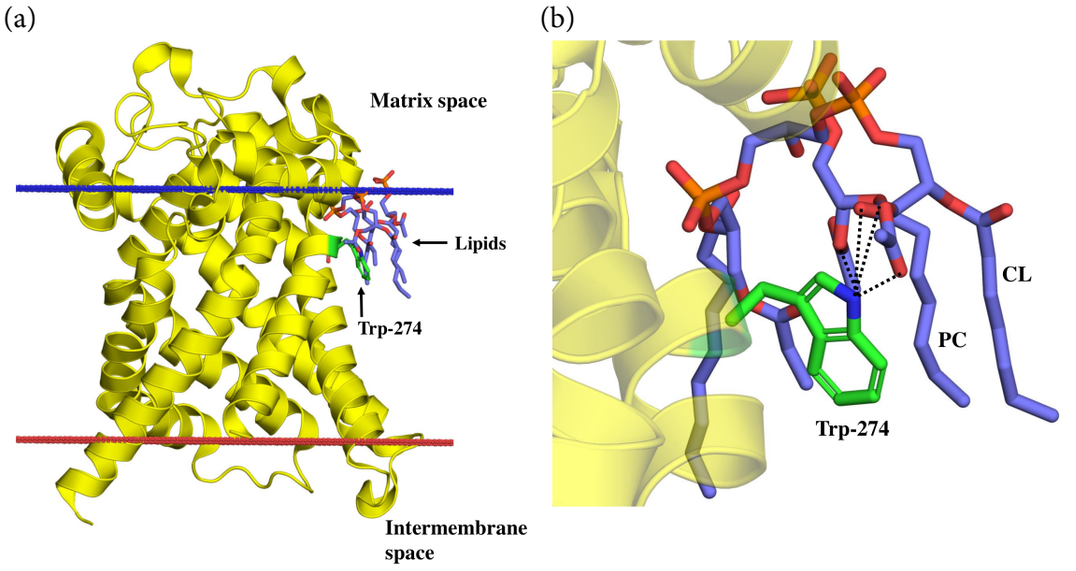

FIGURE 7.25 **Interaction between aromatic residues and lipids in biological membranes.** (a) The structure of the mitochondrial ADP/ATP carrier complex, colored in yellow (PDB entry 1okc). Trp-274 is shown as green sticks, and the adjacent lipids are shown as blue sticks. The red and blue lines mark the predicted boundaries of the membrane (the OPM database [117]). (b) A blowup of the region containing Trp-274, showing the interactions between this residue and two lipids, cardiolipin (CL) and phosphatidylcholine (PC). As explained in the main text, the large ring structure of Trp enables van der Waals and nonpolar interactions to take place between the residue and the nonpolar acyl chains of the lipids, whereas the polar NH group interacts electrostatically with the lipids' ester oxygen atoms and phosphate groups (black dashed lines). For clarity the orientation of the protein is different from that in (a).

phospholipid molecule binds to two Arg residues; each is contributed by a different subunit. This suggests that the role of PG is to help stabilize the quaternary structure of the protein. However, other studies show that KcsA does not require PG specifically, but settles with any negatively charged phospholipid [308]. Thus, it seems that PG's role in this system is to reduce the electrostatic repulsion between positive charges in the subunit interface, rather than to form a specific interaction.

One of the most extensively studied examples of specific protein-lipid interactions is that of PIP_2, a phospholipid that appears in minute quantities in the plasma membrane, almost exclusively on its cytoplasmic side [262,309]. Despite its rarity, PIP_2 is involved in important cellular processes, including endocytosis, exocytosis, phagocytosis, and vesicle transport within the cell. The interest in this molecule began when it was found to be a substrate for the cytoplasmic enzyme *phospholipase C* (*PLC*$_\gamma$). PLC$_\gamma$ splits PIP_2 into *inositol 1,4,5-trisphosphate* (*IP*$_3$) and *diacylglycerol* (*DAG*), two prominent second messengers in signal transduction pathways. Their combined action leads to the activation of the enzyme *protein kinase C* (*PKC*), which phosphorylates numerous targets within the cell and induces significant biological responses. Today we know that PIP_2 is in fact the source for three second messengers, and that its influence on the aforementioned processes is carried out mainly through them [310]. However, it seems that PIP_2 may also directly affect membrane proteins, primarily ion channels [309,311] and transporters [312,313]. What advantage does the PIP_2 dependency confer to these proteins? At least two come to mind, both related

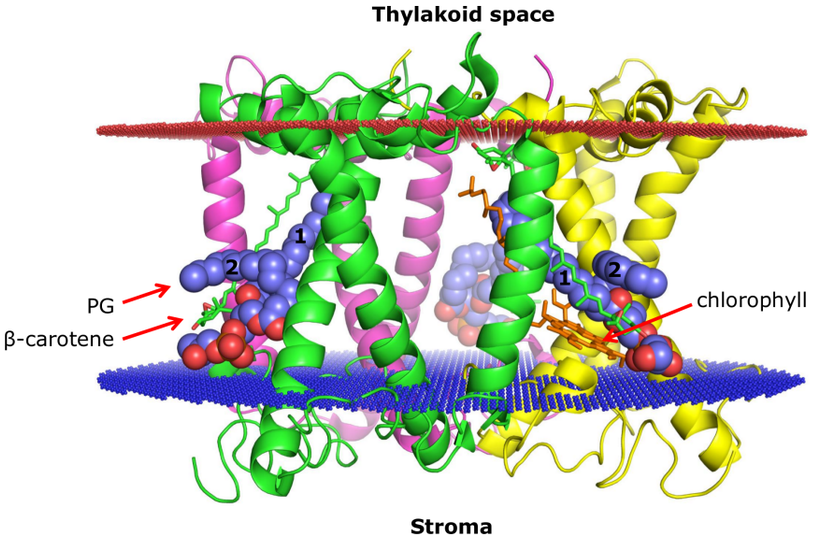

FIGURE 7.26 **Interactions between the light-harvesting complex of photosystem II (LHC-II) and phosphatidylglycerol (PG) in plants.** The backbone structure of the trimeric LHC is shown, with each subunit colored differently. The red and blue lines mark the predicted boundaries of the membrane (the OPM database [117]). The space between any two adjacent monomers contains a PG molecule (blue spheres) with one of its fatty acid chains penetrating into the trimer (1) and the other (2) pointing towards the lipid bilayer. Each PG molecule interacts with protein residues, as well as with a β-carotene pigment molecule (green sticks) that runs parallel to one of PG's chains, and with a chlorophyll molecule (orange sticks) that lies below this chain.

to regulation [309]. The first is simple; the dependency on PIP_2 ensures that these proteins are inactive unless they are attached to the membrane. Indeed, there are many cases in which the plasma membrane acts as a 'meeting place' for signaling proteins. This makes it easier for the different components of the pathway to interact with each other and propagate the signal. The second advantage of the PIP_2 dependency of proteins is indirect; since the levels of PIP_2 are affected by external signals (via the activation of PLC_γ), the dependency of certain proteins on this phospholipid subjects them as well to the same external signals.

Proteins bind PIP_2 in two main forms:

1. **Specifically.** This is carried out via a geometrically and chemically compatible binding site that recognizes PIP_2 using basic and other residues. There are several known binding sites of this kind; the best known is the *pleckstrin homology* (*PH*) domain [315]. This domain contains over 100 residues and has already been found to be present in about 250 human proteins. It is composed of a seven-strand and one α-helix β-sandwich (Figure 7.27). The binding to PIP_2 is carried out using basic residues that form salt bridges with the lipid's phosphate groups, and also via hydrogen bonds to other forming residues [316]. Different PH domains bind different phosphoinositides ($PI(3,4)P_2$, $PI(3,4,5)P_3$), where the spatial arrangement of the residues in the binding site determines the specificity. Other PIP_2 binding sites can be found in other domains, such as *FYVE*, *PX*, and *ENTH* [315].

2. **Non-specifically.** This is carried out via disordered protein segments, which adhere electrostatically and non-specifically to clusters of negatively charged PIP_2 in certain

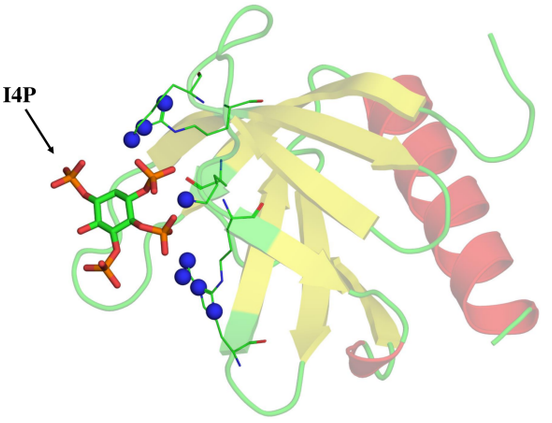

FIGURE 7.27 **Specific binding by the PH domain.** The structure of the PH domain of DAPP1 bound to inositol 1,3,4,5-tetraphosphate (I4P) is shown (PDB entry 1fao). The protein is shown using a ribbon representation. The Arg and Lys residues, interacting electrostatically with I4P, are shown as lines, with the N_ζ of Lys and $N_{\eta 1}$, $N_{\eta 2}$ of Arg shown as small spheres. For clarity, the backbone is rendered partially transparent. The basic residues in the figure are positioned such that they interact optimally and specifically with the phosphate groups of the ligand.

regions of the membrane. The adhesion is made possible by a number of basic residues at proximal positions within the sequence, which provide their corresponding segments with a general positive charge. The proximity of the basic residues to each other is also the cause for the disordered nature of such segments. One frequently used example of this type of binding is the aforementioned MARCKS, a 331-residue protein that is overall acidic, except for a 24-residue stretch, in which 13 residues are basic [261,317]. The positively charged part of this segment allows it to bind PIP_2 molecules and cluster them into a microdomain (Figure 7.28a). Moreover, the binding of MARCKS competes with PIP_2 interactions with other basic cytoplasmic proteins, and it seems that this is used as a regulatory mechanism of PIP_2-dependent signal transduction processes. Indeed, the IP_3-mediated rise in cytoplasmic Ca^{2+} levels (see above) leads to the binding of calmodulin (Ca^{2+}/CaM) to MARCKS, turning the positive electrostatic potential of MARCKS negative, thus inducing the departure of MARCKS from the PIP_2-rich region of the membrane [262] (Figure 7.28b–d). This makes PIP_2 available to other cytoplasmic signaling proteins, thereby allowing the signal to propagate. It should be mentioned that the electric field on MARCKS is also changed by PKC-induced phosphorylation of the protein. As explained above, PKC is activated by the same signal pathway that activates Ca^{2+}/CaM.

The two forms of PIP_2 binding described above differ both in binding specificity and in the structural requirements of the binding site. Although both forms exist, it seems that specific binding is more prominent. A mechanistic characterization of PIP_2 dependency is often not straightforward, although some studies have yielded interesting insights. For example, it has been suggested (based on models) that PIP_2 contributes to the gating mechanism of tetrameric K^+ channel-like proteins, by applying an electrostatic force to parts of the protein, which, as a result, shift and open the channel [309]. Other models that have been suggested are described in [311].

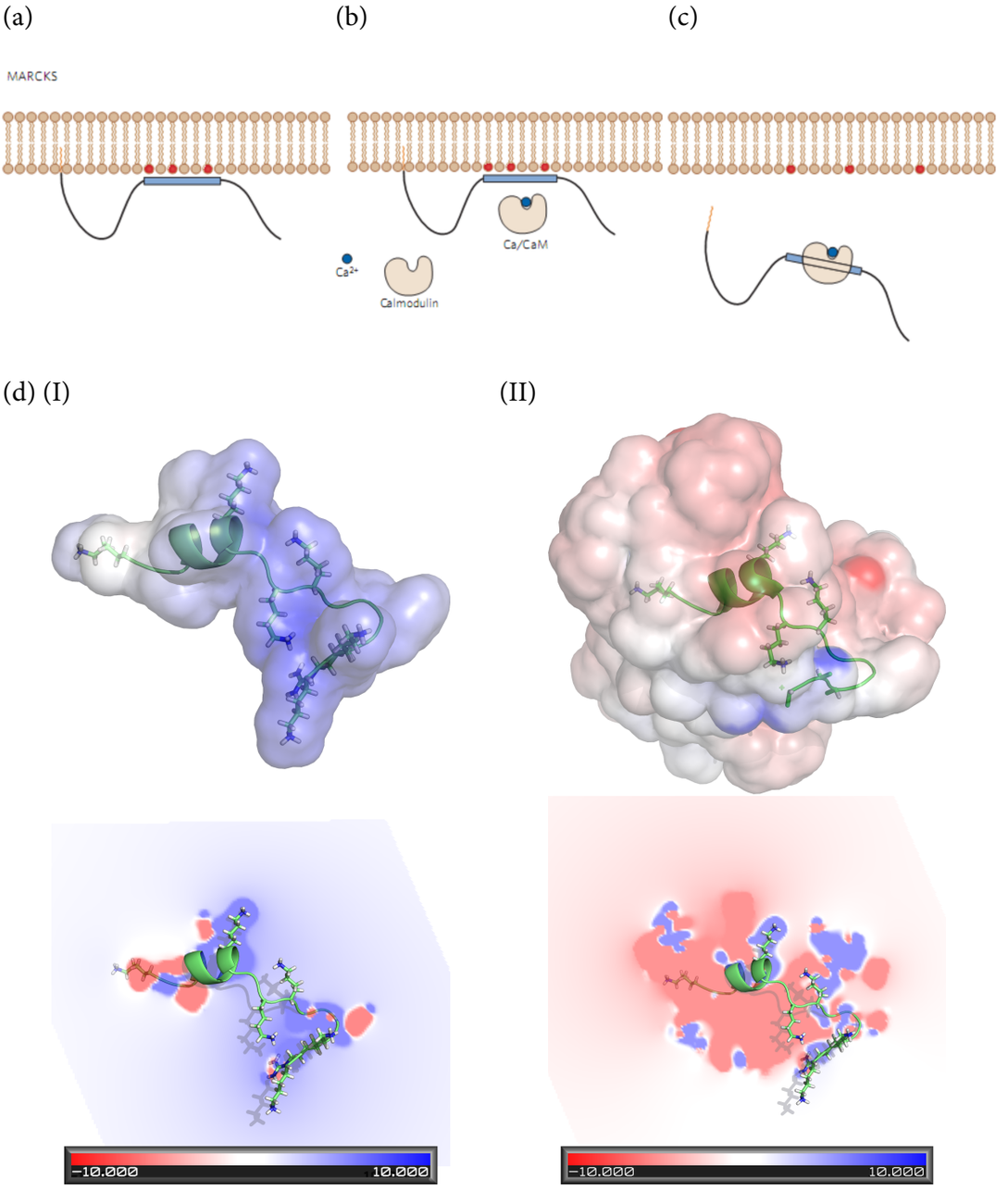

FIGURE 7.28 **Modulation of PIP_2 availability during signal transduction by MARCKS and Ca^{2+}/CaM.** (a) through (c) A schematic depiction. (a) MARCKS binding to PIP_2 lipid (red) via electrostatic interactions, during the resting state. (b) Ca^{2+} binding to CaM following the right signal, and the migration of the complex to the lipid bilayer. (c) Binding of Ca^{2+}/CaM to MARCKS induces detachment of MARCKS from the membrane. The figure was taken from [262]. (d) Electrostatic potential mapped on the surface (top) and on a two-dimensional slice (bottom) of (I) the MARCKS-derived 19-residue basic segment, known to bind to both PIP_2 and calmodulin (CaM), and (II) the complex between the same segment and CaM (PDB entry 1iwq). Negative potentials ($0k_BT/e > \Phi > -10k_BT/e$) are red; positive potentials ($0k_BT/e < \Phi < 10k_BT/e$) are blue; and neutral potentials are white (see color code at the bottom). The electrostatic potential was calculated using APBS [314]. As can clearly be seen, the free MARCKS segment has a strong positive potential, which is reversed upon binding to CaM. As explained in the main text, a similar effect on MARCKS' potential is achieved by PKC-induced phosphorylation of the segment (not shown).

7.4.2 Effects of membrane proteins on lipid bilayer properties

Hydrophobic inclusions such as proteins inside a membrane perturb the lipid order. The perturbation works at several levels, and may lead to different reactions of the bilayer's lipids. In the following subsections we summarize the main effects.

7.4.2.1 Decrease in mobility

Membrane lipids are dynamic, with motions that range from limited vibrations to large-scale movements such as lateral diffusion or flipping between bilayer leaflets. The mere presence of a hydrophobic inclusion in the lipid bilayer reduces the dynamics of lipids bordering the rigid inclusion, and this translates to loss of entropy. Statistical-thermodynamic models show that the insertion of even a single helix into the lipid bilayer reduces the entropy, with a corresponding free energy penalty of +2 kcal/mol [267,318].

7.4.2.2 Deformation and curvature changes

We have seen earlier that, because transmembrane segments vary in length, hydrophobic mismatch may arise between the length of a given transmembrane segment and the thickness of the hydrocarbon region of the lipid bilayer. Such mismatch may prompt changes not only in the structure and/or orientation of the transmembrane segment (see Subsection 7.4.1.1.2 above) but also in the membrane lipids. The primary response of the lipid bilayer to such mismatch is deformation, that is, stretching or compression of the acyl chains around the transmembrane segment, in order to compensate for negative or positive mismatch, respectively [259,266,319] (Figure 7.29a,c). The deformation leads to a local change in the curvature of the lipid bilayer, at the protein-lipid interface. This is made possible by the soft nature of the lipid bilayer, whose compressibility is 10^9 to 10^8 N/m^2 [320,321]. Recent measurements have shown that the effect of protein-induced deformation on membrane thickness is five times more significant than the effect of cholesterol, which was considered for a long time to be the prominent factor determining membrane thickness in higher eukaryotes [57]. Lipid-induced changes in curvature seem to be involved primarily in concentrating certain signaling proteins within the same membrane region [58]. The deformation of the membrane involves an energy cost, which has been assessed at 0.4 kcal/mol for a 4-Å reduction in membrane thickness [259] (see also [322] for other estimates). Interestingly, computational studies suggest that even when the length of the transmembrane segment is equal to or shorter than the hydrophobic thickness of the membrane, the segment may still tilt at least 10° from the membrane's normal, to increase its *entropy of procession* [323–325] (Figure 7.29b). This requires the membrane to deform inwardly, but the deformation penalty is compensated for by the entropy gain. In fact, the deformation penalty is associated with another form of entropy, that of the lipid chains. This is yet another example of two entropy-based terms that balance each other, in this case in the determination of the optimal tilt angle of the transmembrane segment in the lipid bilayer.

Protein shape has also been found to affect membrane curvature. That is, integral proteins with asymmetric profiles, i.e., proteins whose extracellular regions are smaller or wider than the intracellular regions, create either a positive or negative curvature (depending on the location of the wide region), especially when they oligomerize or aggregate [326] (Figure 7.30a).

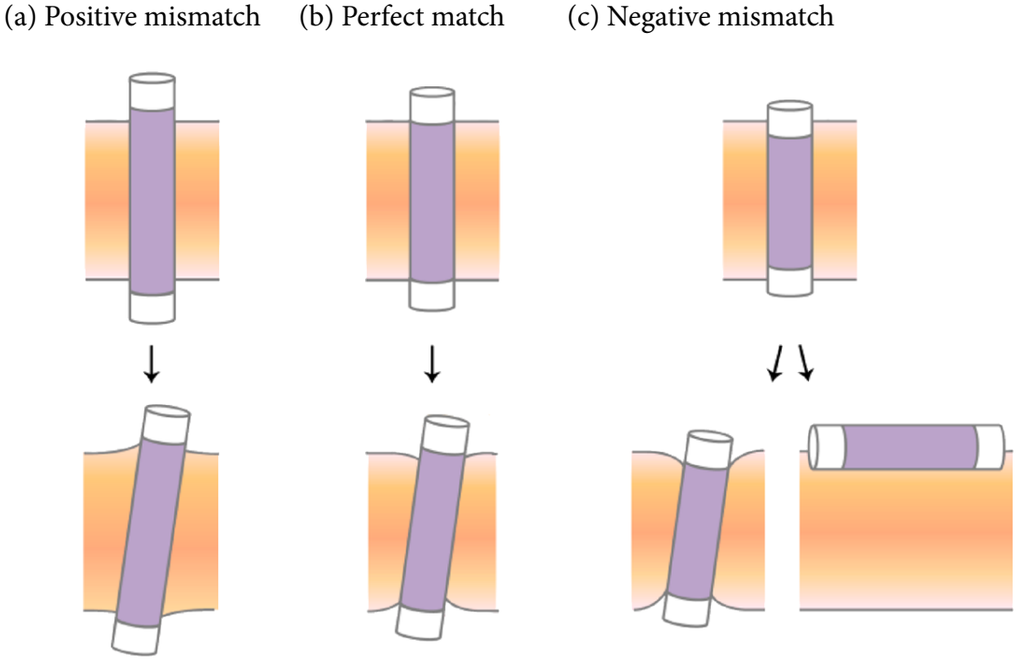

FIGURE 7.29 **Membrane deformation resulting from hydrophobic mismatch between the protein and lipid bilayer.** (a) Positive hydrophobic mismatch. (b) Perfect match. (c) Negative hydrophobic mismatch. The helix is represented as a cylinder, with the hydrophobic core in purple and the hydrophilic termini in white. (a) At positive mismatch, the transmembrane helix tilts, and the membrane expands to match the helix hydrophobic core. (b) At perfect match, the helix tilts because of the favorable increase in precession entropy, and the membrane thins so that the polar helix termini can remain in the lipid head group region rather than partition into the hydrocarbon region of the membrane. (c) At slight negative mismatch (lower left panel), the transmembrane helix tilts and the membrane thins locally as in perfect match. In cases of excessive mismatch, the helix adopts a surface orientation instead of forcing the membrane to thin beyond its elastic limit (lower right panel). The image is taken from [325] (http://pubs.acs.org/doi/full/10.1021/ct300128x).

In addition to these general properties of proteins, some specific cases are known in which the behavior of certain proteins has marked effects on membrane curvature:

1. **Actin polymerization.** The ability of the cytoskeletal protein actin to polymerize in response to certain signals is directly linked to changes in the plasma membrane, including curvature changes. Specifically, the polymerization creates mechanical pressure on the membrane [327], to the point of inducing curvature. This effect is important for several cellular processes, such as the formation of pseudopodia, phagocytic cups, endocytic invaginations, and even axonal growth cones (formed during the creation of the neural synapse) [328,329].

2. **Vesicle formation by coat proteins.** The formation of transport vesicles inside cells is carried out by *coat proteins* such as *clathrin*, *caveolin*, *COPI* and *COPII*, which are bound to the membrane peripherally [330–332]. Their activity leads to the application of mechanical pressure to the bilayer, and this pressure gradually increases the bilayer's curvature until the transport vesicle is formed. It was once assumed that the polymerization of these proteins was responsible for creating pressure on the membrane [333]. However, recent data have shown that clathrin, COPI and COPII do not

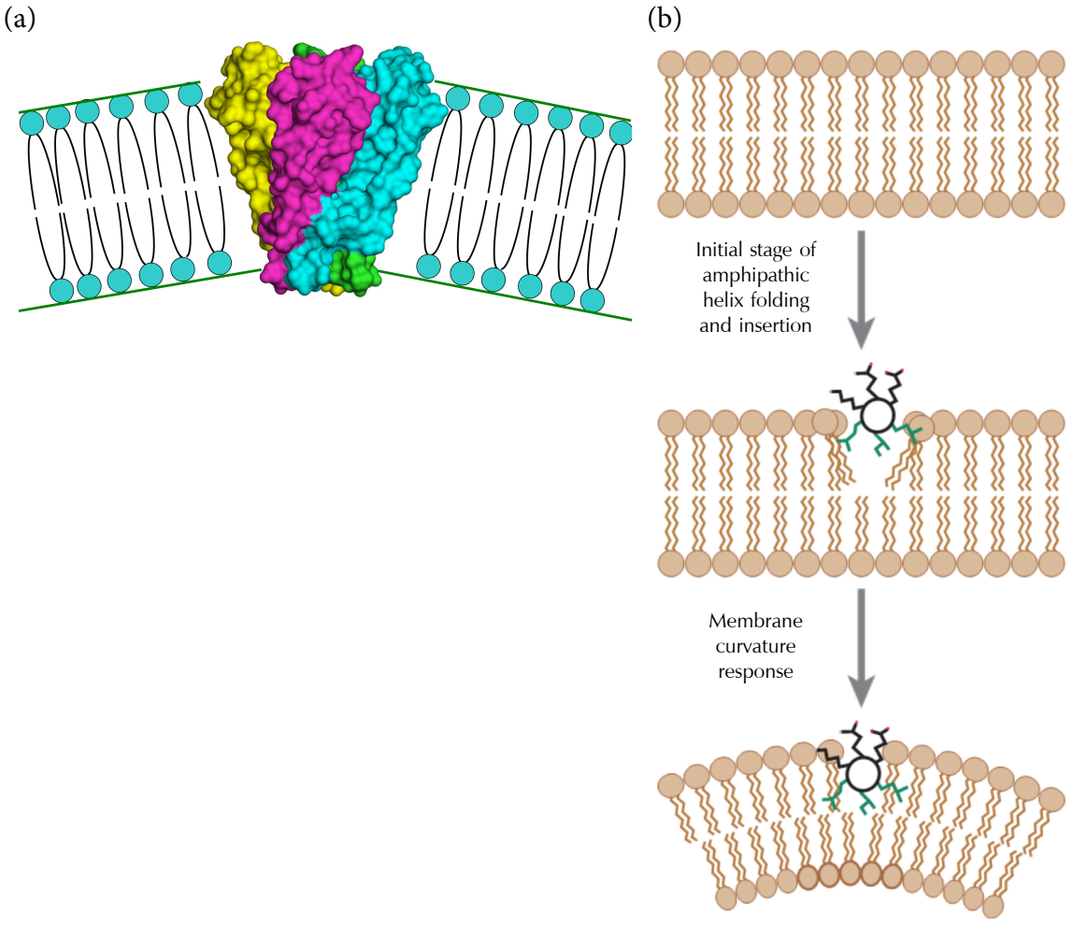

FIGURE 7.30 **Membrane deformation resulting from (a) protein shape and (b) mode of binding.** The protein in (a) is the KcsA voltage-gated potassium channel (PDB entry 1j95). With its teepee-like shape it has an uneven profile along the membrane normal, and is thus expected to cause membrane deformation. Each of the four chains of the channel is in a different color. (b) A model illustrating the bending effect of an epsin-like amphipathic helix, which partially immerses inside the bilayer and may ultimately induce membrane curvature. The figure was taken from [58].

form direct contacts with the membrane, but rather use other proteins (e.g., epsins), which create the mechanical pressure [334]. The latter usually contain amphipathic α-helices that are partially immersed inside the bilayer with their nonpolar side facing the hydrophobic core and their polar side stuck like a wedge between the lipid head groups. The lipids in contact with such α-helices change conformation to compensate for the membrane distortion, and that creates positive curvature in the bilayer [58]. What, then, is the role of clathrin, COPI and COPII? It seems that these proteins are responsible for concentrating the pressure-creating proteins in a particular region of the membrane, and after the vesicle has formed they polymerize to form a scaffold around it.

Formation of transport vesicles is an example of a dramatic, yet physiologically relevant effect of proteins on membrane curvature.

7.5 G PROTEIN-COUPLED RECEPTORS

Despite the limited number of experimentally determined structures of membrane proteins, the extensive research carried out has yielded numerous insights regarding the structural and sequence-related requirements for the function of these proteins. In this subsection we discuss structure-function relationships in G protein-coupled receptors (GPCRs), which play a central role in many physiological processes and related disease, and whose action involves structural complexity, such as changing conformation and binding multiple partners.

7.5.1 Introduction

Single-cell organisms and cells in multicellular organisms communicate with their environments via highly complex signal transduction systems (see Chapter 1, Subsection 1.1.3.5). Such systems contain multiple components, starting from the cell surface and ending in intracellular proteins and small molecules (Figure 7.31a). The first cellular component responding to the incoming message is the membrane-bound receptor. Cells contain a multitude of receptors that respond to different types of messengers. These include external messengers, absorbed from the organism's environment (odorants, pheromones, tastes, etc.), and internal ones (hormones, neurotransmitters, local modulators). When activated, cell-surface receptors can relay the signal into the cell, to a diverse set of enzymes and small molecules or elemental ions. Most of these species function as *transducers-amplifiers*, since they pass on the message while amplifying it by acting on multiple cellular targets. Others act as *end effectors*, i.e., proteins whose activation (or inhibition) leads to an end result. This result may range from relatively small cellular responses, such as the production and/or release of a chemical compound, to more dramatic responses, such as cellular division and even suicide.

Membrane-bound receptors can be classified according to their types of responses to ligand binding:

1. Ion channels
2. Tyrosine kinases
3. Serine and threonine kinases
4. Guanylate cyclases
5. Cytokine receptors (defined by ligand type)
6. G protein-coupled receptors (GPCRs)

GPCRs are by far the largest and most common family of membrane receptors. They are widely represented in most life forms[*1]; in vertebrates they constitute 1% to 5% of the entire genome [336–338], and in the human genome they are encoded by more than 800 genes [339].

[*1] GPCRs seem to be missing in plants, although this matter is controversial. G-proteins do exist in plants, but it has been claimed that they are activated by receptor-like kinases (RLKs) rather than by GPCRs [335].

Another impressive trait of GPCRs is their ability to respond to a huge variety of external messengers, including proteins, peptides, small organic molecules, elemental ions, and even photons of light. These messengers may function as hormones, neurotransmitters, local mediators, pheromones, or environmental factors. Accordingly, GPCRs participate in numerous physiological processes [340], and are involved in many diseases and pathological syndromes, in which they are either inactive or overactive*1. These diseases include hypertension, congestive heart failure, stroke, cancer, thyroid dysfunction, congenital bowel obstruction, abnormal bone development, night blindness, and neonatal hyperparathyroidism [343]. Clearly, GPCRs are promising drug targets, and indeed, it is estimated that 30% to 50% of clinically prescribed drugs act by binding to GPCRs and changing their activity [343–346].

7.5.2 GPCR signaling

7.5.2.1 General view

As their name implies, GPCRs relay signals into cells primarily via large GDP/GTP-binding proteins, called *G-proteins*. Once activated, G-proteins may activate different effector proteins in a process resembling a cascade. That is, each molecule activates a number of effector proteins, and the number of activated proteins grows as the signal advances downstream of the pathway. Thus, the end result of GPCR signaling usually involves either the activation or inhibition of a large number of effector proteins, which include enzymes, ion channels, proteins associated with transport vesicles, and others. **The types of proteins activated in a given GPCR pathway depend on the messenger molecule, GPCR, and G-protein that are activated**. For example, in the *cAMP-PKA pathway* (Figure 7.31b), signaling via certain GPCR and G-protein types leads to activation of *adenylyl cyclase* (*AC*) and the production of the second messenger *cAMP*. The latter activates *protein kinase A* (*PKA*), which in turn phosphorylates numerous cytoplasmic proteins. The phosphorylation activates some of the proteins, while inactivating others. In another universal signaling pathway, the G-protein activates *phospholipase C* (*PLC*) instead of adenylyl cyclase. PLC hydrolyzes the membrane lipid *phosphatidylinositol 4,5-bisphosphate* to two second messengers, *diacylglycerol* (*DAG*) and *inositol 1,4,5-trisphosphate* (IP_3). The combined action of both messengers leads, through a massive, yet short-lived Ca^{2+} influx into the cytoplasm, to the activation of *protein kinase C* (*PKC*), which phosphorylates different proteins than does its PKA counterpart, thus leading to different outcomes.

Because it involves multiple components, GPCR signaling is inherently complex. This complexity is compounded by the following properties:

1. A single GPCR may activate different G-proteins, and even certain non-G proteins [349]. For example, the β_2-adrenergic receptor is known to activate the *MAP kinase* pathway.

2. Most GPCRs tend to have some degree of baseline activity [350]. That is, they are active to some extent even when not binding their activating ligands (*agonists*).

*1 For example, overactive GPCRs may affect the formation and spreading of tumors by trans-activating cancer-related receptors such as the epidermal growth factor receptor (EGFR) [341], and by promoting cell migration during metastasis [342].

(a)

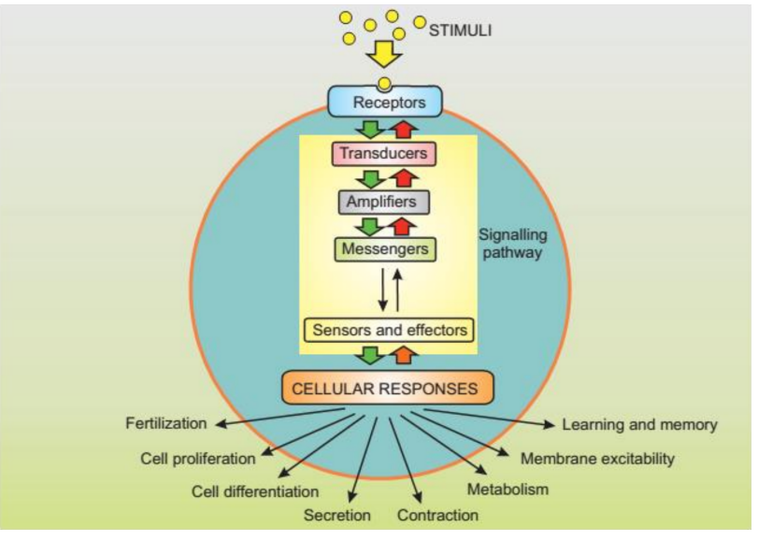

(b)

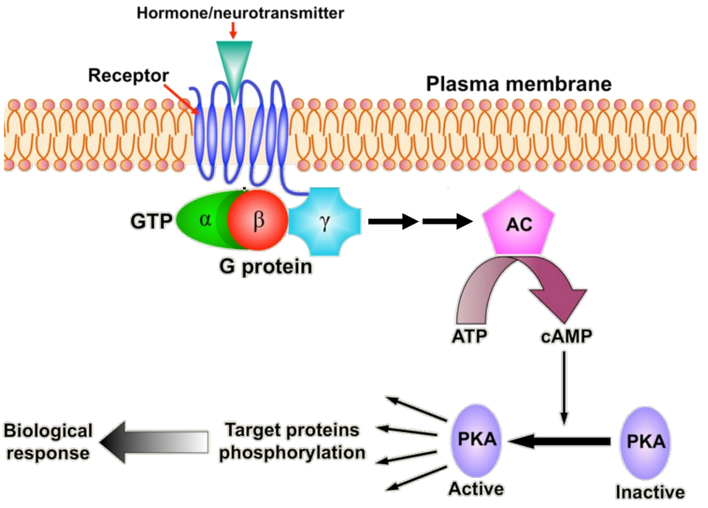

FIGURE 7.31 **The main players in a typical signal transduction cascade.** (a) A general scheme showing the principal components in a signal transduction cascade. Stimuli (e.g., hormones, neurotransmitters or growth factors) act on cell-surface receptors, which activate transducers to relay the signal into the cell. The transducers use amplifiers to generate internal messengers, which either act locally or diffuse throughout the cell. These messengers then engage sensors that are coupled to the effectors responsible for activating cellular responses. Note that the order of some of the components may differ somewhat across different signaling pathways. For example, messengers may be used to activate amplifiers instead of being produced by them (see panel (b)). The green arrows indicate ON mechanisms, which enable information to flow down the pathway, and the red arrows indicate opposing OFF mechanisms, which switch off the different steps of the signaling pathway. Virtually all of the components mentioned above may be proteins. The image is taken from [347]. (b) The cAMP-PKA cascade. Binding of an external chemical messenger (hormone, neurotransmitter, etc.) to a membrane-bound protein receptor induces the activation of an enzyme called a G-protein, which acts as a transducer. The activation of the G-protein leads to the activation of adenylyl cyclase (AC), which catalyzes the conversion of ATP into cyclic AMP. The latter acts as an intracellular messenger. It binds to and activates the enzyme amplifier PKA, which, in turn, phosphorylates a large set of cytoplasmic proteins. The phosphorylated proteins may activate other cellular components, or perform a certain function (that is, they may act as sensors and/or effectors). In any case, this signal transduction eventually leads to changes in the cell's behavior, i.e., to a biological response.

3. A single GPCR may respond to different types of ligands, each eliciting a different outcome [351] (Figure 7.32):

   - *Full agonists* induce maximal receptor activity by stabilizing an active conformation.
   - *Inverse agonists* decrease the baseline (constitutive) activity of the receptor by stabilizing an inactive conformation.
   - *Partial agonists* induce partial activity since they have some affinity to both active and inactive conformations.
   - *Antagonists* prevent other ligands from binding to the GPCR and activating it.

   These observations are in line with two currently accepted models of protein dynamics [350]. The first, referred to as the *'pre-existing equilibrium' model* [352–362] (see Chapter 5), stipulates that even in the absence of a bound agonist, the active conformation of the protein is sampled sufficiently to yield some degree of baseline activity [363]. The second is the so-called *'conformational selection' model* [364–370] (see Chapter 8), which stipulates that each ligand binds and stabilizes a different conformation of the GPCR, which has a different intrinsic activity. Since a single GPCR can modulate different pathways, the same ligand may have opposing effects on two different pathways that are modulated by the same GPCR, by stabilizing a conformation of the GPCR that is compatible with only one of the pathways [371]. This phenomenon is often used in the design of drugs acting on GPCRs.

4. The activity of GPCRs may be affected by their oligomerization (see below), by their localization to certain membrane compartments, or by the lipid composition of the membrane [371].

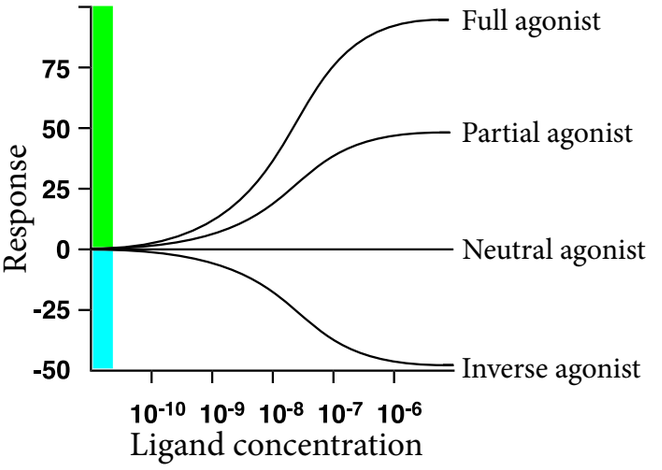

FIGURE 7.32 **Idealized dose response curves of a cellular receptor to a full agonist, partial agonist, neutral antagonist, and inverse agonist.** The constitutive activity of the receptor is assumed to be zero. Note, however, that many receptors have a baseline activity even in the absence of an agonist. Adapted from [348].

7.5.2.2 G-protein mechanisms and regulation

As explained above, GPCRs relay external signals into the cell via G-proteins. Each of these proteins contains three subunits, α, β, and γ (or Gα, Gβ and Gγ, respectively), which may appear in different forms; so far, 23 genes have been found to code for Gα, 5 for Gβ, and 12 for Gγ [338]. Based on the Gα types, G-proteins have been classified into four different families, each of which tends to activate or inhibit specific targets [372]:

- *Gαs* – activates adenylyl cyclase → cAMP-PKA signaling cascade. This family is also over-activated by the *cholera toxin* via covalent modification.
- *G$\alpha i_{/o}$* – inhibits adenylyl cyclase and activates c-Src tyrosine kinases; covalently inactivated by the *pertussis toxin*.
- *G$\alpha q_{/11}$* – activates PLC_{β} → IP_3-PKC signaling cascade.
- *$G\alpha_{12/13}$* – leads to Rho activation.
- *$G\alpha_{transducin}$* – activates cyclic GMP (cGMP) phosphodiesterase (transducin) in the retina.

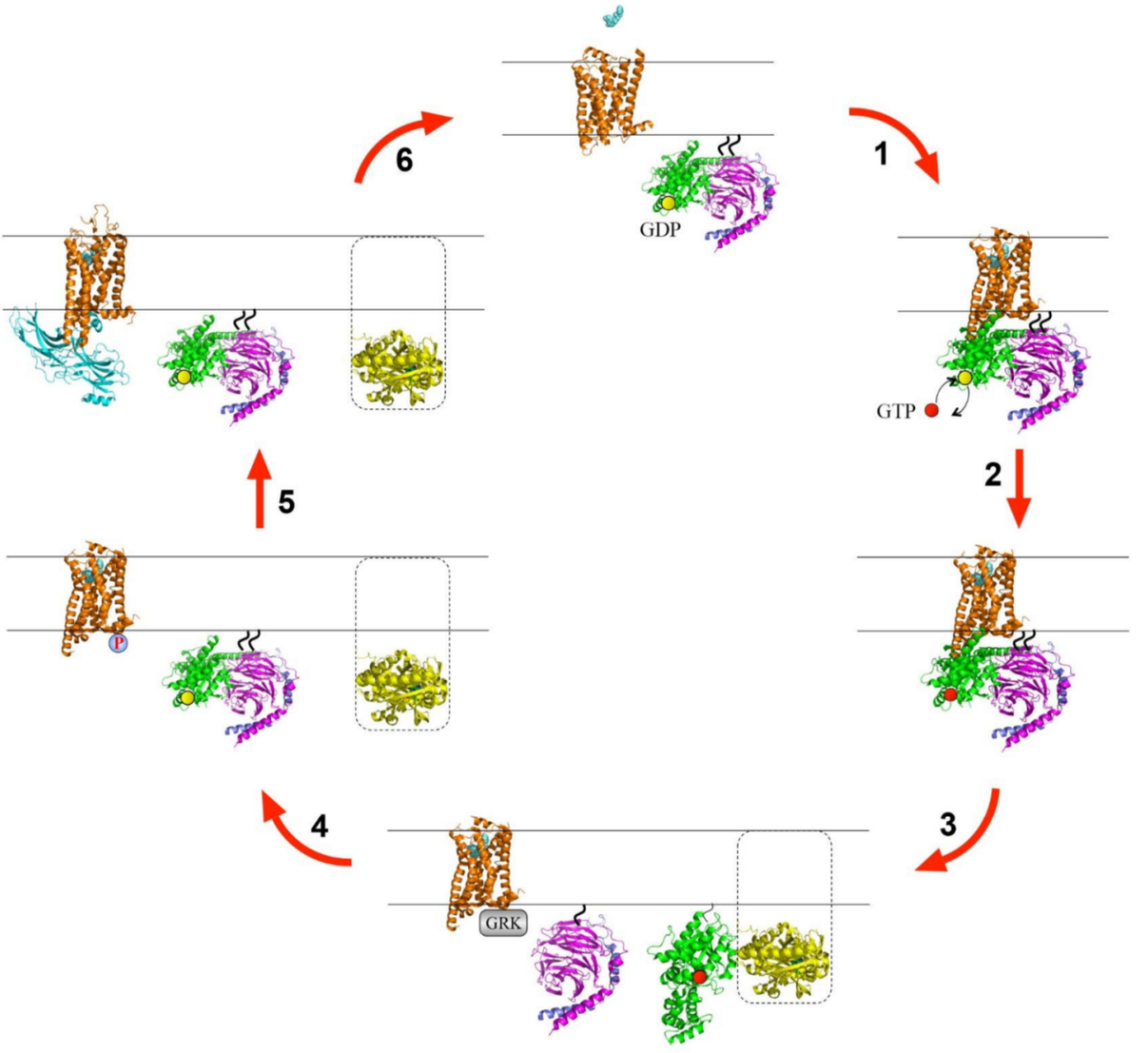

In the G-protein's resting state, its three subunits, Gα, Gβ and Gγ, are bound tightly to each other, and Gα binds the guanine nucleotide GDP (Figure 7.33). The G-protein is attached to the membrane via covalently-bound lipid chains; a palmitoyl or myristoyl chain bound to Gα's *N*-terminus, and an isoprenyl chain bound to the C-terminal *CAAX* motif of Gγ (not shown). Gβ is tightly bound to Gγ via nonpolar interactions and therefore need not be attached to the membrane covalently. The 'resting' G-protein may bind to an active (agonist-bound) or inactive GPCR, or just drift in the membrane. However, when it binds to an active GPCR, it switches from a resting state to an active state. Specifically, **the activated, agonist-induced GPCR conformation induces a conformational change in the G-protein's α subunit (Gα), leading to the exchange of GDP with GTP (Figure 7.33, step 2).** Thus, the immediate role of GPCRs is to act as *GDP/GTP exchange factors* (*GEF*)[*1]. The binding of GTP to Gα leads to the departure of the latter from the G$\beta\gamma$ complex, and the binding of Gα to an effector protein (Figure 7.33, step 3). This binding activates the effector protein. The G$\beta\gamma$ complex also has its effectors, which may be different from or identical to those of Gα (e.g., PLC [376]). Gα possesses GTPase activity, and after a short while hydrolyzes its bound GTP to GDP. This returns Gα to its original conformation, allowing it to reattach to the $\beta\gamma$ subunits (Figure 7.33, step 4). The resting state is restored, and the entire system is ready for another activation cycle. Interestingly, the intrinsic GTPase activity of Gα, though present, is too slow for cellular requirements. G-proteins must therefore use the assistance of proteins referred to as *'regulators of G protein signaling'* (*RGSs*) to accelerate GTP hydrolysis to the required speed [377]. The GPCR cycle also includes regulative steps that ensure the inactivation and internalization of the GPCR (Figure 7.33, steps 4 through 6). The steps are discussed below.

FIGURE 7.33 **The GPCR signaling cycle.** (Opposite) The cycle includes six basic steps: (1) binding of agonist (aquamarine spheres) to the extracellular domain of the inactive GPCR (orange ribbon), followed by the binding of G-protein to the intracellular part of the GPCR. The GPCR structures shown here are those of the β_2-adrenergic receptor: the inactive structure is taken from PDB entry 2rh1 and the active structure is taken from entry 3sn6. In the G-protein's resting state, the Gα subunit, represented by the green ribbon, is attached to the $\beta\gamma$ subunits, represented by the purple and blue ribbons, respectively. Gα in this state is bound to GDP (yellow sphere). The Gα subunit and the Gγ subunit are covalently attached to the membrane (short wavy curves). (2) and (3) Activation of the G-protein, which involves exchange of GDP with GTP (red sphered) in Gα's nucleotide binding site (2), separation of Gα from G$\beta\gamma$ and binding of Gα to an effector protein (3). The Gα-effector complex shown here is taken from PDB entry 1cul. The effector in this complex is the enzyme *adenylyl cyclase*, and only the catalytic subunits are shown (yellow ribbon). The entire region of adenylyl cyclase, which also consists of a transmembrane domain, is marked by the dashed line. The binding of the G$\beta\gamma$ complex to its effector protein is not shown. (4) after a certain amount of time Gα hydrolyses its bound GTP molecule, which causes Gα to separate from its effector protein and re-bind to the G$\beta\gamma$ complex. Following the activation of the GPCR and G-protein, the GPCR undergoes deactivation to terminate the signal. This process includes binding of a G protein-coupled receptor kinase (GRK) to the intracellular domain of the GPCR (3), phosphorylation of the domain by the GRK (4), and binding of arrestin (cyan) to the phosphorylated domain (5, PDB entry 4zwj). The binding prevents the GPCR from re-binding to the G-protein and also induces the internalization and recycling of the GPCR (see Subsection 7.5.5). The entire activation-deactivation cycle is brought to completion with arrestin's departure from the GPCR and return of the system to its resting state (6).

[*1] Note that while GPCRs can bind several types of G-proteins, each GPCR has a strong preference for one G-protein [375].

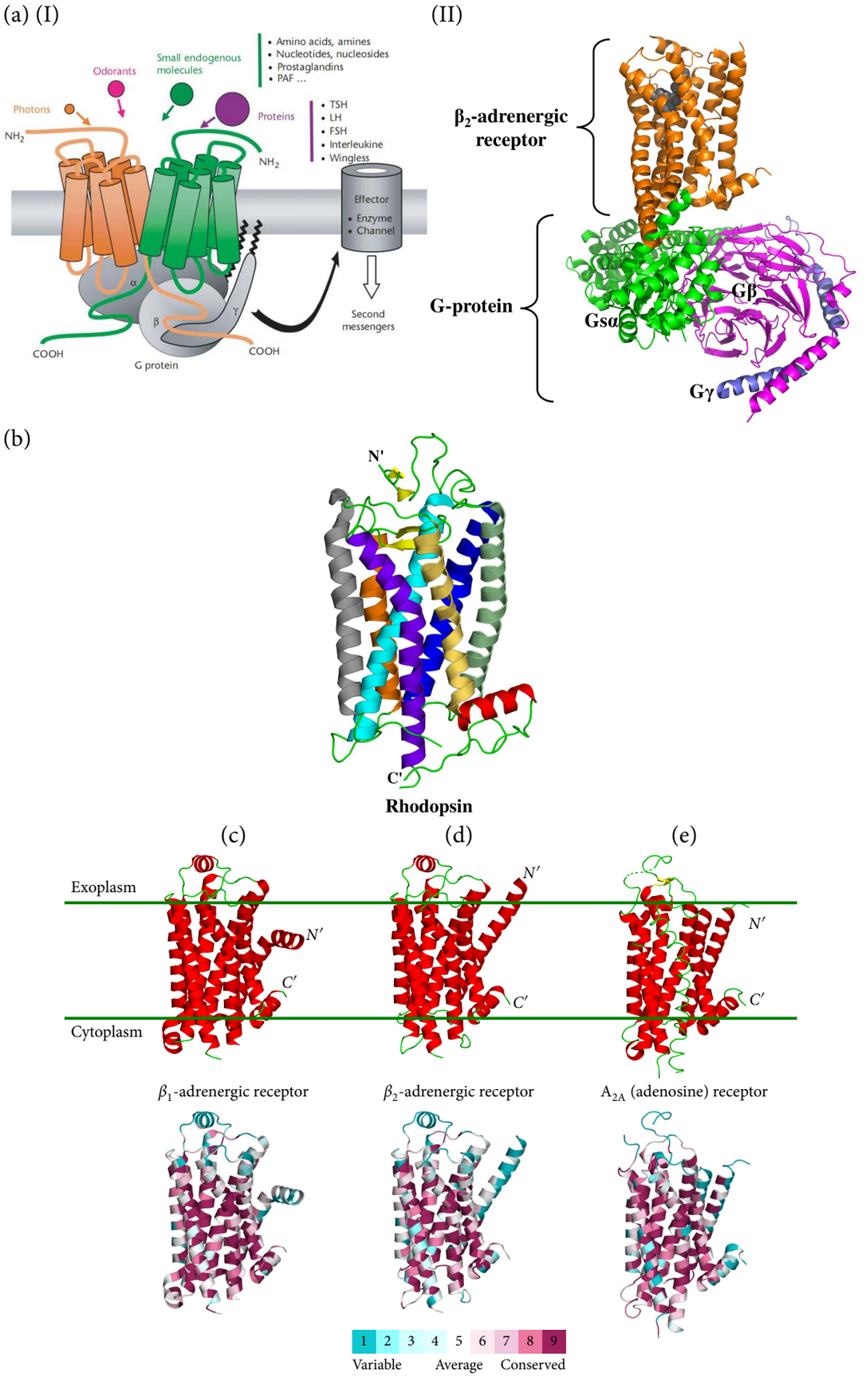
(a) (I)
Amino acids, amines
Nucleotides, nucleosides
Prostaglandins
PAF ...
Small endogenous molecules
Odorants
Photons
Proteins
TSH
LH
FSH
Interleukine
Wingless
NH2
NH2
Effector
Enzyme
Channel
α
β
γ
Second messengers
COOH
COOH
G protein
(II)
β2-adrenergic receptor
G-protein
Gβ
Gsα
Gγ
(b)
N'
C'
Rhodopsin
(c)
(d)
(e)
Exoplasm
Cytoplasm
N′
C′
β1-adrenergic receptor
β2-adrenergic receptor
A2A (adenosine) receptor
1 2 3 4 5 6 7 8 9
Variable
Average
Conserved

7.5.3 GPCR structure

7.5.3.1 General features

As in the case of other membrane-bound proteins, GPCRs' structures have also been late to arrive due to technical difficulties. However, in recent years the difficulties have been successfully tackled, and numerous structures of GPCRs have emerged, although most of these belong to class A[*1]. Many of these structures have been solved by Brian Kobilka's group. Kobilka and Robert Lefkowitz received the 2012 Nobel Prize in Chemistry for their work on GPCRs, starting from the detection of the β-adrenergic receptor and identification of the gene that codes for it. As of the end of 2017, the PDB contained 220 GPCR structures that have been experimentally determined. These correspond to ~25 different receptors (without counting subtypes), including those for adrenaline, adenosine, dopamine, histamine, acetylcholine, serotonin, glutamate, opioids, sphingosine, chemokines, neurotensin, purine nucleosides, and free fatty acids (see reviews in [378,379]). **These studies indicate that GPCRs share several common structural characteristics, the primary characteristic being a transmembrane core containing seven α-helical segments, termed TM1 through TM7, and arranged in a counter-clockwise configuration (when viewed from the extracellular side;** Figure 7.34a–e) [336,372]. Although not all seven-transmembrane receptors are GPCRs, most are. The seven helices are preceded by the extracellular N', and followed by the intracellular C'. The transmembrane segments are interconnected by loops of different lengths at both the extracellular and intracellular sides (these loops are termed ECL1-3 and ICL1-3, respectively). Spectroscopic studies focusing on the refolding of bacteriorhodopsin (a seven-

FIGURE 7.34 **G protein-coupled receptors (GPCRs).** (Opposite) (a) The overall structure of the GPCR–G-protein system. (I) A schematic depiction of GPCRs, taken from [336]. The left side of the image shows a GPCR dimer, bound to its cognate G-protein. The upper-left side shows the different ligands that may bind to the extracellular side of the GPCR and activate it, and the upper-right side shows examples of two of the possible ligands, i.e., proteins and small molecules. The effector molecule, i.e., the enzyme or channel that may be affected by the activated GPCR, and as a result induce the action of a second messenger, is shown on the right side of the figure. (II) The three-dimensional structure of the β_2-adrenergic receptor in complex with Gs-protein (PDB entry 3sn6). The GPCR is shown in orange, with the agonist presented as grey spheres. The α, β, and γ subunits of the G-protein are colored in green, magenta, and blue, respectively. (b) The crystal structure of inactive bovine rhodopsin (PDB entry 1hzx). The N' of the polypeptide chain faces the extracellular side of the membrane. Each of the seven transmembrane helices in the core of the protein is colored differently. (c) through (e) Other GPCRs of known structure positioned similarly to rhodopsin in (b), colored by secondary structure (top) and evolutionary conservation level (bottom). Conservation levels (cyan – lowest, maroon – highest; see color code in figure) are estimated using ConSurf (http://consurf.tau.ac.il) [373,374]). (c) The β_1-adrenergic receptor bound to the antagonist cyanopindolol (PDB entry 2vt4). The structure contains several point mutations in the transmembrane region, as well as deletions in the C' region, which were introduced to increase its stability. (d) The β_2-adrenergic receptor bound to the inverse agonist carazolol (PDB entry 2rh1). (e) The adenosine (A_{2A}) receptor bound to the antagonist ZM241385 (PDB entry 3eml). It is noteworthy that one of the transmembrane spans forms a banana-like helix.

[*1] For a list of all known GPCR structures, including annotations on co-crystallized ligands and their functional effects, see the GPCRDB database (URL: http://gpcrdb.org/).

transmembrane protein that does not interact with a G-protein) in lipid vesicles imply that the common seven-transmembrane core of GPCRs is not accidental, as seven is the minimal number of transmembrane helices required for preserving the environment of the ligand. On the basis of that observation, White speculated that seven helices can "*provide ample space for ligands, through relatively minor helix distortions and reorientations, without the need to increase or decrease the number of transmembrane helices*" [161]. **Besides the number of transmembrane helices and loops, most GPCRs also share certain sequence motifs (see below), and a disulfide bond between a cysteine residue at the extracellular tip of TM3 and another cysteine residue in ECL2**[*1]. The disulfide bond is important in shaping the entrance to the ligand-binding pocket. As we will see below, the extracellular domain (ECD) of GPCRs is the principal ligand-binding site, although in many GPCRs the ligand may also interact with parts of the transmembrane domain (TMD) [380].

Despite sharing several structural characteristics, GPCRs differ in several ways, and these differences give rise to diversity. Most of the differences are localized at the intra- and extracellular regions of the protein, but some are in the transmembrane region. For example, a GPCR may contain additional helices beyond the seven that span the membrane. This is the case in the β-adrenergic receptors, which contain an eighth helix, positioned along the extracellular membrane plane (Figure 7.34c–d). There have also been reports of a μ-opioid receptor variant that has only six transmembrane helices [381,382], as well as of a GPCR-like sequence with a predicted transmembrane domain comprising only five helices [383], but these predictions have not been confirmed structurally. Phylogenetic analysis shows that GPCRs can be grouped into six classes, based on their similarity (see [336] for further detail):

- **Class A or 1 (rhodopsin class).** This class includes most GPCRs (~85%); members of this class respond to both endogenous and exogenous (odorants, pheromones) ligands. Proteins in this class can be further grouped into the following subclasses:

  Subclass I includes receptors that respond to small ligands (e.g., neurotransmitters or even light photons), and whose ligand-binding sites reside within the transmembrane region. Clustering of GPCRs belonging to this subclass [384] suggests that they can be further divided into the following groups: *amine*, *opsin*, *melatonin*, *prostaglandin*, and *MECA* (melatonin, EDG, cannabinoid and adenosine).

  Subclass II includes receptors for peptides. The ligand-binding site of each member of this subclass is built from several segments on the protein's extracellular side.

  Subclass III includes receptors for glycoprotein hormones. The binding site of each protein in this subclass resides primarily in the protein's very large extracellular domain.

- **Class B or 2 (secretin class).** These proteins are similar to class AIII despite a lack of sequence similarity. They respond to large protein and peptide hormones such as:

  Gastrointestinal hormones and factors: glucagon, secretin, vasoactive intestinal peptide (VIP), glucagon-like peptide 1 (GLP-1), glucose-dependent insulinotropic polypeptide (GIP), and others.

[*1] Many GPCRs contain multiple disulfide bonds in the extracellular domain; these bonds stabilize the protein's structure.

Other hormones and factors: corticotropin-releasing factor (CRF), growth hormone-releasing factors (GRF), calcitonin, pituitary adenylate cyclase activating polypeptide (PACAP), and parathyroid hormone (PTH).

Class B GPCRs are also targeted by *α-latrotoxin*, the toxin produced by the black widow spider.

- **Class C or 3 (glutamate class).** This class includes metabotropic glutamate receptors (mGluRs), Ca^{2+}-sensing receptors (CaSRs) of the parathyroid, kidney, and brain [385], $GABA_B$ receptors, pheromone receptors, sweet and amino acid taste receptors (TAS1R), and odorant receptors in fish [386].
- **Class D or 4** includes fungal mating pheromone receptors.
- **Class E or 5** includes *cAMP* receptors in *Dictyostelium discoideum* (slime mold). They are involved in developmental control of the organism.
- **Class F or 6 (Frizzled/Smoothened class).** Members of this class are involved in many cellular and physiological processes (e.g., embryonic development). They activate key signaling pathways, such as the *Wnt pathway*.

Note that all classes also include *orphan receptors*, i.e., proteins that share structural characteristics with known receptors, but are activated by natural ligands that are yet to be found [387].

In the following subsections we will focus on class A GPCRs, for which we have ample structural knowledge. In Subsection 7.5.6 we discuss GPCRs of classes B, C, and F.

GPCRs were initially assumed to work as single polypeptide chains, in contrast to receptor tyrosine kinases, which are known to dimerize. Today, however, it is recognized that **many GPCRs dimerize or oligomerize within biological membranes [336,388–390], and such events are believed to have a role in GPCR signal transduction and crosstalk between different signaling pathways [391,392]**. Much of the information gathered on GPCR dimerization comes from class C receptors, which are active only in their dimeric form [393,394]. Whereas some of these, such as mGluRs, are homodimers, others, such as the $GABA_B$ receptor, are heterodimers. In the case of the $GABA_B$ receptor, one polypeptide chain binds the ligand whereas the other binds the G-protein [395], and is also needed for bringing the entire receptor to the cell surface. Dimerization and oligomerization, with a preference for homodimers, have also been observed in class A GPCRs [396–399] (Figure 7.35). Interestingly, in this class the monomeric form is also active [397,400], and the role of dimerization (or oligomerization) is probably regulatory for the most part. That is, dimerization facilitates better regulation of GPCR activity through cooperativity, crosstalk between different GPCRs in the same heterodimer, etc. [389] Dimerization is usually mediated by the transmembrane region of the GPCRs, but other regions may contribute as well [379]. For example, in the β_1-adrenergic receptor the dimer has two interfaces, involving residues from transmembrane helices, as well as from extracellular and intracellular loops [401]. Moreover, membrane lipids may also contribute to dimerization, as has been suggested in the case of the β_2-adrenergic [402], μ-opioid [403], and mGlu [404] receptors.

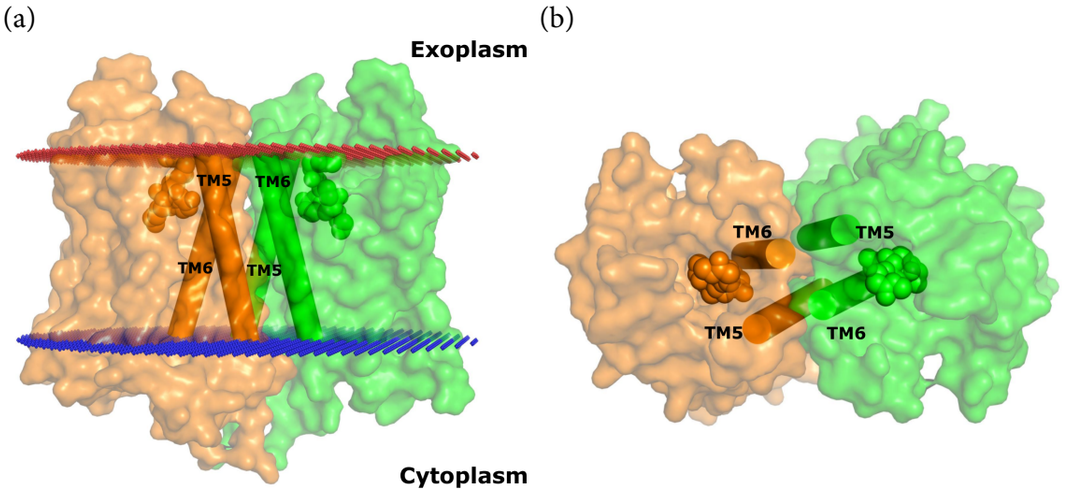

FIGURE 7.35 **A two-fold symmetric dimer formed by the μ-opioid receptor [396].** The receptor (PDB entry 4dkl) is shown in a surface representation from (a) the side and (b) the top (extracellular). Each monomer is colored differently. The two bound ligands (one in each monomer) are shown as spheres. The red and blue lines mark the predicted boundaries of the membrane (the OPM database [117]). The dimerization is mediated by a four-helix bundle motif, formed by TM5 and TM6 (shown as cylinders). On their opposite faces TMs 5 and 6 line the ligand-binding sites, which may be related to the role of dimerization in regulating receptor activity.

7.5.3.2 Structural variations among GPCRs

Since the year 2000, bovine rhodopsin in its inactive state has been the only source for accurate structural analysis of GPCRs. Rhodopsin is a light-activated protein in retinal rod cells, whose function is to convert visual input into neuronal signals that can be transmitted to the brain (via the optic nerves) for processing. Although it has a highly specialized function, rhodopsin has always been a model for the structure of class A GPCRs, mostly because of its overwhelming abundance[*1] and stability; in complete darkness, it assumes only a single (inactive) conformation. These properties enabled scientists to characterize the structure of rhodopsin much earlier compared with other GPCRs, and to study the protein extensively using various approaches [405]. β-adrenergic receptors, which respond to *catecholamines* (see Box 7.2), have also served as popular models of class A GPCRs. As in the case of rhodopsin, their popularity stems from historical reasons; the β-adrenergic receptors were the first GPCRs to be sequenced and cloned after rhodopsin [406], and their three-dimensional structures were also solved quite early. Compared with rhodopsin, however, adrenergic receptors and many other GPCRs are considerably less stable, and their crystallization requires the use of stabilization methods. These usually include mutations or truncation of unstable parts (e.g., the third intracellular loop, ICL3) and attachment of these parts to an antibody fragment or to another protein (e.g., T4-lysozyme). Lower stability is often related to increased flexibility, which suggests that even when the GPCR is agonist-free and inactive, it can still sample other conformations, including the active one. Indeed, as noted above, most GPCRs are characterized by baseline activity even in the absence of an activating signal, whereas rhodopsin has no baseline activity.

[*1] It constitutes 90% of the protein in purified retinal rod outer segments.

As explained above, GPCRs share very similar structures (especially within each class), which is remarkable considering the low sequence identity among members of the group. For example, rhodopsin and the β_2-adrenergic receptor share only 21% identical amino acids, yet the r.m.s.d. between their structures is merely 2.3 Å, and in the transmembrane region it is 1.6 Å. Nevertheless, some differences do exist between GPCRs, and these merit analysis. In the following paragraphs we review the main conclusions obtained thus far for class A GPCRs, by addressing the three different regions of GPCRs (i.e., extracellular, transmembrane and intracellular) separately.

1. **The extracellular (EC) region**
   As expected, **most of the differences between GPCRs are localized to the extracellular domain (ECD), and particularly to the ligand-binding site and adjacent loops** [371]. ECL2 is particularly important in distinguishing among GPCR structures, as it is the largest loop and can therefore assume different conformations. In contrast, ECLs 1 and 3 are much shorter and usually do not have a distinct secondary structure. Here are a few examples:

   Rhodopsin (Figure 7.36a): The EC region has a compact, rigid tertiary structure, which significantly restricts the access of solvent and other molecules to the ligand-binding pocket [407]. This is not surprising; first, rhodopsin's 'ligand' is light (i.e., photons), which does not require a wide entrance. Second, solvent access to the retinal cofactor (see Subsection 7.5.4 below) would result in hydrolysis of the bond connecting the retinal to the polypeptide chain [371]. The main structural element preventing the solvent from reaching the retinal is ECL2, which forms a short β-sheet. It also blocks the main entrance to the ligand-binding pocket and prevents movement of the transmembrane helices [405].

   β-adrenergic receptors (Figure 7.36b): These represent the opposite case, with an open EC region. In particular, ECL3 does not interact with any of the other loops, ECL2 forms a very short helix, and the N' is altogether disordered [371,407].

   Adenosine (A_{2A}) receptor (Figure 7.36c): ECL2 lacks secondary structure, yet remains rigid due to disulfide bridges that stabilize it and the entire extracellular region of the receptor. Polar and van der Waals interactions involving the three loops also contribute to stabilization. It has been suggested that the role of the disulfide bridges is to constrain segments of the EC regions that are involved in ligand binding [407].

   Neurotensin receptor (Figure 7.36d) and other peptide-binding GPCRs: The extracellular region is more open than that in non-peptide-binding GPCRs, and ECL2 forms a hairpin structure.

   Sphingosine 1-phosphate receptor (Figure 7.36e) and other lipid-activated GPCRs: The extracellular region is capped by the N' (organized as a helix) and ECL1, which block the entrance of the ligand to its binding pocket. In these GPCRs, the highly hydrophobic ligands are thought to gain access to their binding pockets through the membrane.

2. **The transmembrane region and ligand-binding pocket**
   This region is where GPCRs vary the least, especially those that belong to the same

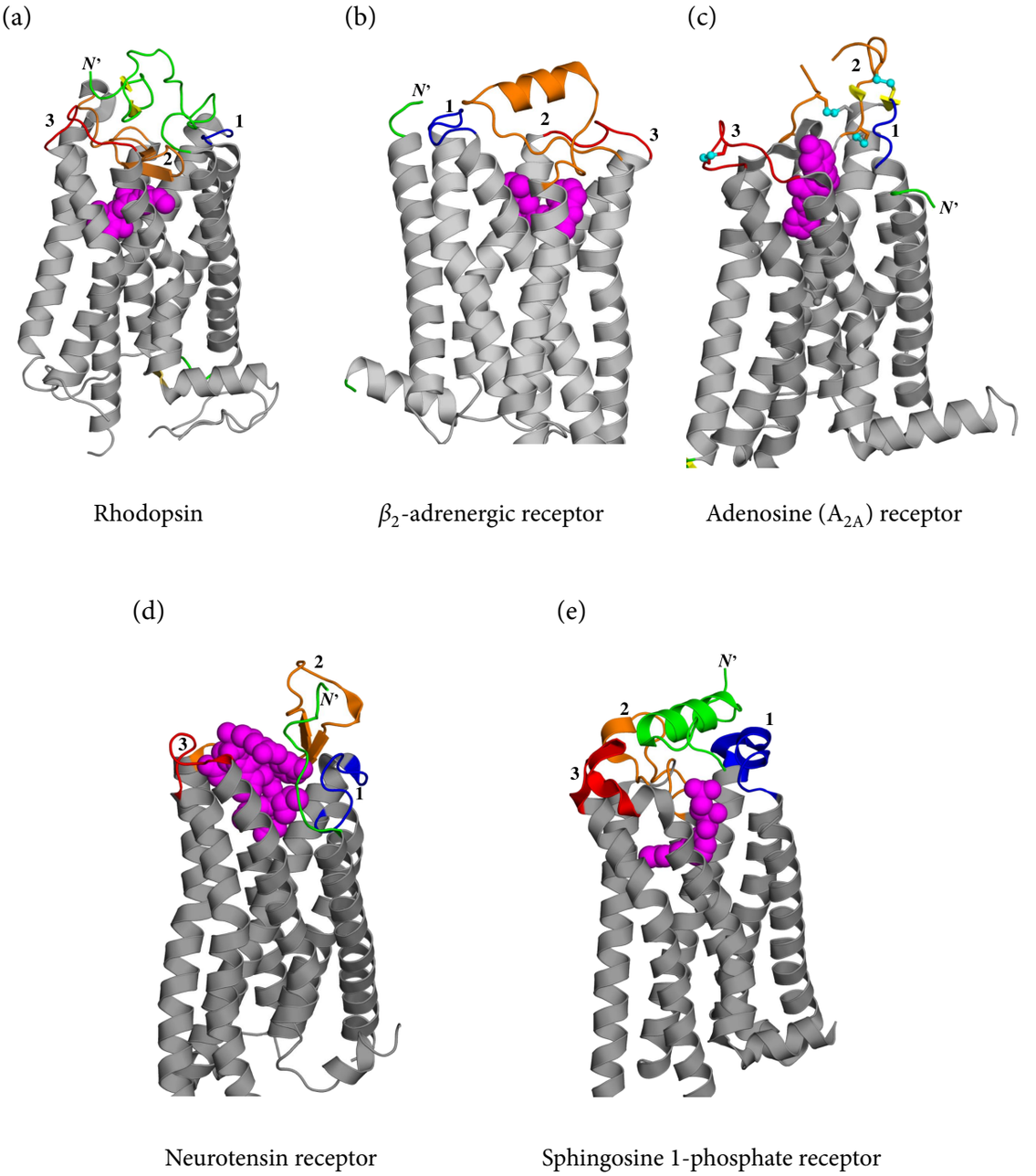

FIGURE 7.36 **The extracellular regions of different class A GPCRs.** (a) Bovine rhodopsin (PDB entry 1hzx). The first, second and third extracellular loops are in blue, orange, and red (respectively), whereas the *N*-terminus is in green (the loop numbers are also noted in the image). The retinal cofactor is presented as magenta spheres, within the transmembrane region (in grey). (b) Human β_2-adrenergic receptor (PDB entry 2rh1). The ligand, carazolol, is presented as magenta spheres. (c) Human adenosine (A_{2A}) receptor (PDB entry 3eml). Sulfur atoms of loop-related disulfide bonds are shown as small cyan spheres, and the ligand as magenta spheres. (d) Rat neurotensin receptor (PDB entry 4xee). (e) Human sphingosine 1-phosphate receptor (PDB entry 3v2w).

class. Still, even this region contains parts that are structurally more similar than others. This is evident in a structural alignment between the various structures, showing a core of 97 residues that have a C_α-r.m.s.d. of only 1.3 Å [407]. The other, less structurally similar residues, are expected to be involved in those functions that make GPCRs distinct from each other, i.e., ligand- and G-protein-binding. One of the common structural characteristics of the GPCRs listed above is the chemical environment of the highly conserved *NPxxY motif*, located at the intracellular end of TM7 [371]. This region is involved in key conformational changes occurring during GPCR activation (see Subsection 7.5.4 below). Interestingly, the helix in all the above GPCR structures is distorted in this region due to the presence of Pro in the sequence motif. The helical distortion is, however, stabilized electrostatically by hydrogen bonds to other residues or adjacent water molecules (Figure 7.37).

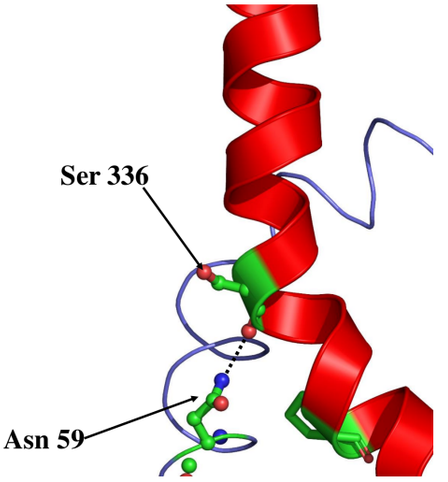

FIGURE 7.37 **Stabilization of helical kink by hydrogen bond.** TM7 of the β_2-adrenergic receptor is shown as a red ribbon. The kink of the helix is seen clearly. The proline residue that induces the kink is presented as sticks. The kink breaks the backbone hydrogen bond involving the carbonyl oxygen of Ser-336. However, the latter is stabilized by Asn-59 of TM1 (blue ribbon), which hydrogen-bonds to Ser-336 (dotted black line).

The structure of the β_2-adrenergic receptor [402,408] provides interesting insights regarding GPCR-lipid interactions. The structure contains a cholesterol-binding site between transmembrane helices 2 through 4, which comprises evolutionarily conserved residues. These include Trp-158 and Ile-154 on TM4, and Ser-74 on TM2 (Figure 7.38). Trp-158, which is highly conserved, is geometrically compatible with the ring(s) of the bound cholesterol. This compatibility optimizes the nonpolar, van der Waals and CH-π interactions between Trp-158 and cholesterol. It has been suggested that the cholesterol-binding residues constitute an allosteric site of GPCRs [407], in accordance with the proposed role of cholesterol as a modulator of the function of membrane proteins in general [409,410], and of GPCRs in particular [411–413]. As mentioned above, cholesterol and other membrane lipids are also thought to contribute to the dimerization of GPCRs, which itself is believed to participate in the regulation of GPCR signaling.

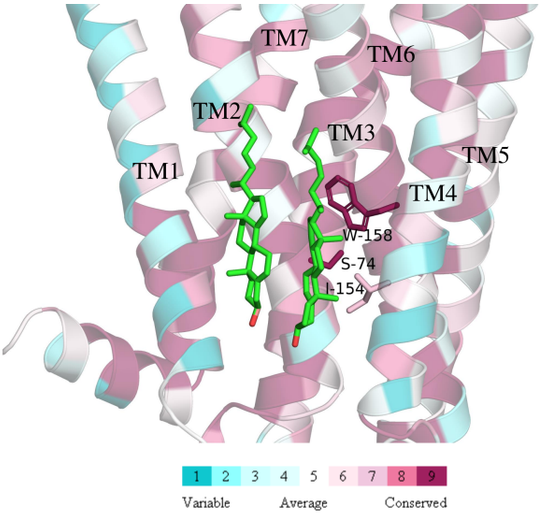

FIGURE 7.38 **Cholesterol binding to the β_2-adrenergic receptor (PDB entry 3d4s).** The cholesterol molecules are shown as sticks (colored by atom type), whereas the receptor is represented as ribbons, colored according to evolutionary conservation level (cyan – lowest, maroon – highest; see color code in figure). The conservation levels are calculated using ConSurf (http://consurf.tau.ac.il) [373,374]. The evolutionarily conserved residues Trp-158, Ile-154 and Ser-74 are shown as sticks. These residues are adjacent to the site of many therapeutic agents that act on class A GPCRs [407], and their location is an attractive target for future drugs.

Though the ligands of all class A GPCRs interact with both the transmembrane and EC domains, the position of the binding pocket varies significantly across the different receptors, although not in all cases. For example, the pockets of rhodopsin and the β-adrenergic receptors are quite similar to each other, with the ligand extending between TMs 3 and 7 and the interface between TMs 5 and 6 [407]. However, in rhodopsin the bound retinal cofactor extends further and is in physical proximity with Trp-265 on TM6, which is part of the conserved *CWxP motif* (Figure 7.39a). This residue, together with Phe-208, is part of a mechanism called the *'transmission switch'* [414], which participates in the propagation of the signal to the intracellular part of rhodopsin upon activation (see Subsection 7.5.4 below). In the β-adrenergic receptors the inverse agonist is separated from Trp-286 (the equivalent of Trp-265) by aromatic residues. In contrast to rhodopsin and the β-adrenergic receptors, the binding pocket of the adenosine (A_{2A}) receptor has a very different location. First, it is located closer to the interface between TM6 and TM7, where the ligand can interact with the second extracellular loop, ECL2. Second, the ligand extends perpendicularly to the membrane plane, and seems to be shifted towards the membrane-solvent interface, where part of it is solvent-exposed [117].

Peptide-binding GPCRs such as the chemokine, neurotensin, and opioid receptors have to accommodate ligands that are larger than biogenic amines like adrenaline, or nucleotides like adenosine. As a result, the binding sites in these GPCRs tend to be shallower than those in the other class A GPCRs, and the peptide ligands tend to bind closer to the extracellular domain (Figure 7.39b). Still, as in GPCRs that bind small molecules, there is variability in ligand locations and interactions within the peptide-binding GPCRs [378].

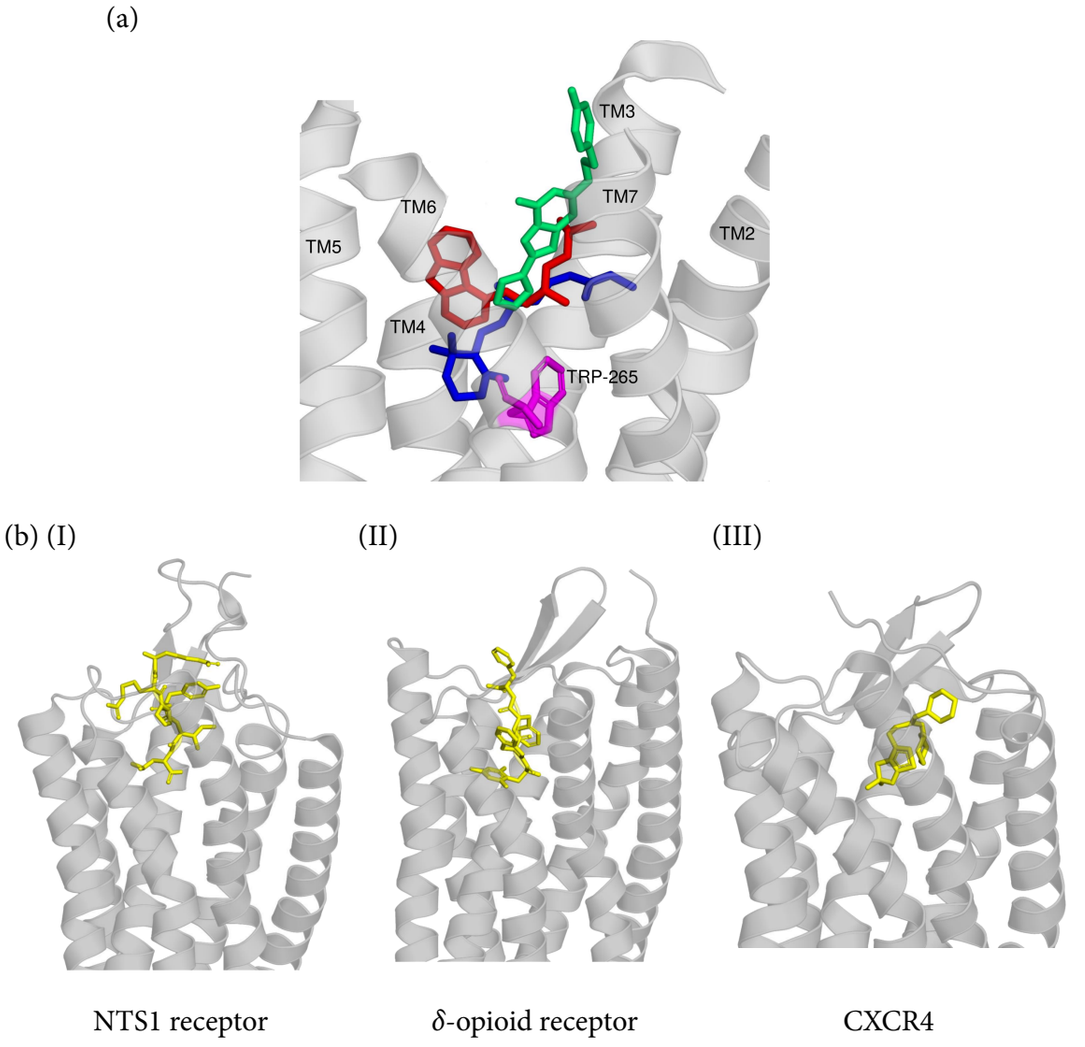

FIGURE 7.39 **Ligand binding sites in class A GPCRs.** (a) The sites of rhodopsin, the β_2-adrenergic receptor, and the A_{2A} receptors are represented by their respective ligands, as blue, red, and green sticks. Rhodopsin's Trp-265 is shown in magenta. For clarity, only rhodopsin's helices are shown, in grey. (b) Peptide binding to class A GPCRs. (I) the neurotensin 1 (NTS1) receptor (PDB entry 4xee), (II) the δ-opioid receptor (PDB entry 4rwa), and (III) CXCR4 (the human chemokine receptor 4, PDB entry 3odu). As the image demonstrates, in peptide-binding receptors, the peptides, shown as yellow sticks, tend to bind closer to the extracellular domain of the GPCR than compared to the small ligands of other class A GPCRs.

3. **The intracellular region**
   The structure of the intracellular region of GPCRs is relatively conserved, probably because of the limited diversity of potential binding partners, which include G-proteins, arrestins, and G protein-coupled receptor kinases (GRKs; see Subsection 7.5.5 below). Members of class A GPCRs have several distinct structural characteristics, one of which is the conserved sequence motif *D/ERY* at the intracellular side of TM3 [336]. The three-dimensional structure of rhodopsin, which was the first GPCR structure to be determined, demonstrated an electrostatic interaction, referred

to as the *'ionic lock'*, between Arg-135 of the motif and the adjacent Glu-247 on TM6 (Figure 7.40). The sequence involved in the ionic lock was conserved, suggesting that the interaction was important. Furthermore, it was found that activation of rhodopsin leads to the disruption of the ionic lock (see below). On the basis of these data, in addition to data obtained from mutational studies, it was suggested that the ionic lock is important for the stabilization of the inactive state of GPCRs, and possibly for their activation or signaling as well [371,407]. However, when the three-dimensional structures of other inactive GPCRs (e.g., the β-adrenergic receptors, the A_{2A} receptor, and the muscarinic (M_2) receptor) were determined, the ionic lock was found to be absent in these structures. **Other studies of β-adrenergic receptors have indicated that the ionic lock is in fact in constant equilibrium between two conformations, one in which it is formed and the other in which it is broken [415,416]. The partial or complete absence of the ionic lock in the inactive forms of β and A_{2A} receptors may explain why these receptors have measurable baseline activity in their inactive states, whereas rhodopsin does not [417].**

Another interesting point emerges from comparing the structures of vertebrate and invertebrate rhodopsins, represented by bovine [418] and squid [419,420] rhodopsins, respectively. As far as their function is concerned, the two proteins respond to the same agonist and differ only in their G-protein specificity. Intriguingly, this difference seems sufficient to create detectible topological differences in the intracellular regions of the two structures [407]. The largest difference is in the third intracellular loop, ICL3, which is attributed to the longer sequence of squid rhodopsin in that region [421]. Indeed, ICL3 is considered to confer specificity to the intracellular binding partner; swapping this part between GPCRs results in switching the receptors' G-protein selectivity [422].

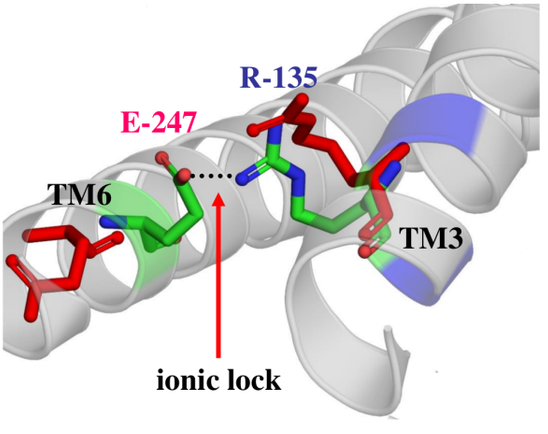

FIGURE 7.40 **The D/ERY motif.** The figure shows the Arg residue of the *D/ERY* motif in the intracellular domain of rhodopsin (colored by atom type) and the β_2-adrenergic receptor (red). In rhodopsin, this residue forms an ionic interaction (dashed line) with an adjacent Glu residue (colored by atom type). However, in the β_2-adrenergic receptor it is too far from its respective Glu (red) to be engaged in a salt bridge.

BOX 7.2 ADRENERGIC RECEPTORS: FIGHT YOUR ASTHMA AND YOUR ENEMIES

Adrenergic receptors mediate the physiological effects of adrenaline and noradrenaline in the animal body [423] (Figure 7.2.1)[*a]. Adrenaline and noradrenaline belong to a group of hormones and neurotransmitters called *'catecholamines'*, which are produced from the amino acid tyrosine [424–426]. There are two sources of catecholamines in the animal body: the nervous system and the medulla (core) or the adrenal glands. The nervous system implicates catecholamines in *neurotransmission*[*b], whereas the medulla implicates them — and particularly adrenaline — in *hormonal action*. The two catecholamines have a very important function; they prepare the body for a situation called *'fight-or-flight'* [428] (Figure 7.2.2). It is easy to understand this situation when considering the lives of wild animals and prehistoric man. In both cases, life in the wild is full of danger for the individual. The danger can appear abruptly, in the form of a predator, competitor, and even a routine, yet catastrophic, act of nature. In such cases, the difference between life and death often lies in the ability of the individual to respond very quickly to the danger. This response involves perceiving the danger and taking appropriate action.

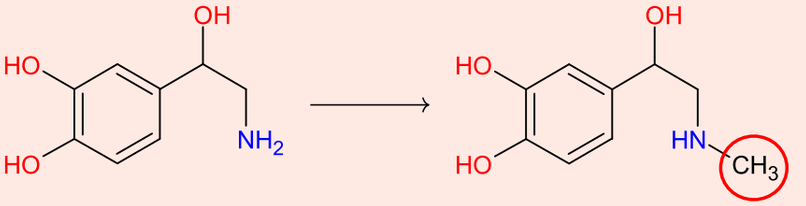

Noradrenaline Adrenaline

FIGURE 7.2.1 **The molecular structures of adrenaline and noradrenaline.** Adrenaline is formed by *N*-methylation of noradrenaline.

Indeed, upon detection of danger, the brain, which collects input from sensory organs, innervates other organs (via sympathetic nerves) in order to get them ready for action. Innervation of the two adrenal glands, located on top of the kidneys, stimulates their neurosecretory cells to secrete adrenaline (and to a lesser extent noradrenaline) into circulation, which further enhances the body's readiness to handle the danger.

As the term 'fight-or-flight' implies, the immediate response of the body to danger, following the action of adrenaline and noradrenaline, may be reduced to two simple options: fighting or fleeing, depending on the situation. Both types of responses require top performance of several body systems. First, sensory organs, such as the eyes, must collect as much information as possible from the environment, so as to be able to alert the body to danger. Second, skeletal muscles must be ready to respond quickly and

[*a] Adrenaline and noradrenaline are also called epinephrine and norepinephrine, respectively.

[*b] Although both adrenaline and noradrenaline are used as neurotransmitters in the central nervous system (CNS), and the *sympathetic* branch of the *autonomic nervous system* (*ANS*), noradrenaline is much more common in this capacity [427].

powerfully. This response involves the functions of several organs; the heart and lungs must supply ample oxygen to the skeletal muscles, and the body's sugar stores in the liver and muscles must be broken down quickly to supply the muscles with available fuel. In addition, bodily functions that usually take place in the resting state and require the functioning of certain organs (e.g., digestion by the gastrointestinal (GI) system), must be inhibited, so as to allow peripheral blood to reach the muscles in high volumes.

FIGURE 7.2.2 **A wolf in a fight-or-flight posture.** The image is taken from [429].

Clearly, some of these responses are neurological in nature (e.g., activation of skeletal muscles), whereas others are metabolic (e.g., breakdown of sugar stores). Adrenaline participates in both types of responses, whereas noradrenaline specializes in the former. The two catecholamines carry out their functions via a set of adrenergic receptors, which reside in various tissues. The specific effects of activating these receptors are detailed in Table 7.2.1. These effects mainly include constriction or dilation of blood vessels (depending on the organ), as well as contraction of some muscles and relaxation of others. Together, these effects create the following physiological outcomes [424]:

1. Increased heart rate and stroke volume[*a].
2. Diversion of blood from the skin and GI tract to the heart, lungs, brain, and skeletal muscles.
3. Increased blood pressure.
4. Pupil dilation.
5. Windpipe dilation.
6. Relaxation of GI smooth muscle.
7. Increased blood clotting rate → less danger of hemorrhages following injury.
8. Increased sweating → cooling down of overworked body.
9. Increased metabolic rate, resulting from the breakdown of both liver lipid stores and muscle glycogen stores.

[*a] The amount of blood the heart can pump out in a single beat.

TABLE 7.2.1 **Some of the physiological effects of adrenergic receptors.**

Receptor Subtype	Location	Effect
α_1	Blood vessels	Smooth muscle contraction $\longrightarrow$ Vasoconstriction
	Heart	Increased cardiac contraction and rate
α_2	Blood vessels	Smooth muscle relaxation $\longrightarrow$ Vasodilation
β_1	Heart	Increased cardiac contraction and rate
	Kidney	Activation of renin-angiotensin-aldosterone system $\longrightarrow$ Na^+–K^+ exchange $\longrightarrow$ Na^+ retention
β_2	Blood Vessels	Smooth muscle relaxation $\longrightarrow$ Vasodilation
	Heart	Increased heart rate and output
	GI tract	Smooth muscle relaxation
	Pancreas	Glucagon secretion $\longrightarrow$ glycogen breakdown and gluconeogenesis
β_3	Liver	Lipid breakdown

The adrenal glands act not only in response to fight-or-flight threats, which are immediate and potentially life-threatening, but also to more prolonged types of threat, called *stress* [430]. In the latter case, however, the adrenal glands are activated hormonally by the brain; the *hypothalamus*, which is the hormonal control center of the brain, stimulates the pituitary *adrenocorticotropic hormone* (*ACTH*). This physiologically-active peptide is secreted from the anterior pituitary gland into circulation under orders from the brain's central metabolic coordinator, the hypothalamus. This mode of stimulation is referred to as the *'hypothalamic-pituitary-adrenal (HPA) axis'*; it also stimulates the cortex of this gland to secrete large amounts of *glucocorticoid hormones*, primarily *cortisol*, into the circulation. Cortisol is implicated in the *stress response*, which is less immediate than the fight-or-flight response. Indeed, like many other steroid hormones, cortisol acts more slowly than adrenaline and noradrenaline, but has extensive effects on the body. For example, its metabolic effects are anabolic in the liver and catabolic in muscle and fat cells, and act to increase blood glucose levels. Cortisol also affects other systems, such as the cardiovascular system, the central nervous system, the immune system, and the kidneys. Most importantly, cortisol inhibits the inflammatory response, which can be potentially hazardous following injury.

The effects of the adrenaline-noradrenaline system on multiple organs have made it a target for many medicinal drugs [425]. These can be separated into the following groups:

1. **Adrenergic agonists.** β_2 receptors can be bound in the trachea (windpipe) and bronchi. Therefore, β_2 agonists, such as albuterol, are used to treat asthma. The α receptors can be found on smooth muscles, such as those controlling the diameter of blood vessels. Whereas the activation of α_1 receptors leads to smooth muscle contraction and the consequent constriction of blood vessels (*vasoconstriction*), α_2 receptors function in regulating their α_1 counterparts, and their activation leads to the opposite effect (*vasodilation*). Thus, α_2 agonists, such as

clonidine, are used as *antihypertensive* drugs, i.e., to treat high blood pressure. High blood pressure has been termed 'the silent killer' because of its devastating effects on untreated individuals and the relative absence of symptoms.

2. **Adrenergic antagonists (blockers).** β_1 receptors reside primarily in the heart, and their antagonists (e.g., atenolol) are used for treating angina pectoris, hypertension, and some arrhythmias.

3. **Reuptake inhibitors.** The action of adrenaline and noradrenaline in the nervous system is stopped primarily by their uptake or reuptake away from the synapse and into their secreting cells. These processes are carried out by transporters, which have become targets for drugs termed *'reuptake inhibitors'*. These drugs block transporters in order to elevate the levels of these neurotransmitters in the synapse, thereby intensifying their action. The primary medical use for adrenaline and noradrenaline reuptake inhibitors is fighting depression. Some of the older-generation antidepressants, such as the *tricyclics* (e.g., *desipramine*) inhibit the reuptake of both catecholamines and indoleamines (e.g., serotonin). Antidepressants of newer generations (SSRIs) are more specific; they are designed to boost only serotonin levels. Yet, a relatively new class of antidepressants (SNRIs) elevate the levels of both serotonin and noradrenaline. The catecholamine reuptake system is also a target for certain types of drugs of abuse, i.e., *amphetamines* (*cocaine*, *MDMA*). These drugs work similarly to the adrenaline-noradrenaline reuptake inhibitors mentioned above, but with much higher intensity. Amphetamines are addictive, and have serious adverse effects on the cardiovascular system.

4. **Monoamine oxidase (MAO) inhibitors.** MAO is an enzyme that catalyzes the oxidative deamination of catecholamines and of indoleamines. Its inhibition therefore increases adrenergic and serotonergic effects. MAO inhibitors (e.g., *selegiline*) are used primarily as antidepressants.

In addition to the drugs listed above, there are other drugs that achieve similar results by acting on the opposite branch of the autonomic nervous system, i.e., the parasympathetic system. For example, an antagonist of the receptor for acetylcholine (the principal neurotransmitter in the parasympathetic system), such as atropine, induces some of the physiological effects of agonists of adrenergic receptors.

7.5.4 GPCR and G-protein activation

Much of what we know today about the changes that GPCRs undergo following activation comes from extensive biochemical and biophysical studies performed on class A receptors [336]. Studying the activation process requires knowledge of GPCRs in both inactive and active states. There are currently many structures of GPCRs, which have been crystallized in complex with an agonist. However, such structures are only partly activated; studies show that in order to assume a fully active conformation, the GPCR must also bind a G-protein or a protein mimicking it (e.g., part of an antibody) on its intracellular side [431–433].

To date, only three GPCRs, all of which belong to class A, have been crystallized in fully active conformations:

- **Rhodopsin.** Two active structures have been determined, one bound on its intracellular side to an 11-amino acid fragment representing the C-terminus of Gα [434], and the other bound to an antibody.
- **The β_2-adrenergic receptor.** Two active structures have been determined in complex with an agonist, one bound to an entire G-protein molecule [435] on its intracellular side, and the other bound to a nanobody (the heavy chain of an antibody) [436].
- **The muscarinic (M_2) receptor.** Two active structures have been determined; each is in complex with an agonist and bound to a nanobody on its intracellular side [437]. One of these structures is also bound to an allosteric activator.

In our discussion of GPCR activation below, we focus on these three GPCRs, but also refer to some of the other GPCRs, such as the A_{2A} receptor, for which a partly active structure is known. In the case of the β_2-adrenergic receptor, we refer only to the active structure bound to a G-protein molecule, as it has been found to be very similar to the nanobody-bound structure. For a more detailed account of the data obtained from known GPCR structures, please see the review by Shonberg et el. [378].

7.5.4.1 Structural changes in GPCRs upon activation

Rhodopsin was the first GPCR for which 3D structures of both the active and inactive states were obtained (Figure 7.41a), and it was therefore the first source of knowledge about the activation process. Rhodopsin is a photoactivated protein residing in the membranes of retinal rod cells; it enables these cells to relay visual input to the brain. Since polypeptide chains are not well suited for responding to electromagnetic photons, rhodopsin uses an organic cofactor called '*11-cis-retinal*' (a *vitamin A* derivate, Figure 7.41b, left) as the photoreactive element. This molecule is covalently, yet reversibly bound to the polypeptide chain via a Schiff base to Lys-296 (on TM7). In the inactive state, the protonated (i.e., positively charged) Schiff base is stabilized by Glu-113 on TM3 (the '*3 to 7 lock*'). When hit by light, the retinal responds by undergoing isomerization. That is, it changes from an 11-*cis* to an *all-trans* configuration (Figure 7.41b, right)[*1]. This, in turn, induces conformational changes in the protein, which create a binding site for rhodopsin's cognate G-proteins[*2]. The α subunit of the G-protein binds to the intracellular side of rhodopsin, and stabilizes its active conformation[*3]. After activation, rhodopsin is *bleached*. That is, the Schiff base binding the retinal is hydrolyzed, allowing the retinal to leave the receptor and render the latter inactive, for about 30 minutes. The retinal-free polypeptide chain that remains, which also represents the active form of rhodopsin, is referred to as '*opsin*'.

In 2011, two structures of fully active rhodopsin were determined in the presence of all-*trans* retinal, one of the structures also bound to a Gs-derived 11-amino-acid fragment in the intracellular domain [434]. A first glance at the superimposed structures of inactive

[*1] Thus, 11-*cis* retinal is in fact a covalently-bound inverse agonist.

[*2] *Transducin* is the main rhodopsin-related G-protein.

[*3] This means that there are two factors stabilizing the active GPCR: its agonist, and its cognate G-protein [405].

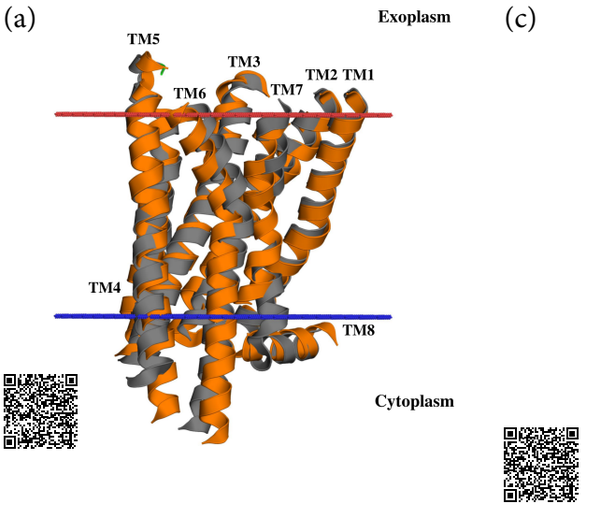
(a)
Exoplasm
TM5
TM3
TM2 TM1
TM6
TM7
TM4
TM8
Cytoplasm

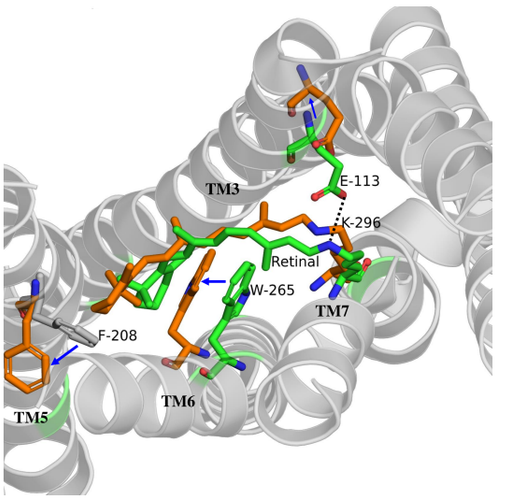
(c)
TM3
E-113
K-296
Retinal
W-265
TM7
F-208
TM5
TM6

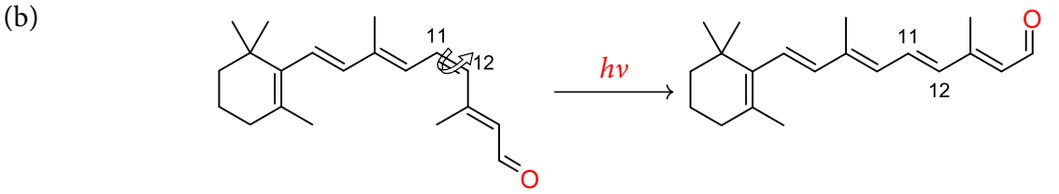
(b)
11
12
O
hv
11
O
12

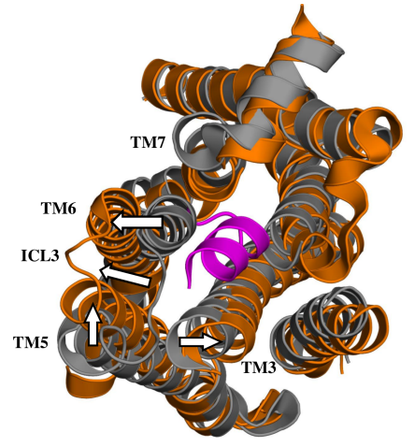
(d) (I)
TM7
TM6
ICL3
TM5
TM3

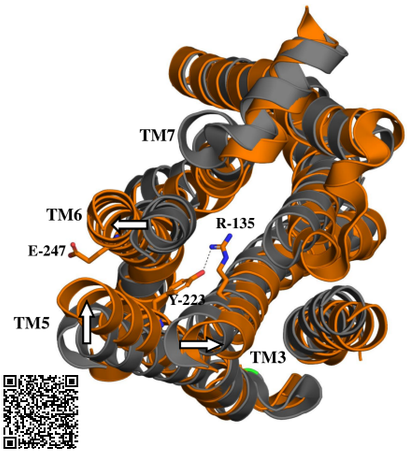
(d) (II)
TM7
TM6
R-135
E-247
Y-223
TM5
TM3

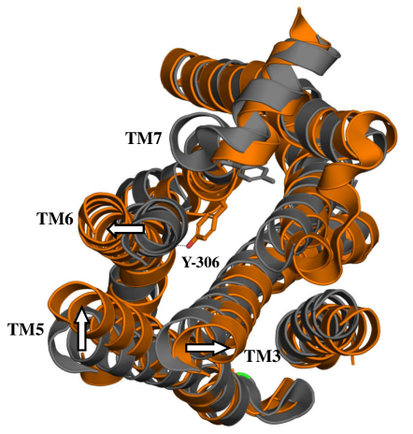
(d) (III)
TM7
TM6
Y-306
TM5
TM3

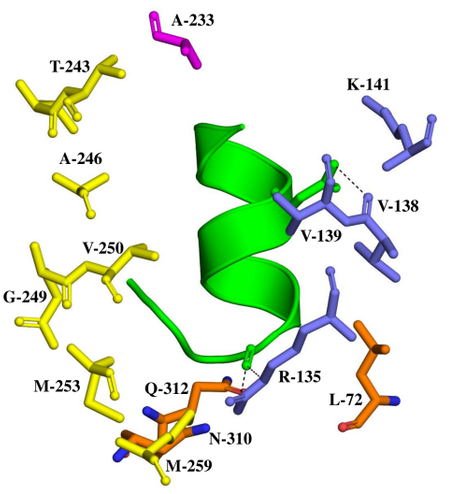
(e)
A-233
T-243
K-141
A-246
V-138
V-139
V-250
G-249
M-253
Q-312
R-135
L-72
N-310
M-259

and active states of rhodopsin reveals only modest changes in conformation, which mostly involve helices 5, 6, and 7 [405] (Figure 7.41a). A closer look at the retinal pocket seems to confirm the first impression, with relatively subtle changes observed in that region. For example:

- Certain side chain movements create room and promote the *cis*-to-*trans* change of the retinal cofactor. These movements involve the side chain of Phe-208 on TM5, and that of Trp-265 on TM6, which moves into a space formerly occupied by the β-ionone ring of the retinal cofactor (Figure 7.41c).
- A distance is created between TM3 and TM7, mainly due to a shift in TM7. This increases the distance between Glu-113 and the Schiff base, from 3.5 Å to 5.3 Å, which disrupts the salt bridge between them (i.e., the 3 to 7 lock). However, the conformational change also strengthens the existing salt bridge between the Schiff base and Glu-181, which replaces Glu-113 as the main stabilizer of the Schiff base.

NMR studies also suggest a disruption of hydrogen bonds between ECL2 and the extracellular parts of helices 4, 5, and 6, occurring just before the dissociation of the retinal cofactor [438].

FIGURE 7.41 **Structural changes in rhodopsin following its activation.** (Opposite) (a) General view of activation-induced shifts of helices. The two structures presented here are of inactive (grey; PDB 1gzm) and active rhodopsin (orange; PDB 3pqr). For clarity, the loops have been removed. The red and blue lines mark the predicted boundaries of the membrane (the OPM database [117]). (b) The retinal cofactor. The figure shows in one step the activation process in which 11-*cis* retinal (left) transitions into all-*trans* retinal (right) using the electromagnetic energy of a photon (*hv*). Carbon atoms 11 and 12 are noted, and the rotation around the bond connecting them is represented by the circular arrow. (c) Conformational changes in the retinal-binding pocket. The backbone of the inactive state (PDB 1gzm) is shown from the extracellular side as grey ribbons. Residue conformations corresponding to the inactive state are colored by atom type, whereas those corresponding to the active state (PDB 3pqr) are in orange. Movements of specific residues are marked by blue arrows. The movements of Trp-265 and Phe-208 are clearly seen, as well as the breaking of the salt bridge between Glu-113 and Lys-296 (dashed line). (d) Changes on the intracellular side of rhodopsin, allowing the binding of transducin. The structures and representation of the active and inactive forms of rhodopsin are the same as in panel (a), but the view is from the intracellular side. (I) Transducin binding. The *C*-terminal 11 amino acids of transducin are presented as a purple ribbon. The white arrows denote the direction of movement of TMs 3, 5, and 6, as well as of ICL3, when rhodopsin shifts from the inactive state to the active state. This movement clearly creates space for the transducin fragment. (II) The conformational change disrupts the inactive state-related ionic lock, which involves Glu-247 of TM6 and Arg-135 of TM3's *D/ERY* motif. In its new position, Arg-135 is stabilized by a hydrogen bond with Tyr-223 (dashed line). (III) The conformational change of rhodopsin also includes a large movement of Tyr-306 of the *NPxxY* motif, which stabilizes the active conformation. A hydrogen bond between Tyr-306 and TM6 is shown. (e) Stabilization of rhodopsin's active conformation by transducin. Transducin is presented as a green ribbon. Residues of rhodopsin that interact with transducin are shown as sticks, colored in magenta (helix 5) cyan (helix 6), and orange (other secondary elements). The hydrogen bonds of transducin with Arg-135 and Val-138 are presented as dashed lines.

However, inspection of the intracellular side of rhodopsin's TMD reveals larger changes in TMs 3, 5, 6, and 7. **The shifts of TMs 3 and 6**[*1] **away from each other and from the center of the protein create a space for transducin binding (Figure 7.41dI). These conformational changes result from the local movements of Trp-265 (the CWxP motif) and Phe-208 in the retinal-binding pocket (i.e., the transmission switch)** [414]**. The space created between TMs 3 and 6 leads to disruption of the 'ionic lock' between Glu-247 and Arg-135 of the D/ERY motif (Figure 7.41dII).** The loss of this interaction is partly compensated for by new interactions formed between Arg-135 and some of the residues of TM5 (e.g., Tyr-223) and TM6, which become closer due to the shifts. As explained above, in the other structurally determined GPCRs the ionic lock is absent, in at least some cases, which has been proposed to account for the differences in baseline activity between the GPCRs. Indeed, whereas rhodopsin is completely inactive in the dark, the other three GPCRs (like many others) retain some activity even when they do not bind their agonists. This activity can be inhibited by inverse agonists, such as carazolol, which acts on the β_2-adrenergic receptor [440].

As mentioned above, the *NPxxY* motif in TM7 differs from the D/ERY motif in that it is involved in the activation of GPCRs, rather than in stabilizing the inactive state. Indeed, Tyr-306 of the motif inserts into a space previously occupied by TM6 (Figure 7.41dIII), which stabilizes the active conformation of rhodopsin. Similar movements are observed also in the equivalent positions of Tyr-306 in the β_1- and β_2-adrenergic receptors, the muscarinic (M_2) receptor, and the A_{2A} receptor upon activation, and it is believed that in these GPCRs, too, the movements participate in the activation process. In the β_2-adrenergic receptor, stabilization of the active site, conferred by the Tyr-306-equivalent position, relies in part on a water-mediated hydrogen-bond with the Tyr-223-equivalent position on TM5 [441]. The active structure of the M_2 receptor does not contain water molecules, but the same water-mediated interaction between the two tyrosine residues is thought to happen there too [437]. The conservation of this interaction and the similar positions of the two tyrosine residues in the three activated GPCRs suggests that the interaction is a hallmark of GPCR activation.

In conclusion, the changes described above, though they involve different parts of rhodopsin, are overall small, i.e., within 2 to 6 Å [421]. **Nevertheless, they serve their purpose, in creating a space between transmembrane helices 3, 5, 6, and 7, which serves as a binding site for transducin** [371,405]**. As we will see later, the β_2-adrenergic receptor and the M_2 receptor display similar changes in their overall conformations upon activation**. The experimentally determined structures of the rhodopsin-transducin complex (PDB entries 3cap and 3pqr) show multiple interactions, both polar and nonpolar, between residues of transducin and those of rhodopsin, which stabilize the active conformation of the latter (Figure 7.41e). The direct interaction between Arg-135 of the *D/ERY* motif and a backbone group in transducin may seem important, considering the high conservation level of Arg-135. However, this interaction is absent in the β_2-adrenergic receptor, which has been crystallized in complex with a complete G-protein molecule (see below). Rhodopsin-transducin binding seems to be driven by nonpolar interactions, with hydrogen bonds rendering the orientation of the transducin-derived peptide specific [371].

[*1] In agreement with spectroscopic data showing a 5 Å outward rotation of TM6 [439].

7.5.4.2 Agonist effect and G-protein activation

In the previous subsection we described the conformational changes that GPCRs undergo when activated. The ultimate goal of GPCR research, however, is to understand how these changes are induced by ligand binding, and how they lead to the activation of the G-protein. This aspect also has important pharmacological implications, since different ligands designed to bind to the same pocket in the GPCR may induce different responses; some may act as agonists, whereas others may act as antagonists or inverse agonists. These questions cannot be answered by the aforementioned structures of rhodopsin, since this GPCR has a non-diffusible agonist (i.e., the covalently-bound all-*trans* retinal)[*1], and the corresponding structure of the activated receptor is bound to a small fragment of the Gs-protein. Fortunately, the fully active structures of both the β_2-adrenergic receptor and the muscarinic (M_2) receptor have been determined.

The active structure of the β_2-adrenergic receptor was crystallized in 2011, bound to a high-affinity agonist (BI-167107) and an entire Gs-protein (see above for details) [435]. The G-protein in the crystallized structure is nucleotide-free, which means it was captured in the middle of the GDP-GTP exchange process. Comparison between the active structure of the β_2-adrenergic receptor and its inactive structure, bound to the inverse agonist carazolol, reveals the following [442]. As in rhodopsin, activation of the β_2-adrenergic receptor induces only small structural changes on the protein's extracellular side and larger changes on its intracellular side (Figure 7.42a). The bound agonist forms three hydrogen bonds with residues in TM5: two with Ser-203 and one with Ser-207. These interactions seem to pull TM5 slightly inward (2 Å at position 207, Figure 7.42b). This small movement leads to rearrangement of the hydrophobic interaction network formed between Phe-208 (TM5), Pro-211 (TM5), Ile-221 (TM3), and Phe-282 (TM6) [443]. As a result, TM6 (and to a lesser extent TM5) undergoes a hinge movement that pushes its intracellular tip outward (Figure 7.42c); this movement is accompanied by much smaller inward movements of TMs 3 and 7 (not shown). **The movements of TMs 5 and 6 create sufficient room for accommodating the carboxyl end of the G-protein's α5 helix, which is pushed to a partial extent into the transmembrane core of the receptor**[*2]**.** This process leads to a large displacement of one of Gα's domains with respect to the other, both of which hold the GDP cofactor in the inactive G-protein (Figure 7.42d), and this displacement is suggested to promote the exchange of GDP with GTP during activation [444]. Note that the overall conformational change of the β_2-adrenergic receptor is relatively similar to the changes observed in rhodopsin, the β_1-adrenergic receptor, and the muscarinic (M_2) receptor (Figure 7.42e, see also below). Interestingly, the displacement of TM6 in the β_1-adrenergic receptor is much smaller than that observed in the β_2-adrenergic receptor. This difference may have to do with the fact that of the two structures, only that of the β_2-adrenergic receptor was crystallized when bound to a G-protein, which was likely to have induced larger conformational changes. Small displacements of helices are also observed in the adenosine (A_{2A}) receptor, whose active structure, like the active structure of the β_1-adrenergic receptor, was crystallized in the absence of a G-protein [445,446]. Indeed, **Gα binding has been shown by NMR**

[*1] Although the all-*trans* and *cis* retinal can be considered as an agonist and an inverse agonist, respectively.

[*2] This is also made possible by conformational changes in the second intracellular loop, ICL2. These changes involve rearrangement of the interactions between Asp-130 of the *D/ERY* motif, Asn-68, and Tyr-141, resulting in displacement of the latter from the space, now occupied by the α5 helix. In its new position, the α5 helix interacts with different residues in TMs 3, 5, and 6, as well as in ICL2.

(a)

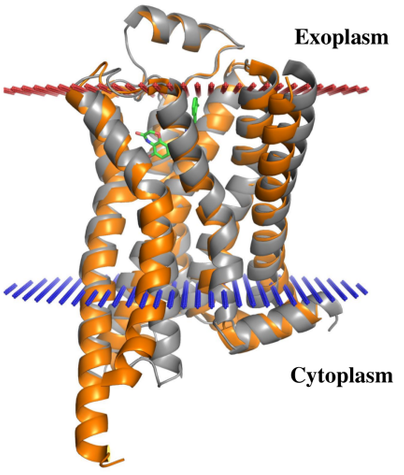

(b)

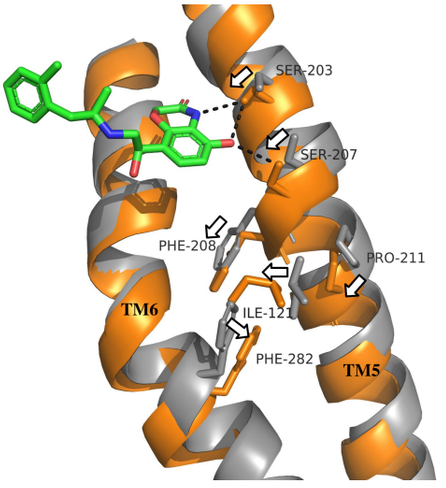

(c)

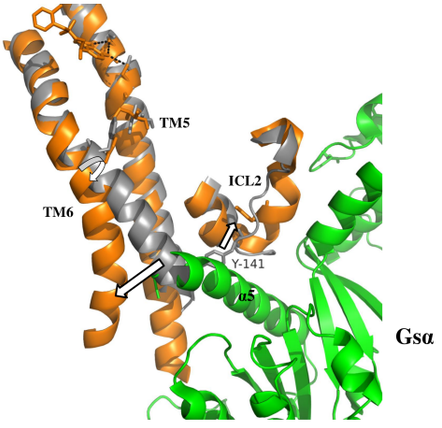

(d)

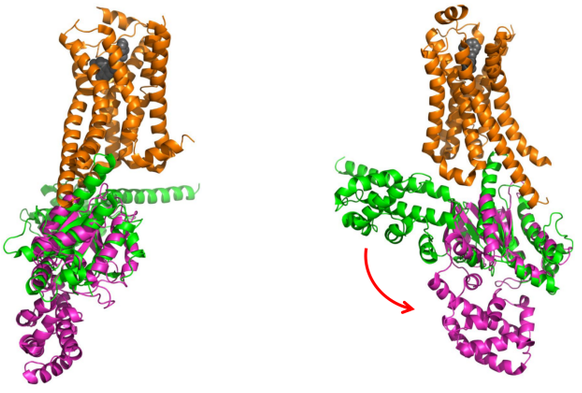

(e) (I)

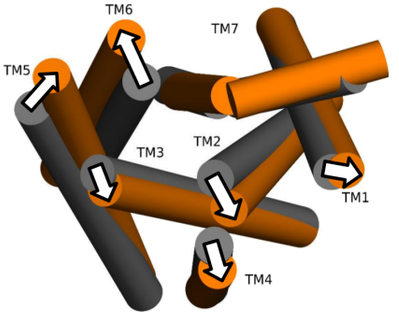

Rhodopsin

(e) (II)

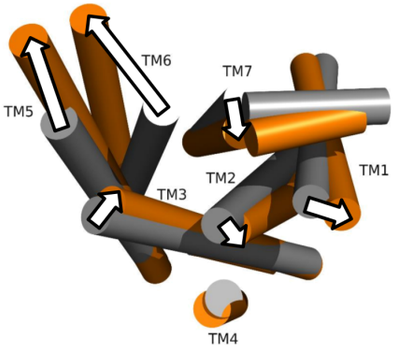

β_2-adrenergic receptor

(e) (III)

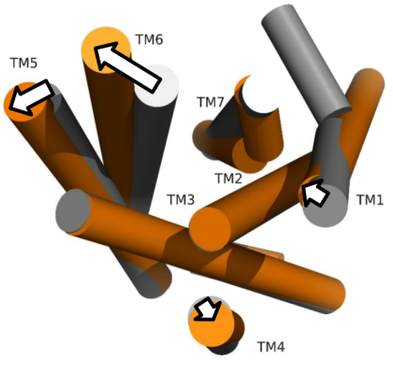

β_1-adrenergic receptor

(e) (IV)

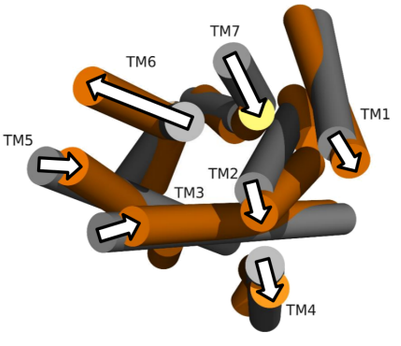

M_2 receptor

and molecular dynamics studies to be required for fully stabilizing the conformational changes induced by the agonist [431–433].

We have seen that the chain of events leading to the large conformational changes on the intracellular side of the β_2-adrenergic receptor starts with the hydrogen bonds formed between the agonist and serines 203 and 207 in TM5. These interactions pull TM5 slightly inward, causing rearrangement of other, more downstream interactions, in addition to movement of TM6. Interestingly, whereas Phe-208 is involved in this rearrangement, the other residue included in the transmission switch, Trp-286, does not seem to play a part in the activation of the β-adrenergic receptor. The involvement of serines 203 and 207 in the activation is not surprising considering their high conservation levels in aminergic receptors [447]. Carazolol, which is bound to the inactive structure of the β_2-adrenergic receptor, also interacts with TM5. However, it forms only a single hydrogen bond with Ser-203, and it seems that this interaction, which is weaker than that of BI-167107 in the active structure, is insufficient to induce the aforementioned structural changes. This may explain why carazolol acts as an inverse agonist, whereas BI-167107 acts as an agonist. The same differential interactions with TM5 are observed in the β_1-adrenergic receptor; in this case, they involve the agonist isoprenaline and the antagonist cyanopindolol, although the resulting conformational changes observed in this GPCR are much smaller. In contrast, in the A_{2A} receptor, TM2 and TM7 are the helices that interact differently with the agonist

FIGURE 7.42 **Structural changes in the β_2-adrenergic receptor following its activation.** (Opposite) (a) Superimposition of the active and inactive structures of the β_2-adrenergic receptor. The inactive structure (grey; PDB entry 2rh1) is bound to the inverse agonist carazolol, and the active structure (orange; PDB entry 3sn6) is bound to the agonist BI-167107. The red and blue lines mark the predicted boundaries of the membrane (the OPM database [117]). (b) Agonist-induced movements of TMs 5 and 6, and of key residues that act as molecular switches. The agonist is shown as sticks, colored by atom type. The hydrogen bonds between the agonist and residues in TM5 are shown as dashed lines. The resulting movement of TM5 leads to local movements of the downstream nonpolar residues Phe-208, Pro-211, Ile-121, and Phe-282, and the hydrophobic contacts between them. The movement of each of the above residues is marked by arrows. (c) Conformational changes on the intracellular side of the receptor upon agonist binding. The changes described in (b) induce a large hinge movement (curved arrow) in TM6, which creates room on the intracellular side for the α5 helix of G_α (marked). In addition, ICL2 shifts away from TM6, with a large change in the position of Tyr-141. Smaller changes in the positions of TM3 and TM7 are not shown. As can be clearly seen, the position of TM6 in the inactive state clashes with the helix of Gα, which prevents the binding of the latter to the GPCR. (d) Superimposition of the structure of Gα in complex with the β_2-adrenergic receptor (PDB entry 3sn6; Gα is colored in green and the β_2-adrenergic receptor is colored in orange) and free Gα bound to 5′-guanosine-diphosphate-monothiophosphate (GTPγS) (PDB entry 1gia; Gα is colored in magenta). The superimposed structures are shown from two angles, rotated 90° from each other. The superimposition shows that the activation of Gα involves a substantial displacement of one of its domains with respect to the other (red arrow). (e) Comparison between movements of helices in rhodopsin and those in the β_2-adrenergic receptor, β_1-adrenergic receptor (where the inactive and active structures correspond to PDB entries 2vt4 and 2y03, respectively) and muscarinic (M_2) receptor. The inactive and active conformations of all three GPCRs are colored in grey and orange, respectively. The arrows mark movements of the intracellular sides of the helices, where the length of each arrow is proportional to the degree of movement. For clarity, the helices are shown as cylinders, and the loops are not shown.

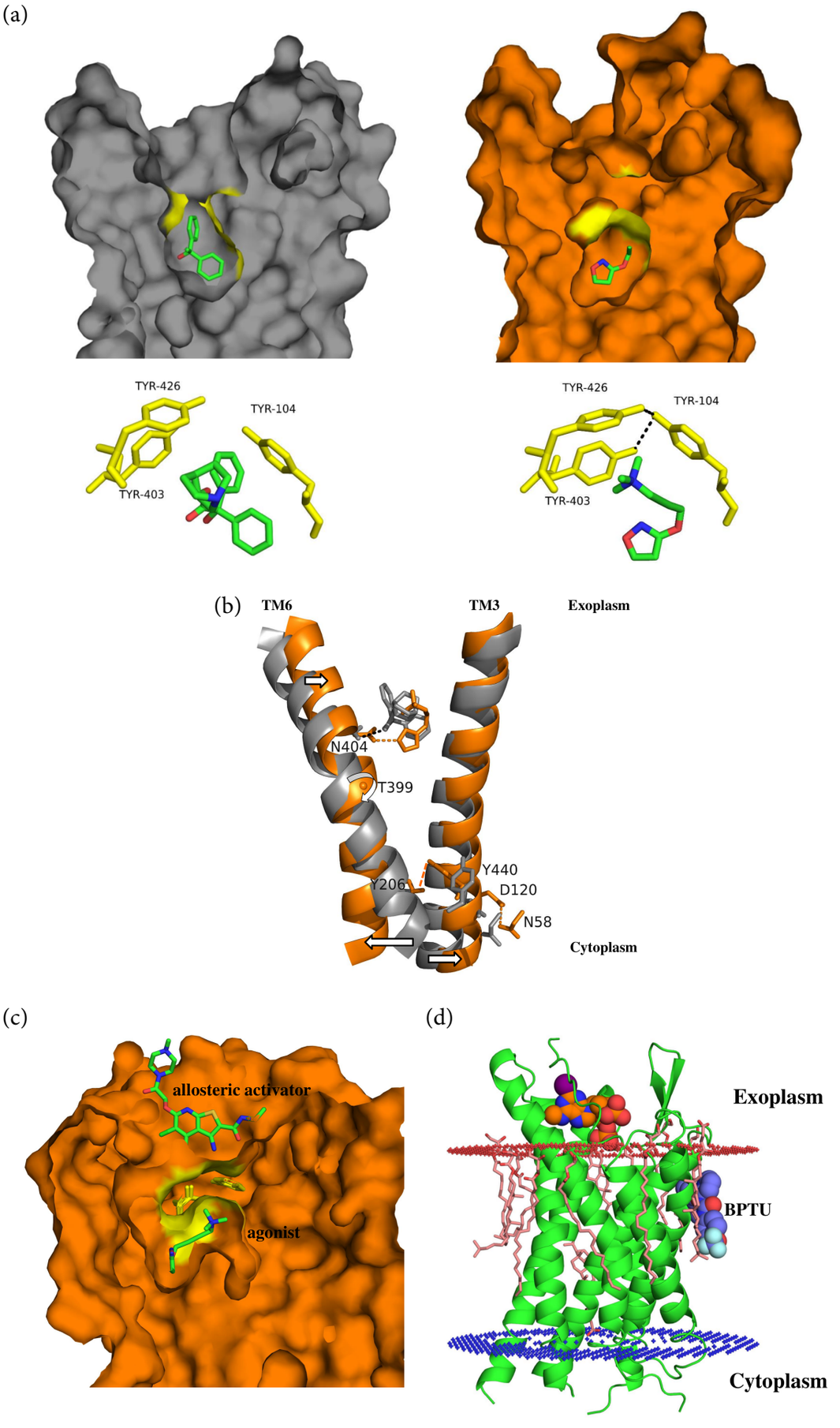
(a)
TYR-426
TYR-104
TYR-403
TYR-426
TYR-104
TYR-403
(b)
TM6
TM3
Exoplasm
N404
T399
Y440
Y206
D120
N58
Cytoplasm
(c)
allosteric activator
agonist
(d)
Exoplasm
BPTU
Cytoplasm

(NECA) as compared to the inverse agonist (ZM241385), and the conformational changes are transmitted to the intracellular side by TMs 3, 6, and 7, rather than TM5 [445]. Thus, **it seems that whereas the interactions of antagonists and inverse agonists with their respective ligand-binding pockets generally differ from the interactions of agonists, the exact mechanisms through which these interactions inhibit or activate the GPCR may differ across GPCRs, and involve different molecular switches and/or transmembrane segments.**

Muscarinic receptors belong to the same class as rhodopsin and the β-adrenergic receptors (class Aα). These receptors, which mediate cholinergic transmission, include five subtypes. They modulate a variety of physiological functions and are targeted by drugs for treating different diseases (e.g., Alzheimer's disease, Parkinson's disease, and schizophrenia). In 2012 the antagonist-bound inactive structures of the M_2 [448] and M_3 [449] receptor subtypes were determined, and a year later the fully active structure of the M_2 receptor was determined, bound to the agonist iperoxo and to a nanobody on its intracellular side [437]. Comparison between the inactive and active structures of the M_2 receptor shows conformational changes at the ligand-binding site that involve TMs 5, 6, and 7, and which are larger than those seen in rhodopsin and the β_2-adrenergic receptor. These changes lead to the complete burial of the agonist inside the pocket, occluded from the solvent (Figure 7.43a, top). This occlusion is created by an 'aromatic lid' above the agonist, composed of Tyr-104,

FIGURE 7.43 **Activation of M_2 receptor and allostery.** (Opposite) (a) Conformational changes in the ligand-binding site of the M_2 receptor. *Top*: A cross-section through the binding site of the inactive (grey; PDB entry 3uon) and active (orange; PDB entry 4mqs) structures of the M_2 receptor. The inactive structure is bound to the antagonist QNB, and the active structure is bound to the agonist iperoxo. The aromatic lid residues above the ligands are colored in yellow. Activation induces conformational changes that lead to the complete occlusion of the agonist from the solvent. *Bottom*: Activation-induced closure of the aromatic lid (yellow sticks). (b) Propagation of the conformational change in TM6 from the ligand-binding site to the intracellular site of the receptor. The image shows a superimposition of the active and inactive structures of the M_2 receptor. For clarity, only TMs 3 and 6 are shown. In the inactive state the antagonist is hydrogen-bonded to Asn-404 on TM6 (black dashed line). Activation of the GPCR induces a small movement of TM6 towards TM3 and allows Asn-404 to remain hydrogen-bonded to the agonist (orange dashed line), which is located further away from TM6 than the antagonist is. The pivot motion of TM6 around Thr-399 (curved white arrow) converts the small movement of the helix near the ligand-binding site into a large movement at the intracellular site, away from TM3. A coordinated movement of TM3 away from TM6 allows a hydrogen bond to be formed between Asp-120 and Asn-58. The activation also involves a conformational change in TM7, which changes the orientation of Tyr-440 (the *NPxxY* motif), thus allowing it to interact with Tyr-206. Note that although the interaction is shown here as a direct hydrogen bond (black dashed line), in reality it is mediated by a water molecule, which is missing in the solved structure. (c) Binding of the allosteric activator LY2119620 to the agonist-bound M_2 receptor (PDB entry 4mqt). LY2119620 binds above the agonist pocket, where it is separated from the agonist iperoxo by the aromatic lid residues (in yellow). (d) Membrane-facing position of an allosteric site in the $P2Y_1$ receptor (PDB entry 4xnv). The allosteric site is occupied by the negative modulator BPTU (with blue carbon spheres). The orthosteric site, which resides in the extracellular loop region of the receptor, is shown with a bound antagonist (orange spheres; PDB entry 4xnw). Co-crystallized lipid molecules are also shown, in pink. The red and blue lines mark the predicted boundaries of the membrane (the OPM database [117]).

Tyr-403, and Tyr-426 (yellow patch in Figure 7.43a, top). In the receptor's inactive state the lid is partly open, but upon activation, movements of these residues, especially Tyr-403 and Tyr-426, allow them to hydrogen-bond with each other and close the lid (Figure 7.43a, bottom).

On the muscarinic receptor's intracellular side, the conformational changes that follow activation are overall similar to those observed in rhodopsin and in the β_2-adrenergic receptor (Figure 7.42eIV). In particular, the outward movements of TMs 6 and 2, and the accompanying inward movements of TMs 7 and 3, are very similar to the movements seen in the β_2-adrenergic receptor, and create the G-protein binding site in a similar manner. As in the other GPCRs, the large conformational change of TM6 begins in the ligand-binding pocket and propagates to the intracellular side. In the ligand-binding pocket both the antagonist and the agonist hydrogen-bond with Asn-404. However, the agonist, which is smaller than the antagonist, is further away from TM6 and closer to TM3 than the antagonist is. The interaction between the agonist and Asn-404 therefore pulls TM6 closer to TM3 in this region (Figure 7.43b). TM6 undergoes a pivot motion around Thr-399, and its intracellular side is displaced farther away from TM3. In light of the above, in addition to the results of mutational studies [437,450], Asn-404 is thought to be a key residue in the activation of the M_2 receptor. The distance created between TMs 3 and 6 upon activation is also the result of a slight displacement of TM3, which involves the formation of a stabilizing hydrogen bond between Asp-120 of the *D/ERY* motif and Asn-58 (the equivalent of Asn-68 in the β-adrenergic receptor). We have already encountered this interaction in the active β_2-adrenergic receptor, suggesting that it plays a general role in GPCR activation, and refuting the association of the *D/ERY* motif with stabilization of the inactive state. The second motif implicated in GPCR activation, *NPxxY*, also seems to be important for the activation of the M_2 receptor. Specifically, Tyr-440 of the motif (the equivalent of rhodopsin's Tyr-306) on TM7 becomes closer to Tyr-206 (the equivalent of rhodopsin's Tyr-223) on TM5, and the water-mediated interaction that is thought to occur between them is expected to stabilize the active state of the receptor.

The study described above also investigated allostery in the M_2 receptor [437]. The protein was crystallized in complex with the agonist iperoxo and the positive allosteric modulator LY2119620. The allosteric activator binds directly above the agonist (Figure 7.43c). **Excluding a few small adjustments of the GPCR structure to the activator, mainly involving residues that interact with the latter, the two structures (i.e., bound and unbound to the activator) are very similar, indicating that the allosteric site is pre-formed by the agonist. This idea is in line with our current view of allostery, which posits that allosteric activators stabilize an active conformation of the protein, whereas allosteric inhibitors stabilize an inactive conformation (see Chapter 5 for more details).** Allosteric modulators have been recognized in many class A GPCRs, including the adenosine, dopamine, histamine, serotonin and chemokine receptors, as well as in class C GPCRs [451]. The allosteric sites identified in these GPCRs reside in the extracellular or transmembrane domains [379]. The modulators are chemically diverse and include lipids (e.g., fatty acids, phospholipids, and cholesterol), amino acids, ions (e.g., Na^+), and various small molecules. In fact, the G-proteins and other intracellular binding partners of GPCRs (e.g., *GRK* and *arrestins*, see following subsection) can also be regarded as allosteric modulators, as each binds preferentially to an active or inactive conformation of the receptor and stabilizes it. As discussed in Section 7.5.7 below, allosteric modulators are highly sought-after by the pharmaceutical industry, for various reasons. Allosteric sites in GPCRs may appear in different locations of

the protein, including the outer, membrane-facing surface. Such a position of an allosteric site is observed, e.g., in the $P2Y_1$ (purine) receptor [452] (Figure 7.43d).

To conclude, the studies discussed above, as well as many others carried out in recent years, have produced the following insights about the activation of class A GPCRs:

- The activation process usually involves relatively small conformational changes in the extracellular and ligand-binding domains. One exception is the $P2Y_{12}$ receptor, where 5 to 10 Å shifts are observed on the extracellular sides of TM6 and TM7.
- The activation results in the transmission of small, local conformational changes from the ligand-binding site of the GPCR to its intracellular side by a variety of molecular triggers, which include ionic locks and transmission switches (see [453] for a more detailed description). Although these triggers do not act identically in all GPCRs, they involve physically similar mechanisms and structurally equivalent positions, which are included in highly conserved motifs, such as *D/ERY* and *NPxxY*.
- The local conformational changes are amplified as they propagate towards the intracellular side, resulting in relatively large shifts of transmembrane helices, especially TM6, and to a lesser extent TMs 3, 5, and 7, which create a binding site for the G-protein.
- The rearrangements of helices on the intracellular side are overall similar in both light-activated rhodopsin and agonist-activated GPCRs.
- Gα undergoes large conformational changes upon binding to its receptor, which in turn promotes nucleotide exchange and activation of downstream signaling.

Nevertheless, there are aspects of the activation process that are yet to be clarified. These include the following:

- The generality of the structural changes observed in rhodopsin and in the β-adrenergic receptors. Evaluating generality would require the determination of additional fully-active GPCR structures, i.e., bound simultaneously to an agonist and to an intracellular binding partner. It is particularly important to gain such information for GPCRs of other classes beyond A, for which no fully active structures are available.
- The GDP-GTP exchange. The β_2-adrenergic receptor was determined in complex with nucleotide-free Gs. To obtain a complete view of the activation process, it is necessary to carry out additional studies on the GTP-bound form of GPCRs, as well as on the intermediates that may exist between the two states. It should be noted that crystallizing the active state of the GPCR with GTP-bound G-protein is not trivial, as the presence of GTP promotes dissociation of the G-protein from the receptor.
- Ligand selectivity. Additional studies are required to understand the mechanistic effects of ligands with different functionality (agonists, antagonists, inverse agonists) and receptor subtype specificity, as well as the effects of *biased ligands*, that is, ligands whose binding to the GPCR leads to activation of specific signaling pathways [454,455]. Moreover, GPCRs may also be affected by allosteric ligands, and it will be interesting to characterize the mechanisms of activation or inhibition employed by such ligands.

- At the system level it is intriguing that GPCRs are an order of magnitude more diverse than their G-proteins (~600 versus ~20). From a signal processing view one may wonder what benefit is obtained from having such a diverse 'sensing end' (GPCRs) that eventually reduces to the limited G-protein repertoire.

7.5.5 GPCR desensitization

Part of the regulation of GPCR action involves GPCR inhibition following short or prolonged activation, so as to prevent over-stimulation of the signaling system [456]. The first type, i.e., downregulation that occurs very soon after the activation of the GPCR, is called *desensitization* [336,457,458]. There are two types of desensitization:

1. **Homologous** desensitization acts on the activated receptor and is mediated by phosphorylation of Ser and Thr residues in ICL3 or the C' of the GPCR (Figure 7.33, step 4). The phosphorylation is carried out by a specific group of Ser/Thr kinases called *GRKs* [459], which act only on the agonist-bound conformation of the receptor. The phosphorylation serves to increase the affinity of the GPCR to proteins of the *arrestin family*, and facilitate their binding to the receptor (Figure 7.33, step 5). The binding to arrestin has two outcomes: first, it prevents the GPCR from interacting with its cognate G-protein, thus stopping the signaling. Second, it recruits *clathrin* and its adaptor protein AP-2, which induces the internalization of the GPCR into the cell via *clathrin-coated vesicles* [460], after which the receptor is recycled or degraded [461]. Interestingly, class A GPCRs lose the clathrin coat and become dephosphorylated following internalization; as a result, it is thought that they may be able to continue signaling even when inside the endosome [462]. In such a case, however, the GPCR and its effectors are closer to the cell's nucleus compared to their initial location in the plasma membrane, which might make the activation of the transcriptional pathway more efficient [463]. In contrast, class B GPCRs remain bound to arrestin following internalization, which leads to their ubiquitylation and degradation. It should be noted that, according to recent studies, arrestins' involvement in cellular signaling is much more complicated than that mentioned above [464]. Specifically, it seems that arrestins are involved in biased agonism: by binding to GPCRs they stabilize certain conformations that block certain signaling pathways and promote other pathways [455,464]. Thus, arrestins should be viewed as multifunctional adapter proteins rather than signal terminators [464].

2. **Heterologous** desensitization acts on other receptors and is mediated by second messenger-activated kinases, such as PKA or PKC.

There are additional downregulation mechanisms that act on activated GPCRs following prolonged stimulation of the receptor. These may act at several levels, including gene transcription and translation [461].

In 2015 the structure of active rhodopsin bound to visual arrestin [465] was determined (Figure 7.44a). Interestingly, the structure showed that arrestin binds to rhodopsin asymmetrically, which should allow arrestin's conserved hydrophobic residues (Phe-197, Phe-198, Met-199, Phe-339, and Leu-343, Figure 7.44a, pink area) to touch, or even insert into the nonpolar region of the membrane. In contrast to G-proteins and GRKs, arrestins are not attached to hydrophobic chains (palmitoyl or prenyl) that anchor them to the membrane. Thus, the conserved hydrophobic patch may be the only means by which arrestins

can become anchored to the membrane, and this anchoring may in turn stabilize arrestin's interaction with the GPCR [465]. Indeed, mutation of any of these residues to alanine affects the binding of arrestin to rhodopsin [466]. The highly asymmetric shape of the rhodopsin-arrestin complex has also been suggested to affect the curvature of the membrane, perhaps as part of arrestin's role in initiating rhodopsin's endocytosis [465].

From the arrestin end, binding to rhodopsin is mediated by several elements. A short helical segment of arrestin inserts into the intracellular side of rhodopsin, in a process similar to the insertion of the Gα subunit of rhodopsin's G-protein, transducin (Figure 7.44b). The helical segment of arrestin interacts with the carboxy-terminus of TM7 and with the amino terminus of helix 8. Indeed, both of these elements have been implicated in previous studies as important for arrestin binding [467,468]. Thus, arrestin directly competes with transducin. Another interesting interaction occurs between arrestin and the second intracellular loop of rhodopsin (ICL2, Figure 7.44b left). In its apo form (detached from rhodopsin), arrestin assumes a closed conformation in which the interaction region is inaccessible (Figure 7.44c, left). Upon binding it opens up, to accommodate rhodopsin's ICL2 (Figure 7.44c, right). In arrestin-bound rhodopsin, ICL2 adopts a helical conformation, whereas in arrestin-free, active rhodopsin it is organized as a loop.

As mentioned above, arrestin binds with high affinity to activated rhodopsin only after the latter has been phosphorylated by a GRK. In the rhodopsin-arrestin structure described above, rhodopsin is not phosphorylated and the binding was made possible by the introduction of mutations into the two binding partners. Thus, the structure of arrestin in that case represents a pre-activated state of the protein. Determining the structure of phosphorylated rhodopsin bound to activated arrestin will enable us to understand the process of arrestin activation and also, hopefully, the initiation of signaling pathways associated with arrestin binding.

7.5.6 GPCRs of other classes

The number of structures determined for GPCRs outside class A is much smaller than the number of class A structures. Known non-class-A structures include the following:

Class B – glucagon and corticotropin-releasing factor (CRF) receptors

Class C – mGlu1, mGlu5, and $GABA_B$ receptors

Class F – Smoothened protein (SMO, a GPCR-like receptor)

7.5.6.1 Class B GPCRs

Class B GPCRs bind large peptide hormones, and therefore constitute attractive targets for therapeutic drugs used to treat diseases associated with glucose metabolism (e.g., diabetes), the stress response, cardiovascular regulation, etc. Unfortunately, the structural data on these GPCRs is relatively scarce, with only two members of the group characterized structurally: the corticotropin-releasing factor (CRF) [469] and glucagon [470] receptors. Moreover, stabilization of the structures for crystallization requires, among other things, the removal of large portions of the *N*- and *C*-termini. Thus, the structures represent mainly the transmembrane domains of the receptors. The structure of CRF receptor subtype 1 (CRFR1) was determined in complex with the non-peptide antagonist CP-376395. There are three striking differences between the structure of CRFR1 and those of the class A GPCRs discussed above:

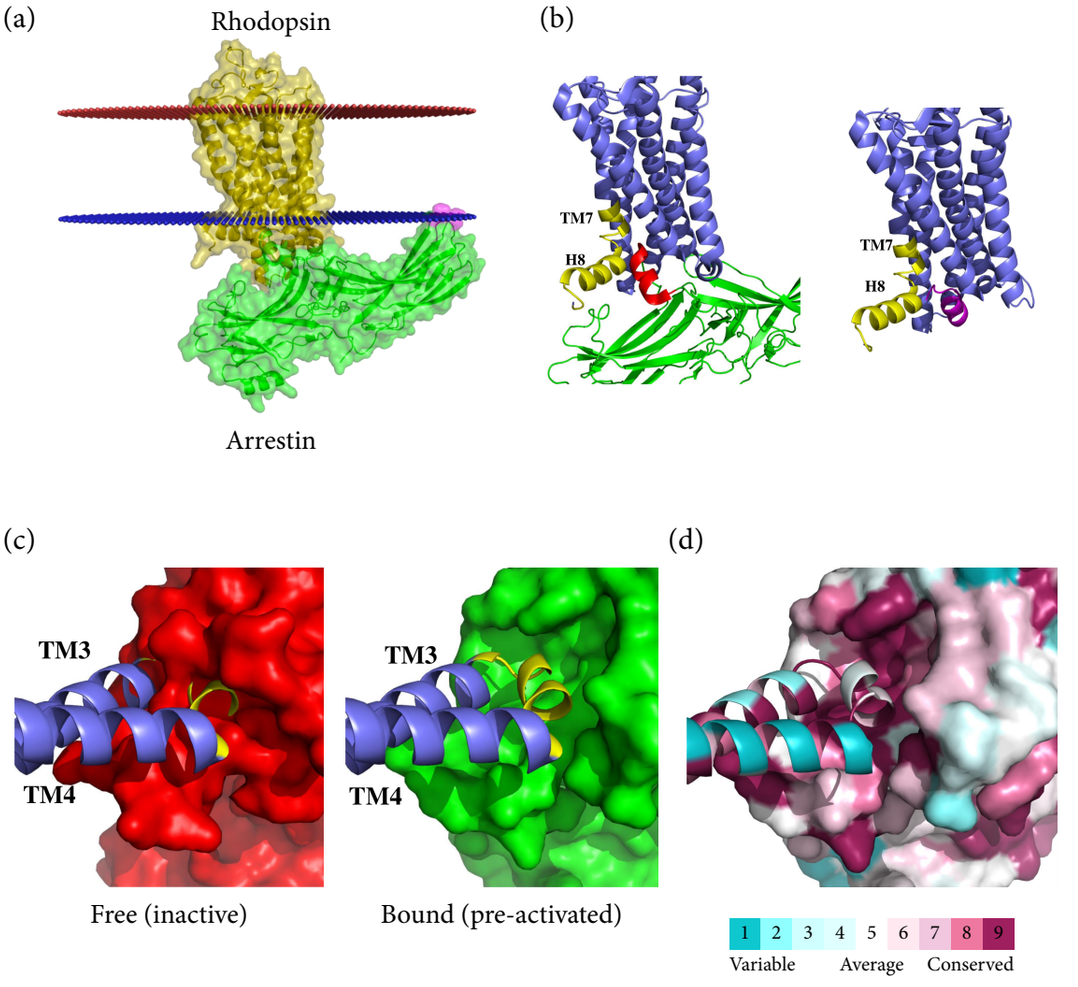

FIGURE 7.44 **Binding of arrestin to active rhodopsin.** (a) The overall structure of the complex (PDB entry 4zwj), where rhodopsin is in gold and arrestin is in green. The conserved hydrophobic patch in arrestin is colored in pink. The red and blue lines mark the predicted boundaries of the membrane (the OPM database [117]). (b) *Left*: The interaction of arrestin's short helical segment with rhodopsin's TM7 and helix 8, where rhodopsin is in blue, the transducin segment is in magenta, and the TM7-H8 binding site is in yellow. *Right*: The structure of active rhodopsin bound to a short segment of the Gα subunit of transducin (PDB entry 3pqr), where the transducin segment is in magenta. The segment binds to the same intracellular pocket of rhodopsin that binds arrestin's short segment, although the orientations of the two segments within the pocket are different. (c) Interaction between arrestin and rhodopsin's ICL2 (colored yellow). *Left*: Free arrestin in its basal (inactive) state (red, PDB entry 1cf1), superimposed on the bound arrestin. *Right*: The rhodopsin-arrestin complex. The rhodopsin is not phosphorylated, and arrestin is therefore said to be in its pre-activated state (see main text). The bound arrestin has an open conformation that accommodates ICL2. For clarity, only TM3, TM4 and ICL2 are shown in rhodopsin. The ICL2-interacting pocket is close, and sterically clashes with the short helix of ICL2. (d) Evolutionary conservation of the rhodopsin-arrestin interface. The image is identical to the one shown on the right side of (c), but both rhodopsin and arrestin are colored according to conservation levels (cyan – lowest, maroon – highest; see color code in figure). The conservation levels are calculated by the ConSurf web server (http://consurf.tau.ac.il) [373,374]. As can clearly be seen, the residues in both proteins that form the interface are evolutionarily conserved.

1. **CRFR1 is V-shaped and has a large cavity** (Figure 7.45a).

2. The antagonist's binding site is located near the intracellular side. Note, however, that the native (peptide) ligands of class B GPCRs bind to both the extracellular and transmembrane domains of the receptor (see more below).

3. TM7 has a sharp kink above the midpoint of the transmembrane domain, around Gly-356. This residue is part of a conserved *QGxxV* motif in class B GPCRs. Gly-356 allows TM7 to acquire the kink, similarly to the *NPxxY* proline in class A GPCRs, which also induces a distortion in TM7. The intracellular side of the transmembrane domain, on the other hand, is similar in shape to that of class A GPCRs (despite the lack of ICL2), indicating that this structure is likely to be able to bind the cognate G-protein.

The glucagon receptor (GCGR), which was crystallized in the same year as CRFR1, was also shown to include a large cavity (Figure 7.45b), but since the ligand could not be resolved, the exact binding location is unknown. The structure of the glucagon receptor does not have the pronounced V shape seen in the CRFR1 structure. Moreover, GCGR seems to be more similar in structure to class A GPCRs than CRFR1 is, in terms of the orientations and positions of the transmembrane helices. One clear difference between the GCGR structure and the structures of class A GPCRs is TM1, which is significantly longer in the former. This region is thought to be involved in glucagon binding and in the positioning of the ECD with respect to the TMD.

The structures described above lack portions of the ECD and a bound peptide. This prevents us from understanding the spatial relation of the ECD to the TMD, how the natural peptide agonist binds to the receptor, and how the receptor is activated. There are, however, biochemical data implicating a *GWGxP* motif in a functionally important network of interactions. These interactions are seen in the CRFR1 structure, but since the active structure of the receptor is unknown, their exact role is yet to be understood. As mentioned above, the natural peptide ligands of class B GPCRs bind to both the ECD and the TMD. Specifically, the *C*-terminus of the peptide agonist binds primarily to the ECD, whereas the *N*-terminus binds to the TMD. This pattern has prompted studies of the isolated ECD of class B GPCRs in complex with a peptide agonist (see review by Parthier and coworkers [471]). The studies indicate that members of this group have similar ECDs, all of which are quite large. This is consistent with the large ligands of class B GPCRs, i.e., peptides comprising ~30 amino acids [472]. The peptide-binding site is composed of two small β-sheets and an adjacent α-helix, and is stabilized by three disulfide bonds (Figure 7.46a). **The binding of the peptide ligands seems to be coupled to their folding (Figure 7.46b), similarly to what we have seen in intrinsically unstructured proteins (Chapter 6).** Upon binding, the C' of the peptide ligand is squeezed between the two β-sheets of the ECD (Figure 7.46b), where it forms mainly nonpolar but also polar contacts with complementary ECD residues of loops 2 and 4, and of the C' of the GPCR (Figure 7.46c). On the other side, the N' of the peptide ligand is held close to the TMD (Figure 7.46a). In this orientation, the N' of the ligand can interact with extracellular loops and transmembrane helices of the GPCR. The binding is also accompanied by conformational changes in ECD loops, which may be transmitted to the TMD, and therefore constitute part of the activation process [471].

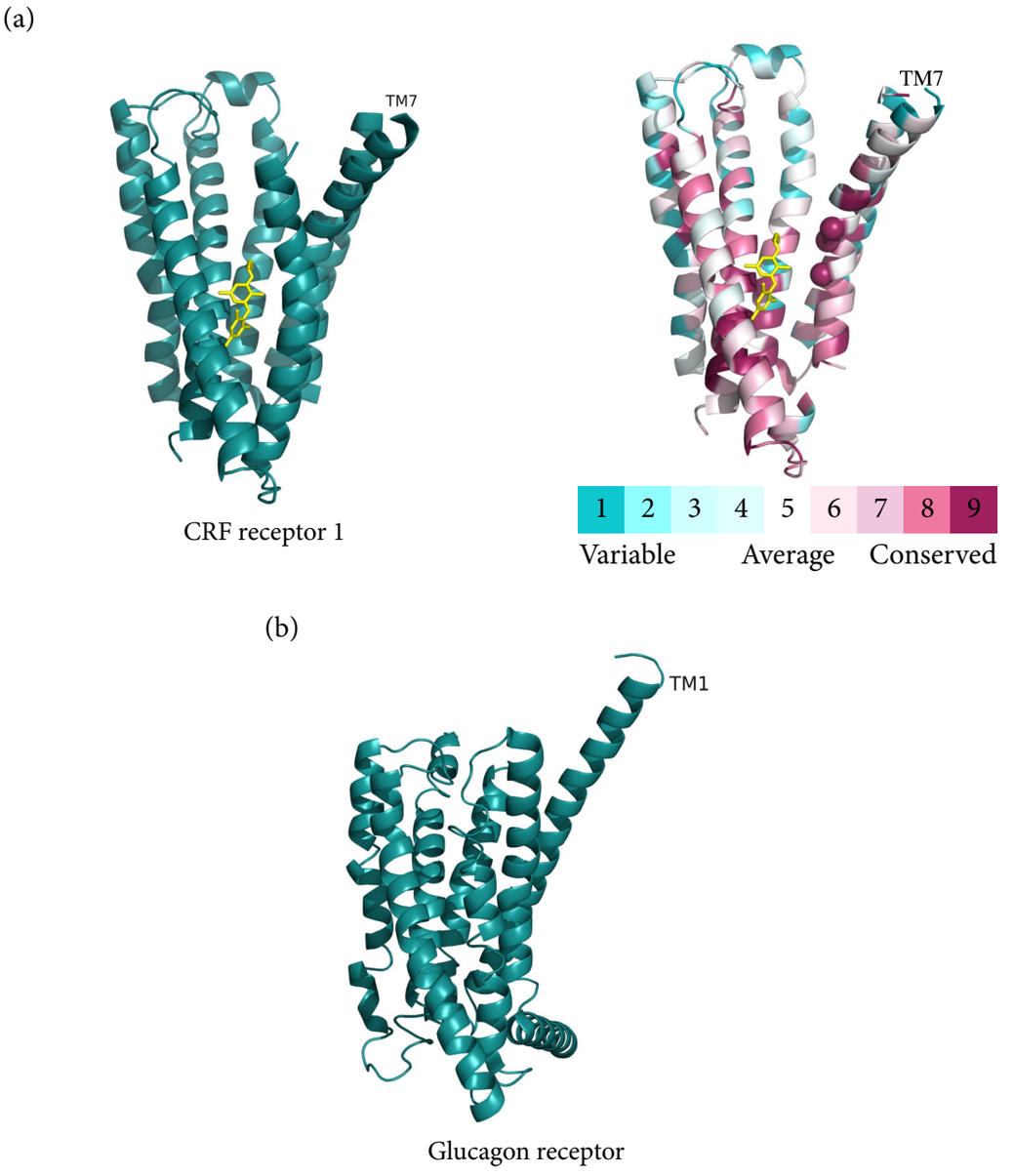

FIGURE 7.45 **The transmembrane domain of class B GPCRs.** (a) The inactive corticotropin-releasing factor receptor 1 (CRFR1) bound to the non-peptide antagonist CP-376395 (PDB entry 4k5y). *Left*: The full structure of the receptor (blue ribbons), with the bound ligand shown as yellow sticks. TM7, which has an unusual kink, is marked. *Right*: The same structure, colored according to evolutionary conservation level (cyan – lowest, maroon – highest; see color code in figure). The Cα atoms of the highly-conserved Gln-355, Gly-356, and Val-359 (the *QGxxV* motif) are shown as spheres. TM5 is removed for clarity. Conservation levels are calculated by the ConSurf web server (http://consurf.tau.ac.il) [373,374]. (b) The inactive glucagon receptor (PDB entry 4l6r). The receptor was crystallized in the presence of the antagonist NNC0640, but the latter was not resolved in the structure.

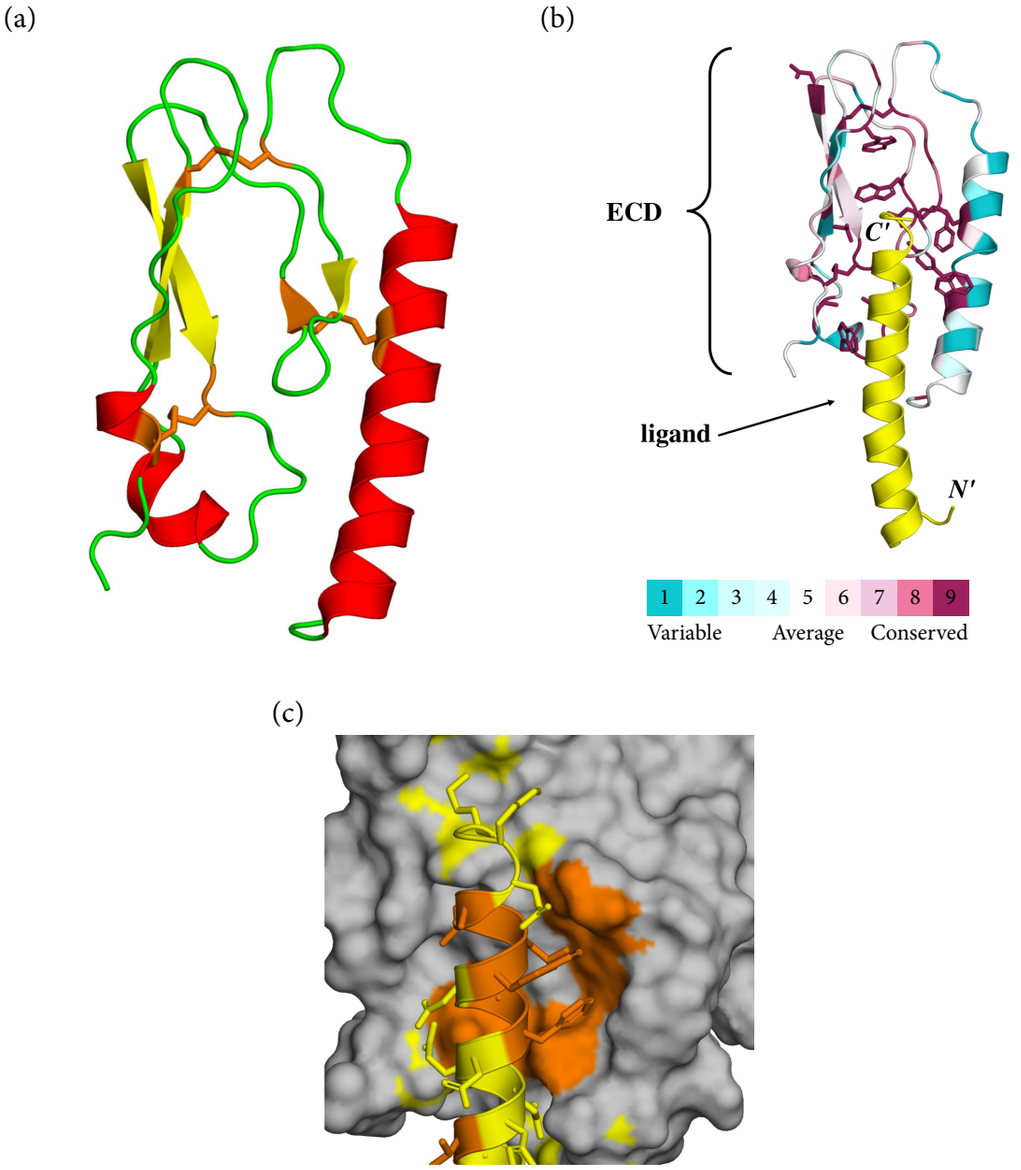

FIGURE 7.46 **Ligand binding in class B GPCRs.** The extracellular domain (ECD) of the human gastric inhibitory peptide (GIP) receptor, in complex with the hormone GIP (PDB entry 2qkh). (a) The structure of the ECD, colored by secondary structure. The disulfide bonds are represented as orange sticks. (b) General view of the ECD-GIP complex. The ECD is colored according to conservation level (cyan – lowest, maroon – highest; see color code in figure), and the peptide ligand is in yellow, with its termini noted. The side chains of the highly conserved residues in the ECD are shown as sticks. As would be expected, most of the highly-conserved residues in the ECD face the peptide ligand. Conservation levels are calculated by the ConSurf web server (http://consurf.tau.ac.il) [373,374]. (c) ECD-ligand interactions. The surface of the receptor's ECD is shown in grey. The ligand peptide is shown as a ribbon, with its side chains represented as sticks. In both the ligand and the ECD, polar residues involved in protein-ligand interactions are in yellow, and nonpolar interacting residues are in orange. The interactions are similar across different class B GPCRs, and the ECD loops 2 and 4, which mediate these interactions, are consistently the parts undergoing the most significant conformational changes following activation.

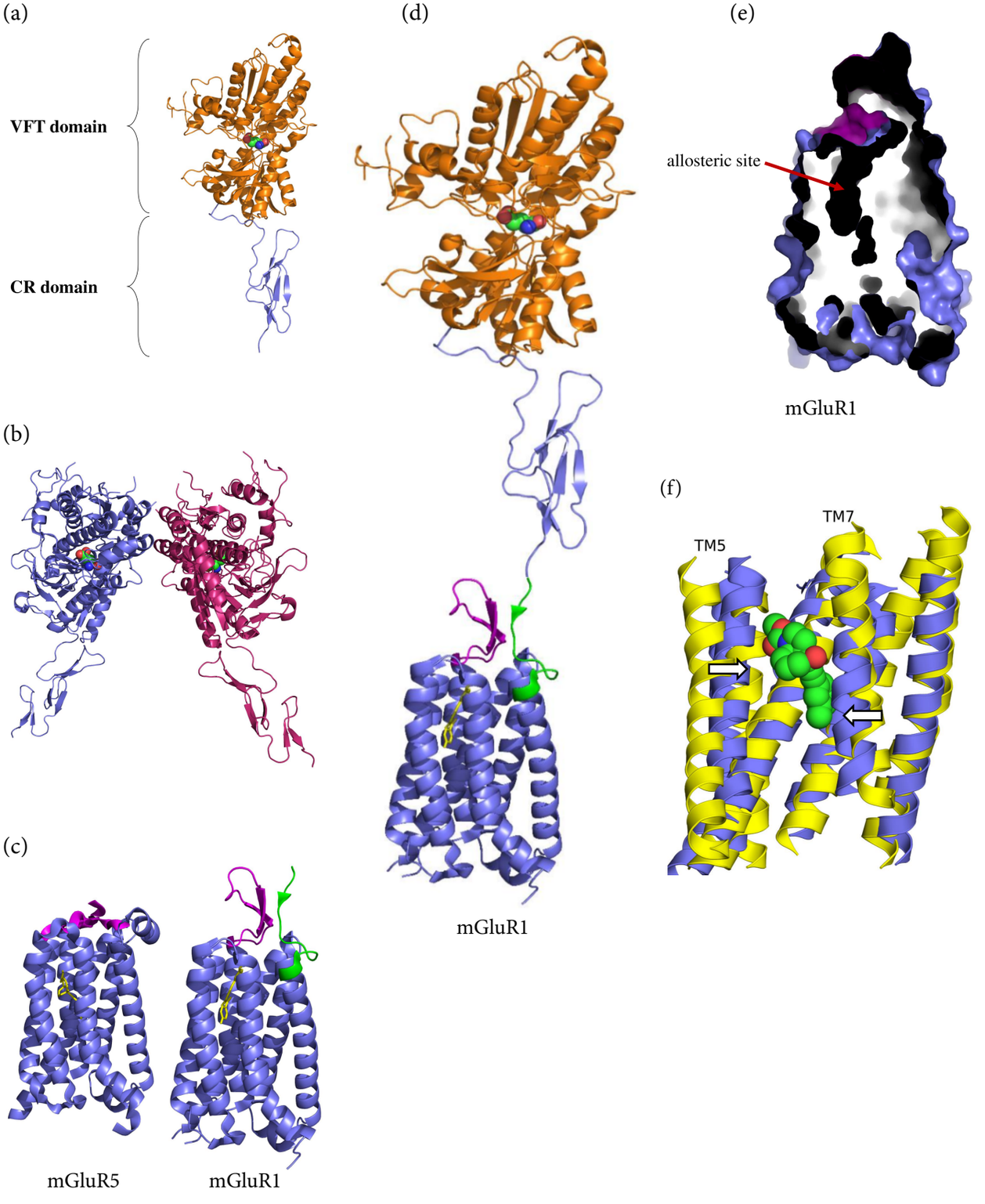
(a)
VFT domain
CR domain
(b)
(c)
mGluR5
mGluR1
(d)
mGluR1
(e)
allosteric site
mGluR1
(f)
TM7
TM5

7.5.6.2 Class C GPCRs

Studies on class C GPCRs have concentrated mainly on the metabotropic glutamate receptors (mGluR), which are classified into three subgroups based on sequence similarity, agonist selectivity, and effector:

I – mGluR subtypes 1 and 5

II – mGluR subtypes 2 and 3

III – mGluR subtypes 4, 6, 7, and 8

The focus on mGlu receptors is not surprising considering their physiological, medical and therapeutic importance. Glutamate, the native agonist of these receptors, is the principal excitatory neurotransmitter in the central and peripheral nervous systems, and it is involved in numerous neurological functions, including memory and learning, sensory and motor functions, emotions, etc. Thus, mGluR malfunctioning leads to diseases such as epilepsy, neurodegeneration, chronic pain, schizophrenia, anxiety, and autism [474]. Accordingly, mGlu receptors are promising targets for different neurological and psychiatric drugs.

The structure of the ECD of mGlu receptors has been determined [473] and shown to consist of a *'Venus fly trap' (VFT) domain*, which binds the glutamate agonist, and a *cysteine-rich (CR) domain*, which links the VFT domain to the TMD (Figure 7.47a). Thus, in contrast to GPCRs of classes A and B, class C GPCRs bind their ligands only through the ECD. The VFT domain also mediates the dimerization of mGluR[*1], and its crystallized structures demonstrate substantial conformational flexibility, which is stabilized by agonist binding. In 2014, the structure of the TMD of mGluR5 was determined in complex with the negative allosteric modulator mavoglurant [475] (Figure 7.47c, left). This structure was of great importance for two reasons. First, allosteric modulation of mGluR5 was postulated to be effective in treating anxiety disorders (negative modulation), as well as schizophrenia and disorders of cognitive function (positive modulation) [476]. Second, as explained earlier, drugs acting on allosteric

FIGURE 7.47 **The structure of the metabotropic glutamate receptor (mGluR).** (Opposite) (a) The extracellular domain of mGlu3 monomer in complex with glutamate [473] (PDB entry 2e4u). The Venus fly trap (VFT) and cysteine-rich (CR) domains are noted. (b) The dimeric structure of the EC domain of mGlu3. Each monomer is in a different color. The monomers interact via the VFT domain. The disulfide bond between the monomers is located in a disordered region that was not resolved in the structure. (c) The transmembrane domains of mGluR5 (PDB entry 4oo9) and mGluR1 (PDB entry 4or2), in complex with the negative allosteric modulators mavoglurant and FITM (respectively), shown as yellow sticks. ECL2, which caps the entrance to the allosteric site, is colored in magenta. The region in mGluR1 linking the TMD to the ECD is colored in green. (d) The postulated structure of the entire monomeric mGluR (for a more elaborate structure and domain interactions, see [404]). The structure was produced by joining the TMD and ECD through the linker regions. (e) A cross-section through mGluR1, showing the narrow allosteric site. (f) Superposition of mGluR5 and rhodopsin (PDB entry 1gzm), showing the differences in the relative orientations of TMs 5 and 7 between them. For clarity, only transmembrane helices are shown.

[*1] mGlu and calcium-sensing receptors create disulfide-linked homodimers (Figure 7.47b; note that the region forming the inter-chain disulfide link is missing in the structure). In contrast, the $GABA_B$ and taste 1 (TAS1) receptors form non-crosslinked heterodimers.

sites are more likely to be subtype-specific, since allosteric sites are less conserved than orthosteric (agonist-binding) sites. As in the case of the class B receptors described above, large flexible portions of the extracellular and intracellular domains of mGluR5 had to be removed for crystallization, so the exact positioning of the ECD with respect to the TMD is still unknown. The structure of the TMD of mGluR1 was determined in the same year, bound to the negative allosteric modulator FITM [404] (Figure 7.47c, right). In the case of mGluR1, however, the linker region to the ECD was resolved, allowing us to postulate the structure of the entire monomeric receptor (Figure 7.47d). Also, the structure was solved as a dimer, with six cholesterol molecules residing at the interface between the monomers (not shown). **These observations support the suggestion made earlier, that cholesterol molecules inside the membrane are involved in GPCR dimerization.**

The TMDs of mGluR1 and mGluR5 are overall similar to the TMDs of class A and class B GPCRs, especially on the intracellular side. As already explained above, this makes sense, considering that there are only a few intracellular binding partners for all GPCRs, such that minimal structural diversity is required in the intracellular region. When the different classes are compared in terms of the conformation of each helix in the TMD, most of the differences seem to be located in TMs 5 through 7 (see more below). As Figure 7.47c shows, in both mGluR structures, the allosteric binding site is deeper than the average class A binding site, yet is not as deep as the (class B) CRF receptor's binding site for the antagonist CP-376395 (see above). Still, FITM extends further towards the extracellular side of the transmembrane domain. The different locations and interactions of the two allosteric modulators with the TMD highlight the aforementioned potential of such modulators to serve as subtype-specific drugs. The entrance to the allosteric site in both structures is occluded by ECL2 (Figure 7.47c), and it is quite narrow (Figure 7.47e), mainly due to TMs 5 and 7, which have a more inward orientation compared to their counterparts in class A and class B GPCRs (Figure 7.47f). The capping of the TMD by ECL2 is consistent with the fact that, unlike in class A GPCRs, the native ligands of mGlu receptors bind to the ECD, so there is no need for a wide entrance to the TMD. Finally, the mGlu receptors include a set of ionic locks and other interactions[*1], which, as we have seen in class A GPCRs, are important for structural stabilization and the activation process. Although the positions involved in these interactions differ among the GPCR classes, their functional mechanisms are similar. A more detailed comparison between the functional motifs of class A GPCRs and those in class C (mGlu5R) is given in [475].

7.5.6.3 Class F GPCRs

Smoothened (SMO) is a GPCR-like protein that constitutes a part of the *hedgehog (Hh) signaling pathway*, which regulates animal embryonic development [477]. Malfunctioning of this pathway leads to embryonic malformations, and sometimes to cancer in adults. Several structures of SMO have been determined since 2013, in complex with different ligands [478–480]. In the first structure, of human SMO in complex with the antagonist LY2940680 [478], the architecture of the TMD was similar to that of class A GPCRs, de-

[*1] For example, in mGluR5 the ionic lock between Lys-665 (the equivalent of rhodopsin's Arg-135) and Glu-770 contributes to the stabilization of the inactive state. Indeed, disrupting the lock by mutating these residues to alanine leads to constitutive activity of the receptor [475].

spite low sequence identity (< 10%) between the two types of proteins (Figure 7.48a)[*1]. The differences in this domain are mostly in TMs 5 through 7, similar to what we have seen in the glutamate (mGlu) receptors. The ligand resides in the interface between the transmembrane and complex extracellular domains, and interacts mainly with ECL2 and ECL3 (Figure 7.48b)[*2]. As in the mGlu receptors, the ligand-binding cavity in SMO is narrow, partly because of the inward positioning of TM5. In the case of SMO, however, ECL2 is located inside the TMD.

In 2014 the antagonist-bound and agonist-bound structures of SMO were determined [479] (Figure 7.48c). One of the most pronounced differences between the two structures involves an ionic lock in the ligand-binding site, between Arg-400 (TM5) and Asp-473 (TM6). This interaction exists in the antagonist-bound structure but is eliminated upon agonist binding, due to a conformational change in Arg-400 (Figure 7.48c). In its new position, Arg-400 hydrogen-bonds with Asn-477, which is also part of TM6. This 'remodeling' of interactions is likely to serve as a molecular switch in the activation of SMO, although the current structures do not reveal the underlying mechanism. On the intracellular side of the transmembrane domain, the only significant difference between the two structures seems to be in the orientation of TM5 (Figure 7.48d), in contrast to the case of class A GPCRS, whose activation primarily involves changes in TM6. This difference, however, does not necessarily constitute a fundamental distinction between class A and class F GPCRs; the agonist-bound SMO lacks an intracellular binding partner[*3], which means it is not fully activated. Complete activation of the receptor may induce changes more reminiscent of those we observed in rhodopsin and in the β_2-adrenergic receptor.

7.5.7 GPCR-targeting drugs

As mentioned above, it is estimated that 30% to 50% of clinically prescribed drugs target GPCRs [343–346]. This is not surprising considering the numerous physiological processes that are regulated by GPCRs and the high accessibility of these cell-surface receptors. Therefore, the pharmaceutical industry constantly attempts to find new drugs that act on GPCRs [482]. GPCR-acting drugs are currently used to treat a plethora of pathological conditions and disorders (see Table 7.2). These drugs may be grouped as follows:

1. **Directly-acting drugs** affect the activity of the GPCR by binding to it. They can be further classified according to binding site type:

    - **Orthosteric drugs** constitute most of the GPCR-acting drugs. This type of compound binds to the orthosteric site of the GPCR and acts as an agonist, antagonist, or inverse agonist. The latter type is particularly interesting, as demonstrated by the antipsychotic drug *aripiprazole*. Psychosis is associated with overactivation of D_2 (dopamine) receptors in certain brain areas, which is why many antipsychotic drugs, e.g., *haloperidol*, act by blocking these receptors. Unfortu-

[*1] The low sequence identity results in the absence of most of the conserved motifs of class A GPCRs, including *D/ERY* (TM3), *CWxP* (TM6) and *NPxxY* (TM7).

[*2] In another antagonist-binding structure the ligand is bound deeper than LY2940680, but it still interacts with both the TMD and ECD [479], a hallmark of class F GPCRs.

[*3] SMO has been shown to activate G-proteins [481], but in the hedgehog pathway it may act (also) by activating other binding partners. For example, in fruit flies, SMO binds the kinesin-like protein *Costal-2* (*Cos2*). The exact way in which SMO activates the mammalian pathway is less understood, and may involve G-proteins.

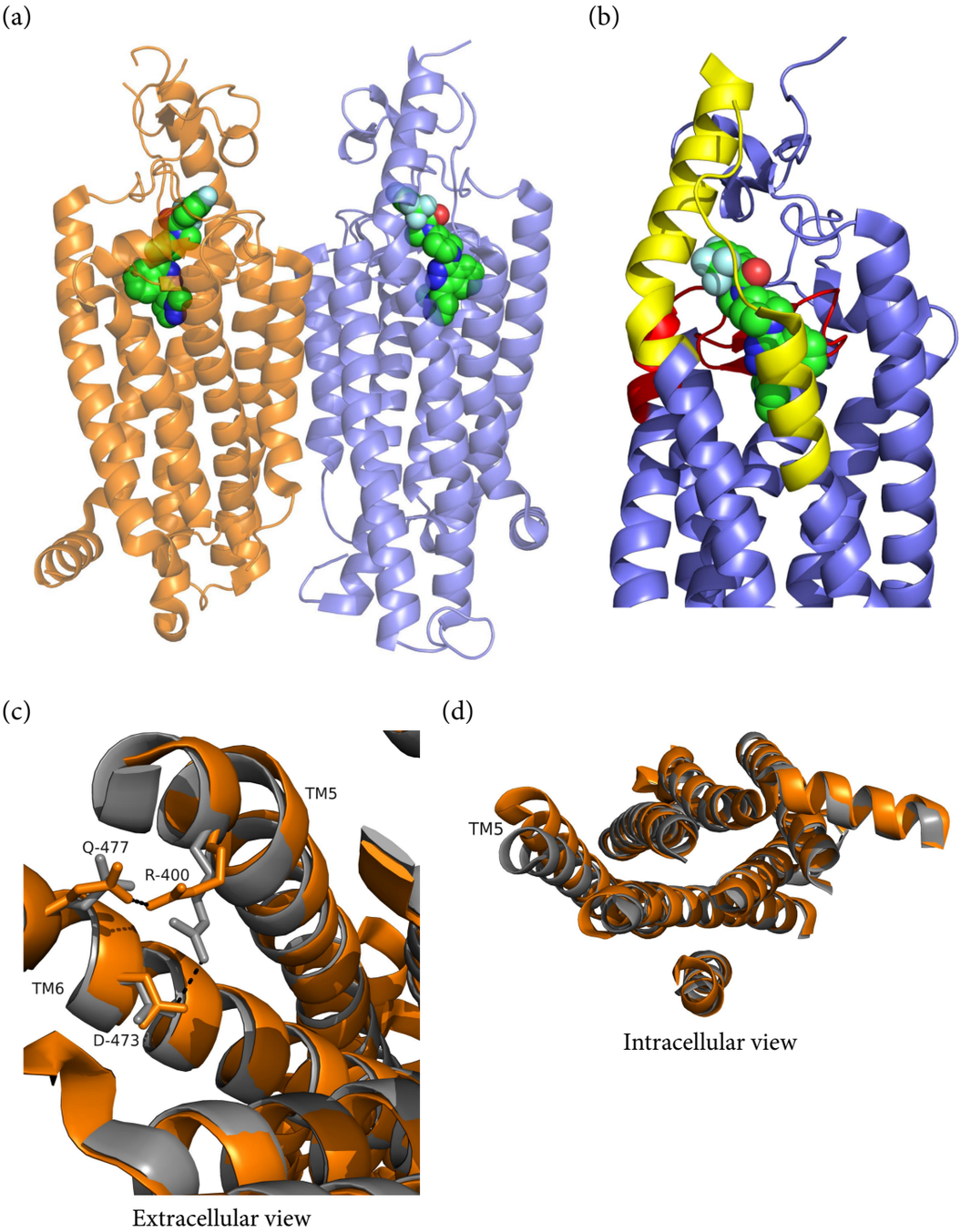

FIGURE 7.48 **The smoothened protein (SMO).** (a) The structure of the dimeric human SMO, bound to the antagonist LY2940680 (PDB entry 4jkv). Each subunit is colored differently, and the ligand is shown as spheres, colored by atom type. (b) The location of the ligand at the interface between the TMD and the ECD allows the ligand to interact extensively with ECL2 (red) and ECL3 (yellow). (c) and (d) Superposition of an antagonist-bound structure and an agonist-bound structure of SMO (PDB entries 4n4w and 4qin, respectively). For clarity, ECD segments and intracellular loops have been removed. (c) An extracellular view of the superposed structures, showing differences in noncovalent interactions that involve Arg-400, Asp-473, and Asn-477. (d) An intracellular view of the superposed structures showing conformational changes in the orientation of transmembrane helices.

nately, this blockage is a double-edged sword, which also leads to neurological side effects such as *tardive dyskinesia* (i.e., tremors). Like haloperidol and other antipsychotics, aripiprazole also acts on D_2 receptors. However, instead of blocking these receptors, it acts as a partial agonist. Not only does this action of aripiprazole lead to alleviation of psychotic symptoms, but it apparently also results in fewer side effects [483]. Finally, some of the directly acting drugs act as *bivalent ligands*, i.e., they bind in a way that promotes dimerization of GPCR [484].

- **Allosteric drugs** bind to an allosteric site and modulate the activity of the GPCR directly, or by changing its affinity to the natural ligand. *Maraviroc* is an example of an allosterically acting therapeutic agent. It is an antiretroviral drug used for the treatment of HIV infection. The drug targets CCR5 (the C-C chemokine receptor type 5), which is a co-receptor of HIV on certain white blood cells. By allosterically stabilizing an inactive conformation of the receptor [485], maraviroc prevents the binding of the virus to CCR5, thus blocking HIV entry into the host cell. The 3D structure of the CCR5-maraviroc complex (Figure 7.49) suggests that the drug stabilizes the inactive conformation via nonpolar interactions with the transmission switch Trp-248 (the equivalent of rhodopsin's Trp-265). This should prevent movement of the tryptophan residue, which, as we saw earlier, is part of the activation process of certain GPCRs. Allosteric drugs are of great interest to the pharmaceutical industry [482], for at least two reasons. First, they constitute an alternative to the veteran orthosteric drugs, which have already been studied extensively. Second, allosteric drugs enable pharmaceutical scientists to control the activity of target GPCRs more accurately (see Chapter 9 for details), and, since allosteric sites are less conserved than orthosteric sites, allosteric drugs tend to be more subtype-selective.

2. **Indirectly-acting drugs** change the activity of GPCRs by affecting other proteins. SSRIs are well-known examples of such drugs; these antidepressants elevate the levels of serotonin in the brain by inhibiting its reuptake from the synapse [486,487] (see Chapter 1). Although SSRIs directly target serotonin transporters rather than GPCRs, the resulting elevation of serotonin levels leads to increased action of this neurotransmitter on its cognate receptor, which is a GPCR [378].

Academic and industrial labs worldwide are continuously searching for GPCR-acting drugs. The drug discovery process is similar to that corresponding to other protein targets, as described in Chapter 8. Briefly, this process relies mostly on the screening of many known molecules with potential to bind to the target protein and change its activity. In the past the screening process was conducted solely in the lab using various binding and functional assays. Such assays were, however, costly and time-consuming, and could only be carried out effectively by large organizations. The subsequent development of computational methods for small molecules enabled pharmaceutical scientists to conduct *structure-activity relationship* (*SAR*) studies, in which the structural and chemical properties of a desired drug were deduced on the basis of the activity of other, yet similar, known drugs. Later, more sophisticated computational methods were developed, in which, given a 3D structure of a protein and a ligand, it became possible to characterize the physicochemical interaction between the two molecules (*receptor-based approach*). The determination of numerous high-resolution

structures of GPCRs in various states and with various bound ligands has enabled scientists to use the receptor-based approach to predict the binding of many millions of potential compounds to a target GPCR, in a relatively short time (*virtual screening*) [482]. The top-ranking compounds are then tested in the lab to confirm the binding and characterize their pharmacological activity.

As mentioned above, there is a growing effort to develop allosteric drugs that will facilitate more accurate modulation of GPCR activity and complement the arsenal of existing drugs, most of which act as agonists or antagonists on orthosteric sites. However, discovering allosteric drugs is not an easy task, as it requires knowledge of active and inactive conformations of the protein, which usually requires crystallization of the GPCR with various ligands or under different conditions. Additional desired goals in GPCR drug discovery include the following drug types [482]:

- **Biased drugs** that activate specific signaling pathways [454,455]. Such drugs render treatment more specific, and their use is therefore expected to result in fewer side effects. This is particularly important in the case of GPCRs, which, as explained above, are involved in virtually all physiological processes in the body. Furthermore, the use of biased drugs is also expected to allow the targeting of the same GPCR for treating different diseases [482]. In such cases, each biased drug inhibits or amplifies a different signaling route that is initiated by the same GPCR.

- **Dual-acting drugs** that can bind to different receptors or other proteins. Such drugs

TABLE 7.2 **Examples of GPCR-targeting drugs.**

Type of Disease or Disorder	Disease or Disorder	Drug	Target GPCR
Psychiatric	Depression or anxiety	Buspirone	5-HT_{1A} and D_2 receptors
	Schizophrenia	Aripiprazole	D_2 (dopamine) receptor
	Insomnia	Suvorexant	Orexin receptor
Cardiovascular	Hypertension Congestive heart failure	Valsartan	Angiotensin receptor
	Thrombosis	Clopidogrel	$P2Y_{12}$ receptor
Neurological	Pain	Oxycodone	Opioid receptors
	Migraine	Sumatriptan	5-HT_1 receptor
	Vomiting or nausea	Dolasetron	5-HT_3 receptor
Respiratory	Asthma or chronic obstructive pulmonary disease (COPD)	Salmeterol	β_2-adrenergic receptor
Metabolic	Diabetes	Albiglutide	GLP-1 receptor
Hormonal	Hypothyroidism	Parathyroid hormone	PTH receptor
	Acromegaly	Octreotide	Somatostatin receptor
Gastrointestinal	Gastric ulcers	Ranitidine	H_2 receptor
Cancer	Prostate cancer	Leuprolide	GNRH receptor

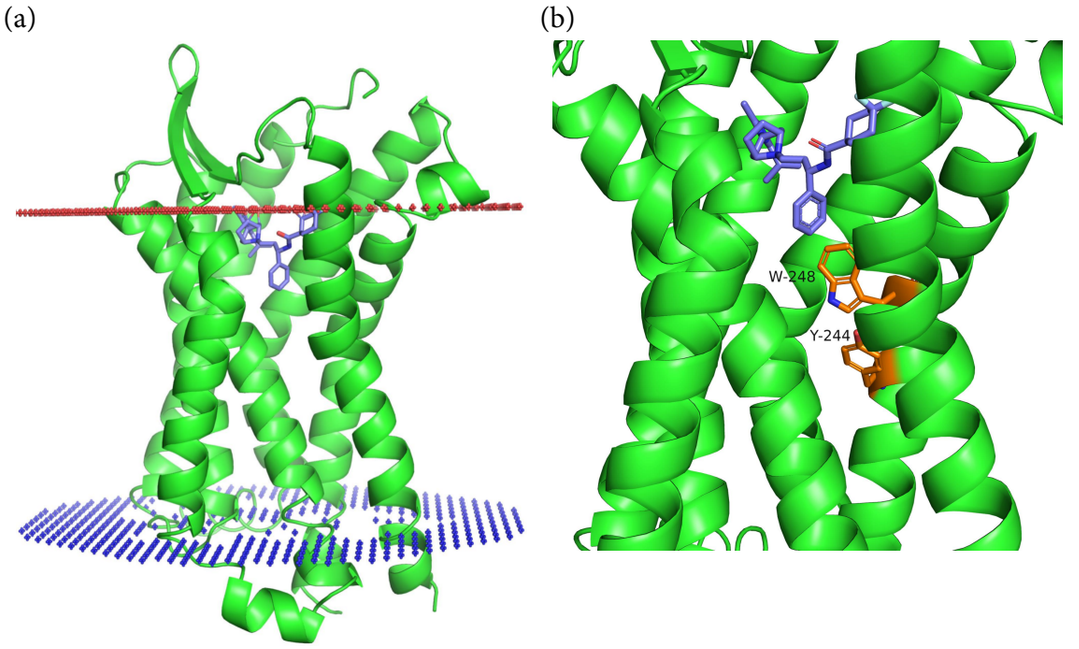

FIGURE 7.49 **Binding of the drug maraviroc to CCR5.** (a) An overall view of the receptor. The receptor is shown as a green ribbon, and maraviroc, which is bound to the ECD-TMD interface, is shown as blue sticks. (b) A magnification of the maraviroc binding site. The drug forms nonpolar interactions with Trp-248, which is thought to prevent the protein from undergoing activation-induced conformational changes. Trp-248 and Tyr-244 constitute a switch that relays the ligand-induced activation process to the intracellular domain. Thus, preventing Trp-248 from moving is expected to inhibit CCR5 activation, which in turn prevents CCR5-HIV binding and viral entry into the cell.

can couple the activity of different GPCRs, or the activity of a GPCR to that of another protein that complements it. For example, the small molecule *donecopride* can both activate 5-HT_4 (serotonin) receptors and inhibit the enzyme acetylcholinesterase. The combined effect of the two activities is potentially beneficial for treating Alzheimer's disease [488].

- **Monoclonal antibodies** that bind to desired GPCRs in a highly specific manner and modulate their activity (e.g., [489]). However, the administration and use of such drugs is much more complicated than in the case of small molecules.
- **Drugs that affect the trafficking or desensitization of the GPCR** (e.g., GRKs and arrestins [490]).

7.6 SUMMARY

- Membrane-bound proteins constitute 20% to 30% of the human genome and are involved in numerous cellular and physiological processes. As such, they are also involved in different pathologies, and therefore constitute prime targets for drugs.
- Membrane proteins reside in a two-layered lipid body referred to as the lipid bilayer.

They are either immersed inside it or anchored to it peripherally. The highly anisotropic lipid bilayer has complex physicochemical properties, such as amphipathicity, asymmetry, quasi-fluidity, and curvature.

- These properties, in addition to specific interactions between membrane proteins and lipids, affect the properties of both. Importantly, the properties of the lipid bilayer significantly constrain the structural space available for membrane proteins. Therefore, despite the limited number of experimentally solved structures of membrane proteins, the principles governing their structure can be deduced.

- At the primary structure level, the transmembrane regions of membrane proteins tend to be highly nonpolar and contain on average 21 to 26 residues. These strong tendencies are the basis for current computer algorithms that trace membrane proteins in raw genomic sequences.

- Transmembrane segments of membrane proteins have an extremely high tendency to form secondary structures, mostly α-helices. This property is mainly driven by a need for lipid-exposed polar backbone groups to be paired in hydrogen bonds.

- At the tertiary structure level, transmembrane domains are mostly arranged as α-helical bundles, and in some cases as β-barrels. The near total dominance of the former structure probably results from its high adaptability. Indeed, helical bundles can form a range of structures, each fulfilling a different role. For example, they can form water-filled ion channels through which ions can diffuse across the membrane, or water-free transporters that undergo considerable conformational changes in order to 'pick up' a ligand on one side of the membrane and release it on the other side. Both of these structures contain domains (or elements) responsible for transport, as well as domains (or elements) that regulate transport according to cellular needs.

- Some membrane proteins have complex structures and are involved in equally complex physiological processes. Examples of such proteins are G protein-coupled receptors (GPCRs), which respond to a variety of hormones, factors, and even light photons. Most GPCRs have a similar seven-transmembrane structures, and they differ mainly in their extracellular domains. The response of a GPCR to its ligand involves conformational changes, which allow the protein to bind and activate its cognate G-protein(s) in the cytoplasm. Thus, an entire signal transduction system is activated, with results that are often dramatic to the cell. The large number of GPCR structures determined in recent years demonstrates that the activation process involves various molecular triggers and switches, which relay the ligand-binding signal to the intracellular side of the protein, thus creating a binding site for the G-protein. Moreover, the binding induces conformational changes in, and activation of, the G-protein. Although the molecular triggers and switches differ to some extent between different classes of GPCRs, many of them are associated with shared conserved motifs, and work in similar ways.

EXERCISES

7.1 Explain why the interest in membrane proteins far exceeds their relative proportion in a cell.

7.2 The lipids found in biological membranes differ significantly from each other in chemical structure and composition. What makes them all suitable as membrane building blocks?

7.3 Unlike other membrane lipids, cholesterol has a bulky, rigid structure. In your opinion, how would this structure affect membrane properties?

7.4 Suggest reasons why membranes of different organelles, cells, and organs differ so significantly in their lipid composition.

7.5 A. Estimate how many encounters between a divalent cation and the plasma membrane are needed in order for the cation to cross the membrane successfully. Assume that the radius of the cation is 1 Å, and that the dielectrics of the membrane and cytoplasm or extracellular matrix are 2 and 80, respectively.

B. If each unsuccessful cation-membrane encounter lasts 10^{-12} s, how much time may be needed for the system to achieve a successful encounter?

7.6 Following the study of Elazar et al. (2016) (*Elife* **5**:e12125), state the expected general locations of the following amino acids in an integral membrane protein: Val, Trp, Arg, Pro, and Asp. Explain your prediction.

7.7 What are the main differences between the driving forces for the folding of globular proteins and those of integral membrane proteins?

7.8 Explain the following observations regarding membrane proteins that function in the transport of ions:

I. Channels contain a water annulus, yet make the passing ions lose their solvation shell for a short part of the way.

II. Carriers do not contain a constant water annulus linking the bulk solvent on both sides of the membrane.

7.9 Peripheral membrane proteins require more than a single type of noncovalent interaction to bind to the membrane. Explain the underlying advantage(s).

7.10 List the different means that the protein-membrane system can use to ameliorate the energy cost of positive hydrophobic mismatch.

7.11 Explain how activation of adrenergic receptors serves the 'fight-or-flight' response in animals.

7.12 Unlike other class A GPCRs, rhodopsin has no baseline activity in the absence of an agonist. Which structural features of GPCRs have been proposed to explain this phenomenon?

7.13 List the structural features of GPCR activation that have emerged from the study of rhodopsin's active and inactive structures.

REFERENCES

1. J. W. Schopf. Microfossils of the Early Archean Apex Chert: new evidence of the antiquity of life. *Science*, 260:640–6, 1993.
2. J. W. Schopf and B. M. Packer. Early Archean (3.3-billion to 3.5-billion-year-old) microfossils from Warrawoona Group, Australia. *Science*, 237:70–3, 1987.
3. S. J. Mojzsis, G. Arrhenius, K. D. McKeegan, T. M. Harrison, A. P. Nutman, and C. R. Friend. Evidence for life on Earth before 3,800 million years ago. *Nature*, 384(6604):55–9, 1996.
4. L. J. Ducka, M. Gliksona, S. D. Goldinga, and R. D. Webb. Microbial remains and other carbonaceous forms from the 3.24 Ga Sulphur Springs black smoker deposit, Western Australia. *Precambrian Res.*, 154(3–4):205–220, 2007.
5. I. Bertini, A. Sigel, and H. Sigel. *Handbook on metalloproteins*. Marcel Dekker, New York, 2001.
6. J. J. R. Frausto da Silva and R. J. P. Williams. *The biological chemistry of the elements: the inorganic chemistry of life*. Oxford University Press, New York, 2001.
7. S. Dorairaj and T. W. Allen. On the thermodynamic stability of a charged arginine side chain in a transmembrane helix. *Proc. Natl. Acad. Sci. USA*, 104(12):4943–8, 2007.
8. A. Kessel and N. Ben-Tal. Free energy determinants of peptide association with lipid bilayers. *Curr. Top. Membr.*, 52:205–253, 2002.
9. G. von Heijne. The membrane protein universe: what's out there and why bother? *J. Intern. Med.*, 261:543–557, 2007.
10. E. Wallin and G. von Heijne. Genome-wide analysis of integral membrane proteins from eubacterial, archaean, and eukaryotic organisms. *Protein Sci.*, 7(4):1029–38, 1998.
11. J. D. Bendtsen, T. T. Binnewies, P. F. Hallin, and D. W. Ussery. Genome update: prediction of membrane proteins in prokaryotic genomes. *Microbiology*, 151(Pt 7):2119–21, 2005.
12. M. Uhlen, L. Fagerberg, B. M. Hallstrom, C. Lindskog, P. Oksvold, A. Mardinoglu, A. Sivertsson, C. Kampf, E. Sjostedt, A. Asplund, I. Olsson, K. Edlund, E. Lundberg, S. Navani, C. A. Szigyarto, J. Odeberg, D. Djureinovic, J. O. Takanen, S. Hober, T. Alm, P. H. Edqvist, H. Berling, H. Tegel, J. Mulder, J. Rockberg, P. Nilsson, J. M. Schwenk, M. Hamsten, K. von Feilitzen, M. Forsberg, L. Persson, F. Johansson, M. Zwahlen, G. von Heijne, J. Nielsen, and F. Ponten. Proteomics. Tissue-based map of the human proteome. *Science*, 347(6220):1260419, 2015.
13. M. A. Yildirim, K.-I. Goh, M. E. Cusick, A.-L. Barabasi, and M. Vidal. Drug–target network. *Nat. Biotechnol.*, 25(10):1119–1126, 2007.
14. D. Salom and K. Palczewski. Structural Biology of Membrane Proteins. In A. S. Robinson, editor, *Production of Membrane Proteins: Strategies for Expression and Isolation*, chapter 9, pages 249–273. Wiley-Vch, 2011.
15. A. L. Hopkins and C. R. Groom. The druggable genome. *Nat. Rev. Drug Discov.*, 1(9):727–30, 2002.
16. A. P. Russ and S. Lampel. The druggable genome: an update. *Drug Discov. Today*, 10(23–24):1607–10, 2005.
17. S. J. Singer and G. L. Nicolson. The fluid mosaic model of the structure of cell membranes. *Science*, 175(23):720–31, 1972.
18. A. D. Dupuy and D. M. Engelman. Protein area occupancy at the center of the red blood cell membrane. *Proc. Natl. Acad. Sci. USA*, 105:2848–2852, 2008.
19. J. E. Rothman and L. Orci. Budding vesicles in living cells. *Sci. Am.*, 274(3):70–5, 1996.
20. N. A. Bright, M. J. Gratian, and J. P. Luzio. Endocytic delivery to lysosomes mediated by concurrent fusion and kissing events in living cells. *Curr. Biol.*, 15(4):360–5, 2005.
21. J. Pietzsch. Mind the membrane. In *Horizon Symposia: Living Frontier*, volume 1. Nature Publishing Group, 2004.
22. S. H. White and G. von Heijne. How translocons select transmembrane helices. *Annu. Rev. Biophys.*, 37:23–42, 2008.
23. E. K. Fridriksson, P. A. Shipkova, E. D. Sheets, D. Holowka, B. Baird, and F. W. McLafferty. Quantitative analysis of phospholipids in functionally important membrane domains from RBL-2H3 mast cells using tandem high-resolution mass spectrometry. *Biochemistry*, 38(25):8056–63, 1999.
24. B. Brugger, G. Erben, R. Sandhoff, F. T. Wieland, and W. D. Lehmann. Quantitative analysis of biological membrane lipids at the low picomole level by nano-electrospray ionization tandem mass spectrometry. *Proc. Natl. Acad. Sci. USA*, 94(6):2339–44, 1997.
25. J. J. Myher, A. Kuksis, and S. Pind. Molecular species of glycerophospholipids and sphingomyelins of human erythrocytes: improved method of analysis. *Lipids*, 24(5):396–407, 1989.

26. J. I. MacDonald and H. Sprecher. Phospholipid fatty acid remodeling in mammalian cells. *Biochim. Biophys. Acta*, 1084(2):105–21, 1991.
27. D. L. Nelson and M. M. Cox. *Lehninger Principles of Biochemistry*. W. H. Freeman and Company, 2004.
28. J. Lecocq and C. E. Ballou. On the Structure of Cardiolipin. *Biochemistry*, 3:976–80, 1964.
29. D. Hishikawa, H. Shindou, S. Kobayashi, H. Nakanishi, R. Taguchi, and T. Shimizu. Discovery of a lysophospholipid acyltransferase family essential for membrane asymmetry and diversity. *Proc. Natl. Acad. Sci. USA*, 105:2830–2835, 2008.
30. A. G. Lee. How lipids affect the activities of integral membrane proteins. *Biochim. Biophys. Acta*, 1666(1–2):62–87, 2004.
31. B. A. Lewis and D. M. Engelman. Lipid bilayer thickness varies linearly with acyl chain length in fluid phosphatidylcholine vesicles. *J. Mol. Biol.*, 166(2):211–7, 1983.
32. F. M. Goni and A. Alonso. Biophysics of sphingolipids I. Membrane properties of sphingosine, ceramides and other simple sphingolipids. *Biochim. Biophys. Acta*, 1758(12):1902–21, 2006.
33. B. Maggio, M. L. Fanani, C. M. Rosetti, and N. Wilke. Biophysics of sphingolipids II. Glycosphingolipids: an assortment of multiple structural information transducers at the membrane surface. *Biochim. Biophys. Acta*, 1758(12):1922–44, 2006.
34. F. R. Maxfield and I. Tabas. Role of cholesterol and lipid organization in disease. *Nature*, 438(7068):612–21, 2005.
35. J. L. Goldstein and M. S. Brown. Molecular medicine. The cholesterol quartet. *Science*, 292(5520):1310–2, 2001.
36. R. Wood and R. D. Harlow. Structural analyses of rat liver phosphoglycerides. *Arch. Biochem. Biophys.*, 135(1):272–81, 1969.
37. M. Schlame, S. Brody, and K. Y. Hostetler. Mitochondrial cardiolipin in diverse eukaryotes. Comparison of biosynthetic reactions and molecular acyl species. *Eur. J. Biochem.*, 212(3):727–35, 1993.
38. A. Yamashita, T. Sugiura, and K. Waku. Acyltransferases and transacylases involved in fatty acid remodeling of phospholipids and metabolism of bioactive lipids in mammalian cells. *J. Biochem.*, 122(1):1–16, 1997.
39. T. K. Ray, V. P. Skipski, M. Barclay, E. Essner, and F. M. Archibald. Lipid composition of rat liver plasma membranes. *J. Biol. Chem.*, 244(20):5528–36, 1969.
40. S. Morein, A. Andersson, L. Rilfors, and G. Lindblom. Wild-type *Escherichia coli* cells regulate the membrane lipid composition in a "window" between gel and non-lamellar structures. *J. Biol. Chem.*, 271(12):6801–9, 1996.
41. M. B. Coren. Biosynthesis and structures of phospholipids and sulfatides. In G. P. Kubica and L. G. Wayne, editors, *The Mycobacteria*, pages 379–415. Marcel Dekker, New York, 1984.
42. P. L. Yeagle. *The structure of biological membranes*. CRC Press, Boca Raton, New York, 2nd edition, 2005.
43. C. Tanford. *The hydrophobic effect*. Wiley, New-York, 1973.
44. T. W. Keenan and D. J. Morre. Phospholipid class and fatty acid composition of Golgi apparatus isolated from rat liver and comparison with other cell fractions. *Biochemistry*, 9(1):19–25, 1970.
45. L. Orci, R. Montesano, P. Meda, F. Malaisse-Lagae, D. Brown, A. Perrelet, and P. Vassalli. Heterogeneous distribution of filipin–cholesterol complexes across the cisternae of the Golgi apparatus. *Proc. Natl. Acad. Sci. USA*, 78(1):293–7, 1981.
46. P. F. Pimenta and W. de Souza. Localization of filipin-sterol complexes in cell membranes of eosinophils. *Histochem. Cell Biol.*, 80(6):563–7, 1984.
47. L. D. Bergelson and L. I. Barsukov. Topological asymmetry of phospholipids in membranes. *Science*, 197(4300):224–30, 1977.
48. J. A. Op den Kamp. Lipid asymmetry in membranes. *Annu. Rev. Biochem.*, 48:47–71, 1979.
49. R. F. Zwaal and A. J. Schroit. Pathophysiologic implications of membrane phospholipid asymmetry in blood cells. *Blood*, 89(4):1121–32, 1997.
50. D. Marquardt, B. Geier, and G. Pabst. Asymmetric lipid membranes: towards more realistic model systems. *Membranes*, 5(2):180–196, 2015.
51. S. Mukherjee and F. R. Maxfield. Membrane domains. *Annu. Rev. Cell. Dev. Biol.*, 20:839–66, 2004.
52. K. Simons and W. L. Vaz. Model systems, lipid rafts, and cell membranes. *Annu. Rev. Biophys. Biomol. Struct.*, 33:269–95, 2004.
53. S. H. White and W. C. Wimley. Membrane protein folding and stability: physical principles. *Annu. Rev. Biophys. Biomol. Struct.*, 28:319–65, 1999.
54. J. C. Holthuis and T. P. Levine. Lipid traffic: floppy drives and a superhighway. *Nat. Rev. Mol. Cell Biol.*, 6(3):209–20, 2005.

55. D. L. Daleke. Regulation of transbilayer plasma membrane phospholipid asymmetry. *J. Lipid Res.*, 44(2):233–42, 2003.
56. D. A. Brown and E. London. Structure and origin of ordered lipid domains in biological membranes. *J. Membr. Biol.*, 164(2):103–14, 1998.
57. K. Mitra, I. Ubarretxena-Belandia, T. Taguchi, G. Warren, and D. M. Engelman. Modulation of the bilayer thickness of exocytic pathway membranes by membrane proteins rather than cholesterol. *Proc. Natl. Acad. Sci. USA*, 101(12):4083–8, 2004.
58. H. T. McMahon and J. L. Gallop. Membrane curvature and mechanisms of dynamic cell membrane remodelling. *Nature*, 438(7068):590–6, 2005.
59. J. M. Seddon. Structure of the inverted hexagonal (HII) phase, and non-lamellar phase transitions of lipids. *Biochim. Biophys. Acta*, 1031(1):1–69, 1990.
60. L. T. Boni and S. W. Hui. Polymorphic phase behaviour of dilinoleoylphosphatidylethanolamine and palmitoyloleoylphosphatidylcholine mixtures. Structural changes between hexagonal, cubic and bilayer phases. *Biochim. Biophys. Acta*, 731(2):177–85, 1983.
61. S. M. Gruner. Intrinsic curvature hypothesis for biomembrane lipid composition: a role for nonbilayer lipids. *Proc. Natl. Acad. Sci. USA*, 82(11):3665–9, 1985.
62. W. C. Wimley. Toward genomic identification of beta-barrel membrane proteins: composition and architecture of known structures. *Protein Sci.*, 11:301–312, 2002.
63. S. Watson and S. Arkinstall. *The C-Protein Linked Receptor-Facts Book*. Academic Press, London, 1994.
64. F. Horn, E. Bettler, L. Oliveira, F. Campagne, F. E. Cohen, and G. Vriend. GPCRDB information system for G protein-coupled receptors. *Nucleic Acids Res.*, 31(1):294–7, 2003.
65. T. M. Bridges and C. W. Lindsley. G-Protein-Coupled Receptors: From Classical Modes of Modulation to Allosteric Mechanisms. *ACS Chem. Biol.*, 3:530–41, 2008.
66. T. H. Ji, M. Grossmann, and I. Ji. G protein-coupled receptors. I. Diversity of receptor-ligand interactions. *J. Biol. Chem.*, 273(28):17299–302, 1998.
67. I. Moraes, G. Evans, J. Sanchez-Weatherby, S. Newstead, and P. D. Stewart. Membrane protein structure determination: the next generation. *Biochim. Biophys. Acta*, 1838(1 Pt A):78–87, 2014.
68. I. D. Pogozheva, H. I. Mosberg, and A. L. Lomize. Life at the border: Adaptation of proteins to anisotropic membrane environment. *Protein Sci.*, 23(9):1165–1196, 2014.
69. A. Oberai, Y. Ihm, S. Kim, and J. U. Bowie. A limited universe of membrane protein families and folds. *Protein Sci.*, 15(7):1723–1734, 2006.
70. S. H. White, A. S. Ladokhin, S. Jayasinghe, and K. Hristova. How membranes shape protein structure. *J. Biol. Chem.*, 276(35):32395–8, 2001.
71. N. Hurwitz, M. Pellegrini-Calace, and D. T. Jones. Towards genome-scale structure prediction for transmembrane proteins. *Philos. Trans. R. Soc. Lond. B: Biol. Sci.*, 361(1467):465–75, 2006.
72. C. Baeza-Delgado, M. A. Marti-Renom, and I. Mingarro. Structure-based statistical analysis of transmembrane helices. *Eur. Biophys. J.*, 42(2–3):199–207, 2013.
73. G. von Heijne. Recent advances in the understanding of membrane protein assembly and structure. *Q. Rev. Biophys.*, 32(4):285–307, 1999.
74. G. von Heijne. Membrane-protein topology. *Nat. Rev. Mol. Cell Biol.*, 7(12):909–18, 2006.
75. F. Cymer, G. von Heijne, and S. H. White. Mechanisms of integral membrane protein insertion and folding. *J. Mol. Biol.*, 427(5):999–1022, 2015.
76. J.-L. Popot and D. M. Engelman. Helical membrane protein folding, stability, and evolution. *Annu. Rev. Biochem.*, 69:881–922, 2000.
77. J. U. Bowie. Helix packing in membrane proteins. *J. Mol. Biol.*, 272(5):780–9, 1997.
78. J. U. Bowie. Understanding membrane protein structure by design. *Nat. Struct. Biol.*, 7(2):91–4, 2000.
79. R. Worch, C. Bökel, S. Höfinger, P. Schwille, and T. Weidemann. Focus on composition and interaction potential of single-pass transmembrane domains. *Proteomics*, 10(23):4196–4208, 2010.
80. K. Illergård, A. Kauko, and A. Elofsson. Why are polar residues within the membrane core evolutionary conserved? *Proteins*, 79(1):79–91, 2011.
81. M. Bañó-Polo, C. Baeza-Delgado, M. Orzáez, M. A. Marti-Renom, C. Abad, and I. Mingarro. Polar/Ionizable residues in transmembrane segments: effects on helix-helix packing. *PLoS One*, 7(9):e44263, 2012.
82. T. H. Walther and A. S. Ulrich. Transmembrane helix assembly and the role of salt bridges. *Curr. Opin. Struct. Biol.*, 27:63–68, 2014.

83. S. Chakrapani, L. G. Cuello, D. M. Cortes, and E. Perozo. Structural dynamics of an isolated voltage-sensor domain in a lipid bilayer. *Structure*, 16(3):398–409, 2008.
84. D. Krepkiy, M. Mihailescu, J. A. Freites, E. V. Schow, D. L. Worcester, K. Gawrisch, D. J. Tobias, S. H. White, and K. J. Swartz. Structure and hydration of membranes embedded with voltage-sensing domains. *Nature*, 462(7272):473–479, 2009.
85. A. G. Lee. Structural biology: Highly charged meetings. *Nature*, 462(7272):420–421, 2009.
86. J. U. Bowie. Solving the membrane protein folding problem. *Nature*, 438(7068):581–9, 2005.
87. M. Gimpelev, L. R. Forrest, D. Murray, and B. Honig. Helical packing patterns in membrane and soluble proteins. *Biophys. J.*, 87(6):4075–4086, 2004.
88. T. A. Eyre, L. Partridge, and J. M. Thornton. Computational analysis of α-helical membrane protein structure: implications for the prediction of 3D structural models. *Protein Eng. Des. Sel.*, 17(8):613–624, 2004.
89. X. Deupi, M. Olivella, C. Govaerts, J. A. Ballesteros, M. Campillo, and L. Pardo. Ser and Thr residues modulate the conformation of pro-kinked transmembrane alpha-helices. *Biophys. J.*, 86(1 Pt 1):105–15, 2004.
90. E. Granseth, G. von Heijne, and A. Elofsson. A study of the membrane-water interface region of membrane proteins. *J. Mol. Biol.*, 346(1):377–85, 2005.
91. C. Landolt-Marticorena, K. A. Williams, C. M. Deber, and R. A. Reithmeier. Non-random distribution of amino acids in the transmembrane segments of human type I single span membrane proteins. *J. Mol. Biol.*, 229(3):602–8, 1993.
92. M. B. Ulmschneider, M. S. Sansom, and A. Di Nola. Properties of integral membrane protein structures: derivation of an implicit membrane potential. *Proteins*, 59(2):252–65, 2005.
93. G. V. Heijne. The distribution of positively charged residues in bacterial inner membrane proteins correlates with the trans-membrane topology. *EMBO J.*, 5(11):3021–3027, 1986.
94. M. Schiffer, C. H. Chang, and F. J. Stevens. The functions of tryptophan residues in membrane proteins. *Protein Eng.*, 5(3):213–4, 1992.
95. A. N. Ridder, S. Morein, J. G. Stam, A. Kuhn, B. de Kruijff, and J. A. Killian. Analysis of the role of interfacial tryptophan residues in controlling the topology of membrane proteins. *Biochemistry*, 39(21):6521–8, 2000.
96. G. von Heijne. Membrane protein structure prediction. Hydrophobicity analysis and the positive-inside rule. *J. Mol. Biol.*, 225(2):487–94, 1992.
97. A. Elazar, J. Weinstein, I. Biran, Y. Fridman, E. Bibi, and S. J. Fleishman. Mutational scanning reveals the determinants of protein insertion and association energetics in the plasma membrane. *eLife*, 5:e12125, 2016.
98. J. P. Segrest, H. De Loof, J. G. Dohlman, C. G. Brouillette, and G. M. Anantharamaiah. Amphipathic helix motif: classes and properties. *Proteins*, 8(2):103–17, 1990.
99. R. Jackups and J. Liang. Interstrand pairing patterns in β-barrel membrane proteins: the positive-outside rule, aromatic rescue, and strand registration prediction. *J. Mol. Biol.*, 354(4):979–993, 2005.
100. J. Qu, S. Behrens-Kneip, O. Holst, and J. H. Kleinschmidt. Binding regions of outer membrane protein A in complexes with the periplasmic chaperone Skp. A site-directed fluorescence study. *Biochemistry*, 48(22):4926–4936, 2009.
101. S. J. Fleishman and N. Ben-Tal. Progress in structure prediction of alpha-helical membrane proteins. *Curr. Opin. Struct. Biol.*, 16(4):496–504, 2006.
102. J. Kyte and R. F. Doolittle. A simple method for displaying the hydropathic character of a protein. *J. Mol. Biol.*, 157(1):105–32, 1982.
103. K. P. Hofmann and W. Stoffel. TMbase: A database of membrane spanning proteins segments. *Biol. Chem.*, 374:166, 1993.
104. TMpred. http://www.ch.embnet.org/software/TMPRED_form.html, 2017.
105. W. C. Wimley and S. H. White. Experimentally determined hydrophobicity scale for proteins at membrane interfaces. *Nat. Struct. Biol.*, 3(10):842–8, 1996.
106. D. M. Engelman, T. A. Steitz, and A. Goldman. Identifying nonpolar transbilayer helices in amino acid sequences of membrane proteins. *Annu. Rev. Biophys. Biophys. Chem.*, 15:321–53, 1986.
107. D. Eisenberg, W. Wilcox, and A. D. McLachlan. Hydrophobicity and amphiphilicity in protein structure. *J. Cell Biochem.*, 31(1):11–7, 1986.
108. W. C. Wimley, T. P. Creamer, and S. H. White. Solvation energies of amino acid side chains and backbone in a family of host-guest pentapeptides. *Biochemistry*, 35(16):5109–5124, 1996.
109. T. Hessa, H. Kim, K. Bihlmaier, C. Lundin, J. Boekel, H. Andersson, I. Nilsson, S. H. White, and G. von Heijne. Recognition of transmembrane helices by the endoplasmic reticulum translocon. *Nature*, 433(7024):377–81, 2005.
110. T. Hessa, N. M. Meindl-Beinker, A. Bernsel, H. Kim, Y. Sato, M. Lerch-Bader, I. Nilsson, S. H. White,

and G. Von Heijne. Molecular code for transmembrane-helix recognition by the Sec61 translocon. *Nature*, 450(7172):1026–1030, 2007.

111. K. Öjemalm, S. C. Botelho, C. Stüdle, and G. von Heijne. Quantitative analysis of SecYEG-mediated insertion of transmembrane α-helices into the bacterial inner membrane. *J. Mol. Biol.*, 425(15):2813–2822, 2013.
112. A. Bernsel, H. Viklund, J. Falk, E. Lindahl, G. von Heijne, and A. Elofsson. Prediction of membrane-protein topology from first principles. *Proc. Natl. Acad. Sci. USA*, 105(20):7177–7181, 2008.
113. D. Shental-Bechor, S. J. Fleishman, and N. Ben-Tal. Has the code for protein translocation been broken? *Trends Biochem. Sci.*, 31(4):192–6, 2006.
114. A. C. V. Johansson and E. Lindahl. Protein contents in biological membranes can explain abnormal solvation of charged and polar residues. *Proc. Natl. Acad. Sci. USA*, 106(37):15684–15689, 2009.
115. A. Senes, D. C. Chadi, P. B. Law, R. F. S. Walters, V. Nanda, and W. F. DeGrado. E(z), a depth-dependent potential for assessing the energies of insertion of amino acid side-chains into membranes: derivation and applications to determining the orientation of transmembrane and interfacial helices. *J. Mol. Biol.*, 366(2):436–448, 2007.
116. C. A. Schramm, B. T. Hannigan, J. E. Donald, C. Keasar, J. G. Saven, W. F. DeGrado, and I. Samish. Knowledge-based potential for positioning membrane-associated structures and assessing residue-specific energetic contributions. *Structure*, 20(5):924–935, 2012.
117. M. A. Lomize, A. L. Lomize, I. D. Pogozheva, and H. I. Mosberg. OPM: orientations of proteins in membranes database. *Bioinformatics*, 22:623–625, 2006.
118. S. J. Fleishman, V. M. Unger, and N. Ben-Tal. Transmembrane protein structures without X-rays. *Trends Biochem. Sci.*, 31(2):106–13, 2006.
119. D. A. Doyle, J. Morais Cabral, R. A. Pfuetzner, A. Kuo, J. M. Gulbis, S. L. Cohen, B. T. Chait, and R. MacKinnon. The structure of the potassium channel: molecular basis of K^+ conduction and selectivity. *Science*, 280(5360):69–77, 1998.
120. J. M. Cuthbertson, D. A. Doyle, and M. S. Sansom. Transmembrane helix prediction: a comparative evaluation and analysis. *Protein Eng. Des. Sel.*, 18(6):295–308, 2005.
121. D. T. Jones, W. R. Taylor, and J. M. Thornton. A model recognition approach to the prediction of all-helical membrane protein structure and topology. *Biochemistry*, 33(10):3038–49, 1994.
122. E. L. Sonnhammer, G. von Heijne, and A. Krogh. A hidden Markov model for predicting transmembrane helices in protein sequences. *Proc. Int. Conf. Intell. Syst. Mol. Biol.*, 6:175–82, 1998.
123. A. Krogh, B. Larsson, G. von Heijne, and E. L. Sonnhammer. Predicting transmembrane protein topology with a hidden Markov model: application to complete genomes. *J. Mol. Biol.*, 305(3):567–80, 2001.
124. D. O. Daley, M. Rapp, E. Granseth, K. Melen, D. Drew, and G. von Heijne. Global topology analysis of the *Escherichia coli* inner membrane proteome. *Science*, 308(5726):1321–3, 2005.
125. T. Nugent and D. T. Jones. Transmembrane protein topology prediction using support vector machines. *BMC Bioinformatics*, 10:1–11, 2009.
126. A. Elazar, J. J. Weinstein, J. Prilusky, and S. J. Fleishman. Interplay between hydrophobicity and the positive-inside rule in determining membrane-protein topology. *Proc. Natl. Acad. Sci. USA*, pages 10340–5, 2016.
127. S. Hayat and A. Elofsson. BOCTOPUS: improved topology prediction of transmembrane β barrel proteins. *Bioinformatics*, 28(4):516–522, 2012.
128. J. Koehler Leman, M. B. Ulmschneider, and J. J. Gray. Computational modeling of membrane proteins. *Proteins: Struct., Funct., Bioinf.*, 83(1):1–24, 2015.
129. A. Senes, M. Gerstein, and D. M. Engelman. Statistical analysis of amino acid patterns in transmembrane helices: the GxxxG motif occurs frequently and in association with beta-branched residues at neighboring positions. *J. Mol. Biol.*, 296(3):921–36, 2000.
130. K. T. O'Neil and W. F. DeGrado. A thermodynamic scale for the helix-forming tendencies of the commonly occurring amino acids. *Science*, 250(4981):646–51, 1990.
131. M. S. Sansom and H. Weinstein. Hinges, swivels and switches: the role of prolines in signalling via transmembrane alpha-helices. *Trends Pharmacol. Sci.*, 21(11):445–51, 2000.
132. C. Govaerts, C. Blanpain, X. Deupi, S. Ballet, J. A. Ballesteros, S. J. Wodak, G. Vassart, L. Pardo, and M. Parmentier. The TXP motif in the second transmembrane helix of CCR5. A structural determinant of chemokine-induced activation. *J. Biol. Chem.*, 276(16):13217–25, 2001.
133. A. Peralvarez, R. Barnadas, M. Sabes, E. Querol, and E. Padros. Thr-90 is a key residue of the bacteriorhodopsin proton pumping mechanism. *FEBS Lett.*, 508(3):399–402, 2001.
134. Y. Ri, J. A. Ballesteros, C. K. Abrams, S. Oh, V. K. Verselis, H. Weinstein, and T. A. Bargiello. The role of a

conserved proline residue in mediating conformational changes associated with voltage gating of Cx32 gap junctions. *Biophys. J.*, 76(6):2887–98, 1999.
135. W. C. Wigley, M. J. Corboy, T. D. Cutler, P. H. Thibodeau, J. Oldan, M. G. Lee, J. Rizo, J. F. Hunt, and P. J. Thomas. A protein sequence that can encode native structure by disfavoring alternate conformations. *Nat. Struct. Mol. Biol.*, 9(5):381–388, 2002.
136. S. K. Buchanan. Beta-Barrel proteins from bacterial outer membranes: Structure, function and refolding. *Curr. Opin. Struct. Biol.*, 9:455–461, 1999.
137. G. E. Schulz. Beta-barrel membrane proteins. *Curr. Opin. Struct. Biol.*, 10(4):443–7, 2000.
138. R. Benz and K. Bauer. Permeation of hydrophilic molecules through the outer membrane of Gram-negative bacteria. Review on bacterial porins. *Eur. J. Biochem.*, 176(1):1–19, 1988.
139. T. Schirmer. General and specific porins from bacterial outer membranes. *J. Struct. Biol.*, 121(2):101–9, 1998.
140. R. Benz. Permeation of hydrophilic solutes through mitochondrial outer membranes: review on mitochondrial porins. *Biochim. Biophys. Acta*, 1197(2):167–96, 1994.
141. D. C. Bay and D. A. Court. Origami in the outer membrane: the transmembrane arrangement of mitochondrial porins. *Biochem. Cell Biol.*, 80(5):551–62, 2002.
142. D. Duy, J. Soll, and K. Philippar. Solute channels of the outer membrane: from bacteria to chloroplasts. *Biol. Chem.*, 388(9):879–89, 2007.
143. B. Bolter and J. Soll. Ion channels in the outer membranes of chloroplasts and mitochondria: open doors or regulated gates? *EMBO J.*, 20(5):935–40, 2001.
144. S. Bhakdi and J. Tranum-Jensen. Alpha-toxin of *Staphylococcus aureus*. *Microbiol. Rev.*, 55(4):733–751, 1991.
145. G. von Heijne. Principles of membrane protein assembly and structure. *Prog. Biophys. Mol. Biol.*, 66(2):113–39, 1996.
146. K. Zeth and M. Thein. Porins in prokaryotes and eukaryotes: common themes and variations. *Biochem. J.*, 431(1):13–22, 2010.
147. K. Seshadri, R. Garemyr, E. Wallin, G. von Heijne, and A. Elofsson. Architecture of beta-barrel membrane proteins: analysis of trimeric porins. *Protein Sci.*, 7(9):2026–32, 1998.
148. T. J. Stevens and I. T. Arkin. Are membrane proteins "inside-out" proteins? *Proteins*, 36(1):135–43, 1999.
149. D. C. Rees, L. DeAntonio, and D. Eisenberg. Hydrophobic organization of membrane proteins. *Science*, 245(4917):510–3, 1989.
150. D. Donnelly, J. P. Overington, S. V. Ruffle, J. H. Nugent, and T. L. Blundell. Modeling alpha-helical transmembrane domains: the calculation and use of substitution tables for lipid-facing residues. *Protein Sci.*, 2(1):55–70, 1993.
151. D. T. Moore, B. W. Berger, and W. F. DeGrado. Protein-protein interactions in the membrane: sequence, structural, and biological motifs. *Structure*, 16(7):991–1001, 2008.
152. M. Eilers, A. B. Patel, W. Liu, and S. O. Smith. Comparison of helix interactions in membrane and soluble alpha-bundle proteins. *Biophys. J.*, 82(5):2720–36, 2002.
153. W. P. Russ and D. M. Engelman. The GxxxG motif: a framework for transmembrane helix-helix association. *J. Mol. Biol.*, 296(3):911–9, 2000.
154. B. K. Mueller, S. Subramaniam, and A. Senes. A frequent, GxxxG-mediated, transmembrane association motif is optimized for the formation of interhelical Cα–H hydrogen bonds. *Proc. Natl. Acad. Sci. USA*, 111(10):E888–E895, 2014.
155. A. Senes, D. E. Engel, and W. F. DeGrado. Folding of helical membrane proteins: the role of polar, GxxxG-like and proline motifs. *Curr. Opin. Struct. Biol.*, 14(4):465–479, 2004.
156. R. F. S. Walters and W. F. DeGrado. Helix-packing motifs in membrane proteins. *Proc. Natl. Acad. Sci. USA*, 103(37):13658–13663, 2006.
157. N. A. Noordeen, F. Carafoli, E. Hohenester, M. A. Horton, and B. Leitinger. A transmembrane leucine zipper is required for activation of the dimeric receptor tyrosine kinase DDR1. *J. Biol. Chem.*, 281(32):22744–22751, 2006.
158. B. North, L. Cristian, X. Fu Stowell, J. D. Lear, JG. Saven, and W. F. Degrado. Characterization of a membrane protein folding motif, the Ser zipper, using designed peptides. *J. Mol. Biol.*, 359:930–939, 2006.
159. S. Kim, T.-J. Jeon, A. Oberai, D. Yang, J. J. Schmidt, and J. U. Bowie. Transmembrane glycine zippers: physiological and pathological roles in membrane proteins. *Proc. Natl. Acad. Sci. USA*, 102(40):14278–14283, 2005.
160. A. Marsico, K. Scheubert, A. Tuukkanen, A. Henschel, C. Winter, R. Winnenburg, and M. Schroeder. MeM-

otif: a database of linear motifs in α-helical transmembrane proteins. *Nucleic Acids Res.*, 38:D181–D189, 2010.
161. S. H. White. Biophysical dissection of membrane proteins. *Nature*, 459:344–6, 2009.
162. J.-L. Popot, S.-E. Gerchman, and D. M. Engelman. Refolding of bacteriorhodopsin in lipid bilayers: a thermodynamically controlled two-stage process. *J. Mol. Biol.*, 198(4):655–676, 1987.
163. R. E. Jacobs and S. H. White. The nature of the hydrophobic binding of small peptides at the bilayer interface: implications for the insertion of transbilayer helices. *Biochemistry*, 28(8):3421–37, 1989.
164. D. M. Engelman and T. A. Steitz. The spontaneous insertion of proteins into and across membranes: the helical hairpin hypothesis. *Cell*, 23(2):411–422, 1981.
165. C. M. Deber and N. K. Goto. Folding proteins into membranes. *Nat. Struct. Mol. Biol.*, 3(10):815–818, 1996.
166. J.-L. Popot. Integral membrane protein structure: transmembrane α-helices as autonomous folding domains. *Curr. Opin. Struct. Biol.*, 3(4):532–540, 1993.
167. K. G. Fleming. Energetics of membrane protein folding. *Annu. Rev. Biophys.*, 43:233–255, 2014.
168. N. Ben-Tal, A. Ben-Shaul, A. Nicholls, and B. Honig. Free-energy determinants of alpha-helix insertion into lipid bilayers. *Biophys. J.*, 70(4):1803–12, 1996.
169. N. Ben-Tal, D. Sitkoff, I. A. Topol, A. S. Yang, S. K. Burt, and B. Honig. Free energy of amide hydrogen bond formation in vacuum, in water, and in liquid alkane solution. *J. Phys. Chem. B*, 101(3):450–457, 1997.
170. C. Chothia. Hydrophobic bonding and accessible surface area in proteins. *Nature*, 248(446):338–339, 1974.
171. J. A. Reynolds, D. B. Gilbert, and C. Tanford. Empirical Correlation Between Hydrophobic Free Energy and Aqueous Cavity Surface Area. *Proc. Natl. Acad. Sci. USA*, 71(8):2925–2927, 1974.
172. S. Vajda, Z. Weng, and C. DeLisi. Extracting hydrophobicity parameters from solute partition and protein mutation/unfolding experiments. *Protein Eng.*, 8(11):1081–1092, 1995.
173. P. Andrew Karplus. Hydrophobicity regained. *Protein Sci.*, 6(6):1302–1307, 1997.
174. K. Öjemalm, T. Higuchi, Y. Jiang, Ü. Langel, I. Nilsson, S. H. White, H. Suga, and G. von Heijne. Apolar surface area determines the efficiency of translocon-mediated membrane-protein integration into the endoplasmic reticulum. *Proc. Natl. Acad. Sci. USA*, 108(31):E359–E364, 2011.
175. D. J. Müller, M. Kessler, F. Oesterhelt, C. Möller, D. Oesterhelt, and H. Gaub. Stability of bacteriorhodopsin α-helices and loops analyzed by single-molecule force spectroscopy. *Biophys. J.*, 83(6):3578–3588, 2002.
176. F. Cymer and D. Schneider. Oligomerization of polytopic α-helical membrane proteins: causes and consequences. *Biol. Chem.*, 393:1215–30, 2012.
177. A. J. Venkatakrishnan, E. D. Levy, and S. A. Teichmann. Homomeric protein complexes: evolution and assembly. *Biochem. Soc. Trans.*, 38(4):879–882, 2010.
178. Y.-C. Chang and J. U. Bowie. Measuring membrane protein stability under native conditions. *Proc. Natl. Acad. Sci. USA*, 111(1):219–224, 2014.
179. S. Faham, D. Yang, E. Bare, S. Yohannan, J. P. Whitelegge, and J. U. Bowie. Side-chain contributions to membrane protein structure and stability. *J. Mol. Biol.*, 335(1):297–305, 2004.
180. V. Helms. Attraction within the membrane. Forces behind transmembrane protein folding and supramolecular complex assembly. *EMBO Rep.*, 3(12):1133–8, 2002.
181. F. X. Zhou, M. J. Cocco, W. P. Russ, A. T. Brunger, and D. M. Engelman. Interhelical hydrogen bonding drives strong interactions in membrane proteins. *Nat. Struct. Biol.*, 7(2):154–60, 2000.
182. C. Choma, H. Gratkowski, J. D. Lear, and W. F. DeGrado. Asparagine-mediated self-association of a model transmembrane helix. *Nat. Struct. Biol.*, 7(2):161–6, 2000.
183. W. F. DeGrado, H. Gratkowski, and J. D. Lear. How do helix-helix interactions help determine the folds of membrane proteins? Perspectives from the study of homo-oligomeric helical bundles. *Protein Sci.*, 12(4):647–65, 2003.
184. N. H. Joh, A. Min, S. Faham, J. P. Whitelegge, D. Yang, V. L. Woods, and J. U. Bowie. Modest stabilization by most hydrogen-bonded side-chain interactions in membrane proteins. *Nature*, 453(7199):1266–70, 2008.
185. E. Arbely and I. T. Arkin. Experimental measurement of the strength of a Cα–H···O bond in a lipid bilayer. *J. Am. Chem. Soc.*, 126:5362–5363, 2004.
186. S. Yohannan, S. Faham, D. Yang, D. Grosfeld, A. K. Chamberlain, and J. U. Bowie. A Cα–H···O hydrogen bond in a membrane protein is not stabilizing. *J. Am. Chem. Soc.*, 126:2284–2285, 2004.
187. S. Kumar and R. Nussinov. Salt bridge stability in monomeric proteins. *J. Mol. Biol.*, 293(5):1241–55, 1999.
188. S. Albeck, R. Unger, and G. Schreiber. Evaluation of direct and cooperative contributions towards the strength of buried hydrogen bonds and salt bridges. *J. Mol. Biol.*, 298(3):503–20, 2000.
189. D. Lee, J. Lee, and C. Seok. What stabilizes close arginine pairing in proteins? *Phys. Chem. Chem. Phys.*, 15(16):5844–53, 2013.

190. E. Gouaux and R. Mackinnon. Principles of selective ion transport in channels and pumps. *Science*, 310(5753):1461–5, 2005.
191. U. G. Hacke and J. Laur. Aquaporins: Channels for the Molecule of Life. In *Encyclopedia of Life Sciences*. John Wiley & Sons, Ltd., 2016.
192. J. S. Hub and B. L. De Groot. Mechanism of selectivity in aquaporins and aquaglyceroporins. *Proc. Natl. Acad. Sci. USA*, 105(4):1198–1203, 2008.
193. Y. Fujiyoshi, K. Mitsuoka, B. L. de Groot, A. Philippsen, H. Grubmuller, P. Agre, and A. Engel. Structure and function of water channels. *Curr. Opin. Struct. Biol.*, 12(4):509–15, 2002.
194. A. Barati Farimani, N. R. Aluru, and E. Tajkhorshid. Thermodynamic insight into spontaneous hydration and rapid water permeation in aquaporins. *Appl. Phys. Lett.*, 105(8):083702, 2014.
195. Y. Arinaminpathy, E. Khurana, D. M. Engelman, and M. B. Gerstein. Computational analysis of membrane proteins: the largest class of drug targets. *Drug Discov. Today*, 14(23–24):1130–5, 2009.
196. A. Lange, K. Giller, S. Hornig, M. F. Martin-Eauclaire, O. Pongs, S. Becker, and M. Baldus. Toxin-induced conformational changes in a potassium channel revealed by solid-state NMR. *Nature*, 440(7086):959–62, 2006.
197. J. H. Chill, J. M. Louis, J. L. Baber, and A. Bax. Measurement of 15N relaxation in the detergent-solubilized tetrameric KcsA potassium channel. *J. Biomol. NMR*, 36(2):123–36, 2006.
198. S. Y. Noskov, S. Berneche, and B. Roux. Control of ion selectivity in potassium channels by electrostatic and dynamic properties of carbonyl ligands. *Nature*, 431(7010):830–4, 2004.
199. A. N. Thompson, I. Kim, T. D. Panosian, T. M. Iverson, T. W. Allen, and C. M. Nimigean. Mechanism of potassium-channel selectivity revealed by Na^+ and Li^+ binding sites within the KcsA pore. *Nat. Struct. Mol. Biol.*, 16(12):1317–1324, 2009.
200. Q. Kuang, P. Purhonen, and H. Hebert. Structure of potassium channels. *Cell. Mol. Life Sci.*, 72(19):3677–3693, 2015.
201. D. M. Kim and C. M. Nimigean. Voltage-gated potassium channels: a structural examination of selectivity and gating. *Cold Spring Harb. Perspect. Biol.*, 8(5):a029231, 2016.
202. S. Chakrapani, J. F. Cordero-Morales, and E. Perozo. A quantitative description of KcsA gating I: macroscopic currents. *J. Gen. Physiol.*, 130(5):465–478, 2007.
203. S. Imai, M. Osawa, K. Takeuchi, and I. Shimada. Structural basis underlying the dual gate properties of KcsA. *Proc. Natl. Acad. Sci. USA*, 107(14):6216–6221, 2010.
204. S. Uysal, L. G. Cuello, D. M. Cortes, S. Koide, A. A. Kossiakoff, and E. Perozo. Mechanism of activation gating in the full-length KcsA K^+ channel. *Proc. Natl. Acad. Sci. USA*, 108(29):11896–11899, 2011.
205. L. G. Cuello, V. Jogini, D. M. Cortes, and E. Perozo. Structural mechanism of C-type inactivation in K^+ channels. *Nature*, 466(7303):203–208, 2010.
206. Y.-S. Liu, P. Sompornpisut, and E. Perozo. Structure of the KcsA channel intracellular gate in the open state. *Nat. Struct. Mol. Biol.*, 8(10):883–887, 2001.
207. L. G. Cuello, D. M. Cortes, V. Jogini, A. Sompornpisut, and E. Perozo. A molecular mechanism for proton-dependent gating in KcsA. *FEBS Lett.*, 584(6):1126–1132, 2010.
208. L. G. Cuello, V. Jogini, D. M. Cortes, A. Sompornpisut, M. D. Purdy, M. C. Wiener, and E. Perozo. Design and characterization of a constitutively open KcsA. *FEBS Lett.*, 584(6):1133–1138, 2010.
209. L. G. Cuello, V. Jogini, D. M. Cortes, A. C. Pan, D. G. Gagnon, O. Dalmas, J. F. Cordero-Morales, S. Chakrapani, B. Roux, and E. Perozo. Structural basis for the coupling between activation and inactivation gates in K^+ channels. *Nature*, 466(7303):272–275, 2010.
210. T. Hoshi, W. N. Zagotta, and R. W. Aldrich. Two types of inactivation in Shaker K^+ channels: Effects of alterations in the carboxy-terminal region. *Neuron*, 7(4):547–556, 1991.
211. O. Jardetzky. Simple Allosteric Model for Membrane Pumps. *Nature*, 211(5052):969–970, 1966.
212. Y. Lee, T. Nishizawa, K. Yamashita, R. Ishitani, and O. Nureki. Structural basis for the facilitative diffusion mechanism by SemiSWEET transporter. *Nat. Commun.*, 6:6112, 2015.
213. S. Wilkens. Structure and mechanism of ABC transporters. *F1000Prime Rep*, 7, 2015.
214. R. J. P. Dawson and K. P. Locher. Structure of a bacterial multidrug ABC transporter. *Nature*, 443(7108):180–185, 2006.
215. N. Livnat-Levanon, A. I. Gilson, N. Ben-Tal, and O. Lewinson. The uncoupled ATPase activity of the ABC transporter BtuC2D2 leads to a hysteretic conformational change, conformational memory, and improved activity. *Sci. Rep.*, 6:21696, 2016.
216. P. A. Mitchell. General theory of membrane transport from studies of bacteria. *Nature*, 180:134–136, 1957.

217. C. F. Higgins and K. J. Linton. The ATP switch model for ABC transporters. *Nat. Struct. Mol. Biol.*, 11(10):918–926, 2004.
218. L. Reuss. Ion Transport across Nonexcitable Membranes. In *Encyclopedia of Life Sciences*. John Wiley & Sons, Ltd., 2001.
219. J. P. Morth, B. P. Pedersen, M. J. Buch-Pedersen, J. P. Andersen, B. Vilsen, M. G. Palmgren, and P. Nissen. A structural overview of the plasma membrane Na^+,K^+-ATPase and H^+-ATPase ion pumps. *Nat. Rev. Mol. Cell Biol.*, 12(1):60–70, 2011.
220. U. Hasler, G. Crambert, J.-D. Horisberger, and K. Geering. Structural and Functional Features of the Transmembrane Domain of the Na,K-ATPase β Subunit Revealed by Tryptophan Scanning. *J. Biol. Chem.*, 276(19):16356–16364, 2001.
221. T. Shinoda, H. Ogawa, F. Cornelius, and C. Toyoshima. Crystal structure of the sodium-potassium pump at 2.4 Å resolution. *Nature*, 459(7245):446–450, 2009.
222. J. P. Morth, B. P. Pedersen, M. S. Toustrup-Jensen, T. L. M. Sorensen, J. Petersen, J. P. Andersen, B. Vilsen, and P. Nissen. Crystal structure of the sodium-potassium pump. *Nature*, 450(7172):1043–1049, 2007.
223. V. B. Chen, W. B. Arendall, J. J. Headd, D. A. Keedy, R. M. Immormino, G. J. Kapral, L. W. Murray, J. S. Richardson, and D. C. Richardson. MolProbity: all-atom structure validation for macromolecular crystallography. *Acta Crystallogr. Sect. D*, 66(1):12–21, 2010.
224. C. Toyoshima, M. Nakasako, H. Nomura, and H. Ogawa. Crystal structure of the calcium pump of sarcoplasmic reticulum at 2.6 Å resolution. *Nature*, 405(6787):647–655, 2000.
225. J. Zhao, S. Benlekbir, and J. L. Rubinstein. Electron cryomicroscopy observation of rotational states in a eukaryotic V-ATPase. *Nature*, 521(7551):241–245, 2015.
226. O. M. Becker, Y. Marantz, S. Shacham, B. Inbal, A. Heifetz, O. Kalid, S. Bar-Haim, D. Warshaviak, M. Fichman, and S. Noiman. G protein-coupled receptors: in silico drug discovery in 3D. *Proc. Natl. Acad. Sci. USA*, 101(31):11304–9, 2004.
227. O. Schueler-Furman, C. Wang, P. Bradley, K. Misura, and D. Baker. Progress in Modeling of Protein Structures and Interactions. *Science*, 310(5748):638–642, 2005.
228. Y. Pilpel, N. Ben-Tal, and D. Lancet. kPROT: a knowledge-based scale for the propensity of residue orientation in transmembrane segments. Application to membrane protein structure prediction. *J. Mol. Biol.*, 294(4):921–35, 1999.
229. W. R. Taylor, D. T. Jones, and N. M. Green. A method for alpha-helical integral membrane protein fold prediction. *Proteins*, 18(3):281–94, 1994.
230. S. J. Fleishman, S. Harrington, R. A. Friesner, B. Honig, and N. Ben-Tal. An automatic method for predicting transmembrane protein structures using cryo-EM and evolutionary data. *Biophys. J.*, 87(5):3448–59, 2004.
231. T. A. Hopf, L. J. Colwell, R. Sheridan, B. Rost, C. Sander, and D. S. Marks. Three-dimensional structures of membrane proteins from genomic sequencing. *Cell*, 149(7):1607–21, 2012.
232. S. J. Fleishman and N. Ben-Tal. A novel scoring function for predicting the conformations of tightly packed pairs of transmembrane alpha-helices. *J. Mol. Biol.*, 321(2):363–78, 2002.
233. M. Schushan and N. Ben-Tal. Modeling and Validation of Transmembrane Protein Structures. In *Introduction to Protein Structure Prediction: Methods and Algorithms*, pages 369–401. John Wiley & Sons, Inc., 2010.
234. V. Yarov-Yarovoy, J. Schonbrun, and D. Baker. Multipass membrane protein structure prediction using Rosetta. *Proteins*, 62(4):1010–25, 2006.
235. R. Das and D. Baker. Macromolecular modeling with Rosetta. *Annu. Rev. Biochem.*, 77:363–82, 2008.
236. P. Barth, J. Schonbrun, and D. Baker. Toward high-resolution prediction and design of transmembrane helical protein structures. *Proc. Natl. Acad. Sci. USA*, 104(40):15682–7, 2007.
237. A. Roy, A. Kucukural, and Y. Zhang. I-TASSER: a unified platform for automated protein structure and function prediction. *Nat. Protoc.*, 5(4):725–38, 2010.
238. J. Zhang, J. Yang, R. Jang, and Y. Zhang. GPCR-I-TASSER: A hybrid approach to G protein-coupled receptor structure modeling and the application to the human genome. *Structure*, 23(8):1538–49, 2015.
239. P. Barth, B. Wallner, and D. Baker. Prediction of membrane protein structures with complex topologies using limited constraints. *Proc. Natl. Acad. Sci. USA*, 106(5):1409–14, 2009.
240. Y. Zhang, M. E. Devries, and J. Skolnick. Structure modeling of all identified G protein-coupled receptors in the human genome. *PLoS Comput. Biol.*, 2(2):e13, 2006.
241. A. Sali and T. L. Blundell. Comparative protein modelling by satisfaction of spatial restraints. *J. Mol. Biol.*, 234(3):779–815, 1993.

242. W. Zheng and S. Doniach. Protein structure prediction constrained by solution X-ray scattering data and structural homology identification. *J. Mol. Biol.*, 316(1):173–87, 2002.
243. W. Zheng and S. Doniach. Fold recognition aided by constraints from small angle X-ray scattering data. *Protein Eng. Des. Sel.*, 18(5):209–19, 2005.
244. D. Schneidman-Duhovny, S. J. Kim, and A. Sali. Integrative structural modeling with small angle X-ray scattering profiles. *BMC Struct. Biol.*, 12:17, 2012.
245. P. D. Adams, D. Baker, A. T. Brunger, R. Das, F. DiMaio, R. J. Read, D. C. Richardson, J. S. Richardson, and T. C. Terwilliger. Advances, interactions, and future developments in the CNS, Phenix, and Rosetta structural biology software systems. *Annu. Rev. Biophys.*, 42:265–87, 2013.
246. S. J. Hirst, N. Alexander, H. S. McHaourab, and J. Meiler. RosettaEPR: an integrated tool for protein structure determination from sparse EPR data. *J. Struct. Biol.*, 173(3):506–14, 2011.
247. P. Rossi, L. Shi, G. Liu, C. M. Barbieri, H. W. Lee, T. D. Grant, J. R. Luft, R. Xiao, T. B. Acton, E. H. Snell, G. T. Montelione, D. Baker, O. F. Lange, and N. G. Sgourakis. A hybrid NMR/SAXS-based approach for discriminating oligomeric protein interfaces using Rosetta. *Proteins*, 83(2):309–17, 2015.
248. F. DiMaio, M. D. Tyka, M. L. Baker, W. Chiu, and D. Baker. Refinement of protein structures into low-resolution density maps using Rosetta. *J. Mol. Biol.*, 392(1):181–90, 2009.
249. Y. Shen, O. Lange, F. Delaglio, P. Rossi, J. M. Aramini, G. Liu, A. Eletsky, Y. Wu, K. K. Singarapu, A. Lemak, A. Ignatchenko, C. H. Arrowsmith, T. Szyperski, G. T. Montelione, D. Baker, and A. Bax. Consistent blind protein structure generation from NMR chemical shift data. *Proc. Natl. Acad. Sci. USA*, 105(12):4685–90, 2008.
250. F. DiMaio, Y. Song, X. Li, M. J. Brunner, C. Xu, V. Conticello, E. Egelman, T. C. Marlovits, Y. Cheng, and D. Baker. Atomic-accuracy models from 4.5-Å cryo-electron microscopy data with density-guided iterative local refinement. *Nat. Methods*, 12(4):361–5, 2015.
251. A. Cavalli, X. Salvatella, C. M. Dobson, and M. Vendruscolo. Protein structure determination from NMR chemical shifts. *Proc. Natl. Acad. Sci. USA*, 104(23):9615–20, 2007.
252. D. S. Wishart, D. Arndt, M. Berjanskii, P. Tang, J. Zhou, and G. Lin. CS23D: a web server for rapid protein structure generation using NMR chemical shifts and sequence data. *Nucleic Acids Res.*, 36(suppl 2):W496–502, 2008.
253. M. A. dos Reis, R. Aparicio, and Y. Zhang. Improving protein template recognition by using small-angle x-ray scattering profiles. *Biophys. J.*, 101(11):2770–81, 2011.
254. D. Murray, N. Ben-Tal, B. Honig, and S. McLaughlin. Electrostatic interaction of myristoylated proteins with membranes: simple physics, complicated biology. *Structure*, 5(8):985–9, 1997.
255. D. Murray and B. Honig. Electrostatic control of the membrane targeting of C2 domains. *Mol. Cell*, 9(1):145–54, 2002.
256. N. Ben-Tal, B. Honig, R. M. Peitzsch, G. Denisov, and S. McLaughlin. Binding of small basic peptides to membranes containing acidic lipids: theoretical models and experimental results. *Biophys. J.*, 71(2):561–75, 1996.
257. S. J. Dunne, R. B. Cornell, J. E. Johnson, N. R. Glover, and A. S. Tracey. Structure of the Membrane Binding Domain of CTP:Phosphocholine Cytidylyltransferase†. *Biochemistry*, 35(37):11975–11984, 1996.
258. B. Antonny, S. Beraud-Dufour, P. Chardin, and M. Chabre. N-Terminal Hydrophobic Residues of the G-Protein ADP-Ribosylation Factor-1 Insert into Membrane Phospholipids upon GDP to GTP Exchange. *Biochemistry*, 36(15):4675–4684, 1997.
259. A. Kessel, D. S. Cafiso, and N. Ben-Tal. Continuum solvent model calculations of alamethicin-membrane interactions: thermodynamic aspects. *Biophys. J.*, 78(2):571–83, 2000.
260. K. V. Damodaran, K. M. Merz Jr, and B. P. Gaber. Interaction of small peptides with lipid bilayers. *Biophys. J.*, 69(4):1299–308, 1995.
261. E. Yamauchi, T. Nakatsu, M. Matsubara, H. Kato, and H. Taniguchi. Crystal structure of a MARCKS peptide containing the calmodulin-binding domain in complex with Ca^{2+}-calmodulin. *Nat. Struct. Biol.*, 10(3):226–31, 2003.
262. S. McLaughlin and D. Murray. Plasma membrane phosphoinositide organization by protein electrostatics. *Nature*, 438(7068):605–11, 2005.
263. A. Kessel, D. Shental-Bechor, T. Haliloglu, and N. Ben-Tal. Interactions of hydrophobic peptides with lipid bilayers: Monte Carlo simulations with M2delta. *Biophys. J.*, 85(6):3431–44, 2003.
264. O. S. Andersen and R. E. Koeppe 2nd. Bilayer thickness and membrane protein function: an energetic perspective. *Annu. Rev. Biophys. Biomol. Struct.*, 36:107–30, 2007.

265. M. P. Sheetz and S. J. Singer. Biological membranes as bilayer couples. A molecular mechanism of drug-erythrocyte interactions. *Proc. Natl. Acad. Sci. USA*, 71(11):4457–61, 1974.
266. O. G. Mouritsen and M. Bloom. Mattress model of lipid-protein interactions in membranes. *Biophys. J.*, 46(2):141–53, 1984.
267. D. R. Fattal and A. Ben-Shaul. A molecular model for lipid-protein interaction in membranes: the role of hydrophobic mismatch. *Biophys. J.*, 65(5):1795–809, 1993.
268. D. C. Mitchell, M. Straume, J. L. Miller, and B. J. Litman. Modulation of metarhodopsin formation by cholesterol-induced ordering of bilayer lipids. *Biochemistry*, 29(39):9143–9, 1990.
269. J. A. Lundbaek, P. Birn, S. E. Tape, G. E. Toombes, R. Sogaard, R. E. Koeppe 2nd, S. M. Gruner, A. J. Hansen, and O. S. Andersen. Capsaicin regulates voltage-dependent sodium channels by altering lipid bilayer elasticity. *Mol. Pharmacol.*, 68(3):680–9, 2005.
270. K. Simons and E. Ikonen. Functional rafts in cell membranes. *Nature*, 387(6633):569–72, 1997.
271. H. Sprong, P. van der Sluijs, and G. van Meer. How proteins move lipids and lipids move proteins. *Nat. Rev. Mol. Cell Biol.*, 2(7):504–13, 2001.
272. R. J. Schroeder, S. N. Ahmed, Y. Zhu, E. London, and D. A. Brown. Cholesterol and sphingolipid enhance the Triton X-100 insolubility of glycosylphosphatidylinositol-anchored proteins by promoting the formation of detergent-insoluble ordered membrane domains. *J. Biol. Chem.*, 273(2):1150–7, 1998.
273. M. D. Resh. Membrane targeting of lipid modified signal transduction proteins. *Subcell. Biochem.*, 37:217–32, 2004.
274. T. Y. Wang, R. Leventis, and J. R. Silvius. Partitioning of lipidated peptide sequences into liquid-ordered lipid domains in model and biological membranes. *Biochemistry*, 40(43):13031–40, 2001.
275. S. Munro. An investigation of the role of transmembrane domains in Golgi protein retention. *EMBO J.*, 14(19):4695–704, 1995.
276. A. P. Starling, J. M. East, and A. G. Lee. Effects of phosphatidylcholine fatty acyl chain length on calcium binding and other functions of the (Ca^{2+}–Mg^{2+})-ATPase. *Biochemistry*, 32(6):1593–600, 1993.
277. P. A. Baldwin and W. L. Hubbell. Effects of lipid environment on the light-induced conformational changes of rhodopsin. 2. Roles of lipid chain length, unsaturation, and phase state. *Biochemistry*, 24(11):2633–9, 1985.
278. F. Cornelius. Modulation of Na,K-ATPase and Na-ATPase activity by phospholipids and cholesterol. I. Steady-state kinetics. *Biochemistry*, 40(30):8842–51, 2001.
279. J. D. Pilot, J. M. East, and A. G. Lee. Effects of bilayer thickness on the activity of diacylglycerol kinase of *Escherichia coli*. *Biochemistry*, 40(28):8188–95, 2001.
280. C. Montecucco, G. A. Smith, F. Dabbeni-sala, A. Johannsson, Y. M. Galante, and R. Bisson. Bilayer thickness and enzymatic activity in the mitochondrial cytochrome c oxidase and ATPase complex. *FEBS Lett.*, 144(1):145–8, 1982.
281. O. S. Andersen, R. E. Koeppe 2nd, and B. Roux. Gramicidin channels. *IEEE Trans. Nanobioscience*, 4(1):10–20, 2005.
282. A. M. O'Connell, R. E. Koeppe 2nd, and O. S. Andersen. Kinetics of gramicidin channel formation in lipid bilayers: transmembrane monomer association. *Science*, 250(4985):1256–9, 1990.
283. S. Bransburg-Zabary, A. Kessel, M. Gutman, and N. Ben-Tal. Stability of an ion channel in lipid bilayers: implicit solvent model calculations with gramicidin. *Biochemistry*, 41(22):6946–54, 2002.
284. A. Johannsson, G. A. Smith, and J. C. Metcalfe. The effect of bilayer thickness on the activity of ($Na^+ + K^+$)-ATPase. *Biochim. Biophys. Acta*, 641(2):416–21, 1981.
285. F. Dumas, J. F. Tocanne, G. Leblanc, and M. C. Lebrun. Consequences of hydrophobic mismatch between lipids and melibiose permease on melibiose transport. *Biochemistry*, 39(16):4846–54, 2000.
286. M. Sinensky. Homeoviscous adaptation: a homeostatic process that regulates the viscosity of membrane lipids in *Escherichia coli*. *Proc. Natl. Acad. Sci. USA*, 71(2):522–5, 1974.
287. M. F. Brown. Influence of nonlamellar-forming lipids on rhodopsin. *Curr. Top. Membr.*, 44:285–356, 1997.
288. A. P. Starling, K. A. Dalton, J. M. East, S. Oliver, and A. G. Lee. Effects of phosphatidylethanolamines on the activity of the Ca^{2+}-ATPase of sarcoplasmic reticulum. *Biochem. J.*, 320 (Pt 1):309–14, 1996.
289. O. P. Hamill and B. Martinac. Molecular basis of mechanotransduction in living cells. *Physiol. Rev.*, 81(2):685–740, 2001.
290. C. Hunte. Specific protein-lipid interactions in membrane proteins. *Biochem. Soc. Trans.*, 33(Pt 5):938–42, 2005.
291. A. C. Simmonds, J. M. East, O. T. Jones, E. K. Rooney, J. McWhirter, and A. G. Lee. Annular and non-annular binding sites on the (Ca^{2+} + Mg^{2+})-ATPase. *Biochim. Biophys. Acta*, 693(2):398–406, 1982.

292. P. F. Knowles, A. Watts, and D. Marsh. Spin-label studies of lipid immobilization in dimyristoylphosphatidylcholine-substituted cytochrome oxidase. *Biochemistry*, 18(21):4480–7, 1979.
293. T. Murata, I. Yamato, Y. Kakinuma, A. G. Leslie, and J. E. Walker. Structure of the rotor of the V-Type Na^+-ATPase from *Enterococcus hirae*. *Science*, 308(5722):654–9, 2005.
294. H. Palsdottir and C. Hunte. Lipids in membrane protein structures. *Biochim. Biophys. Acta*, 1666(1–2):2–18, 2004.
295. C. Lange, J. H. Nett, B. L. Trumpower, and C. Hunte. Specific roles of protein-phospholipid interactions in the yeast cytochrome bc1 complex structure. *EMBO J.*, 20(23):6591–600, 2001.
296. T. Tsukihara, K. Shimokata, Y. Katayama, H. Shimada, K. Muramoto, H. Aoyama, M. Mochizuki, K. Shinzawa-Itoh, E. Yamashita, M. Yao, Y. Ishimura, and S. Yoshikawa. The low-spin heme of cytochrome c oxidase as the driving element of the proton-pumping process. *Proc. Natl. Acad. Sci. USA*, 100(26):15304–9, 2003.
297. S. S. Deol, P. J. Bond, C. Domene, and M. S. Sansom. Lipid-protein interactions of integral membrane proteins: a comparative simulation study. *Biophys. J.*, 87(6):3737–49, 2004.
298. P. C. van der Wel, N. D. Reed, D. V. Greathouse, and R. E. Koeppe 2nd. Orientation and motion of tryptophan interfacial anchors in membrane-spanning peptides. *Biochemistry*, 46(25):7514–24, 2007.
299. K. Boesze-Battaglia and R. Schimmel. Cell membrane lipid composition and distribution: implications for cell function and lessons learned from photoreceptors and platelets. *J. Exp. Biol.*, 200(Pt 23):2927–36, 1997.
300. F. Jiang, M. T. Ryan, M. Schlame, M. Zhao, Z. Gu, M. Klingenberg, N. Pfanner, and M. L. Greenberg. Absence of cardiolipin in the crd1 null mutant results in decreased mitochondrial membrane potential and reduced mitochondrial function. *J. Biol. Chem.*, 275(29):22387–94, 2000.
301. S. Heimpel, G. Basset, S. Odoy, and M. Klingenberg. Expression of the mitochondrial ADP/ATP carrier in *Escherichia coli*. Renaturation, reconstitution, and the effect of mutations on 10 positive residues. *J. Biol. Chem.*, 276(15):11499–506, 2001.
302. B. Hoffmann, A. Stockl, M. Schlame, K. Beyer, and M. Klingenberg. The reconstituted ADP/ATP carrier activity has an absolute requirement for cardiolipin as shown in cysteine mutants. *J. Biol. Chem.*, 269(3):1940–4, 1994.
303. S. Nussberger, K. Dorr, D. N. Wang, and W. Kuhlbrandt. Lipid-protein interactions in crystals of plant light-harvesting complex. *J. Mol. Biol.*, 234(2):347–56, 1993.
304. J. Standfuss, A. C. Terwisscha van Scheltinga, M. Lamborghini, and W. Kuhlbrandt. Mechanisms of photoprotection and nonphotochemical quenching in pea light-harvesting complex at 2.5 Å resolution. *EMBO J.*, 24(5):919–28, 2005.
305. Z. Liu, H. Yan, K. Wang, T. Kuang, J. Zhang, L. Gui, X. An, and W. Chang. Crystal structure of spinach major light-harvesting complex at 2.72 Å resolution. *Nature*, 428(6980):287–92, 2004.
306. R. Horn and H. Paulsen. Folding In vitro of Light-harvesting Chlorophyll a/b Protein is Coupled with Pigment Binding. *J. Mol. Biol.*, 318(2):547–556, 2002.
307. C. Arnarez, S. J. Marrink, and X. Periole. Identification of cardiolipin binding sites on cytochrome c oxidase at the entrance of proton channels. *Sci. Rep.*, 3:1263, 2013.
308. L. Heginbotham, L. Kolmakova-Partensky, and C. Miller. Functional reconstitution of a prokaryotic K^+ channel. *J. Gen. Physiol.*, 111(6):741–9, 1998.
309. B. C. Suh and B. Hille. PIP2 is a necessary cofactor for ion channel function: how and why? *Annu. Rev. Biophys.*, 37:175–95, 2008.
310. M. J. Berridge and R. F. Irvine. Inositol phosphates and cell signalling. *Nature*, 341(6239):197–205, 1989.
311. M. A. Zaydman and J. Cui. PIP(2) regulation of KCNQ channels: biophysical and molecular mechanisms for lipid modulation of voltage-dependent gating. *Front. Physiol.*, 5, 2014.
312. P. J. Hamilton, A. N. Belovich, G. Khelashvili, C. Saunders, K. Erreger, J. A. Javitch, H. H. Sitte, H. Weinstein, H. J. Matthies, and A. Galli. PIP2 regulates psychostimulant behaviors through its interaction with a membrane protein. *Nat. Chem. Biol.*, 10(7):582–9, 2014.
313. F. Buchmayer, K. Schicker, T. Steinkellner, P. Geier, G. Stübiger, P. J. Hamilton, A. Jurik, T. tockner, J.-W. Yang, T. Montgomery, M. Holy, T. Hofmaier, O. Kudlacek, H. J. G. Matthies, V. Ecker, G. F. nd Bochkov, A. Galli, S. Boehm, and H. H. Sitte. Amphetamine actions at the serotonin transporter rely on the availability of phosphatidylinositol 4,5-bisphosphate. *Proc. Natl. Acad. Sci. USA*, 110(28):11642–11647, 2013.
314. N. A. Baker, D. Sept, S. Joseph, M. J. Holst, and J. A. McCammon. Electrostatics of nanosystems: Application to microtubules and the ribosome. *Proc. Natl. Acad. Sci. USA*, 98(18):10037–10041, 2001.
315. M. A. Lemmon. Phosphoinositide recognition domains. *Traffic*, 4(4):201–13, 2003.
316. K. M. Ferguson, J. M. Kavran, V. G. Sankaran, E. Fournier, S. J. Isakoff, E. Y. Skolnik, and M. A. Lem-

mon. Structural basis for discrimination of 3-phosphoinositides by pleckstrin homology domains. *Mol. Cell*, 6(2):373–84, 2000.
317. H. Tapp, I. M. Al-Naggar, E. G. Yarmola, A. Harrison, G. Shaw, A. S. Edison, and M. R. Bubb. MARCKS is a natively unfolded protein with an inaccessible actin-binding site: evidence for long-range intramolecular interactions. *J. Biol. Chem.*, 280(11):9946–56, 2005.
318. A. Ben-Shaul, N. Ben-Tal, and B. Honig. Statistical thermodynamic analysis of peptide and protein insertion into lipid membranes. *Biophys. J.*, 71(1):130–7, 1996.
319. J. A. Killian. Hydrophobic mismatch between proteins and lipids in membranes. *Biochim. Biophys. Acta*, 1376(3):401–15, 1998.
320. N. I. Liu and R. L. Kay. Redetermination of the pressure dependence of the lipid bilayer phase transition. *Biochemistry*, 16(15):3484–6, 1977.
321. E. A. Evans and R. M. Hochmuth. Mechanochemical properties of membranes. *Curr. Top. Membr. Transp.*, 10:1–64, 1978.
322. D. Marsh. Energetics of Hydrophobic Matching in Lipid-Protein Interactions. *Biophys. J.*, 94(10):3996–4013, 2008.
323. T. Kim and W. Im. Revisiting hydrophobic mismatch with free energy simulation studies of transmembrane helix tilt and rotation. *Biophys. J.*, 99(1):175–83, 2010.
324. S. K. Kandasamy and R. G. Larson. Molecular dynamics simulations of model trans-membrane peptides in lipid bilayers: a systematic investigation of hydrophobic mismatch. *Biophys. J.*, 90(7):2326–43, 2006.
325. Y. Gofman, T. Haliloglu, and N. Ben-Tal. The Transmembrane Helix Tilt May Be Determined by the Balance between Precession Entropy and Lipid Perturbation. *J. Chem. Theory. Comput.*, 8(8):2896–2904, 2012.
326. D. P. Siegel, V. Cherezov, D. V. Greathouse, R. E. Koeppe 2nd, J. A. Killian, and M. Caffrey. Transmembrane peptides stabilize inverted cubic phases in a biphasic length-dependent manner: implications for protein-induced membrane fusion. *Biophys. J.*, 90(1):200–11, 2006.
327. D. Raucher and M. P. Sheetz. Cell spreading and lamellipodial extension rate is regulated by membrane tension. *J. Cell Biol.*, 148(1):127–36, 2000.
328. M. D. Ledesma and C. G. Dotti. Membrane and cytoskeleton dynamics during axonal elongation and stabilization. *Int. Rev. Cytol.*, 227:183–219, 2003.
329. M. P. Sheetz. Cell control by membrane-cytoskeleton adhesion. *Nat. Rev. Mol. Cell Biol.*, 2(5):392–6, 2001.
330. B. Antonny, P. Gounon, R. Schekman, and L. Orci. Self-assembly of minimal COPII cages. *EMBO Rep.*, 4(4):419–24, 2003.
331. R. Nossal. Energetics of clathrin basket assembly. *Traffic*, 2(2):138–47, 2001.
332. B. Razani and M. P. Lisanti. Caveolins and caveolae: molecular and functional relationships. *Exp. Cell Res.*, 271(1):36–44, 2001.
333. R. J. Mashl and R. F. Bruinsma. Spontaneous-curvature theory of clathrin-coated membranes. *Biophys. J.*, 74(6):2862–75, 1998.
334. M. G. Ford, I. G. Mills, B. J. Peter, Y. Vallis, G. J. Praefcke, P. R. Evans, and H. T. McMahon. Curvature of clathrin-coated pits driven by epsin. *Nature*, 419(6905):361–6, 2002.
335. M. N. Aranda-Sicilia, Y. Trusov, N. Maruta, D. Chakravorty, Y. Zhang, and J. R. Botella. Heterotrimeric G proteins interact with defense-related receptor-like kinases in Arabidopsis. *J. Plant Physiol.*, 188:44–48, 2015.
336. J. Bockaert. G Protein-coupled Receptors. In *Encyclopedia of Life Sciences*. John Wiley & Sons, Ltd., 2009.
337. R. Fredriksson, M. C. Lagerstrom, L. G. Lundin, and H. B. Schioth. The G-protein-coupled receptors in the human genome form five main families. Phylogenetic analysis, paralogon groups, and fingerprints. *Mol. Pharmacol.*, 63:1256–1272, 2003.
338. C. D. Hanlon and D. J. Andrew. Outside-in signaling: a brief review of GPCR signaling with a focus on the Drosophila GPCR family. *J. Cell Sci.*, 128(19):3533–3542, 2015.
339. T. K. Bjarnadóttir, D. E. Gloriam, S. H. Hellstrand, H. Kristiansson, R. Fredriksson, and H. B. Schiöth. Comprehensive repertoire and phylogenetic analysis of the G protein-coupled receptors in human and mouse. *Genomics*, 88(3):263–273, 2006.
340. N. Wettschureck and S. Offermanns. Mammalian G Proteins and Their Cell Type Specific Functions. *Physiol. Rev.*, 85(4):1159–1204, 2005.
341. N. E. Bhola and J. R. Grandis. Crosstalk between G-protein-coupled receptors and epidermal growth factor receptor in cancer. *Front. Biosci. J. Virtual Library*, 13:1857–1865, 2008.
342. A. Madeo and M. Maggiolini. Nuclear Alternate Estrogen Receptor GPR30 Mediates 17β-Estradiol–

Induced Gene Expression and Migration in Breast Cancer–Associated Fibroblasts. *Cancer Res.*, 70(14):6036–6046, 2010.
343. G. Sliwoski, S. Kothiwale, J. Meiler, and E. W. Lowe Jr. Computational methods in drug discovery. *Pharmacol. Rev.*, 66(1):334–95, 2014.
344. Y. Fang, T. Kenakin, and C. Liu. Editorial: Orphan GPCRs As Emerging Drug Targets. *Front. Pharmacol.*, 6:295, 2015.
345. J. A. Salon, D. T. Lodowski, and K. Palczewski. The Significance of G Protein-Coupled Receptor Crystallography for Drug Discovery. *Pharmacol. Rev.*, 63(4):901–937, 2011.
346. S. L. Garland. Are GPCRs Still a Source of New Targets? *J. Biomol. Screen.*, 18(9):947–966, 2013.
347. M. J. Berridge. Introduction. In *Cell Signalling Biology*, chapter 1, pages 1–69. Portland Press, 2014.
348. Boghog. Dose response curves of a full agonist, partial agonist, neutral antagonist, and inverse agonist. Wikipedia, the free encyclopedia. https://en.wikipedia.org/wiki/Inverse_agonist#/media/File:Inverse_agonist_3.svg, 2014.
349. J. Bockaert, L. Fagni, A. Dumuis, and P. Marin. GPCR interacting proteins (GIP). *Pharmacol. Ther.*, 103(3):203–21, 2004.
350. W. I. Weis and B. Kobilka. Structural insights into G-protein-coupled receptor activation. *Curr. Opin. Struct. Biol.*, 18:734–740, 2008.
351. B. K. Kobilka. G protein coupled receptor structure and activation. *Biochim. Biophys. Acta – Biomembranes*, 1768(4):794–807, 2007.
352. A. Kitao, S. Hayward, and N. Go. Energy landscape of a native protein: jumping-among-minima model. *Proteins*, 33(4):496–517, 1998.
353. J. A. McCammon, B. R. Gelin, and M. Karplus. Dynamics of folded proteins. *Nature*, 267(5612):585–90, 1977.
354. R. H. Austin, K. W. Beeson, L. Eisenstein, H. Frauenfelder, and I. C. Gunsalus. Dynamics of ligand binding to myoglobin. *Biochemistry*, 14(24):5355–73, 1975.
355. G. A. Petsko and D. Ringe. Fluctuations in protein structure from X-ray diffraction. *Annu. Rev. Biophys. Bio.*, 13:331–71, 1984.
356. H. Frauenfelder, F. Parak, and R. D. Young. Conformational substates in proteins. *Annu. Rev. Biophys. Biophys. Chem.*, 17:451–79, 1988.
357. K. S. Kim and C. Woodward. Protein internal flexibility and global stability: effect of urea on hydrogen exchange rates of bovine pancreatic trypsin inhibitor. *Biochemistry*, 32(37):9609–13, 1993.
358. Y. Bai, T. R. Sosnick, L. Mayne, and S. W. Englander. Protein folding intermediates: native-state hydrogen exchange. *Science*, 269(5221):192–7, 1995.
359. R. Elber and M. Karplus. Multiple conformational states of proteins: a molecular dynamics analysis of myoglobin. *Science*, 235(4786):318–21, 1987.
360. L. Fetler, E. R. Kantrowitz, and P. Vachette. Direct observation in solution of a preexisting structural equilibrium for a mutant of the allosteric aspartate transcarbamoylase. *Proc. Natl. Acad. Sci. USA*, 104(2):495–500, 2007.
361. L. C. James and D. S. Tawfik. Conformational diversity and protein evolution: a 60-year-old hypothesis revisited. *Trends Biochem. Sci.*, 28(7):361–8, 2003.
362. A. Malmendal, J. Evenas, S. Forsen, and M. Akke. Structural dynamics in the C-terminal domain of calmodulin at low calcium levels. *J. Mol. Biol.*, 293(4):883–99, 1999.
363. B. K. Kobilka and X. Deupi. Conformational complexity of G-protein-coupled receptors. *Trends Pharmacol. Sci.*, 28(8):397–406, 2007.
364. K. Henzler-Wildman and D. Kern. Dynamic personalities of proteins. *Nature*, 450(7172):964–72, 2007.
365. M. Vendruscolo and C. M. Dobson. Dynamic Visions of Enzymatic Reactions. *Science*, 313(5793):1586–1587, 2006.
366. K. Gunasekaran, B. Ma, and R. Nussinov. Is allostery an intrinsic property of all dynamic proteins? *Proteins*, 57(3):433–43, 2004.
367. G. Weber. Ligand binding and internal equilibrium in proteins. *Biochemistry*, 11(5):864–878, 1972.
368. I. Bahar, C. Chennubhotla, and D. Tobi. Intrinsic dynamics of enzymes in the unbound state and relation to allosteric regulation. *Curr. Opin. Struct. Biol.*, 17(6):633–40, 2007.
369. O. F. Lange, N. A. Lakomek, C. Fares, G. F. Schroder, K. F. Walter, S. Becker, J. Meiler, H. Grubmuller, C. Griesinger, and B. L. de Groot. Recognition dynamics up to microseconds revealed from an RDC-derived ubiquitin ensemble in solution. *Science*, 320(5882):1471–5, 2008.

370. J. Gsponer, J. Christodoulou, A. Cavalli, J. M. Bui, B. Richter, C. M. Dobson, and M. Vendruscolo. A coupled equilibrium shift mechanism in calmodulin-mediated signal transduction. *Structure*, 16(5):736–46, 2008.
371. D. M. Rosenbaum, S. G. F. Rasmussen, and B. K. Kobilka. The structure and function of G-protein-coupled receptors. *Nature*, 459:356–363, 2009.
372. K. L. Pierce, R. T. Premont, and R. J. Lefkowitz. Seven-transmembrane receptors. *Nat. Rev. Mol. Cell Biol.*, 3(9):639–50, 2002.
373. H. Ashkenazy, S. Abadi, E. Martz, O. Chay, I. Mayrose, T. Pupko, and N. Ben-Tal. ConSurf 2016: an improved methodology to estimate and visualize evolutionary conservation in macromolecules. *Nucleic Acids Res.*, 44(W1):W344–W350, 2016.
374. F. Glaser, T. Pupko, I. Paz, R. E. Bell, D. Bechor-Shental, E. Martz, and N. Ben-Tal. ConSurf: identification of functional regions in proteins by surface-mapping of phylogenetic information. *Bioinformatics*, 19(1):163–4, 2003.
375. R. A. Cerione, C. Staniszewski, J. L. Benovic, R. J. Lefkowitz, M. G. Caron, P. Gierschik, R. Somers, A. M. Spiegel, J. Codina, and L. Birnbaumer. Specificity of the functional interactions of the beta-adrenergic receptor and rhodopsin with guanine nucleotide regulatory proteins reconstituted in phospholipid vesicles. *J. Biol. Chem.*, 260(3):1493–500, 1985.
376. W. W. I. Lau, A. S. L. Chan, L. S. W. Poon, J. Zhu, and Y. H. Wong. G$\beta\gamma$-mediated activation of protein kinase D exhibits subunit specificity and requires G$\beta\gamma$-responsive phospholipase Cβ isoforms. *Cell Commun. Signal.*, 11:22, 2013.
377. H. G. Dohlman and J. Thorner. RGS proteins and signaling by heterotrimeric G proteins. *J. Biol. Chem.*, 272:3871–3874, 1997.
378. J. Shonberg, R. C. Kling, P. Gmeiner, and S. Löber. GPCR crystal structures: Medicinal chemistry in the pocket. *Bioorg. Med. Chem.*, 23(14):3880–3906, 2015.
379. D. Zhang, Q. Zhao, and B. Wu. Structural Studies of G Protein-Coupled Receptors. *Mol. Cells*, 38(10):836–842, 2015.
380. A. J. Venkatakrishnan, Xavier Deupi, Guillaume Lebon, Christopher G. Tate, Gebhard F. Schertler, and M. Madan Babu. Molecular signatures of G-protein-coupled receptors. *Nature*, 494(7436):185–194, 2013.
381. S. A. Shabalina, D. V. Zaykin, P. Gris, A. Y. Ogurtsov, J. Gauthier, K. Shibata, I. E. Tchivileva, I. Belfer, B. Mishra, C. Kiselycznyk, M. R. Wallace, R. Staud, N. A. Spiridonov, M. B. Max, D. Goldman, R. B. Fillingim, W. Maixner, and L. Diatchenko. Expansion of the human μ-opioid receptor gene architecture: novel functional variants. *Hum. Mol. Genet.*, 18(6):1037, 2009.
382. M. Convertino, A. Samoshkin, J. Gauthier, M. S. Gold, W. Maixner, N. V. Dokholyan, and L. Diatchenko. μ-Opioid receptor 6-transmembrane isoform: A potential therapeutic target for new effective opioids. *Prog. Neuropsychopharmacol. Biol. Psychiatry*, 62:61–67, 2015.
383. N. Kamesh, Gopala K. Aradhyam, and Narayanan Manoj. The repertoire of G protein-coupled receptors in the sea squirt *Ciona intestinalis*. *BMC Evol. Biol.*, 8(1):129, 2008.
384. J. A. Hanson, K. Duderstadt, L. P. Watkins, S. Bhattacharyya, J. Brokaw, J. W. Chu, and H. Yang. Illuminating the mechanistic roles of enzyme conformational dynamics. *Proc. Natl. Acad. Sci. USA*, 104:18055–18060, 2007.
385. J. Bockaert, S. Claeysen, C. Bécamel, S. Pinloche, and A. Dumuis. G protein-coupled receptors: dominant players in cell-cell communication. *Int. Rev. Cytol.*, 212:63–132, 2002.
386. L. Chun, W.-h. Zhang, and J.-f. Liu. Structure and ligand recognition of class C GPCRs. *Acta Pharm. Sin.*, 33(3):312–323, 2012.
387. H. P. Nothacker. Orphan Receptors. In S. Offermanns and W. Rosenthal, editors, *Encyclopedia of Molecular Pharmacology*, pages 914–917. Springer, Heidelberg, 2008.
388. S. P. Lee, B. F. O'Dowd, and S. R. George. Homo- and hetero-oligomerization of G protein-coupled receptors. *Life Sci.*, 74(2–3):173–180, 2003.
389. S. Ferré, V. Casadó, L. A. Devi, M. Filizola, R. Jockers, M. J. Lohse, G. Milligan, J.-P. Pin, and X. Guitart. G Protein–Coupled Receptor Oligomerization Revisited: Functional and Pharmacological Perspectives. *Pharmacol. Rev.*, 66(2):413–434, 2014.
390. S. Ferré. The GPCR heterotetramer: challenging classical pharmacology. *Trends Pharmacol. Sci.*, 36(3):145–152, 2015.
391. M. J. Lohse. Dimerization in GPCR mobility and signaling. *Curr. Opin. Pharmacol.*, 10(1):53–58, 2010.
392. G. Milligan. G protein-coupled receptor hetero-dimerization: contribution to pharmacology and function. *Br. J. Pharmacol.*, 158(1):5–14, 2009.

393. J. Kniazeff, L. Prézeau, P. Rondard, J.-P. Pin, and C. Goudet. Dimers and beyond: The functional puzzles of class C GPCRs. *Pharmacol. Ther.*, 130(1):9–25, 2011.
394. X. C. Zhang, J. Liu, and D. Jiang. Why is dimerization essential for class-C GPCR function? New insights from mGluR1 crystal structure analysis. *Protein Cell*, 5(7):492–495, 2014.
395. J. P. Pin, J. Kniazeff, V. Binet, J. Liu, D Maurel, T. Galvez, B. Duthey, M. Havlickova, J. Blahos, L. Prézeau, and P. Rondard. Activation mechanism of the heterodimeric GABA(B) receptor. *Biochem. Pharmacol.*, 68(8):1565–1572, 2004.
396. A. Manglik, A. C. Kruse, T. S. Kobilka, F. S. Thian, J. M. Mathiesen, R. K. Sunahara, L. Pardo, W. I. Weis, B. K. Kobilka, and S. Granier. Crystal structure of the micro-opioid receptor bound to a morphinan antagonist. *Nature*, 485(7398):321–326, 2012.
397. R. Franco, E. Martínez-Pinilla, J. L. Lanciego, and G. Navarro. Basic Pharmacological and Structural Evidence for Class A G-Protein-Coupled Receptor Heteromerization. *Front. Pharmacol.*, 7:76, 2016.
398. B. Wu, E. Y. T. Chien, C. D. Mol, G. Fenalti, W. Liu, V. Katritch, R. Abagyan, A. Brooun, P. Wells, F. C. Bi, D. J. Hamel, P. Kuhn, T. M. Handel, V. Cherezov, and R. C. Stevens. Structures of the CXCR4 Chemokine GPCR with Small-Molecule and Cyclic Peptide Antagonists. *Science*, 330(6007):1066–1071, 2010.
399. H. Wu, D. Wacker, V. Katritch, M. Mileni, G. W. Han, E. Vardy, W. Liu, A. A. Thompson, X.-P. Huang, F. I. Carroll, S. W. Mascarella, R. B. Westkaemper, P. D. Mosier, B. L. Roth, V. Cherezov, and R. C. Stevens. Structure of the human kappa opioid receptor in complex with JDTic. *Nature*, 485(7398):327–332, 2012.
400. M. R. Whorton, B. Jastrzebska, P. S. Park, D. Fotiadis, A. Engel, K. Palczewski, and R. K. Sunahara. Effcient coupling of transducin to monomeric rhodopsin in a phospholipid bilayer. *J. Biol. Chem.*, 283(74387–4394), 2008.
401. J. Huang, S. Chen, J. J. Zhang, and X.-Y. Huang. Crystal structure of oligomeric β1-adrenergic G protein–coupled receptors in ligand-free basal state. *Nat. Struct. Mol. Biol.*, 20(4):419–425, 2013.
402. V. Cherezov, D. M. Rosenbaum, M. A. Hanson, S. G. F. Rasmussen, F. S. Thian, T. S. Kobilka, H. J. Choi, P. Kuhn, W. I. Weis, B. K. Kobilka, and R. C. Stevens. High-resolution crystal structure of an engineered human beta2-adrenergic G protein-coupled receptor. *Science*, 318(5854):1258–65, 2007.
403. H. Zheng, E. A. Pearsall, D. P. Hurst, Y. Zhang, J. Chu, Y. Zhou, P. H. Reggio, H. H. Loh, and P.-Y. Law. Palmitoylation and membrane cholesterol stabilize μ-opioid receptor homodimerization and G protein coupling. *BMC Cell Biology*, 13(1):6, 2012.
404. H. Wu, C. Wang, K. J. Gregory, G. W. Han, H. P. Cho, Y. Xia, C. M. Niswender, V. Katritch, J. Meiler, V. Cherezov, P. J. Conn, and R. C. Stevens. Structure of a Class C GPCR Metabotropic Glutamate Receptor 1 Bound to an Allosteric Modulator. *Science*, 344(6179):58–64, 2014.
405. T. W. Schwartz and W. L. Hubbell. Structural biology: A moving story of receptors. *Nature*, 455(7212):473–474, 2008.
406. R. J. Lefkowitz. A Brief History of G-Protein Coupled Receptors (Nobel Lecture). *Angew. Chem. Int. Ed.*, 52(25):6366–6378, 2013.
407. M. A. Hanson and R. C. Stevens. Discovery of New GPCR Biology: One Receptor Structure at a Time. *Structure*, 17:8–14, 2009.
408. S. G. F. Rasmussen, H. J. Choi, D. M. Rosenbaum, T. S. Kobilka, F. S. Thian, P. C. Edwards, M. Burghammer, V. R. Ratnala, R. Sanishvili, R. F. Fischetti, G. F. Schertler, W. I. Weis, and B. K. Kobilka. Crystal structure of the human beta2 adrenergic G-protein-coupled receptor. *Nature*, 450(7168):383–7, 2007.
409. E. M. Bastiaanse, K. M. Hold, and A. Van der Laarse. The effect of membrane cholesterol content on ion transport processes in plasma membranes. *Cardiovasc. Res.*, 33(2):272–83, 1997.
410. K. Burger, G. Gimpl, and F. Fahrenholz. Regulation of receptor function by cholesterol. *Cell. Mol. Life Sci.*, 57(11):1577–92, 2000.
411. T. J. Pucadyil and A. Chattopadhyay. Role of cholesterol in the function and organization of G-protein coupled receptors. *Prog. Lipid Res.*, 45(4):295–333, 2006.
412. J. Oates and A. Watts. Uncovering the intimate relationship between lipids, cholesterol and GPCR activation. *Curr. Opin. Struct. Biol.*, 21(6):802–807, 2011.
413. Y. D. Paila and A. Chattopadhyay. The function of G-protein coupled receptors and membrane cholesterol: specific or general interaction? *Glycoconj. J.*, 26(6):711, 2009.
414. X. Deupi and J. Standfuss. Structural insights into agonist-induced activation of G-protein-coupled receptors. *Curr. Opin. Struct. Biol.*, 21(4):541–551, 2011.
415. R. Moukhametzianov, T. Warne, P. C. Edwards, M. J. Serrano-Vega, A. G. W. Leslie, C. G. Tate, and G. F. X. Schertler. Two distinct conformations of helix 6 observed in antagonist-bound structures of a β1-adrenergic receptor. *Proc. Natl. Acad. Sci. USA*, 108(20):8228–8232, 2011.

416. R. O. Dror, D. H. Arlow, D. W. Borhani, M. Ø. Jensen, S. Piana, and D. E. Shaw. Identification of two distinct inactive conformations of the β2-adrenergic receptor reconciles structural and biochemical observations. *Proc. Natl. Acad. Sci. USA*, 106(12):4689–4694, 2009.
417. R. A. Bond and A. P. Ijzerman. Recent developments in constitutive receptor activity and inverse agonism, and their potential for GPCR drug discovery. *Trends Pharmacol. Sci.*, 27:92–96, 2006.
418. K. Palczewski, T. Kumasaka, T. Hori, C. A. Behnke, H. Motoshima, B. A. Fox, I. Le Trong, D. C. Teller, T. Okada, R. E. Stenkamp, M. Yamamoto, and M. Miyano. Crystal structure of rhodopsin: A G protein-coupled receptor. *Science*, 289(5480):739–45, 2000.
419. M. Murakami and T. Kouyama. Crystal structure of squid rhodopsin. *Nature*, 453(7193):363–7, 2008.
420. T. Shimamura, K. Hiraki, N. Takahashi, T. Hori, H. Ago, K. Masuda, K. Takio, M. Ishiguro, and M. Miyano. Crystal structure of squid rhodopsin with intracellularly extended cytoplasmic region. *J. Biol. Chem.*, 283(26):17753–6, 2008.
421. D. Mustafi and K. Palczewski. Topology of class A G protein-coupled receptors: insights gained from crystal structures of rhodopsins, adrenergic and adenosine receptors. *Mol. Pharmacol.*, 75(1):1–12, 2009.
422. B. K. Kobilka, T. S. Kobilka, K. Daniel, J. W. Regan, M. G. Caron, and R. J. Lefkowitz. Chimeric alpha 2-,beta 2-adrenergic receptors: delineation of domains involved in effector coupling and ligand binding specificity. *Science*, 240(4857):1310–1316, 1988.
423. C. C. Malbon and H. Y. Wang. Adrenergic Receptors. In *Encyclopedia of Life Sciences*. John Wiley & Sons, Ltd., 2005.
424. S. Nussey and S. Whitehead. *Endocrinology: An Integrated Approach*. BIOS Scientific Publishers Ltd, Oxford, England, 2001.
425. D. S. Goldstein. Adrenaline and noradrenaline. In *Encyclopedia of Life Sciences*. John Wiley & Sons, Ltd., 2001.
426. S. C. Stanford. Adrenaline and Noradrenaline: Introduction. In *Encyclopedia of Life Sciences*. John Wiley & Sons, Ltd., 2009.
427. J. H. Schwartz. Neurotransmitters. In *Encyclopedia of Life Sciences*. John Wiley & Sons, Ltd., 2001.
428. W. B. Cannon. *Bodily Changes in Pain, Hunger, Fear and Rage: An Account of Recent Research Into the Function of Emotional Excitement*. Appleton-Century-Crofts, New York, 1929.
429. A. Hachmon. An Arabian woof bristling its hair. Wikipedia, the free encyclopedia. http://en.wikipedia.org/wiki/File:Canis_lupus_arabic.JPG, 2008.
430. E. Charmandari, C. Tsigos, and G. Chrousos. Endocrinology of the stress response. *Annu. Rev. Physiol.*, 67:259–84, 2005.
431. D. M. Rosenbaum, C. Zhang, J. A. Lyons, R. Holl, D. Aragao, D. H. Arlow, S. G. F. Rasmussen, H.-J. Choi, B. T. DeVree, R. K. Sunahara, P. S. Chae, S. H. Gellman, R. O. Dror, D. E. Shaw, W. I. Weis, M. Caffrey, P. Gmeiner, and B. K. Kobilka. Structure and function of an irreversible agonist-β2 adrenoceptor complex. *Nature*, 469(7329):236–240, 2011.
432. R. Nygaard, Y. Zou, R. O. Dror, T. J. Mildorf, D. H. Arlow, A. Manglik, A. C. Pan, C. W. Liu, J. J. Fung, M. P. Bokoch, F. S. Thian, T. S. Kobilka, D. E. Shaw, L. Mueller, R. S. Prosser, and B. K. Kobilka. The Dynamic Process of β2-Adrenergic Receptor Activation. *Cell*, 152(3):532–542, 2013.
433. A. Manglik, T. H. Kim, M. Masureel, C. Altenbach, Z. Yang, D. Hilger, M. T. Lerch, T. S. Kobilka, F. S. Thian, W. L. Hubbell, R. S. Prosser, and B. K. Kobilka. Structural Insights into the Dynamic Process of β2-Adrenergic Receptor Signaling. *Cell*, 161(5):1101–1111, 2015.
434. H.-W. Choe, Y. J. Kim, J. H. Park, T. Morizumi, E. F. Pai, N. Krausz, K. P. Hofmann, P. Scheerer, and O. P. Ernst. Crystal structure of metarhodopsin II. *Nature*, 471(7340):651–655, 2011.
435. S. G. F. Rasmussen, B. T. DeVree, Y. Zou, A. C. Kruse, K. Y. Chung, T. S. Kobilka, F. S. Thian, P. S. Chae, E. Pardon, D. Calinski, J. M. Mathiesen, S. T. A. Shah, J. A. Lyons, M. Caffrey, S. H. Gellman, J. Steyaert, G. Skiniotis, W. I. Weis, R. K. Sunahara, and B. K. Kobilka. Crystal structure of the β2 adrenergic receptor-Gs protein complex. *Nature*, 477(7366):549–555, 2011.
436. S. G. F. Rasmussen, H.-J. Choi, J. J. Fung, E. Pardon, P. Casarosa, P. S. Chae, B. T. DeVree, D. M. Rosenbaum, F. S. Thian, T. S. Kobilka, A. Schnapp, I. Konetzki, R. K. Sunahara, S. H. Gellman, A. Pautsch, J. Steyaert, W. I. Weis, and B. K. Kobilka. Structure of a nanobody-stabilized active state of the β2 adrenoceptor. *Nature*, 469(7329):175–180, 2011.
437. A. C. Kruse, A. M. Ring, A. Manglik, J. Hu, K. Hu, K. Eitel, H. Hubner, E. Pardon, C. Valant, P. M. Sexton, A. Christopoulos, C. C. Felder, P. Gmeiner, J. Steyaert, W. I. Weis, K. C. Garcia, J. Wess, and B. K. Kobilka. Activation and allosteric modulation of a muscarinic acetylcholine receptor. *Nature*, 504(7478):101–106, 2013.

438. S. Ahuja, V. Hornak, E. C. Yan, N. Syrett, J. A. Goncalves, A. Hirshfeld, M. Ziliox, T. P. Sakmar, M. Sheves, P. J. Reeves, S. O. Smith, and M. Eilers. Helix movement is coupled to displacement of the second extracellular loop in rhodopsin activation. *Nat. Struct. Mol. Biol.*, 16:168–175, 2009.
439. C. Altenbach, A. K. Kusnetzow, O. P. Ernst, K. P. Hofmann, and W. L. Hubbell. High-resolution distance mapping in rhodopsin reveals the pattern of helix movement due to activation. *Proc. Natl. Acad. Sci. USA*, 105:7439–7444, 2008.
440. S. R. Sprang. A receptor unlocked. *Nature*, 450:355–6, 2007.
441. A. M. Ring, A. Manglik, A. C. Kruse, M. D. Enos, W. I. Weis, K. C. Garcia, and B. K. Kobilka. Adrenaline-activated structure of β2-adrenoceptor stabilized by an engineered nanobody. *Nature*, 502(7472):575–579, 2013.
442. I. Bang and H.-J. Choi. Structural Features of β2 Adrenergic Receptor: Crystal Structures and Beyond. *Mol. Cells*, 38(2):105–111, 2015.
443. R. O. Dror, D. H. Arlow, P. Maragakis, T. J. Mildorf, A. C. Pan, H. Xu, D. W. Borhani, and D. E. Shaw. Activation mechanism of the β2-adrenergic receptor. *Proc. Natl. Acad. Sci. USA*, 108(46):18684–18689, 2011.
444. K. Y. Chung, S. G. F. Rasmussen, T. Liu, S. Li, B. T. DeVree, P. S. Chae, D. Calinski, B. K. Kobilka, V. L. Woods, and R. K. Sunahara. Conformational changes in the G protein Gs induced by the β2 adrenergic receptor. *Nature*, 477(7366):611–615, 2011.
445. G. Lebon, T. Warne, P. C. Edwards, K. Bennett, C. J. Langmead, A. G. W. Leslie, and C. G. Tate. Agonist-bound adenosine A_{2A} receptor structures reveal common features of GPCR activation. *Nature*, 474(7352):521–525, 2011.
446. F. Xu, H. Wu, V. Katritch, G. W. Han, K. A. Jacobson, Z.-G. Gao, V. Cherezov, and R. C. Stevens. Structure of an Agonist-Bound Human A_{2A} Adenosine Receptor. *Science*, 332(6027):322–327, 2011.
447. G. Liapakis, J. A. Ballesteros, S. Papachristou, W. C. Chan, X. Chen, and J. A. Javitch. The forgotten serine. A critical role for Ser-2035.42 in ligand binding to and activation of the β2-adrenergic receptor. *J. Biol. Chem.*, 275(48):37779–37788, 2000.
448. K. Haga, A. C. Kruse, H. Asada, T. Yurugi-Kobayashi, M. Shiroishi, C. Zhang, W. I. Weis, T. Okada, B. K. Kobilka, T. Haga, and T. Kobayashi. Structure of the human M2 muscarinic acetylcholine receptor bound to an antagonist. *Nature*, 482(7386):547–551, 2012.
449. A. C. Kruse, J. Hu, A. C. Pan, D. H. Arlow, D. M. Rosenbaum, E. Rosemond, H. F. Green, T. Liu, P. S. Chae, R. O. Dror, D. E. Shaw, W. I. Weis, J. Wess, and B. K. Kobilka. Structure and dynamics of the M3 muscarinic acetylcholine receptor. *Nature*, 482(7386):552–556, 2012.
450. F. Heitz, J. A. Holzwarth, J.-P. Gies, R. M. Pruss, S. Trumpp-Kallmeyer, M. F. Hibert, and C. Guenet. Site-directed mutagenesis of the putative human muscarinic M2 receptor binding site. *Eur. J. Pharmacol.*, 380(2–3):183–195, 1999.
451. P. R. Gentry, P. M. Sexton, and A. Christopoulos. Novel Allosteric Modulators of G Protein-coupled Receptors. *J. Biol. Chem.*, 290(32):19478–19488, 2015.
452. D. Zhang, Z.-G. Gao, K. Zhang, E. Kiselev, S. Crane, J. Wang, S. Paoletta, C. Yi, L. Ma, W. Zhang, G. W. Han, H. Liu, V. Cherezov, V. Katritch, H. Jiang, R. C. Stevens, K. A. Jacobson, Q. Zhao, and B. Wu. Two disparate ligand-binding sites in the human P2Y1 receptor. *Nature*, 520(7547):317–321, 2015.
453. B. Trzaskowski, D. Latek, S. Yuan, U. Ghoshdastider, A. Debinski, and S. Filipek. Action of molecular switches in GPCRs–theoretical and experimental studies. *Curr. Med. Chem.*, 19(8):1090–109, 2012.
454. J. Shonberg, L. Lopez, P. J. Scammells, A. Christopoulos, B. Capuano, and J. R. Lane. Biased Agonism at G Protein-Coupled Receptors: The Promise and the Challenges: A Medicinal Chemistry Perspective. *Med. Res. Rev.*, 34(6):1286–1330, 2014.
455. E. Reiter, S. Ahn, A. K. Shukla, and R. J. Lefkowitz. Molecular Mechanism of β-Arrestin-Biased Agonism at Seven-Transmembrane Receptors. *Annu. Rev. Pharmacol. Toxicol.*, 52(1):179–197, 2012.
456. P. Tsao and M. von Zastrow. Downregulation of G protein-coupled receptors. *Curr. Opin. Neurobiol.*, 10(3):365–9, 2000.
457. S. K. Bohm, E. F. Grady, and N. W. Bunnett. Regulatory mechanisms that modulate signalling by G-protein-coupled receptors. *Biochem. J.*, 322(part 1):1–18, 1997.
458. S. S. Ferguson. Evolving concepts in G protein-coupled receptor endocytosis: the role in receptor desensitization and signaling. *Pharmacol. Rev.*, 53:1–24, 2001.
459. J. A. Pitcher, N. J. Freedman, and R. J. Lefkowitz. G protein-coupled receptor kinases. *Annu. Rev. Biochem.*, 67:653–92, 1998.
460. O. B. Goodman Jr, J. G. Krupnick, F. Santini, V. V. Gurevich, R. B. Penn, A. W. Gagnon, J. H. Keen, and J. L.

Benovic. Beta-arrestin acts as a clathrin adaptor in endocytosis of the beta2-adrenergic receptor. *Nature*, 383(6599):447–50, 1996.

461. S. Danner and M. J. Lohse. Regulation of beta-adrenergic receptor responsiveness modulation of receptor gene expression. *Rev. Physiol., Biochem. Pharmacol.*, 136:183–223, 1999.
462. F. Mullershausen, F. Zecri, C. Cetin, A. Billich, D. Guerini, and K. Seuwen. Persistent signaling induced by FTY720-phosphate is mediated by internalized S1P1 receptors. *Nat. Chem. Biol.*, 5(6):428–434, 2009.
463. N. G. Tsvetanova and M. von Zastrow. Spatial encoding of cyclic AMP signaling specificity by GPCR endocytosis. *Nat. Chem. Biol.*, 10(12):1061–1065, 2014.
464. J. S. Smith and S. Rajagopal. The β-Arrestins: Multifunctional regulators of G protein-coupled receptors. *J. Biol. Chem.*, 291(17):8969–8977, 2016.
465. Y. Kang, X. E. Zhou, X. Gao, Y. He, W. Liu, A. Ishchenko, A. Barty, T. A. White, O. Yefanov, G. Won Han, Q. Xu, P. W. de Waal, J. Ke, M. H. E. Tan, C. Zhang, A. Moeller, G. M. West, B. D. Pascal, N. Van Eps, L. N. Caro, S. A. Vishnivetskiy, R. J. Lee, K. M. Suino-Powell, X. Gu, K. Pal, J. Ma, X. Zhi, S. Boutet, G. J. Williams, M. Messerschmidt, C. Gati, N. A. Zatsepin, D. Wang, D. James, S. Basu, S. Roy-Chowdhury, C. E. Conrad, J. Coe, H. Liu, S. Lisova, C. Kupitz, I. Grotjohann, R. Fromme, Y. Jiang, M. Tan, H. Yang, J. Li, M. Wang, Z. Zheng, D. Li, N. Howe, Y. Zhao, J. Standfuss, K. Diederichs, Y. Dong, C. S. Potter, B. Carragher, M. Caffrey, H. Jiang, H. N. Chapman, J. C. H. Spence, P. Fromme, U. Weierstall, O. P. Ernst, V. Katritch, V. V. Gurevich, P. R. Griffin, W. L. Hubbell, R. C. Stevens, V. Cherezov, K. Melcher, and H. E. Xu. Crystal structure of rhodopsin bound to arrestin by femtosecond X-ray laser. *Nature*, 523(7562):561–567, 2015.
466. M. K. Ostermaier, C. Peterhans, R. Jaussi, X. Deupi, and J. Standfuss. Functional map of arrestin-1 at single amino acid resolution. *Proc. Natl. Acad. Sci. USA*, 111(5):1825–1830, 2014.
467. J. J. Liu, R. Horst, V. Katritch, R. C. Stevens, and K. Wuthrich. Biased Signaling Pathways in 2-Adrenergic Receptor Characterized by 19F-NMR. *Science*, 335(6072):1106–1110, 2012.
468. K. Kirchberg, T.-Y. Kim, M. Möller, D. Skegro, G. Dasara Raju, J. Granzin, G. Büldt, R. Schlesinger, and U. Alexiev. Conformational dynamics of helix 8 in the GPCR rhodopsin controls arrestin activation in the desensitization process. *Proc. Natl. Acad. Sci. USA*, 108(46):18690–18695, 2011.
469. K. Hollenstein, J. Kean, A. Bortolato, R. K. Y. Cheng, A. S. Doré, A. Jazayeri, R. M. Cooke, M. Weir, and F. H. Marshall. Structure of class B GPCR corticotropin-releasing factor receptor 1. *Nature*, 499(7459):438–443, 2013.
470. F. Y. Siu, M. He, C. de Graaf, G. W. Han, D. Yang, Z. Zhang, C. Zhou, Q. Xu, D. Wacker, J. S. Joseph, W. Liu, J. Lau, V. Cherezov, V. Katritch, M.-W. Wang, and R. C. Stevens. Structure of the human glucagon class B G-protein-coupled receptor. *Nature*, 499(7459):444–449, 2013.
471. C. Parthier, S. Reedtz-Runge, R. Rudolph, and M. T. Stubbs. Passing the baton in class B GPCRs: peptide hormone activation via helix induction? *Trends Biochem. Sci.*, 34:303–10, 2009.
472. H. A. Watkins, M. Au, and D. L. Hay. The structure of secretin family GPCR peptide ligands: Implications for receptor pharmacology and drug development. *Drug Discov. Today*, 17(17–18):1006–1014, 2012.
473. T. Muto, D. Tsuchiya, K. Morikawa, and H. Jingami. Structures of the extracellular regions of the group II/III metabotropic glutamate receptors. *Proc. Natl. Acad. Sci. USA*, 104(10):3759–3764, 2007.
474. C. M. Niswender and P. J. Conn. Metabotropic Glutamate Receptors: Physiology, Pharmacology, and Disease. *Annu. Rev. Pharmacol. Toxicol.*, 50(1):295–322, 2010.
475. A. S. Doré, K. Okrasa, J. C. Patel, M. Serrano-Vega, K. Bennett, R. M. Cooke, J. C. Errey, A. Jazayeri, S. Khan, B. Tehan, M. Weir, G. R. Wiggin, and F. H. Marshall. Structure of class C GPCR metabotropic glutamate receptor 5 transmembrane domain. *Nature*, 511(7511):557–562, 2014.
476. P. J. Conn, A. Christopoulos, and C. W. Lindsley. Allosteric modulators of GPCRs: a novel approach for the treatment of CNS disorders. *Nat. Rev. Drug Discov.*, 8(1):41–54, 2009.
477. A. Ruiz-Gómez, C. Molnar, H. Holguín, F. Mayor, and J. F. de Celis. The cell biology of Smo signalling and its relationships with GPCRs. *Biochim. Biophys. Acta Biomembranes*, 1768(4):901–912, 2007.
478. C. Wang, H. Wu, V. Katritch, G. W. Han, X.-P. Huang, W. Liu, F. Y. Siu, B. L. Roth, V. Cherezov, and R. C. Stevens. Structure of the human smoothened receptor 7TM bound to an antitumor agent. *Nature*, 497(7449):338–343, 2013.
479. C. Wang, H. Wu, T. Evron, E. Vardy, G. W. Han, X.-P. Huang, S. J. Hufeisen, T. J. Mangano, D. J. Urban, V. Katritch, V. Cherezov, M. G. Caron, B. L. Roth, and R. C. Stevens. Structural basis for Smoothened receptor modulation and chemoresistance to anticancer drugs. *Nat. Commun.*, 5, 2014.
480. U. Weierstall, D. James, C. Wang, T. A. White, D. Wang, W. Liu, J. C. H. Spence, B. R. Doak, G. Nelson, P. Fromme, R. Fromme, I. Grotjohann, C. Kupitz, N. A. Zatsepin, H. Liu, S. Basu, D. Wacker, G. Won Han, V. Katritch, S. Boutet, M. Messerschmidt, G. J. Williams, J. E. Koglin, M. Marvin Seibert, M. Klinker,

C. Gati, R. L. Shoeman, A. Barty, H. N. Chapman, R. A. Kirian, K. R. Beyerlein, R. C. Stevens, D. Li, S. T. A. Shah, N. Howe, M. Caffrey, and V. Cherezov. Lipidic cubic phase injector facilitates membrane protein serial femtosecond crystallography. *Nat. Commun.*, 5(3309), 2014.

481. N. A. Riobo, B. Saucy, C. Dilizio, and D. R. Manning. Activation of heterotrimeric G proteins by Smoothened. *Proc. Natl. Acad. Sci. USA*, 103(33):12607–12612, 2006.
482. K. A. Jacobson. New paradigms in GPCR drug discovery. *Biochem. Pharmacol.*, 98(4):541–555, 2015.
483. N. M. Urs, P. J. Nicholls, and M. G. Caron. Integrated approaches to understanding antipsychotic drug action at GPCRs. *Curr. Opin. Cell. Biol.*, 27(1):56–62, 2014.
484. J. Shonberg, P. J. Scammells, and B. Capuano. Design strategies for bivalent ligands targeting GPCRs. *ChemMedChem*, 6(6):963–974, 2011.
485. Q. Tan, Y. Zhu, J. Li, Z. Chen, G. W. Han, I. Kufareva, T. Li, L. Ma, G. Fenalti, J. Li, W. Zhang, X. Xie, H. Yang, H. Jiang, V. Cherezov, H. Liu, R. C. Stevens, Q. Zhao, and B. Wu. Structure of the CCR5 Chemokine Receptor-HIV Entry Inhibitor Maraviroc Complex. *Science*, 341(6152):1387–1390, 2013.
486. G. J. Siegel. *Basic neurochemistry: molecular, cellular and medical aspects*. Lippincott Williams & Wilkins, Philadelphia, 6th edition, 1999.
487. R. B. Russell and D. S. Eggleston. New roles for structure in biology and drug discovery. *Nat. Struct. Biol.*, 7 Suppl:928–30, 2000.
488. C. Rochais, C. Lecoutey, F. Gaven, P. Giannoni, K. Hamidouche, D. Hedou, E. Dubost, D. Genest, S. Yahiaoui, T. Freret, V. Bouet, F. Dauphin, J. S. De Oliveira Santos, C. Ballandonne, S. Corvaisier, A. Malzert-Fréon, R. Legay, M. Boulouard, S. Claeysen, and P. Dallemagne. Novel multitarget-directed ligands (MTDLs) with acetylcholinesterase (AChE) inhibitory and serotonergic subtype 4 receptor (5-HT_4R) agonist activities as potential agents against Alzheimer's disease: the design of donecopride. *J. Med. Chem.*, 58(7):3172–3187, 2015.
489. G. L. Harris, M. B. Creason, G. B. Brulte, and D. R. Herr. In vitro and in vivo antagonism of a G protein-coupled receptor (S1P3) with a novel blocking monoclonal antibody. *PLoS One*, 7(4):e35129, 2012.
490. S. M. Schumacher, E. Gao, W. Zhu, X. Chen, J. K. Chuprun, A. M. Feldman, J. J. G. Tesmer, and W. J. Koch. Paroxetine-mediated GRK2 inhibition reverses cardiac dysfunction and remodeling after myocardial infarction. *Sci. Transl. Med.*, 7(277):277ra31–277ra31, 2015.